UNIVERSITÀ DEGLI STUDI DI MILANO

Doctoral School in Biochemical Science

Dipartimento di Biotecnologie Mediche e Medicina Traslazionale

XXXII Cycle

PhD thesis

EX VIVO MONOCYTES SIGNATURES FROM CORONARY ARTERY DISEASE PATIENTS AND HEALTHY SUBJECTS THROUGH A LIPIDOMIC APPROACH

Chiara Maria MANEGA

Matr. n. R11601

Tutor: Professor Donatella Caruso

Coordinatore del dottorato: Professor Alessandro Prinetti

A.A. 2018-2019

Index

Abbreviations

β-1,4 GalT-V: β-1,4 Galactosyltransferase-V
ACS: acute coronary syndromes
AMI: acute myocardial infarction
BMI: body mass index
CAD: Coronary artery disease
CE: Cholesteryl esters
CER: ceramides
Cho: cholesterol
CV: coefficient of variation
CVD: cardiovascular disease
DG: diglycerides
D-PDMP: D-1-phenyl-2-2-decanoylamino-3-morpholino-1-propanol
ESI: electrospray ionization
FA: fatty acids
FBS: fetal bovine serum
FC: fold change
FDR: false discovery rate
GL: Glycerolipids
GlcCer: glucosylceramide
GM-CSF: granulocyte macrophage-colony stimulating factor
GP: glycerophospholipids
GSL: glycosphingolipids
HDL: high-density lipoprotein
HexCer: hexosylceramide
ICAM-1: intercellular adhesion molecule-1
IL: interleukin
LacCer: lactosylceramide
LDL: low-density lipoprotein
LDLR: low-density lipoprotein receptor
LPL: lysophospholipids
m/z: mass to charge
Mac-1: macrophage-1 antigen
MCP-1: monocyte chemoattractant protein-1
M-CSF: macrophage-colony stimulating factor
MG: monoglycerides
MI: myocardial infarction
MS: mass spectrometry
MS/MS: tandem mass spectrometry
MUFA: monounsaturated fatty acid
NADPH: nicotinamide adenine dinucleotide phosphate
NSTEMI: non-ST elevation myocardial infarction
OxLDL: oxidized low-density lipoprotein
PA: phosphatidic acid
PC: phosphatidylcholine
PC1, PC2: principal component 1,2
PC-O/-P: Plasmanyl/Plasmenyl **PC**
PCA: Principal Component Analysis
PE: phosphatidylethanolamine
PECAM-1: platelet-endothelial cell adhesion molecule-1
PG: phosphatidylglycerol
PI: phosphatidylinositol
PKC: protein kinase C
PL: phospholipids
PLA_2: phospholipase A2
PS: phosphatidylserine
PUFA: polyunsaturated fatty acid
QC: quality control
QTOF: quadrupole time of flight
ROS: reactive oxygen species
RT: retention time
S1P: sphingosine-1-phosphate
SA: stable angina
SD: standard deviation
SM: sphingomyelin
SMCs: smooth muscle cells
SP: Sphingolipids
Sph: sphingosine
STEMI: ST elevation myocardial infarction
TAG/TG: triglycerides
TGF- β transforming growth factor-β
TIC: total ion current
TNF-α: tumor necrosis factor-α
UA: unstable angina
UPLC: ultra-high pressure liquid chromatography
VCAM-1: vascular cell adhesion molecule-1
VLA-4: very late antigen-4
VLDL: very low-density lipoproteins
VEGF: vascular endothelial growth factor

1. Abstract

Monocytes play a major role in atherosclerosis, a chronic inflammatory disease of the arterial wall and specifically, the recruitment of circulating monocytes to the site of injury and their diapedesis through the endothelium (extravasation) are crucial events in atherosclerotic plaque progression.

Monocytes are classified into three subsets according to the differential expression of the lipopolysaccharide receptor (CD14) and the FcγIII receptor (CD16): $CD14^{++}CD16^{-}$ classical monocytes, intermediate $CD14^{++}CD16^{+}$ monocytes and non-classical $CD14^{+}CD16^{++}$.

During circulation, monocytes are exposed to several environmental stimuli that may alter their metabolic state thus inducing a cellular reprogramming with important effects on their functional profile. Recent data indicated that subjects with altered blood lipid levels display circulating monocytes with an inflammatory profile.

Most of researches investigated the mechanisms by which lipids and lipoproteins affects the monocyte functions leading to plaque formation, but no information about the relationship between cellular lipid composition and monocyte function are available.

Aim of the study was to investigate a lipid profile of monocytes in healthy subjects (HS) and coronary artery disease (CAD) patients, and its influence on monocyte migration.

Monocyte lipidomic profile was evaluated through an untargeted liquid chromatography-time of flight mass spectrometry platform operating in positive and negative ionization mode. Monocyte migration assay was performed using fetal bovine serum (FBS), or autologous serum as chemotactic stimuli.

By means of an untargeted lipidomics approach, we evidence a different profile in CAD monocytes compared to HS, with a marked increase in lactosylceramide (d34:1) (d18:1/16:0) in patient's monocytes. Moreover, we demonstrate that monocytes obtained from CAD patients show a significant increase in FBS- and autologous serum-mediated migration compared to HS. The lactosylceramide levels positive correlate with monocyte migration and the treatment with the inhibitor of lactosylceramide synthase significantly reduces the monocyte migration. The results of this study suggest that lipidomics profile may dysregulate cell function, such as migration in CAD patients' monocytes.

2. Introduction

2.1 Atherosclerosis

2.1.1 Definition and overview

Atherosclerosis is a chronic and degenerative inflammatory disease characterized by alterations of the vascular wall of medium and large arteries resulting in the atherosclerotic plaque formation and its progression[1]. Atherosclerotic plaques show heterogeneity in terms of both morphology and composition leading to different clinical outcomes. Most plaques remain asymptomatic, some become obstructive characterizing the stable angina (SA) condition, while others elicit thrombus formation and may result in acute coronary syndromes (ACS)[2].

The underlying causes of the disease have been studied since 1900 when atherosclerosis was supposed to be mainly related to the aging process[3]. In 1913, Anitschkov's work demonstrated, for the first time, that high cholesterol (Cho) level can increase the incidence of the pathology[4] which was also later confirmed in the 1950s by Keys[5]. The role of Cho has become increasingly important when the presence of low-density lipoprotein (LDL) cellular receptors (LDLR), capable of removing Cho from blood, has been discovered[6]. On this basis, it was observed that subjects showing an insufficient number of LDLR or carrying genetic mutation of the receptor structure are more prone to develop hypercholesterolemia and Cho-related diseases[7]. In the 1990s, Ross formulated the "response to injury" hypothesis according to which endothelial damage represents the first step in the development of an atherosclerotic lesion, followed by migration to the vessel wall of circulating monocytes and T lymphocytes[8]. Since these cells have a crucial role in local and systemic infection, others theories have been formulated indicating infectious diseases as possible causes of atherosclerosis[9]. In support of this, the presence of lesions of the vessel walls similar to that observed in human with atherosclerotic disease was reported in animal infected with avian herpes virus[10]. In addition, observational studies in humans proposed an association of infectious agents such as certain viruses and bacteria with atherosclerosis, coronary events, or restenosis after arterial intervention[11]. However, currently the involvement of bacterial or viral infections in the development of atheromasic pathology has been completely ruled out. In the last two decades, the results of numerous studies have led to the definition of atherosclerosis as a disease on an inflammatory basis, rather than a disease due only to an alteration in the accumulation and distribution of Cho[1, 12].

Atherosclerosis is a complicated and multifactorial disease, indeed, several epidemiological studies have identified several risk factors that can contribute to the onset of the disease and that can be classified, according to European Society of Cardiology (ESC), as modifiable or not modifiable. Not modifiable risk factors include age and gender. The incidence of atherosclerosis increases with advancing age and specifically the risk increases after the age of 45 for men while in women after 55[13]. This effect in women coincides with the onset of menopause when estrogens levels decrease. Consequently, the estrogenic protective role, consisting in the improvement of the lipoprotein profile, is reduced[14, 15]. Genetic predispositions also promote the development of atherosclerosis. Indeed, people with a family history of cardiovascular disease (CVD) or hereditary alterations in the genes involved in lipid, glucose and amino acid metabolism, show an increased CVD risk[14, 16]. On the other hand, modifiable risk factors can be monitored and controlled thus allowing a prevention or a delay in the onset of the disease. These include diet, lifestyle (smoking and/or lack of physical exercise) and metabolic syndromes, which are a cluster of conditions such as hypertension, hyperglycemia, obesity and dyslipidaemia[17]. Concerning the food intake, several epidemiological studies have shown that plasma Cho levels and death from CVD are lower in Japan and southern Europe compared to the northern countries. This difference is associated with saturated fatty acids (FA), animal proteins, sodium and sugar increased consumption combined also with a sedentary lifestyle[18]. Moreover, an unhealthy diet can lead to other conditions such as overweight or obesity, which increase mortality risk for men and women of all racial and ethnic groups. About half of the obese population also exhibits insulin resistance defined as a defective uptake or utilization of glucose in response to insulin. Clinically, this pathology can be diagnosed by a fasting plasma glucose test (glucose level of 100 to 125 mg/dL) or by an oral glucose tolerance test defined as 2 hours plasma glucose value of 140 to 199 mg/dL[19]. These glucose levels are also associated with type-2 diabetes mellitus. High blood glucose concentration can injure the vascular wall by inducing reactive oxygen species (ROS) production, stimulating the endothelial cells apoptosis and inactivating proteins through their glycation[20-22]. Moreover, elevated insulin levels promote the development of atheromasic plaque by stimulating smooth muscle cells (SMCs) proliferation and activating hepatic Cho biosynthesis[23]. Diabetes is characterized by the development of microvascular and macrovascular complications that can be exacerbated by the presence of concomitant diagnosis of hypertension. Guidelines from the *Seventh Report of the Joint National Committee on Prevention, Detection, Evaluation and Treatment of High Blood Pressure* recommend a systolic blood pressure below of 140 mmHg and a diastolic blood pressure above 90 mmHg. These goals have been lowered to 130 mmHg and 80 mmHg respectively, for patients with diabetes or chronic kidney disease specifically[24]. The rising incidence of hypertension is of interest since even moderate increase in blood pressure can increase the CVD risk. Indeed, hypertensive

patients are characterized by high angiotensin II level, a vasoconstrictor mediator that stimulate SMCs proliferation but also induce inflammation and LDL oxidation (oxLDL)[25]. Furthermore, a high blood pressure leads to an increased permeability of the vessel wall to lipoproteins thus promoting the onset of atherosclerosis[26]. Hypertension but also smoking habits can cause narrowing and hardening of arteries that decrease the blood flow and thus the supply of oxygen to the tissues. This lumen reduction also led to deposit of Cho that characterizes the first phase of atherosclerotic plaque formation. Moreover cigarette smoking is also associated with endothelial dysfunction, increased oxidation of atherogenic lipids and reduced high-density lipoprotein (HDL) levels[27]. Another major risk factor for CVD is hypercholesterolemia characterized by high blood total Cho levels[28]. Cho is transported by several classes of lipoproteins such as very low-density lipoproteins (VLDL), LDL and HDL. Specifically, the risk of CVD increases linearly with LDL levels, indeed LDL levels represents the most used diagnostic test to evaluate the risk of atherosclerosis. The goal is an LDL level below 70 mg/dL for high-risk patients and statins are the most effective and most frequently prescribed medications to decrease LDL cholesterol levels. It was demonstrated that every 1 mmol/l reduction in LDL cholesterol is associated with 10–20% reduction in the risk of cardiovascular events[29]. However, statin therapy only modestly improved the HDL cholesterol whose low level (below 40 mg/dL) is an independent and predictive risk factor for CVD[30].

The identification of the different risk factors and their mechanisms of action has already led to the development of some successful therapeutic strategies. For example, intensive lifestyle modifications clearly have the potential to reduce CVD risk however many patients are reluctant to follow a healthy regimen for long periods of time[31]. In addition, several medications such as lipid-lowering or antihypertensive drugs have been prescribed to inhibit the progression of atherosclerotic disease and reduce its complications. Most of the currently available drugs, however, are specific for a single risk factor with a little effect on the others. Thus, the goal of the new-developed treatments is to address several CVD risk factors with a single agent that in conjunction with an improvement in lifestyle habits may reduce CVD risk.

2.1.2 Atherosclerotic plaque formation

Atherosclerosis is characterized by the formation, in the vascular lumen, of an atherosclerotic plaque consisting of lipids, activated SMCs, immune cells, foam cells, a necrotic core and calcified areas[9]. Atherosclerotic plaques mainly develop in specific region of the arterial tree that are most susceptible to low or oscillatory endothelial shear stress. These sites are located near branching points or along internal curvatures, indeed, abdominal aorta, coronary and carotid arteries appear to be the most affected[32]. Before development of atheromasic plaques, these sites are characterized by an adaptive intimal thickening consisting in an early accumulation of SMCs (**Figure 1A**).

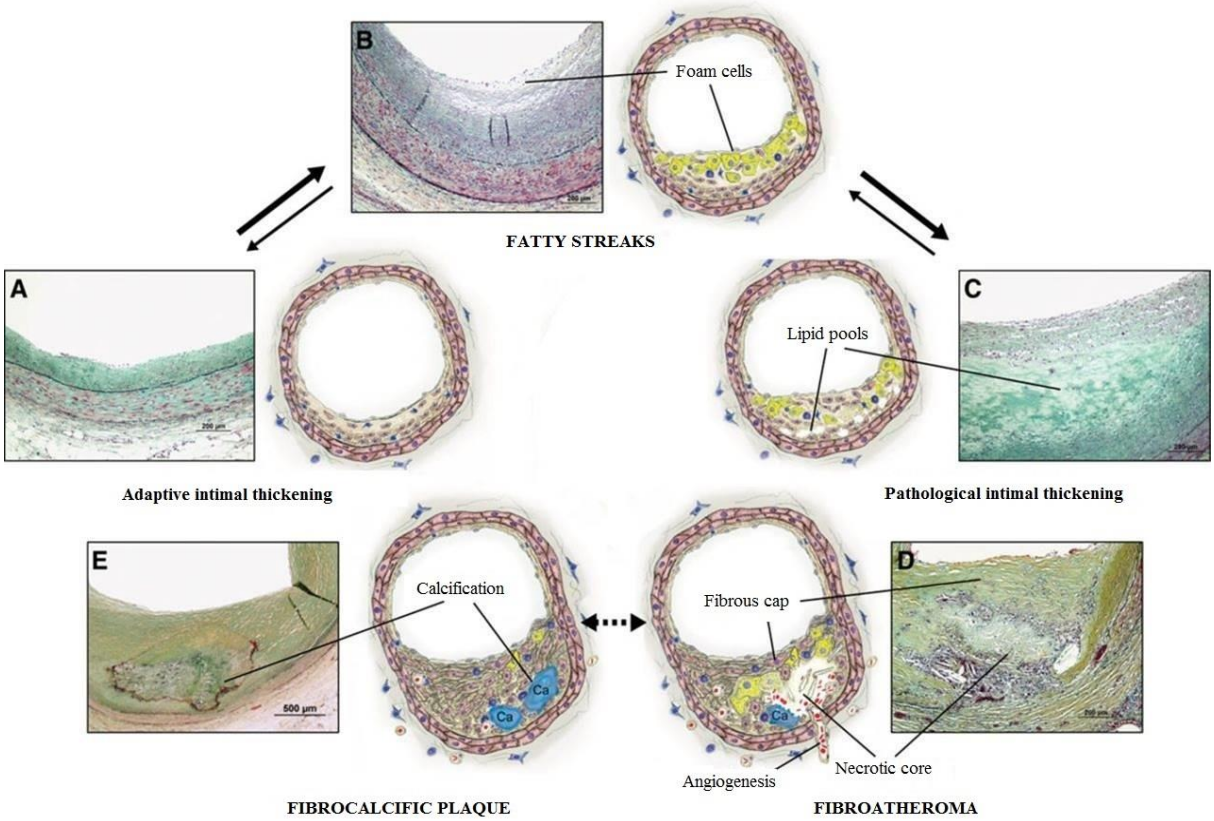

Figure 1 **Atherosclerotic plaque development and progression**
A: Adaptive intimal thickening characterized by smooth muscle cell accumulation.
B: Fatty streak formation following accumulation of foam cells.
C: Pathological intimal thickening and lipid pools accumulation in the absence of necrosis.
D: Fibroatheroma and necrotic core formation.
E: Calcification and fibrocalcific plaque formation.

Plaque formation begins with an accumulation of LDL in the arterial intima, where they may be subjected to modifications as oxidation (oxLDL) or aggregation[33]. OxLDL stimulate the response of the innate and adaptive immune system, inducing the expression by endothelial cells and SMCs, of adhesion molecules such as intercellular adhesion molecule-1 (ICAM-1) and vascular cell adhesion molecule-1 (VCAM-1), chemoattractant factors such as monocyte chemoattractant protein-1 (MCP-1), and growth factors as granulocyte macrophage-colony stimulating factor (GM-CSF) and macrophage-colony stimulating factor (M-CSF), that interact with monocyte receptors to promote their migration and the subsequent differentiation to macrophages[34]. Macrophages are heterogeneous cells, which show different phenotypes, thus exerting multiple functions during the development of atheromasic lesions. Indeed, macrophages characterized by a pro-inflammatory phenotype (M1), produce pro-inflammatory cytokines as interleukin-1β (IL-1β) and tumor necrosis factor-α (TNF-α) and ROS that may stimulate LDL retention and their oxidation, and other mediators that may participate in the process of atherosclerosis such as plasminogen activators, cathepsins and matrix metallo-proteinases[35]. On the contrary, macrophages showing an anti-inflammatory phenotype (M2) secrete factors such as transforming growth factor-β (TGF-β) that favor the resolution of inflammation[36]. Macrophages participate in the clearance of oxLDL, accumulate lipids thus transforming into foam cells through a mechanism that involves scavenger receptors. These receptors mediate mainly the uptake of oxLDL, that can be hydrolyzed in intracellular lithic compartments, but also the uptake of native LDL[37]. Foam cells accumulation is a hallmark of an inflammatory state of the vascular wall. These cells accrue within the proteoglycan layer of the intima forming several overlapping layers, which appear as yellow-colored fatty streaks (**Figure 1B**). These are completely reversible in the absence of the stimuli that caused their formation. They may already be present in fetal or neonatal aortas during the first six months of life, probably as a consequence of the mother risk factors; however, their number declines in the following years. During adolescence, fatty streaks can reappear especially in atherosclerotic-prone regions of the coronary arteries and the aorta[38].

2.1.2.1 Necrotic core formation

While many fatty streaks do not progress further, others, especially those that develop in predilection sites, evolve into atherosclerotic lesions. The distinctive feature is an accumulation of lipid material in the intima[39-41]. At first, small pools of lipids are visible under the layer of foam cells, without alterations of the normal structure of the vessel wall. This type of lesion is called pathological intimal thickening (**Figure 1C**) and is commonly observed from 20 to 30 years of age in the coronary arteries[39]. A necrotic core (or lipid-rich core) characterize the more advance lesions. The necrotic core formation, following invasion by macrophages, is a process that irreversibly destroys the normal structure of the intima[28]. In the presence of a necrotic core, the lesion is called fibroatheroma (**Figure 1D**). Apoptosis and necrosis play an important role during the development of the necrotic core[42]. Whilst a high number of apoptotic macrophages and SMCs is detectable in the atherosclerotic lesion, specifically at the margins of the necrotic core[43], the presence of free apoptotic debris in lesions which are not associated with phagocytic cells, suggests that an altered process of apoptotic cell removal (i.e. efferocytosis) occurs thus promoting the growth of the necrotic core[36, 44]. In addition, the chemical composition of the necrotic core suggests that the accumulation of lipids from different sources, such as Cho esters from LDL and free Cho from erythrocyte membranes, released during intraplaque hemorrhagic events, may also contribute to the development of atheroma[45].

2.1.2.2 Plaque angiogenesis and intraplaque hemorrhage

During the progression of atheromasic plaque, new blood vessels are formed which originate from the adventitial vasa vasorum and provide an alternative route of entry to monocytes and immune cells[46]. These vessels are fragile and leaky, leading to the extravasation of plasma proteins and erythrocytes, which in turn promote the necrotic core expansion and inflammation[45, 47]. It has been observed that intraplaque bleeding is associated with the presence of macrophages expressing CD163, a scavenger receptor that binds the haptoglobin-hemoglobin complex thus preventing cytotoxic effects caused by free hemoglobin. These macrophages lack the typical markers of M1 phenotype (TNF-α and inducible nitric oxide synthase), but express the mannose receptor, characterizing M2 macrophages, and are resistant to foam cell formation[48].

2.1.2.3 Fibrous cap formation

The connective tissue, present in the initial stages of the lesion, is gradually replaced by fibrous tissue rich in collagen fibers that becomes the dominant component as the atheromasic plaque progresses[49]. Collagen, elastin and proteoglycans of the fibrous matrix are mainly produced by damaged SMCs. SMCs are present in small quantities in normal intima, however, their number rises significantly during the development of the lesion. This increase is due to both local proliferation of synthetic SMCs, or migration from media to intima of contractile SMCs with a subsequent shift towards the synthetic phenotype. These cells, showing a synthetic phenotype, are characterized by an abundant rough endoplasmic reticulum and Golgi apparatus and scattered myofilaments[50].

2.1.2.4 Calcification

The presence of calcifications is a common aspect in the progression of atherosclerotic plaque and the incidence of fibrocalcific plaques (**Figure 1E**) increases with age. These plaques are characterized by microscopic calcium granules that can then expand to form larger calcium deposits utilizing apoptotic cells, the extracellular matrix and the necrotic core content as focal points for the development[51, 52]. The necrotic nucleus may then completely calcify, and the calcifications may occupy most of the surface of the plaque. Sometimes calcified lesions can evolve into osseous metaplasia; however, this is a rare event that only occurs in arteries with a high calcification status[51].

2.1.3 Histological classification of atherosclerotic plaque

The histological classification of atherosclerotic plaques has been studied since the beginning of the 20th century when two types of lesions were recognized. The former, "fatty streak", was associated with an intimal thin lipid deposit in children. The latter, "fibrous plaque", represented a thick fibrolipidic layer presents in adults. The pathologist Aschoff was a strong promoter of the theory supporting the intimal lipid and fibrolipidic deposits as an early and late stage of one disease. He defined the first stage as "atherosis" or "atheromatosis" mainly characterized by lipid deposition, while, the fibrolipidic stage was defined "atherosclerosis"[50]. Thereafter, the pathogenesis of atherosclerotic lesions was studied on the basis of microscopic analysis of arteries obtained from different subjects affected by atherosclerotic disease and divided into groups according to age. Following the research of Stary et al. (1994)[39], the histological classification, proposed by the American Heart Association, distinguished six different stages of atherosclerotic lesion[53].

The type I lesion is defined as intimal thickening or "initial lesion" and it appears to be most common in children. It is characterized by small deposits of lipids and limited endothelial changes. The human intima changes are minimal, indeed small isolated groups of foam cells are observed and SMCs show low proliferative activity[54].

Type II lesions refer to the presence of fatty streaks, yellow-colored streaks on the intimal surface of arteries. Macrophages are the most numerous cells present at the level of the lesion, however, an increase in the number of T lymphocytes and mast cells compared to the type I lesion and normal intima is also observed. Moreover, abundant macrophage foam cells form layers rather than single isolated spots and they are interspersed with SMCs containing lipid droplets[39]. Lipids that characterize the type II lesion are mainly phospholipids (PL), free Cho and Cho esters and among these cholesteryl oleate and cholesteryl linoleate[55]. Type II lesions can be divided into two subgroups: type IIa and type IIb also defined as advance lesion-prone and advance lesion-resistant, respectively. While the former represents a small class of lesions localized at the level of specific adaptive intimal thickenings in predictable areas, the latter subgroup is larger, and it includes lesions that are found at the level of a thin intima. Morphologically, these two categories differ in terms of presence of SMCs, abundance of intercellular matrix, accumulation of lipoproteins and macrophages and localization of foam cells and extracellular lipid droplets. Furthermore, type IIa lesions are the first to evolve into type III lesions, while type IIb lesions may progress slowly or not at all[39]. The designation 'type III lesions' refers to lesions that show intermediate morphological characteristics between type II lesions and advanced lesions. The intimal pathological thickening (type III) is characterized by a layer of SMCs in a proteoglycan-collagen matrix above the underlying lipid pools rich in hyaluronan and versican. The structural modifications of the glycosaminoglycan chains in proteoglycans represent one of the initial triggers for the development

of the lesion favoring the binding of atherogenic plasma lipoproteins to the extracellular matrix in the lipid pools[56]. Another characteristic of type III injury is a higher content of free Cho, FA, sphingomyelin (SM), lysolecithin and triglycerides (TG) compared to type II lesions. Moreover, Cho esters contain a high percentage of linoleic acid and low levels of oleic acid while the opposite occurs in type II lesions[57].

Type III lesions represent a transitional state between type I and II, which are defined as "early" lesions, and the other "later" advanced lesions. Atherosclerotic lesions are considered advanced when an accumulation of lipids is observed in association with disorganization and thickening of the intima of the vessel and deformation of the vessel wall. In addition, complications such as fissures, hematomas and thrombosis often occur in these conditions[39].

Advanced lesions are in turn subdivided into types IV, V and VI.

The type IV lesion, also known as atheroma, is characterized by a dense accumulation of extracellular lipids (lipid cores) formed as a result of the confluence of the small isolated lipid pools typical of type III lesions. In the region between the lipid core and the endothelial surface there are SMCs, macrophages and macrophage foam cells but also lymphocytes and mast cells. In addition, there is a severe disorganization of the intima and consequent formation of fibrous tissue above the lipid core. When an increase in fibrous connective tissue, mainly collagen, is observed, the lesion is defined as type V and it is characterized by a large lipid-rich necrotic core covered by a thick fibrous cap[50]. The necrotic core evolves thus an "early" and "later" ones can be distinguished. An early necrotic core is described by the presence of foamy macrophages that infiltrate the luminal surface of the lipid pools. Moreover, the presence of proteoglycans, versican and hyaluronan, typically absent in the late necrotic core, was observed. Late necrotic cores are distinguished by the increased presence of cell debris resulting from a defective phagocytic clearance of apoptotic cells. Another discriminating feature is the presence of free Cho partly attributed to the apoptotic death of macrophages[58]. According to the morphology, type V lesions can be classified into three subtypes. Type Va lesion is multi-layered: different lipid cores surrounded by thick fibrous connective tissue are superimposed and for this reason, it is called "multilayered fibroatheroma". Lesions, with a high calcium content, are called type Vb or calcific lesions; on the contrary, lesions with minimal presence of lipids but high fibrous connective tissue are type Vc or fibrotic lesions[59].

The last stage of atherosclerotic plaque is the type VI or complicated lesions. Specifically, these are type IV or V lesions in which disruptions of the lesion surface (type VIa), hematoma or hemorrhage (type VIb) and thrombosis (type VIc) occur. These events may occur individually or simultaneously as in the VIabc type.

2.1.4 Clinical manifestation of atherosclerosis

Since the beginning of the 21st century, a dramatic increase in the incidence of cardiovascular disease was observed. Although statistics indicate that the death rates are now decreasing, CVD remain the leading cause of mortality and morbidity in Europe. Therefore, 3.9 million deaths from cardiovascular disease (45% of all deaths), are recorded each year in Europe[60].

Coronary artery disease (CAD) is the most common of the cardiovascular diseases and it includes SA, unstable angina (UA), myocardial infarction (MI) and sudden cardiac death. Moreover, myocardial infarctions are clinically classified into ST elevation MI (STEMI) and non-ST elevation MI (NSTEMI) based on changes on electrocardiogram. Atherosclerosis, especially plaque rupture and thrombosis, is the main leading cause of these clinical manifestations. Patients diagnosed with SA show a stenotic lesion that tends to be stable, fibrotic and less prone to rupture. A severe stenosis may progress to total thrombotic occlusion but less frequently will result in a heart attack[50]. On the contrary, ACS (UA and AMI) are often caused by luminal thrombus formation or by sudden plaque hemorrhage[61]. Specifically, thrombus appear to be mostly occlusive in STEMI while UA and NSTEMI are characterized by either the formation of a non-occlusive thrombus or complete thrombosis. Luminal thrombosis occurs mainly as a result of plaque rupture (55-65% of cases), plaque erosion (30-35%) and less frequently as a result of calcific nodules formation (2-7%)[40]. Plaque rupture is typically observed in a lesion characterized by a large necrotic core (usually >30% of plaque area), a damaged fibrous cap (thickness < 65 μm) and high macrophage infiltration. Thrombus is formed as a consequence of the contact between blood flow and the thrombogenic necrotic core[62] (**Figure 2B**).

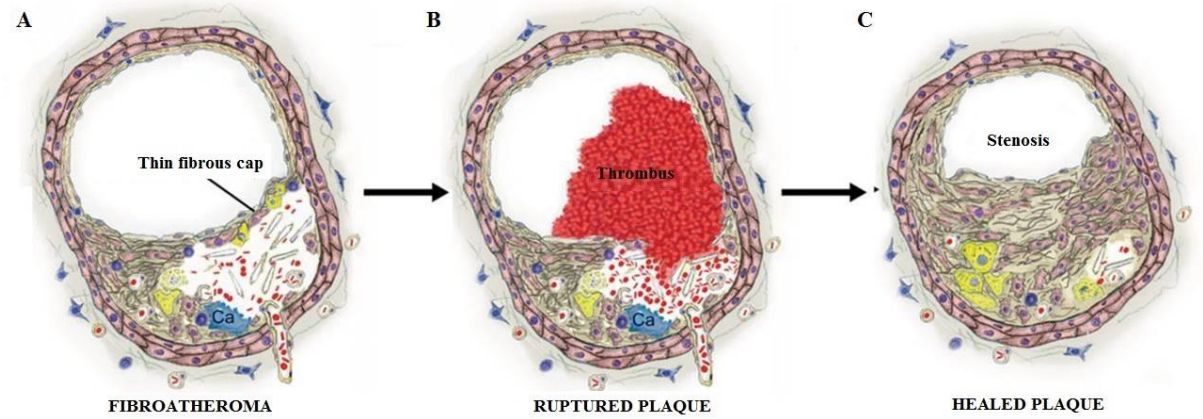

Figure 2 **Plaque rupture and healing**
A. Fibroatheroma with a thin fibrous cap.
B. Plaque ruptured and thrombus formation.
C. Healed plaque with fibrous tissue formation and constrictive remodeling.

Thinning of the fibrous cap can be due to the gradual loss of SMCs and collagen which constitute the cap itself[63]. In addition, infiltrated macrophages can degrade the collagen-rich cap matrix by secreting proteolytic enzymes, such as plasminogen activators, cathepsins and metalloproteinases[64]. The rupture of a thin fibrous cap and subsequent thrombus formation may occur spontaneously, but in some cases, it may be triggered also by emotional or physical stress as a consequence of sympathetic nervous system activation that in turn increase heart rate and blood pressure[65]. Thrombus formation can also occur after plaque erosion, without plaque rupture. Eroded plaques are typically poorly calcified, usually associated with negative remodeling and less inflamed than ruptured plaques. At the point of erosion there is a loss of the integrity of the endothelial surface, resulting in exposure of the SMCs of the intima and proteoglycans leading to thrombus formation, however the mechanism by which this occurs is not yet fully known. Vasospasm was proposed as trigger of endothelial damage and following thrombosis[66]. Calcified nodules are the least frequent cause of thrombosis. These, which occur in highly calcified arteries, penetrated the lumen of the vessels destroying the collagen layer and the endothelium. The nodules are surrounded by fibrin and often associated with small platelet-rich thrombi that are non-occlusive. Calcified nodules are more likely found in elderly patients and specifically observed in the tortuous regions of coronary arteries[58]. In addition, thrombi from ruptured, eroded or calcified plaques can be silent and eventually repaired to form healed lesions (**Figure 2C**). These lesions are characterized by a fibrous cap rich in type I collagen which is overlaid with a new layer rich in proteoglycans and type III collagen with interspersed SMCs. Luminous thrombus may be non-occlusive or occlusive leading to the development of a chronic total occlusion. Histological studies have shown that the frequency of healed plaques correlates with the degree of vessel wall narrowing. Indeed, it has been observed that the incidence of healed lesions rises from 20% of lesions with a stenosis <50%, to 70% with a stenosis degree >50%[67].

2.1.5 Perspective for prevention

In research and clinical practice, it is necessary to characterize the atherosclerotic disease and atheromasic plaques, defining some important and measurable parameters that highlight the stage of the disease and the risk of progression. Some of the parameters used are plaque burden, activity and vulnerability. Plaque burden is a measure of the extent of atherosclerosis, regardless of cellular composition and plaque activity. It can be calculated as the volume of plaque, (arterial surface covered by the lesion), or through the measurement of the calcium amount by computed tomography, or as the intima-media thickness defined by ultrasound[68]. Plaque activity, on the other hand, is a tool for identifying causal factors that can contribute to the progression of the disease. This parameter, which can be evaluated through imaging techniques, or through the measurement of circulating plasma biomarkers, can be used to verify the effectiveness of pharmacological therapies. Usually, the term plaque activity refers to the inflammatory state, measured for example in terms of macrophage density in plaques. However, there is a profound difference between the inflammation that characterizes the initial stages of the lesion and the specific inflammation of fibrous cap that causes rupture and thrombosis[69]. Several other processes can be classified as factors that modulate plaque activity, including the extent of intimal necrosis, which is perhaps the most damaging consequence of the disease. Angiogenesis, endothelial damage and intraplaque hemorrhage that often accompany inflammation are other potential biomarkers[69]. Many efforts have been made to identify the peculiar characteristics of vulnerable plaques in order to predict which plaques are at risk of developing a thrombotic condition and to understand the mechanism leading to their formation[70]. The term "vulnerable plaque" is used to indicate plaques with a high risk of rupture or erosion or to describe a set of histological features that increase the risk of thrombus formation. On this basis, patients with a high short-term risk of developing an acute clinical event are classified as "vulnerable". This propensity is indeed influenced by the parameters described above such as the extent and activity of plaque, but also by the systemic thrombotic predisposition and the susceptibility of the myocardium to ischemia and arrhythmia[71].

In summary, the mechanisms that lead to the narrowing of the fibrous cap and the consequent plaque rupture, are still unclear and the trigger for thrombotic event in eroded plaques are even less known. Extensive research in this field could lead to the definition of new therapeutic treatments for the prevention and limitation of the progression of atherosclerotic disease. For example, periodic evaluations of plaque burden in middle-aged people can improve the risk stratification of patients, thus enabling preventive therapies in a larger number of patients at risk[72]. However, to achieve an improvement of prevention strategies, the importance of lifestyle aspects such as quality of diet, physical activity and weight control should also be taken into account.

2.2 Monocytes

The definition of atherosclerosis as an inflammatory disease has delineate a pathophysiological role of cells such as monocytes and macrophages. Monocytes are fundamental during the development of atherosclerosis from the early lesion to the final plaque rupture. After the initial injury, the attachment and subsequent migration of monocytes to the subendothelial space is stimulated by activated endothelial cells expressing adhesion molecules. Monocytes can then differentiate into macrophages that incorporate oxLDL and produce cytokines by promoting inflammation. The perpetuation of this cycle promotes the progression of early lesions in advanced atherosclerotic plaques.
The study of the development and functional characterization of monocytes and their pathophysiological role in atherosclerosis is therefore fundamental.

2.2.1 Definition and overview

The first observations on monocytes can be traced back to the second half of the 19th century and are specifically linked to the introduction of microscopy. In 1880, Ehrlich developed a technique of cytological staining and through the use of aniline and neutral dyes, he described white blood cells (WBC) according to nuclear morphology. By this way, he classified mononuclear leukocytes, characterized by a large kidney-shaped nucleus that he called "Übergangszelle" or "transitional cells" now known as monocytes, and polymorphonuclear cells with neutrophilic (neutrophils), acidophilic (eosinophils) or basophilic (basophils) granules[73]. The introduction of the denomination "monocytes" seems to be attributable to the scientist Artur Pappenheim in 1910[74]. Subsequently, the first *in vitro* studies were conducted describing the migratory capacity of these cells and their differentiation into tissue macrophages following acute insults as inflammatory stimuli[75].
Actually, monocytes represent a highly plastic and heterogeneous cell population that refers to the mononuclear phagocytic system. These cells are characterized by a kidney/bean-shaped nucleus. As blood circulating cells, these amount to about 10% of total peripheral leukocytes in humans and 4% in mice.

2.2.2 Monocyte heterogeneity and subsets

Monocytes are a heterogeneous cell population showing differences in terms of morphology, phenotype and functions.

Monocytes show distinct phenotypes due to the different expression, on the cell surface, of two markers: the lipopolysaccharide (LPS) receptor antigen, CD14, and the immunoglobulin G Fcγ receptor, CD16. According to the nomenclature approved by the Nomenclature Committee for the International Union of Immunological Societies, human monocytes are then classified into three subpopulations: classical $CD14^{++}CD16^{-}$, intermediate $CD14^{++}CD16^{+}$ and non-classical $CD14^{+}CD16^{++}$ monocytes[76]. Each of these subsets show peculiar characteristics in terms of expression of cell adhesion molecules and chemokine receptors resulting in different phenotypes with different functions (**Figure 3**).

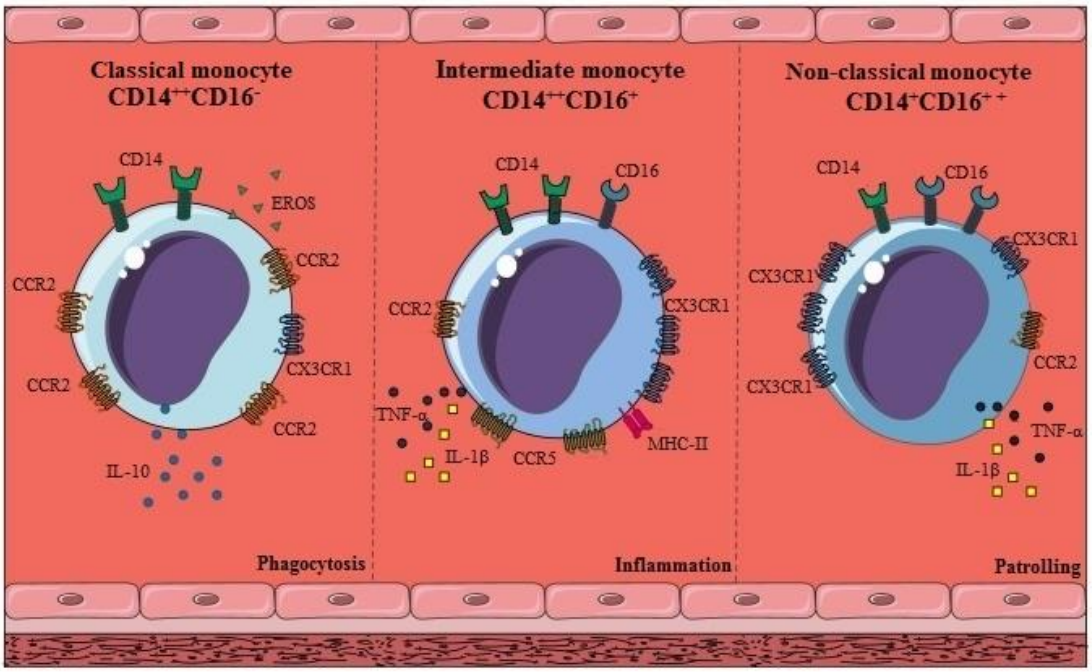

Figure 3 **Human monocyte subsets**
Human monocytes are classified into three subsets based on the different expression on the cell surface of specific receptor: classical $CD14^{++}CD16^{-}$ monocytes, intermediate $CD14^{++}CD16^{+}$ monocytes and non-classical $CD14^{+}CD16^{++}$ monocytes.

Classical monocytes represent the largest subgroup: 80-90% of the total monocyte count. These cells display a high expression of the chemokine receptor (CCR) type 2, that is the receptor of MCP-1, of chemokine receptor (CXCR) 1,2 and 4 and high levels of the cell adhesion molecule L-Selectin (CD62L) while CX3CR1 (the fractalkine receptor) and CCR5 show lower levels. Following stimulation with LPS, this subset produces several chemokines and cytokines such as interleukin (IL)-10, IL-6, IL-8, IL-1β, TNF-α and CCL2 (chemokine ligand also known as MCP-1). The main function is linked to the immune response, specifically, due to the high expression of

myeloperoxidase, several receptors such as, CD32, CD64, signal-regulatory protein α (SIRPα), and CD36 that highlights their role in the phagocytic process. These cells are considered as inflammatory mediators as they are rapidly recruited to inflamed tissue due to the recognition, by their receptor CCR2, of MCP-1 produced by tissue resident-macrophages. Furthermore, classical monocytes are rich in genes related to angiogenesis and coagulation thus underlining their involvement in tissue repair and wound healing[77].

Non-classical monocytes (2-8% of total circulating monocytes) show phagocytic competences too; these are also ROS producers; however, their production of cytokines is greatly reduced. Concerning molecule expression on cell surface, non-classical monocytes display ICAM-1, opsonin receptors FcγRI and FcγRII, major histocompatibility complex (MHC) class II and CX3CR1 but low levels of CD11b and CD33 while they do not express CCR2 and CD62L at all. The main function is the patrolling of the blood circulation for the control and removal of damaged cells. This activity is due to the interaction between fractalkine (CX3CL1) expressed on endothelial cells, and its receptor CX3CR1 allowing the attraction and arresting of monocytes to the endothelium. Moreover, non-classical monocytes show a high expression of genes involved in the rearrangement of the cytoskeleton[77].

Intermediate monocytes (2-10% of total circulating monocytes) appear as an intermediate state between classical and non-classical monocytes, as these cells show the expression of a mixture of markers that characterize both classical and non-classical subsets. The expression of CCR1, CCR2 and CXCR2 characterizes the intermediate monocytes. Furthermore, CX3CR1 and CCR5 are present on the cell surface, as well as MHC class II that is more expressed in this group than the others are. Intermediate monocytes produce large quantities of ROS and pro-inflammatory cytokines such as TNF-α and IL-1β following stimulation with LPS; however, they are also the main producers of the anti-inflammatory IL-10[78].

To conclude, monocyte population is composed by three subsets showing different phenotypes, however, whether these phenotypes are distinct or constitute a wide continuum is still unclear. To date it is assumed that dynamic changes rather than marked differences appear between the subset of monocytes in terms of phenotype and functionality. In *in vivo* studies performed with deuterium labelling, show that during steady state but also during endotoxemia, monocytogenesis proceeds from the onset of classical monocytes, which subsequently become intermediate and finally non-classical. The evidence that circulating monocytes change their phenotype from one subset to another followed by an increasing of the degree of CD16 expression, support this hypothesis. The dynamic changes of monocyte subsets also occur during pathologies such as major systemic inflammation[79].

2.2.3 Monocyte development

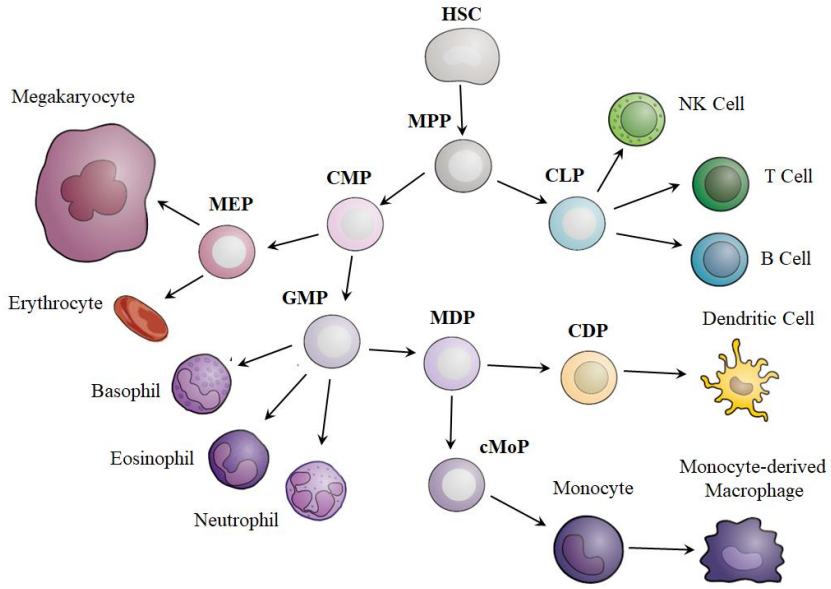

Figure 4 **Hematopoietic development in the bone marrow**
Representation of the tree-like hierarchy model of hematopoietic cell development in the bone marrow.
CDP: Common Dendritic cells Precursors; **CLP**: Common Lymphocyte Precursors; **cMoP**: common Monocyte Precursors; **CMP**: Common Myeloid Precursors; **GMP**: Granulocyte Macrophage Precursors; **HSC**: Hematopoietic Stem Cells; **MDP**: Monocyte-Macrophage/Dendritic cell Precursors; **MEP**: Megakaryocyte/Erythrocyte Precursors; **MPP**: Multipotent Precursors;

Monocytes originate in the bone marrow (**Figure 4**) from hematopoietic stem cells (HSC) which in turn generate a heterogeneous population of multipotent progenitors (MPP) that differentiate into two separate precursors: common lymphoid progenitors (CLP) or common myeloid progenitors (CMP). While the former originates lymphoid cells such as B, T, and natural killer cells, the latter gives rise to megakaryocyte and erythrocyte progenitors (MEP) or granulocyte and macrophage progenitors (GMP). Basophils, neutrophils and eosinophils originate directly from GMP as does the monocyte-macrophage/dendritic cells progenitors (MDP). At this point, two distinct lineages are distinguished: dendritic cells differentiate from the common dendritic cell precursors (CDP) while the common monocyte progenitors (cMoP) give rise to monocytes[80]. The differentiation of monocytes from cMoP involves an intermediate stage of pre-monocytes characterized by a high expression of CXCR4. These cells differentiate in 24h to monocytes poor in CXCR4 but rich in CCR2[81]. It has been observed that in CCR2-deficient mice, monocytes remain trapped in the bone marrow with a consequent reduction in the number of circulating monocytes[82]. Consequently, it is likely that CCR2 and its ligands CCL2 and CCL7, rather than CXCR4 regulate the exit of monocytes from the bone marrow into the blood flow.

Although the generation of monocytes is considerable in the bone marrow, a small amount of MDP and cMoP was also observed in the spleen[83]. In fact, the spleen represents a small reservoir of

monocytes and, in particular, during the inflammatory state, there is an increase in emergency extramedullary monopoiesis mediated by IL-1β[84]. Thus, splenic monocytes are then mobilized and recruited towards the injured tissue as observed in atherosclerosis[85].

Under homeostatic conditions, classical monocytes remain in the circulation for about a day before they migrate to the tissues to differentiate into local tissue-resident macrophages. Monocyte-derived macrophages show significant differences compared to their circulating precursors, indeed, they adapt to the local environment and acquire functions similar to those of the macrophages they are replacing[86]. On the other hand, monocytes may also migrate towards tissue and retain their characteristics and identity thus constituting a local reservoir of monocytes[87]. An alternative pathway is the transition of classical monocytes to the non-classical subset through intermediate monocytes, which remain in the circulation for about 4 days[79]. Non-classical monocytes show a longer life span of about 2 days in mice and up to 7 days in humans. This increased life span ensures a constant number of non-classical monocytes even during pathological conditions and especially following inflammatory stimuli that promote the differentiation of classical monocyte to macrophage thus blocking the transition to non-classical ones. The number of non-classical monocytes is therefore deeply affected by the physiological state of the organism in fact even exercise and age can influence the balance of monocyte subsets[79].

2.2.4 Monocyte in atherosclerosis

Monocytes have been observed to play a key role in atherosclerosis both during the process of initiation and formation of atherosclerotic plaque, which is accelerated by different risk factors, but also during the acute inflammatory phase leading to destabilization and plaque rupture. In addition, monocytes are also involved during healing by promoting the accumulation of myofibroblasts, angiogenesis process and myocardial healing and remodeling[88] (**Figure 5**).

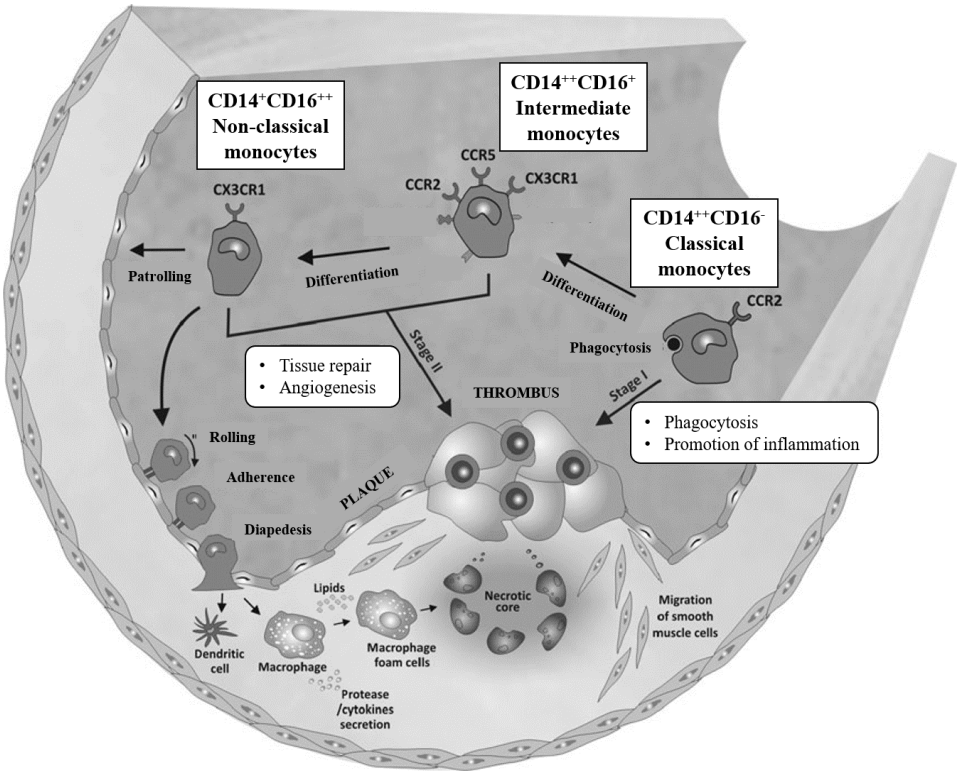

Figure 5 **Role of monocytes in atherosclerosis**
The key roles of the three monocyte subsets in atherosclerosis are depicted. At first (stage I), classical monocytes promote inflammation and phagocyte necrotic debris. During stage II, non-classical and intermediate monocytes attenuate inflammation and promote healing, angiogenesis, tissue repair and remodelling.

2.2.4.1 Monocyte recruitment and transmigration

A key factor in the pathogenesis of atherosclerotic disease is the recruitment of circulating monocytes to the vascular endothelium. This process consists of three fundamental steps: the adherence of monocytes, their rolling along the vascular wall and finally the transmigration into the subendothelial space. The capture and rolling of monocytes are mediated by the interaction between the CCL5 and CXCL1 chemokines present on the endothelial surface and the corresponding monocyte receptors[89]. Several adhesion molecules are also involved in the process and these belong to four families: selectins, immunoglobulins, integrins and mucin-like glycoproteins. The family of selectins, transmembrane monomeric glycoproteins, comprises several classes, each characterized

by a different site of expression. L-selectin, is expressed by monocytes and most types of leukocyte, interacts with the ligands expressed by the endothelium and allows a transient adhesion; E-selectin or CD62E is expressed on activated endothelial cells and binds the sialylated oligosaccharides groups present on protein surface of leukocytes; P-selectin or CD62P, can be expressed by both endothelial cells and platelets. P-selectin, under physiological conditions, is located in intracellular granules, while during inflammation, the release of chemical mediators stimulates its translocation on the cell surface making it available for interaction with leukocyte ligands[90]. This last selectin appears to be the most responsible for monocyte rolling in atherosclerosis. Immunoglobulins such as VCAM-1 and ICAM-1 are present on the endothelial surface and represent the ligands for the integrins expressed by leukocytes[91]. Integrins, integral membrane glycoproteins, are heterodimers formed by α and β subunits: monocytes express integrin-β1 that recognize VCAM-1, and integrin-β2 that bind ICAM-1. The α4β1 integrin known as very late antigen-4 (VLA-4) also plays an important role in the adhesion of monocytes to the endothelial surface; it binds to some isoforms of fibronectin and to VCAM-1[90-92]. The macrophages present in the atherosclerotic lesion are involved in the migration of monocytes; in fact, they produce cytokines such as TNF-α and IL-1 β that induce the expression of ligands for integrins, especially VCAM-1 and ICAM-1. In response to lipid oxidation, macrophages also produce chemokines such as MCP-1, abundantly expressed in atheromasic lesions and involved in the amplification of the recruitment process of monocytes[93]. Another factor that can increase the migration of monocytes is represented by oxLDL. These lipoproteins can stimulate the expression of adhesion molecule on endothelial cells and induce the synthesis of chemotactic or growth factors. OxLDL can also act directly on monocytes or through the promotion of the formation of platelet-monocyte aggregates thus promoting the adhesion of monocytes to the endothelium[94]. Platelets are also considered mediators of monocyte recruitment in atherosclerosis. Through the formation of platelet-monocyte aggregates, an inflammatory reaction is triggered that promotes the release of chemokines CCL2 and CCL5, and cytokine IL-1β, inducing monocyte activation. In addition, the release from platelet α-granules of CXCL4, CCL5, and other chemokines involves endothelial activation thus promoting the adhesion of monocytes[95]. After diapedesis, monocytes are temporarily retained in the subendothelial space and then the cells are able to cross the basal membrane. CD44 and integrins-β1 are the mediators involved in the monocytes delay in the extracellular matrix[96] but CCL5 (also known as RANTES), CXCL1 and IL-8 are also implicated in the process[93]. Finally, monocyte transendothelial transmigration is regulated by adhesion molecules present on endothelial cell surface or in endothelial cells junctions including platelet-endothelial cell adhesion molecule or CD31 (PECAM-1) a member of the immunoglobulin superfamily[97].

2.2.4.2 Monocyte differentiation into macrophages

Macrophage accumulation in atherosclerotic plaque occurs both as a result of the differentiation of monocytes recalled from the blood circulation, and of the activation or proliferation, even if in a modest extent, of local macrophages that are immobilized at the site of inflammation[98]. Similar to monocytes, macrophages represent a heterogeneous population that reflects the complexity and diversity of the microenvironment to which monocytes are exposed[99]. The exposition to different cytokines and growth factors during the process of monocyte differentiation induces a polarization towards different macrophage phenotypes with extremely different and even opposing properties. Among several cytokines and growth factors, M-CSF and GM-CSF play a fundamental role in the differentiation process[100]. M-CSF, in the bloodstream, favours the survival of circulating monocytes and induces their differentiation into macrophages by modulating the levels of CD14 and CD68[101, 102]. In *In vitro* model, the differentiation of monocytes in the presence of M-CSF, gives rise to macrophages with anti-inflammatory properties (M2 macrophages) characterized by a marked phagocytic activity and able to produce high amounts of IL-10[99]. On the contrary, macrophages obtained in the presence of GM-CSF display pro-inflammatory characteristics (M1 macrophages) and produce high levels of TNF-α, IL-12, IL-1, IL-6, IL-8 and IL-23 after activation with LPS[103]. These cytokines can exacerbate the endothelial dysfunction and promote oxidative stress[104]. M2 phenotype, characterized by the presence of the scavenger receptors (SR-A) and CD36, and the mannose receptor, display an atheroprotective role as they secrete TGF-β and anti-inflammatory cytokines such as IL-10, and reduce the recruitment of pro-inflammatory cells[105]. While M1 macrophages sustain the expansion of the necrotic core and plaque rupture[106]. Thus, based on their anti-inflammatory characteristics, M2 macrophages appear to mainly derive from the differentiation of non-classical monocytes while extravasated classical monocytes start a differentiation process, which involves the upregulation of markers characteristics of M1 macrophages. In human atherosclerotic plaques, phenotypes M1 and M2 are simultaneously present throughout the evolution of plaque, as evidenced by a recent study conducted in plaques at different lesional stages[107]. Specifically, a preponderance of M2 macrophages has been described at the level of the vascular adventitious layer. On the contrary, M1 macrophages appear to be mainly distributed at the plaque rupture site while in the fibrous cap there is no significant difference in the prevalence of the two subgroups[107].

2.2.4.3 Monocytes subsets and cardiovascular outcomes

An increasing number of evidences highlights an association between the development of atherosclerosis and $CD16^+$ monocytes (both intermediate and non-classical)[108-115]. $CD16^+$ monocytes are correlated with traditional cardiovascular risk factors such as Body Mass Index (BMI), diabetes, obesity and insulin resistance[111-113], but also with high serum levels of TNF-α[114]. A significant relationship is demonstrated between increased levels of $CD16^+$ monocytes and thickening of the intima or the occurrence of vulnerable atherosclerotic plaque in patients with both SA and UA[111, 112, 115]. Further studies are carried out with specific reference to the two distinct subsets intermediate and non-classical monocytes. The number of non-classical monocytes are positively correlated with high levels of total plasma Cho, LDL and TG while a negative correlation is observed with HDL levels[108, 109]. Moreover, Rogacev et al investigated the heterogeneity of monocytes more thoroughly through the HOM SWEET HOMe study (Heterogeneity of Monocytes in Subjects Who Undergo Elective Coronary Angiography-The Homburg Evaluation). The results show an association between cardiovascular events and a high count of total monocytes, classical and intermediate monocytes, but not with non-classical monocytes[116]. Moreover, an association between low levels of HDL and intermediate monocytes count is reported, pointing out that a high count of this subset may represent an independent determinant of cardiovascular events[110]. More specifically, there is a strong association between the monocyte count and ACS, due to the fact that the evolution from stable CAD to ACS is partly linked to the upsurge of the inflammatory state linked to the monocyte activity. A rise in monocyte count following AMI, which is maintained for 7 months, is observed. Following AMI, monocytes invade the infarct area promoting healing and remodelling of myocardial tissue[117]. Interestingly, classic monocytes reach their highest levels 3 days after the onset of AMI while $CD16^+$ monocytes increase at day 5[118]. A similar study conducted in STEMI patients, shows an association between levels of classical monocytes and a larger extent of transmural infarction with a larger infarct size while a high count of non-classical monocytes is found in patients with increased tissue recovery. Therefore, these results confirm the role of classical monocytes in amplifying the inflammatory response and of non-classical monocytes in the healing process[119]. Moreover, at the level of the infarct area, within the first 5 days after AMI, the classical monocytes are predominant and are placed in the infarct border zone. However, during the following days, $CD16^+$ monocytes invade the infarct core zone[120]. Intermediate monocytes are also linked to myocardial infarction: their count rises after 3 days from the event (in both STEMI and NSTEMI patients) and then returns to values comparable to stable patients in 30 days[121].

2.3 Lipids

Lipids play a central role in CVD since atherosclerotic plaque formation is initiated as lipid particles accumulate and become trapped in vessel walls. The interplay between lipids and immune cells is believed to be a driving force in the chronic inflammation of the arterial wall during atherosclerosis. Therefore, the study of the lipid composition of immune cells, such as monocyte, could evidence a possible association between lipid species and cardiovascular events.

2.3.1 Lipid classification, nomenclature and structures

Lipids have always been recognized as a group of hydrophobic molecules and therefore highly soluble in organic solvents[122]. However, this definition is not exhaustive because complex lipids such as glycosphingolipids (GSL), precursors of lipid biosynthesis or their degradation products, are also soluble in water[123]. An alternative was proposed by Christie who defined lipids as ' FA, their derivatives and substances biosynthetically or functionally related'[124]. The Lipid Library[125] and Cyberlipids[126] divide lipids into "simple" and "complex", the former include molecules that after hydrolysis generate two distinct products (e.g. acylglycerols → fatty acids + glycerol) while complex lipids lead to the production of three or more distinct entities (glycerophospholipids → fatty acids + glycerol + head group). Currently, the Lipid Metabolites and Pathways Strategy (LIPID MAPS) consortium, a multi-institutional group created in 2003, has defined a classification of lipids based on their structural and biosynthetic characteristics. Therefore, lipids are defined as hydrophobic or amphiphilic molecules that are formed, at least in part, by condensation of ketoacyl or isoprene groups[127, 128]. Based on this assumption, lipids are classified into 8 groups: FA, glycerolipids (GL), glycerophospholipids (GP), sphingolipids (SP), saccharolipids, polyketides (resulting from condensation of ketoacyl subunits), sterol lipids and prenol lipids[127, 128].

The nomenclature of lipids includes systematic names and common names. Systematic names have been assigned following the guidelines formulated by the International Union of Pure and Applied Chemists and the International Union of Biochemistry and Molecular Biology (IUPAC-IUBMB) Commission on Biochemical Nomenclature in 1975[129]. Common names, on the other hand, are abbreviations that allow to easily identify acyl/alkyl chains in GL, SP and GP. By this way, lipids are represented by the marks that identify the lipid class (e.g. TG for triglycerides) or the lipid head group (e.g. PC for phosphocholines) followed by the side-chains indicated in brackets. Side-chains are represented by the number of carbons that make up the chain and the number of chain unsaturation (e.g. TG (16:0/18:1/16:0)). If the composition of the side-chains is not known, abbreviations such as TG (52:1) are used where the numbers in brackets refer to the total number of carbons and the total number of double bonds of the all side-chains[127, 128].

2.3.1.1 Fatty acids

FA are fundamental molecules as they represent the basic structure for the construction of complex lipids. FA are chains that are built up by successive repetitions of a methylene group that impart the characteristic hydrophobicity and contained a terminal carboxylic acid[127, 128]. Hydrocarbon chains diversify in terms of length, structure (linear or branched) and degree of unsaturation (presence of double bonds). According to these characteristics, FA can be further divided into short-chain FA (less than 6 carbons), medium-chain FA (from 6 to 12 carbons) and long-chain FA (more than 12 carbons). Moreover, FA can be saturated (no double bonds) or the degree of unsaturation can vary from 1 double bond (monounsaturated FA or MUFA) to two or more (polyunsaturated FA or PUFA). These double bonds may differ in the position along the chain and in orientation (*cis* or *trans*). The number, position and orientation of the double bonds are fundamental characteristics of FA in that they alter the arrangement in the lipid membrane thus modifying its biophysical characteristics such as curvature, fluidity and structure[130]. FA biosynthesis takes place in the cytoplasm and is catalysed by the multienzyme complex fatty acid synthase. The first reaction consists in the formation of malonyl-CoA from acetyl-CoA and CO_2. Then a cyclic repetition of reactions occurs that lead to the elongation of the FA chain through the repetitive addition of two carbon atoms donated by malonyl-CoA. After the addition of each 2-carbons-unit, double bond reduction reactions occur for the formation of saturated FA. The final product is palmitic acid, a saturated FA constituted by 16 carbon atoms (16:0). However, longer FA chains can be obtained through elongation reactions catalysed by elongases; alternatively, FA with a higher unsaturation degree can be obtained through the activity of desaturases enzymes. Elongation and desaturation pathways occur mainly in the liver[130].

2.3.1.2 Glycerolipids and glycerophospholipids

GL and GP share the presence of a molecule of glycerol in their structure. GL include acylglycerols mono-, di-, tri- fatty acid esters of glycerol: monoglycerides or monoacylglycerols (MG or MAG), diglycerides or diacylglycerols (DG or DAG) and triglycerides or triacylglycerols (TG or TAG) (**Figure 6**). FA linked at the *sn*-1 and *sn*-3 carbons of glycerol are usually saturated while the fatty acid esterified at the *sn*-2 carbon is more flexible and usually unsaturated. TG synthesis occurs in adipose tissue from dihydroxyacetone phosphate (DHAP), produced during glycolysis. The enzyme glycerol-3-phosphate dehydrogenase reduces DHAP to glycerol 3-phosphate with subsequent direct esterification of FA to carbon 1 and 2 and while carbon 3 esterification occurs after dephosphorylation[130].

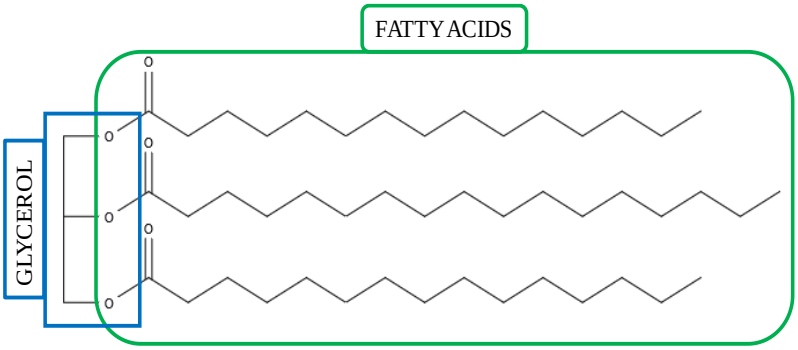

Figure 6 **Triacylglycerol structure**
General structure of a saturated triacylglycerol. Triacylglycerol is an ester derived from glycerol (blue) linked to three fatty acids (green).

GP or more simply PL are characterized by the presence of a phosphate group esterified to a hydroxyl group (*sn*-3 position) of the glycerol backbone. Typically, the remaining two hydroxyl groups of glycerol exhibit acylated long-chain FA, however, alkyl-linked and alkenyl-linked (plasmalogen) GP may also be found. Thus, PL with a saturated 1-O-alkyl ether group are called plasmanyl-PL ("O"-prefix for the nomenclature) while the presence of a monounsaturated 1-O-alkenyl ether groups appoints the denomination plasmenyl-PL ("P"-prefix for the nomenclature). Moreover, lysophospholipids (LPL) are PL whose FA chain has been removed from either the *sn*-1 or *sn-2* position. PL can be divided into additional categories based on the nature of the polar head group linked to phosphate. The common head groups are choline, ethanolamine, serine, glycerol and inositol; thus, the following classes of PL are categorized: phosphatidylcholine (PC), phosphatidylethanolamine (PE), phosphatidylserine (PS), phosphatidylglycerol (PG) and phosphatidylinositol (PI) respectively (**Figure 7**). The simplest PL is phosphatidic acid (PA). Further diversity of these molecular species is due to the different combination of the FA composition at the *sn*-1 and *sn*-2 position[127, 128]. PC are the most abundant PL in cell membrane (40-50% of total PL) followed by PE which are enriched in mitochondrial inner membranes (40% of total PL). The Kennedy pathway is the main mechanism of *de novo* biosynthesis of PC and PE, the most abundant PL. The first reaction occurs in the cytosol and involves the phosphorylation of choline (or ethanolamine) by kinase forming phosphocholine (or phosphoethanolamine). In the rate-limiting step, starting from cytidine triphosphate (CTP), the formation of the intermediate CDP-choline (or CDP-ethanolamine) occurs with pyrophosphate release. The final reaction occurs in Golgi or in the endoplasmic reticulum and leads to the formation of PC (or PE) using DAG as lipid anchor and release cytidine monophosphate[131]. The FA configuration characterizing the newly synthetized PC and PE can experience further variation by acyl-remodelling reactions in the Lands pathway[132].

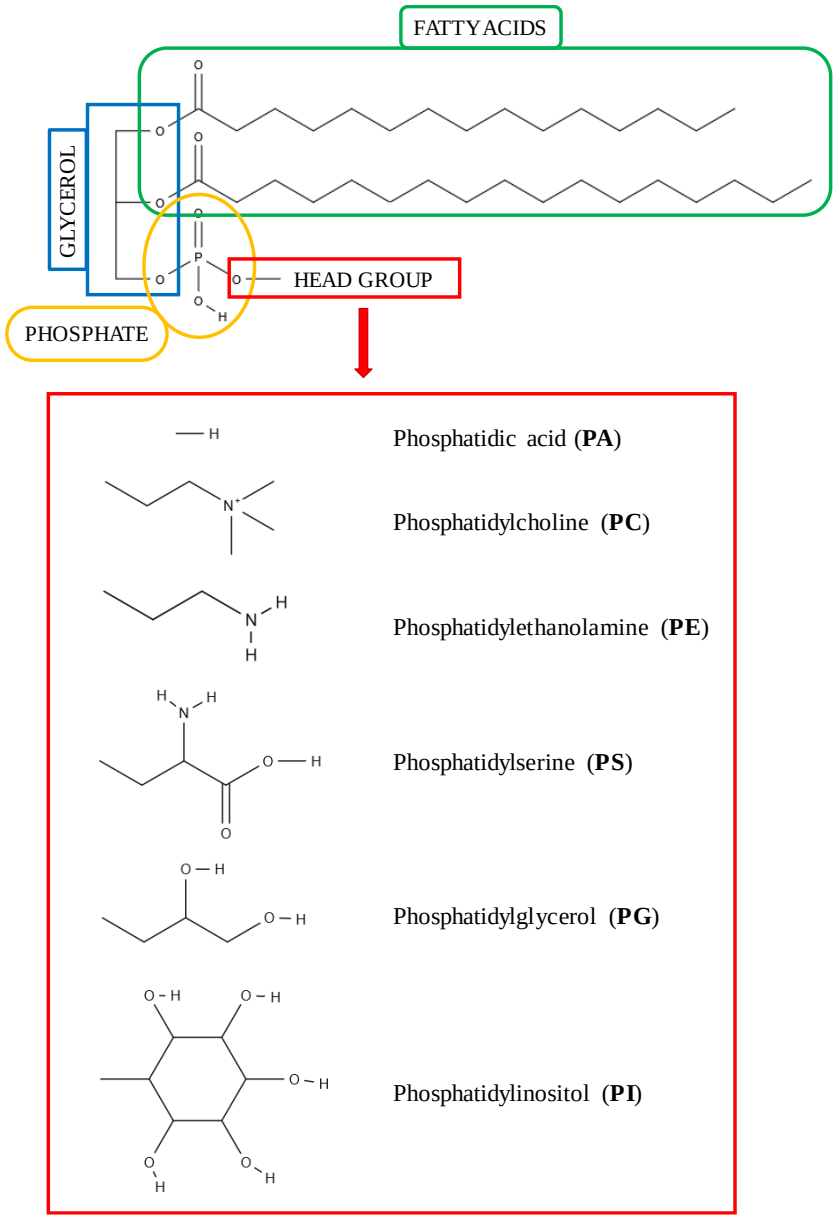

Figure 7 **Phospholipid structures**
The structure of phospholipids consist of a glycerol backbone (blue) with two fatty acid tails (green) and a polar head group (red) linked to phosphate (yellow). According to the nature of the head group, the following classes of phospholipids are categorized: phosphatidic acid, phosphatidylcholine, phosphatidylethanolamine, phosphatidylglycerol, phosphatidylserine and phosphatidylinositol.

2.3.1.3 Sphingolipids

SP are a complex family of molecules that share a common structure, a long-chain nitrogenous base, sphingosine (Sph), a sphingoid base that display amphiphilic properties due to the presence of two hydroxyl groups and an amino group in its polar portion.

SPH is synthesized *de novo* from serine and a long-chain fatty acyl-CoA, palmitoyl-CoA by serine palmitoyl-transferase. SP can be divided into different classes: sphingosine derivatives such as sphingosine-1-phosphate (S1P), ceramides (CER), phosphosphingolipids and GSL (**Figure 8**).

CER derived from Sph to which a FA is bound with amide bond. These FA are usually saturated or monounsaturated and have a chain length from 14 to 26 carbon atoms. Depending on the FA chain length, CER can be classified as medium chain (12-14 carbons), long chain (16-18 carbons), very-long chain (20-24 carbons) and ultra-long chain (>26 carbons)[133]. Carbon 2 can be characterized by the presence of a hydroxyl group; in this case, the designation "t" is assigned to identify these ceramides while in the absence of the hydroxyl group, "d" is assigned. CER can be generated by *de novo* synthesis, by ceramide synthase enzymes that produce dihydroceramide from dihydrosphingosine and FA, or they can be derived from the salvage pathway that produces CER from SPH and FA[133]. CER are precursors of more complex SP.

Phosphosphingolipids present a polar head and a phosphate group linked to the free hydroxyl group of CER. Among the phosphosphingolipids, the most abundant are the SM, which are characterized by the presence of phosphocholines.

GSL are divided on the basis of the carbohydrate linked: neutral GSL contain one or more uncharged sugars such as glucose (glucosylceramide (GlcCer)) or galactose (galactosylceramide (GalCer)) and lactose (lactosylceramide (LacCer)) Acid GSL contain ionized functional groups (phosphate or sulphate) bound to sugar such as sialic acid (gangliosides), and finally there are basic and amphoteric GSL[127, 128].

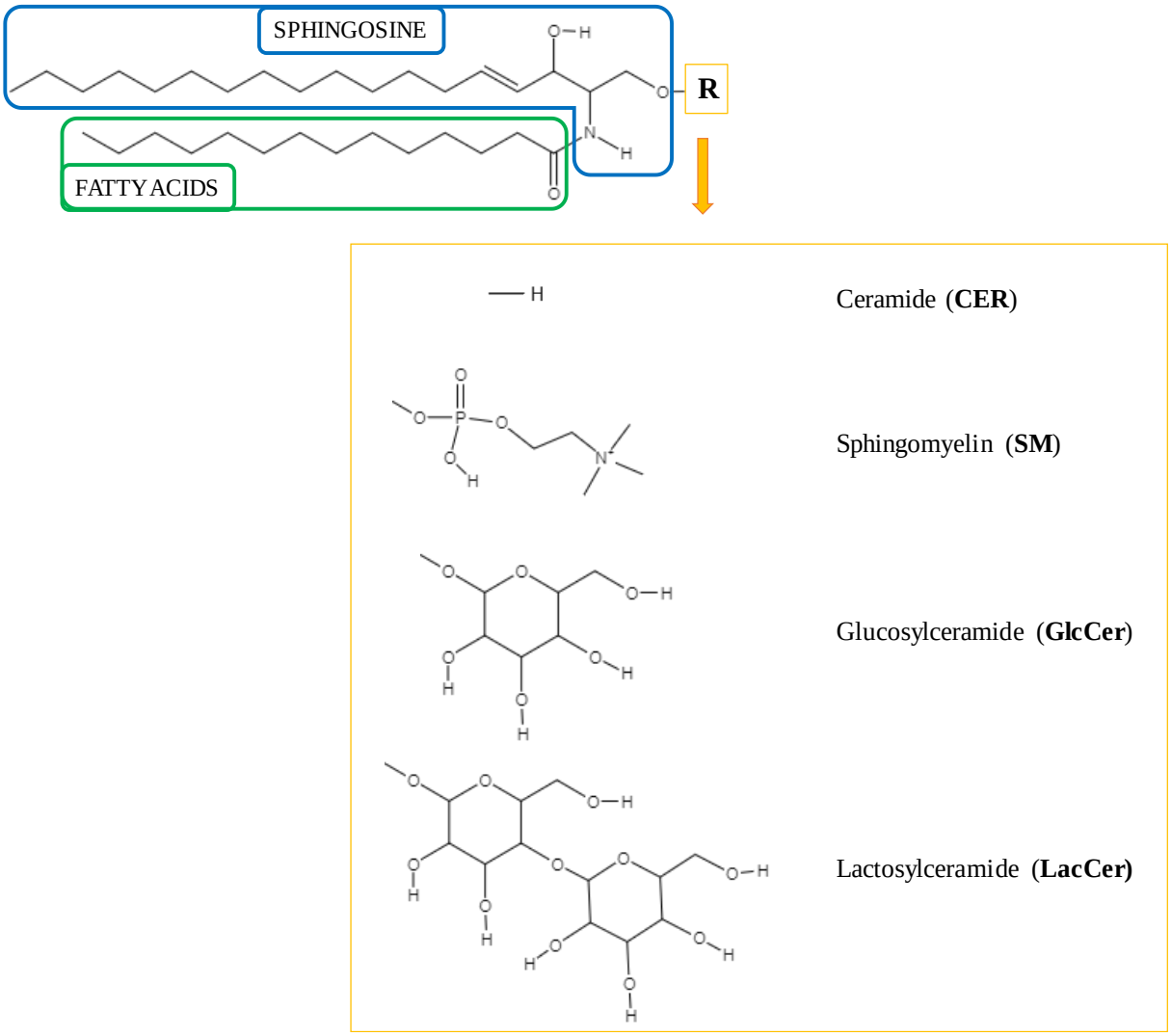

Figure 8 **Sphingolipid structures**
Sphingolipids share sphingosine (blue) as common backbone structure to which a fatty acid (green) is bound with amide bond. Sphingolipid with a hydrogen atom as R group is a ceramide. Other common R groups include phosphocholine (yielding a sphingomyelin), glucose (glucosylceramide) or lactose (lactosylceramide).

2.3.1.4 Sterol lipids and prenol lipids

Sterol and prenol lipids share a common biosynthetic pathway as they result from condensation of isoprene subunits, however display differences in the structure and functions. Among sterols, Cho and its derivatives constitute an important component of membrane lipids. Cho is characterized by a planar structure constituted by four fused rings and a hydrocarbon side chain[130]. The first reaction in Cho biosynthesis is the acetoacetyl-CoA formation, which is transformed to hydroxymethylglutaryl-CoA (HMG-CoA) by HMG-CoA reductase. HMG-CoA is finally converted to Cho through several condensation and isomerisation reactions[134]. Cholesteryl esters (CE) are Cho derivate in which a FA is esterified with the hydroxyl group present on Cho carbon C3. This reaction is catalysed by lecithin: cholesterol acyl transferase[130].

2.3.1.5 Saccharolipids and polyketides

Saccharolipids (SL) are molecules in which fatty acyl groups are directly linked to a sugar backbone. These differ from glycolipids in which the fatty acyl portion of the molecule is linked to a glycerol backbone. SL include glycans and phosphorylated derivatives. The most common SL are the acylated glucosamine precursors of the lipid A component of the lipopolysaccharides in Gram-negative bacteria[127, 128].

Polyketides (PK) include several characteristic molecules of animals, plants and microbes[127, 128].

2.3.2 Lipid biological functions

Lipids are a heterogeneous group of molecules abundant in the diet, and present in blood, tissues and cells in which these molecules are not casually dispersed but extremely ordered according to their function[135]. Both free FA and the FA components of complex lipids show different biological functions influenced by their structural characteristics. Complex lipids show a role in lipid transport, cell membrane structure and cell signalling.

2.3.2.1 Membrane components

The fundamental role that lipids play at the level of biological membranes consists in modulating the physical assets of the membrane and consequently lipid dynamics, hydrophobic thickness, intrinsic contraction tendency, and electrostatic surface[136]. Plasma membrane is asymmetric: the inner leaflet is typically composed of charged PS, large amounts of PE and a smaller content of PC. On the contrary, the outer surface is mostly composed of SP, GL and a larger number of PC. This configuration is fundamental, and its alteration leads to cell death.

Specifically, PE and PS play a key role in membrane architecture. PE are characterised by a conical structure with a small polar head group that allows the formation of reversible non-lamellar structures required, for example, for the formation of intermediate assemblies during membrane fusion processes. Furthermore, PE generate pressure stress involved in the membrane curvature, modulating the structure, folding and activity of the membrane proteins[137].

Moreover, PS, maintain membrane asymmetry and curvature. PS modulate the assembly and activation of different enzyme complexes present on the cell surface. These lipids are also essential for the recognition by phagocytes of apoptotic or senescent cells[138].

The inner surface of the plasma membrane is also rich in plasmalogens. Due to their vinyl ether bond, these lipids play an important role as endogenous antioxidants and regulate the fluidity, fusion tendency and thickness of the membrane[139]. The increase membrane rigidity due to an increased plasmalogens concentration, leads to an improved interaction of receptors with signalling proteins involved in the phagocytosis process[140].

Overall, the plasma membrane is formed by a mixture of Cho and saturated (mainly SP) and unsaturated lipids mostly represented by PC. Specifically, it is composed of saturated and unsaturated FA in an approximate 1:1 ratio. Under homeostatic conditions, , the membrane bilayer is fluid allowing lipids of the membrane to migrate within it[130]. Consequently, alterations of this proportion can induce changes in the fluidity of the membrane and thus in its functions. The saturated FA that predominantly composed plasma membrane are palmitic acid and stearic acid, while the unsaturated FA present in greater quantities are oleic acid and palmitoleic acid[141]. Both

the FA composition of the lipid bilayer and the FA structure (number, position and orientation of the double bonds) influence the membrane fluidity, which in turn modulates the activity and functions of the integral membrane proteins.

2.3.2.2 Energy source, cell signaling and gene expression

FA modulate different cellular functions, as they are not only structural constituents of membrane but also energy sources. In fact, FA released following TG hydrolysis are used as fuels through β-oxidation in mitochondria and peroxisomes. The *β*-oxidation rate is controlled by the concentration of intracellular free FA in turn influenced by the plasmatic concentration of free FA[130].

Moreover, membrane lipids and PL are substrates for the formation of second lipid messengers involved in signal transduction. Eicosanoids for example are signalling molecules made by the enzymatic or non-enzymatic oxidation of arachidonic acid or other 20-carbon PUFA. These PUFA are released from membrane PC by the phospholipase A_2 (PLA_2) enzyme. Alternatively, the release from phosphatidylinositol-4,5-biphosphate is catalysed by phospholipase C or a DAG lipase. Furthermore, the hydrolysis of PL by phospholipase C and D leads to the production of second messengers such as DAG and PA that activate enzymes such as protein kinase C (PKC). PA are also regulators of membrane trafficking as well as key step in PL biosynthesis[142].

In addition to their effect on the cellular signalling process, FA can influence gene expression by acting on PPARs transcriptional factors. FA in fact bind directly to PPAR which in turn interacts with PPAR response elements in gene promoters specifically those of enzymes involved in the FA β-oxidation[143].

Moreover, lipids regulate protein anchor to membrane by protein-lipid interactions. Specifically, membrane proteins are linked to glycosyl phosphatidylinositol or sterol, palmitoyl, prenyl moieties modulating protein bound to membranes[144].

2.3.3 Lipids and atherosclerosis

Lipids are implicated in the pathogenesis of several diseases and alterations of lipid metabolism play a key role in various pathologies related to atherosclerosis. For example, a correlation between obesity and SM, PC, PE, CE, PI and TAG levels detected in obese patients has been observed[145]. Moreover, patients with familiar hypercholesterolemia are characterized by different ratios of SM/PC and PC/LPC compared to normolipidemic subjects as well as by a positive correlation between SM and LPC versus LDL and VLDL respectively[146]. Recent advances in the field of lipidomics have made possible to determine the lipidome of atherosclerotic plaques by highlighting the presence of CE, SM, PC and LPC[128, 147]. In particular, unstable plaques are characterized by a high lipid content, especially free Cho and CE[148], while PL and TAG are present in greater quantities in stable plaques. Considering the plasma lipid profile of SA and UA patients, a positive association between SA and CER, PI or PE and a negative correlation with LPC and plasmalogens have been observed[149]. Lipids have a specific role in plasmatic lipoprotein structure and a specific lipid composition has been observed for each class of plasmatic lipoproteins: LDL are rich in CE and SM while HDL have a high content of PC, PE and plasmalogen[150]. PL are necessary for the formation and stability of lipoproteins, which therefore consist of a monolayer of Cho and PL (especially PC) surrounding a neutral lipid core composed of TAG and CE. DAG and SP with lower concentration are also present in lipoproteins[151]. In addition, the role of PC biosynthesis in the secretion of VLDL[152] has been demonstrated since low levels of PC in the endoplasmic reticulum lead to an impairment of VLDL formation[153].

As circulating cells, monocytes in blood are exposed to lipoproteins before their migration to the injured endothelium. It has been observed that dyslipidaemia can influence the recall of monocytes, migration and their phenotype[154]. In hypertriglyceridemic conditions, the accumulation of non-classical monocytes and the CCL4-mediated extravasion are increased[155].

TAG are present in plasma often associated with proteins forming triglyceride-rich lipoproteins (i.e. VLDL). Recent research shows that VLDL deposit at the level of the endothelium damaging it and promoting the recruitment and adhesion of circulating monocytes through the upregulation of ICAM-1 and VCAM-1. In addition, VLDL participate in the development of atherosclerotic plaque by stimulating the inflammatory process and the production of cytokines[156]. Hypercholesterolemia also stimulates the production of classical monocytes as well as their CCR5-mediated recruitment. In patients with familiar hypercholesterolemia, increased levels of CCR2 are observed on circulating monocytes that positively correlate with LDL levels and with the accumulation of lipids in monocytes[157]. This shift in the phenotype of monocytes is associated with an increase in the number of monocytes and their migratory capacity due to the increased expression of adhesion

molecules, chemokine receptors and CD11b, CD11c and CD18 integrins[158]. Thus, monocytes in the extravascular tissue compartment can incorporate circulating lipids transforming into 'foamy monocytes', which transport lipids from the blood to peripheral tissues contributing to the formation of foam cells. Lipid uptake occurs via LDLR or the scavenger receptors CD36 and SRA1. A high lipid loading in monocytes affects the cytoskeleton by blocking the signalling of RhoA family molecules leading to an impairment of monocyte migration[159].

2.3.3.1 Role of sphingolipids and lactosylceramide on cellular functions

SP and their derivatives such as SM, CER, SPH and S1P and GSL are important mediators of cell proliferation, differentiation and apoptosis[160]. SM are related to atherosclerosis due to the observation that high levels of these lipids have been observed in atherosclerotic lesions compared to normal artery tissues[161]. In addition, in human carotid plaques, increased levels of SP associated with symptoms and production of inflammatory cytokines and histological markers of plaque instability, are observed[160]. Plasma levels of SM and CER are also increased in CAD patients (both SA and AMI) compared to healthy subjects[162]. Moreover, the atherogenic lipoproteins VLDL and LDL are rich in SM[163]. High levels of platelet SM and TAG are observed in STEMI patients compared to control subjects[164]. In addition, plasma concentrations of SM are independent risk factors for coronary heart disease and these levels are prognostic in ACS patients[165].

Regarding to S1P, it shows a positive correlation with HDL, its major plasma carrier, and S1P-HDL reduce atherosclerosis through inhibition of adhesion molecule expression in endothelial cells and production of MCP-1 in SMCs[166]. However free-S1P shows an opposite effect as it is an extracellular ligand for its G protein-coupled receptor and can contribute to inflammatory reactions and several cellular responses such as differentiation, survival, apoptosis, proliferation and angiogenesis[167] through the activation of downstream effectors like adenylate cyclase, phospholipase C, phosphatidylinositol-3 kinase, Ras and RhoA[168].

CER mediate several cellular processes such as apoptosis, autophagy, inflammation, FA β-oxidation and endoplasmic reticulum stress[169]. Their activity is due to the effect exerted on the membranes and by the direct interaction with target proteins. It has been observed that CER form large ceramide-rich platforms (CRPs) that play a role in different cellular processes such as cell death and immune response through membrane protein recruitment and the formation of receptor clustering[170]. The characteristics of FA that constituted CER, length and saturation of the acyl chain specifically, but also the proportion of long-chain and very long-chain species, influence membrane fluidity and consequently cell migration[171, 172]. In addition, CER regulate membrane permeability through the formation of channels on lysosomal and mitochondrial membranes[173]. It has been observed that high levels of 16-carbons CER, through the modulation of membrane fluidity, inhibit

FA β-oxidation and destroy receptors for insulin signalling[174, 175]. Indeed, CER appear to be strongly related to obesity and insulin resistance[176]. A role of CER in the formation of atherosclerotic plaque has also been highlighted. Specifically, the reduction of plasma levels of very-long chain CER correlates with a reduced infiltration of monocytes/macrophages and prevents the formation of plaques in atherosclerosis-prone mice[177]. These results are in agreement with a recent clinical study that indicates a high very long chain/long chain CER ratio in plasma as a possible biomarker for several heart diseases[178].

GSL play an important role in several cellular functions such as cell-cell recognition, cell adhesion, protein trafficking, and signal transducuction[179-182]. Typically, they are present at low concentrations on the outer membrane, however high levels can be observed on the surface of specialized cells such as neurons and endothelial cells[183]. GSL are synthesized by glucose transfer from the nucleotide-sugar UDP-glucose, to CER to form GlcCer. Similarly, the addition of galactose from UDP-galactose to GlcCer by galactosyltransferase leads to the production of lactosylceramide (LacCer)[184] (**Figure 9**).

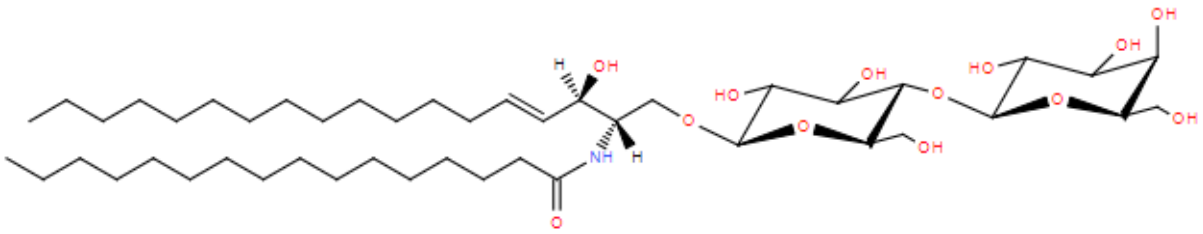

Figure 9 **Lactosylceramide**
The structure of lactosylceramide d34:1 (d18:1/16:0) is represented. It is composed by two sugar molecule (glucose and galactose), sphingoid base (d18:1) and a 16 carbon chain fatty acid.

Galactosyltransferase, also called lactosylceramide synthase, belongs to the family of β-1,4GalT-transferases and mainly localized in the Golgi apparatus. To date two isoforms, with 68% homology[185], are known to be present in mammalian tissues: β-1,4GalT-V constitutively expressed in most adult tissues and β-1,4GalT-VI whose expression is tissue-specific, and it is predominant in adult brain cells and present at low levels in other adult tissues[186]. The gene encoding for the isoform V is for example highly expressed in human endothelial cells[185] and is activated by inflammatory cytokines such as TNF-α[187, 188]. In addition, growth factors such as platelet-derived growth factor and epidermal growth factor or oxLDL increase enzyme activity in cultured human kidney cells, SMCs and human aortic endothelial cells[189]. The increase in enzyme activity leads to a consequent increased production of LacCer. Furthermore, the enzyme activity is inhibited dose-dependently by D-1-phenyl-2-2-decanoylamino-3-morpholino-1-propanol (D-PDMP), a GlcCer analogue[190] and inhibitor of both GlcCer and LacCer synthase[191]. In contrast, the L-isoform of PDMP induce enzyme activation[191]. Interest in LacCer synthase and its product LacCer has

increased due to the involvement in cell proliferation[190], cell adhesion, transendothelial migration and angiogenesis[187, 192, 193]. *In vitro* studies have demonstrated the ability of exogenously added LacCer to bind to glycosaminoglycan present on the outer surface of eukaryotic cells[194]. In addition, human macrophages treated with LDL show an augmented expression of LacCer on cell surface revealed by confocal microscopy[195]. However, influence of LDL on LacCer synthase seems to be cell-specific since in normal human kidney cells[196] and aortic SMCs[197], LDLs decrease enzyme activity resulting in inhibition of cell proliferation while a stimulatory effect is observed in human renal cancer proximal tubular cells[196]. Furthermore, LDL are likely to be the transporters of LacCer, and subjects with family hypercholesterolemia characterized by non-functional LDLR do not efficiently metabolize LacCer[198].

In human aortic SMCs, LacCer have been observed to increase cell proliferation[199], an effect also shared by oxLDL in a dose-dependent manner[190]. This action is counteracted by the antibody against LacCer and by D-PDMP. These observations suggest that oxLDL-mediated proliferation involves the activation of LacCer synthase resulting in the production of LacCer[200] which in turn promote proliferation through the activation of a signalling cascade involving ROS, p21 Ras GTP, MEK and Raf kinases, p44mitogen activated protein kinase and c-fos expression[201]. In addition, the nature of the FA that compose these lipids directly influences the proliferation and production of ROS. In fact, in human atherosclerotic plaques, C16:0, C22:0 and C24:0 participate to a greater extent in cell proliferation than stearoyl (C18:0)-LacCer[202]. To carry out this effect, LacCer specifically stimulates the activity of nicotinamide adenine dinucleotide phosphate (NADPH) oxidase, enzymes that produce ROS. This has been demonstrated in studies conducted on human neutrophils in which the addition of exogenous LacCer leads to a production of ROS and increased expression of cell surface glycoprotein macrophage-1 antigen (Mac-1) promoting the adhesion of neutrophils to endothelial cells[203]. In a further study on human monocytes U937, LacCer was observed to activate PKC and PLA_2 thus stimulating the expression of PECAM-1 and adhesion to endothelial cells[193]. Moreover, LacCer and LacCer synthase play a role in mediating the pro-inflammatory effect of TNF-α released in inflammatory conditions such as atherosclerosis. In endothelial cells, TNF-α or oxLDL stimulates LacCer synthase leading to an overproduction of LacCer which in turn modulates the NADPH oxidase activity and production of ROS. Through this pathway (**Figure 10**), an increased expression of ICAM-1 by modulation of nuclear factor NF-κB and increased adhesion to endothelial cells of monocytes and neutrophils that express Mac-1 occur. However, pre-incubation of endothelial cells with D-PDMP, reverse the LacCer-mediated effect. This inhibition is avoided by treatment with exogenous LacCer but no other GSL such as GluCer[187]. LacCer is also involved in the angiogenesis that occurs during atherosclerosis. Its involvement is demonstrated in both *in vitro* studies conducted with human aortic endothelial cells and human

umbilical vein endothelial cell and *in vivo* studies in a mouse model of angiogenesis[192]. These studies show how vascular endothelial growth factor (VEGF), mediator of all processes involved in angiogenesis such as cell migration, proliferation and differentiation to capillary loops[204], dose-dependently increases the activity of LacCer synthase and LacCer levels as much as TNF-α. Similarly, the signalling pathway involves the activation NF-κB that modulates β-1,4GalT-V expression and consequently, the formation of ROS, the production of PECAM-1 and the recruitment of PLA_2 for the induction of angiogenesis. This effect is reverted through the use of D-PDMP, antibody against LacCer, PECAM-1 and β-1,4GalT-V peptide. In addition, pre-treatment of human umbilical vein endothelial cell with antioxidants as N-acetyl-L-cysteine or NF-κB inhibitor pyrolidine dithiocarbamate, significantly diminished VEGF- and LacCer- mediated PECAM-1 expression[192].

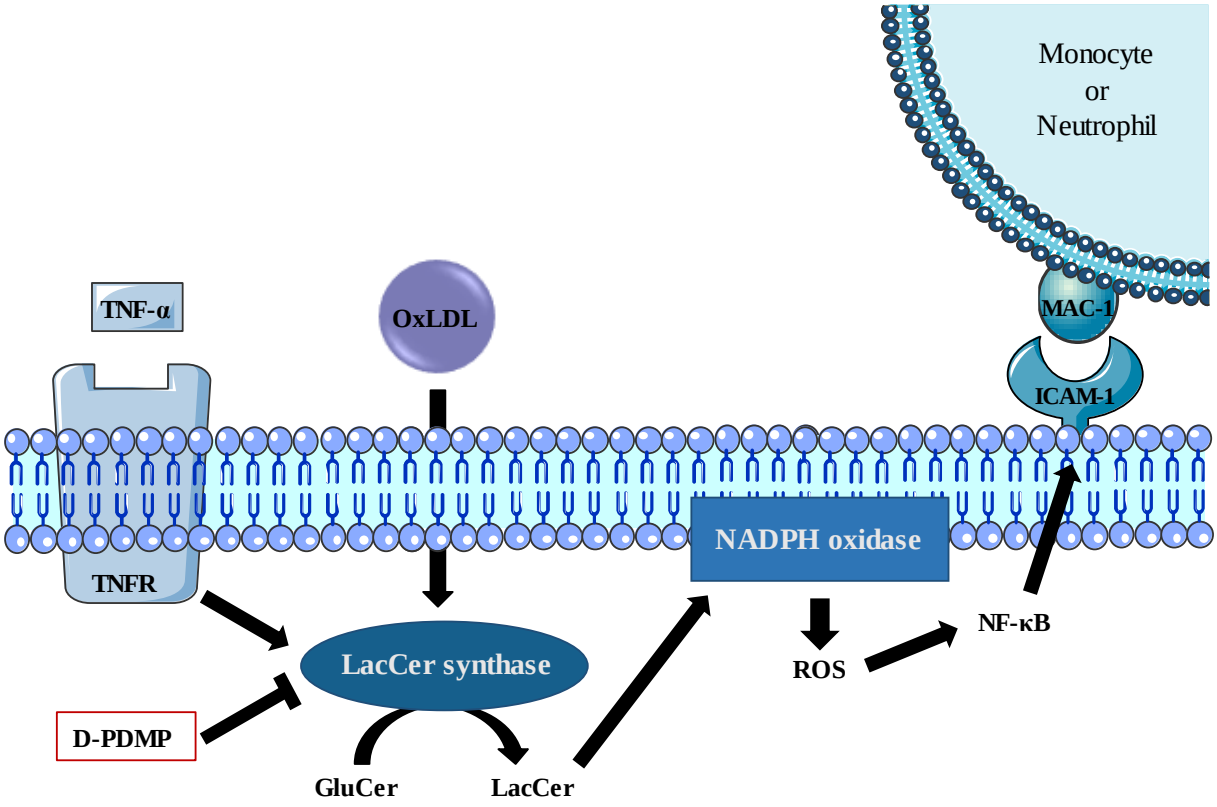

Figure 10 **Lactosylceramide signalling pathway**
Tumor necrosis factor-α (TNF- α) and oxidized-low-density lipoproteins (OxLDL) stimulate lactosylceramide synthase (LacCer synthase) and lactosylceramide (LacCer) synthesis, which in turn activates nicotinamide adenine dinucleotide phosphate (NADPH) oxidase leading to reactive oxygen species (ROS) production. ROS modulate nuclear transcription factor NF-κB that ultimately involves the overexpression of intercellular adhesion molecule-1 (ICAM-1) on cell surface and allows monocyte or neutrophil adhesion through the interaction with macrophage antigen-1 (MAC-1). D-1-phenyl-2-2-decanoylamino-3-morpholino-1-propanol (D-PDMP) is an inhibitor of this signalling pathway.

2.3.4 Lipidomics

The term 'lipidome' describes the complete lipid composition of a cell, tissue or organism[205]. The application of mass spectrometry (MS) to lipidome analysis has extended the knowledge of the wide variety of lipid molecular species. In 2003, Han and Gross coined the term 'lipidomics' to indicate a wide-ranging analysis of cellular lipidome through a comprehensive MS approach[206]. Lipidomics aims to identify lipid alterations in a system such as health and disease states, and to characterize molecular species involved in lipid metabolism and lipid-mediated signalling[207]. Due to the complexity and heterogeneity of lipid structures, the use of a single experimental approach makes the analysis challenging. Thus, lipidomics practices two approaches, the target study of individual lipid classes or the untargeted profiling of the entire lipid extracts. The typical workflow of an untargeted lipidomics experiment begins with the experimental design followed by sample collection and preparation, analytical instrument analysis (data acquisition), data processing, statistical analysis and, finally, results interpretation (**Figure 11**).

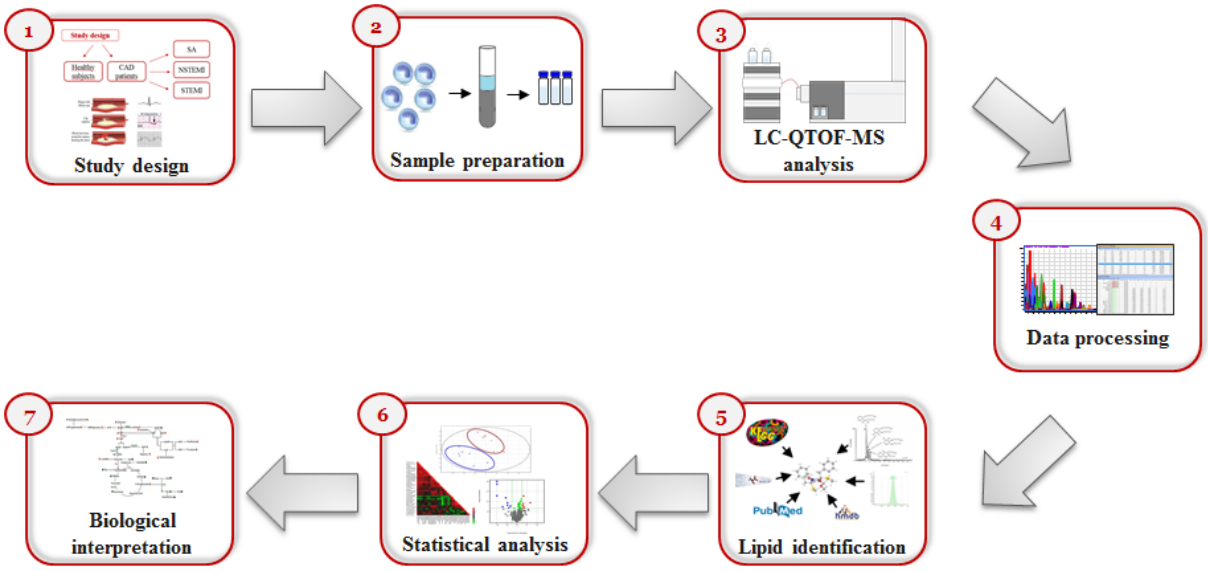

Figure 11 **Lipidomics workflow**
A schematic representation of the untargeted lipidomics workflow is depicted: study design, sample preparation, data acquisition (liquid chromatography-quadrupole time of flight-mass spectrometry analysis), data processing, lipid identification, statistical analysis and biological data interpretation

2.3.4.1 Study design, sample collection and preparation

The first step, experimental design, is of fundamental importance: in fact, it is necessary to pay great attention to sampling the population so that the selected individuals best represent the study groups. Furthermore, it is necessary to reduce the variability among the collected samples, since different variables can affect the experimental outcome[208]. In order to determine and examine the most influential factors that are relevant for the hypothesis under investigation, external factors that can affect the variables have to be eliminated or identified so that they can be accounted for during data analysis. In the study design, factors like sample size, randomisation and storage must be all be taken into account to guarantee reproducible and successful experiments that minimise incorrect variability and yet highlight the metabolites of interest and their potential interactions.

Sample preparation optimisation is essential to maximise the throughput and reproducibility of the analysis. Firstly, the lipid extraction from samples must be highly efficient, reproducible and ensure the complete removal of non-lipid contents. The suitable extraction solvents for lipids, consisting of both hydrophobic and hydrophilic groups, are methanol and chloroform. The most common technique of lipid extraction is the Folch method which uses a mixture of chloroform and methanol in a 2:1 ratio followed by a washing step with water for the removal of non-lipid components[209]. The Bligh and Dyer method is a modification of the previous one as it uses chloroform: methanol, 1:2, thus making it easier to apply to biological fluids[210]. In this procedure, the adjustment of the pH of the aqueous phase and in particular the acidification allows to increase the hydrophobicity of lipids, by disturbing their ion interactions, thus increasing the extraction efficiency. In this way, the recovery of charged polar molecules such as GP is increased. In addition, acidification improves the efficiency of lipid ionization in mass spectrometry analyses. However, the pH must be monitored as the ester bonds are susceptible to acid and may encounter hydrolysis. Another factor influencing the sample preparation that must be monitored, is temperature as it has been observed that cold reduces degradation and increases the stability of lipids[211].

2.3.4.2 Data acquisition

The most common analytical platform applied for lipidomics is MS. A first method applied to lipidomic studies is the 'shotgun' approach[207] which does not require any chromatographic separation of lipids before the infusion in the mass spectrometer. This approach is simple, high-throughput and fast as it requires short data acquisition times. However, many compounds, such as PL, after concurrent infusion can compete for ionization in the electrospray ionization (ESI) source resulting in ion suppression. This effect can affect the detection of some molecular species. In addition, the separation of isobaric molecules is not possible. Other analytical methods provide a separation phase. In particular, gas chromatography can be applied for PL analysis. In this method, the compounds must be derivatized and high column temperatures are also applied which can lead to the degradation of some of them[212]. Ultra-high pressure liquid chromatography (UPLC), compared to other chromatographic methods, displays wide application possibilities in lipidomic studies. Typically, for lipid analysis is used the reversed-phase liquid chromatography that is based on a stationary non-polar phase (C18 or C8 columns) and mobile phases such as methanol, isopropanol or acetonitrile[213]. In this way, based on lipophilicity, lipids are separated according to class and within the same lipid class are separated according to the carbon chain length and the amount of double bonds[214].

During the MS analysis, lipids undergo ionization and vaporization in the source and are sorted by mass to charge ratio (*m/z*) in the mass analyser[215]. The most appropriate method for lipid ionization is ESI, a soft ionization technique effective for example for polar lipids that can ionize both positively (protonation $[M+H]^+$) and negatively (deprotonation $[M-H]^-$)[216]. In the so-called 'top-down lipidomics', lipids can be directly identified on the basis of their *m/z* value. However this approach requires the use of high-resolution mass spectrometers that allow fast scanning and high mass accuracy (<5 ppm)[217]. The Quadrupole Time Of Flight (QTOF) mass spectrometer meets such requirements as it combines the stability of a quadrupole with the high efficiency, sensitivity and accuracy of a TOF. In the top-down lipidomic, the aim is to identify differences in the lipid pattern expressed rather than quantify specific molecules. The latter objective is in fact often pursued by the 'bottom-up' lipidomics approach with tandem mass spectrometry (MS/MS) analysis in which specific fragments ions allow to identify the related molecules so as to facilitate the analyte identification[144].

2.3.4.3 Data processing

Data extraction is the first significant step after data acquisition. MS data are characterized by information about retention time (RT), *m/z* values and signal intensity. There are several software from instrument companies (e.g. Mass Profile by Agilent Technologies) that propose algorithms to process the instrument-generated raw data transforming them into a two-dimensional data matrix that reports the measurement of abundance of different metabolites detected in the samples. Data processing stages are pre-processing, annotation, post-processing and finally statistical analysis performed in order to find metabolites differently expressed in the sample groups analyzed[208].

Data pre-processing includes chromatographic peak integration and alignment, filtering of the data by presence in blank samples or by eliminating peaks that do not appear in sample majority. This step of data cleaning is of extreme importance because lipidomics experiments often present a large amount of noise that can negatively affect the outcome of the analysis. This stage increases the quality of the data obtained and the statistical power reducing false positives[218].

Depending on the data processing, peak list can include adducts, isomers or fragments leading to several features detected *per* metabolite. Adduct-finding algorithms and de-isotope procedure are usually performed to avoid multiple features for one metabolite. In addition missing values can be imputed and data can be normalized and transformed[208]. This step reduces the variability between data by facilitating comparison between different samples.

Missing values imputation could be performed by different approaches as introducing zero, the mean or the median of other samples, k-nearest neighbors (kNN) and random forest (RF) [219].

Normalization includes statistical methods such as log transformation or auto-scaling or biologically-derived methods such as those that take into account the dilution effect of samples[208].

Quality control (QC) strategy is a technique applied to monitor unwanted signal instrumental variations that can occur in large number samples analysis and that can be minimized by normalization methods. QC is a sample, prepared mixing small and equal amount of all samples that should be analyzed repeatedly throughout an individual batch and across different batches. The signal variation of each molecular feature in QCs during the run allow correcting the signal of the same feature in each sample in relationship to the order of injection[220].

2.3.4.4 Data analysis

After data processing, the statistical analysis that can be performed are both univariate (Student's *t*-test, Wilcoxon *t*-test, ANOVA or Kruskal-Wallis test) and multivariate such as Principal Component Analysis (PCA), Partial Least Square (PLS) or Partial Least Squares-Discriminant Analysis (PLS-DA)[208]. Multivariate analyses can be supervised or unsupervised. Unsupervised methods investigate possible patterns or trends in data that can be either technical artifacts or biological effects. Among these, the PCA is the most widely used technique to obtain an overview of the data. PCA is a method of dimensionality reduction that consists in representing, in a 2D or 3D scatter plot, the maximum variation of the data through the first principal components (PC1 and PC2) that are linear combinations of the original variables. The PCA allows therefore to observe possible groupings of the analyzed samples and to identify the variables that determine their clustering. Supervised methods such as PLS-DA evaluate data variations according to the class labels, which can be groups or categories that are assigned to the samples. PLS-DA through the score plots represent the separation of the analyzed samples according to the class label. This separation, as supervised, is stronger than that given by the PCA; however, it can be misleading as it is susceptible to data overfitting. Therefore the results of the PLS-DA must be validated[208].

The molecular features need to be identified as specific metabolites and this identification is based on the accurate mass, RT (indicating hydro-lipophilic properties), MS/MS spectra and isotope distribution. The acquired MS/MS spectra can be compared with the ones available on in-house metabolite spectral libraries or online databases including Human Metabolome Database (HMDB)[221], Lipid Maps database[222] and METLIN Metabolite Database[223]. All of these, report metabolite information about the molecular name, molecular weight, chemical formula, structure and physical properties. MS/MS spectra specific for each metabolite can be also found on the online databases. In addition, new tools for in silico mass spectra generation using quantum chemistry coupled to machine learning methods are emerging[224]. The Metabolomics Standard Initiative defined four levels of identification[225]: identified metabolites (level 1), putatively annotated compounds (level 2), putatively characterized compound classes (level 3), and unknown compounds (level 4). Level 1 requires the comparison of experimental metabolite to an authentic chemical standard analyzed with the same analytical methods. By contrast, level 2 and 3 annotation does not require matching to data for authentic chemical standards but is enough the comparison to spectra databases. Level 2 is assigned when a compound matches the online database spectrum while level 3 is assigned when only the class to which the compound belongs to, is defined. Finally, level 4 represents a discernible spectral signal that can be reproducibly detected and quantified.

3. Objective

The development of new therapeutic approaches directed towards monocytes/macrophages, pivotal cells in the atherosclerotic plaque formation, is becoming a focal point of interest for many research groups. In particular, the definition of a molecular and functional profile of circulating monocytes can represent a useful tool for the characterization of inflammatory condition in cardiovascular disease.

In the circulation, monocytes are exposed to various soluble mediators that can lead to cell activation and/or metabolic profile alterations.

Recently it has been observed that an intracellular lipid accumulation alters some cellular functions and changes in the composition and organization of cellular lipids can profoundly influence the plasticity of membranes and the signal transduction following receptor activation. However, to date, information on the relationship between cellular lipid composition and inflammatory response of monocytes is still scantly.

The aim of the study was to determine the lipid profile, through an untargeted lipidomic analysis, of monocytes isolated from coronary artery disease patients and healthy subjects, in relation to the migratory capacity of these cells. The characterization of a lipidic and functional profile could allow to identify markers that could predict the progression of the atherosclerotic disease.

4. Materials and Methods

4.1 Study population

Sixty-two consecutive CAD patients undergoing coronary angiography due to SA or ACS as their first manifestation of ischaemic heart disease were enrolled in the study performed at Centro Cardiologico Monzino IRCCS (Milan, Italy). SA was defined as angina with stable symptoms for at least six months before admission (n=20). ACS diagnosis included NSTEMI (n=21) and STEMI (n=21) patients. NSTEMI was defined as chest pain at rest in the last 48 hours prior to admission, associated with evidence of transient depression of the ST segment in the 12-lead electrocardiogram tracing and elevated serum troponin I levels. STEMI condition was defined by the presence of prolonged chest pain (up to 30 min) with a pain onset of less than 12 h, and ST-elevation at the J point in ≥2 contiguous leads (≥0.2 mV in V1 through V3 and ≥0.1 mV in other leads). NSTEMI patients underwent coronary angiography within 24 h from admission while STEMI patients within 12 h of symptom onset. All patients underwent a venous blood sample for evaluation of biological parameters at the time of the admission. The exclusion criteria from the study were: previous history of CAD (i.e. any previous diagnosis of stable or unstable coronary artery disease), severe chronic heart failure (NYHA class III-IV), severe heart valve disease, acute and chronic infections, liver diseases, neoplasia, evidence of immunologic disorders, use of anti-inflammatory or immunosuppressive drugs and recent (<3 months) surgical procedure or trauma. For each patients the following cardiovascular risk factors were annotated: family history of early CAD (first degree relative with a history of myocardial infarction <60 years), diabetes (fasting blood glucose >126 mg/dl or treated diabetes), hypercholesterolemia (total Cho >200 mg/dl or treated hypercholesterolemia), smoking and hypertension (systolic blood pressure >140 mmHg and/or diastolic blood pressure >90 mmHg, or treated hypertension). BMI and laboratory data including complete blood count, serum glucose, serum creatinine, and lipid profile were recorded. Drug assumption at the time of admission were recorded too.

Twenty-seven healthy subjects (HS), defined as healthy on the basis of clinical and haematological investigations, with no history of CAD, cardiovascular risk factors, inflammatory diseases, and no drug therapy for cardiovascular disease, were recruited as control group.

The study was approved by the institutional ethics committee and was conducted in accordance with the Helsinki Declaration. All study participants signed the informed consent at the time of enrolment.

4.2 Monocyte isolation

Venous blood samples from healthy volunteers and CAD patients were collected in tubes containing ethylenediaminetetaacetic acid as anti-coagulant (EDTA) (9.3 mM; Vacutainer Systems, Becton Dickinson, Franklin Lakes, NJ, USA). The laboratory data were recorded for all enrolled subjects. Samples were then centrifuged (Megafuge 1.0R centrifuge, Hareaus) at room temperature (700xg, 4 min) and platelet-rich-plasma was removed. Mononuclear cells were isolated by Ficoll-Paque Plus (GE Healthcare, Milan, Italy) density centrifugation (450xg, 20 min, room temperature). To remove platelet contamination, the lymphocytes/monocyte-rich layer was washed with PBS (Lonza Italia SRL, Bergamo, Italy) containing 1 mM EDTA (Sigma-Aldrich, Milan, Italy).
To isolate monocytes two different techniques are applied.

4.2.1 Monocytes isolation by adhesion

Lymphocytes/monocytes pellet was suspended in RPMI 1640 (Lonza) supplemented with 2mM L-glutamine (Lonza), 100µg/ml penicillin and 100µg/ml streptomycin (Lonza) and 10% autologous serum, freshly obtained from blood clotted for 2h at 37°C. Mononuclear cells were then plated ($2x10^6$ cells/ml) in 35 mm well plates (PrimariaTM, Falcon, Sacco S.r.l, Como, Italy) and kept at 37°C (5% CO_2). After 2h, non-adherent cells were removed. Adherent monocytes were detached with trypsin-EDTA (0,1% trypsin + 0,04% EDTA) and later analyzed by flow cytometry.

4.2.2 Monocytes isolation by negative selection

Monocytes isolation was performed using the EasySep Negative Selection Human Monocytes Enrichment Kit (Stem Cell Technologies, Voden medical instruments, Monza Brianza, Italy). Lymphocytes/monocytes pellet was suspended in PBS at a concentration of $5x10^7$ cells/ml. A cocktail of monoclonal antibodies (mAb) was added (1 µl/10^6 cells); then cells were incubated for 10 minutes at 4°C. The cocktail is composed by antibodies against specific surface receptors of lymphocytes, dendritic cells and erythrocyte i.e. CD2, CD3, CD19, CD20, CD56, CD66b, CD123 and glycophorin A. Subsequently magnetic particles were added (1 µl/10^6 cells) and samples incubated for 5 minutes at 4°C to let the antibodies bind to the magnetic particles. Cell suspension was brought up to a total volume of 2.5 ml with PBS. Samples were then put into the magnet and the desired fraction (monocytes) was poured off. The magnetically labelled unwanted cells remain held by the magnetic field. Monocytes so obtained were analyzed by flow cytometry to verify the samples purity degree.

4.3 Flow cytometry

4.3.1 CD14 monocyte retrieval

Monocytes obtained through the two different technique, were stained for 15 min at room temperature with mAb against CD14 conjugated with fluorophore allophycocyanin (APC, 10 µl). Isotype-matched irrelevant antibodies were used as reference. Samples were analyzed by FACSCalibur (BD Biosciences) and $1x10^4$ events/sample were recorded. All data were analyzed using CellQuest Pro software (BD Biosciences).

4.3.2 CD14 CD16 monocyte subset analysis in whole blood

Whole blood (100µl) was stained for 15 min at RT with mAbs against CD14 APC-conjugated (10µl) and CD16 conjugated with fluorophore FITC (5µl). FACS lysing solution (700 µl) was added in order to remove interference of red blood cells. Isotype-matched irrelevant antibodies were used as reference. Samples were analyzed by Gallios (Beckman coulter) and $1x10^4$ events/sample were recorded. All data were analyzed using Kaluza analysis software (Beckman coulter).

4.4 Monocyte migration

Monocytes obtained by a negative selection isolation, were suspended, after washing, in RPMI 1640 (Lonza) supplemented with L-glutamine (2 mM) (Lonza), penicillin and streptomycin (100 µg/ml) (Lonza) and seeded into a transwells ($2x10^5$ cells/well). Transwells for migration assay are cell culture inserts with a permeable membrane (5 µm pore diameter) (Corning ®Costar® 24 well). Cells are placed in the upper layer while cell culture medium is placed in the lower chamber. Cell culture medium was supplemented with 10% fetal bovine serum (FBS) or autologous serum. In addition, to test the migration towards human non-autologous serum, CAD monocytes were exposed to a medium supplemented with a pool of sera obtained from healthy subjects (HS serum pool); conversely HS monocytes were exposed to a medium supplemented with a CAD serum pool. Sera were freshly obtained from blood clotted for 2h at 37°C. Following an incubation period (3h, 37°C), non-migrated cells were removed from the upper chamber with a cotton swab and cells that have migrated through the membrane were fixed in 4% paraformaldehyde and stained with Hoechst dyes (Sigma-Aldrich). Migrated cells were counted in a total of 10 randomly selected fields in duplicate wells through the Axiovert fluorescence microscope (Axiovert 200M, Zeiss). Migration Index is expressed as the ratio between the number of cells migrated into a medium supplemented with serum and the number of cells spontaneously migrated in the absence of stimulus.

To evaluate the contribution of the *de novo* synthesis of LacCer on monocyte migration, cells were pre-incubated for 1 hour prior to the migration assay with the lactosylceramide synthase enzyme inhibitor D-PDMP (20 µM). Experiments using TNF-α (10 ng/ml) as a chemotactic agent were used as a positive control. The monocyte migration was also evaluated after the treatment of monocytes with standard Lactosylceramide (d18:1/16:0) (Avanti Polar Lipids) 2 µM for 30 min.

4.5 Untargeted lipidomic analysis

4.5.1 Sample preparation

Monocytes were thawed in ice, re-suspended in 1 ml of CH_3OH and transferred into 7 ml borosilicate tubes. Lipids were extracted by adding 2 ml of CH_3Cl containing 20 mg/l butylated hydroxytoluene (BHT); samples were vortexed for 10 seconds at RT and sonicated in ice in an ultrasonic bath for 15 min (Falc, LabService, Milan). One ml of deionized H_2O was added, samples were vortexed 10 sec and centrifuged (10000xg, 4°C, 10 min). The organic phase was collected, and a second extraction of the aqueous phase was performed by adding 50 µl of HCl 37% and 2 ml of CH_3Cl containing BHT (20 mg/l). The organic phases were pooled, dried in a Speedvac and re-suspended in 150 µl of CH_3OH: CH_3Cl 9:1 (v:v). A pool of these lipid extracts for quality control (QC) was created by combining 20 µl of each sample. Lipid extracts were aliquoted in two vials for the LC-QTOF-MS full scan analysis and the LC-QTOF-MS/MS analysis. Samples were randomized prior to injection

4.5.2 LC-QTOF-MS sample analysis

LC-QTOF-MS analysis was performed by an ultra-high performance liquid chromatography (UHPLC) system (1290 Infinity series, Agilent Technologies) coupled to a QTOF mass spectrometry detector (Agilent 6550 iFunnel QTOF) outfitted with Dual-Jet ESI source (Agilent Technologies). Samples were analyzed both in positive and in negative detection mode. Two µl was injected onto the Zorbax Eclipse Plus C18 Rapid Resolution HD reverse phase column (2.1 x 150 mm, 1.8 µm, Agilent Technologies), maintained at 35°C, using a constant flow rate of 0.3 ml/min. For both positive and negative ionization mode, the mobile phases and their gradients (**Table 1**) are reported.

A) CH_3CN 50% + NH_4COOH 10 mM + 0.1% HCOOH

B) IPA 88% + H_2O 2% + CH_3CN 10% + NH_4COOH 10 mM + 0.1% HCOOH

Time (min)	A (%)	B (%)
0	65	35
20	5	95
25	0	100
27.5	0	100
27.6	65	35
36	65	35

Table 1 **Gradient elution of the mobile phases**

The detector operated in full scan mode, acquiring mass spectra over the m/z range 100-1200 Da in positive ion mode and 50-1200 Da in negative mode with a scan rate of 1.5 scan per second. Source parameters for both ion modes were: drying gas temperature 230°C, drying gas flow 12 l/min, nebulizer pressure 35 psig, sheath gas temperature 350 °C, sheath gas flow 12 l/min, nozzle voltage 1000 V and fragmentor 150 V, skimmer 1,65 V, octopole RF peak 750 V. Capillary voltage was set at 3500 V in positive ionization mode and 4000 V in negative one. The references masses, 121.0509 m/z, 922.0098 m/z (ESI+) and 112.9856 m/z, 1033.9881 m/z (ESI-), were continuously infused to correct instrument variability, at a flow rate 0.05 ml/min. Data were acquired by MassHunter Workstation Data Acquisition software (Agilent Technologies).

4.5.3 Performance evaluation

Performance evaluation was assessed using QC samples approach[226]. QC samples were obtained by pooling together equal volumes of all samples of monocyte lipid extracts (CAD + HS). Subsequently, QCs were injected at the beginning of the analytical sequence (n=7), every nine injections and at the end of the analysis.

4.5.4 Data processing

Raw acquired data were imported in MassHunter Qualitative software (Agilent Technologies), converted in mzData and then analyzed by the software MZmine 2.3[227] which use peak detection algorithm that provides a list of features, which represent possible metabolites, combining different information from co-eluting ions such as charge-state, isotopic distribution, presence of adducts and/or dimers. The most relevant parameters selected for the feature's extraction were as follow: signal-to-noise ratio of 5, intensity threshold of $1x10^3$ (to clean background noise), mass range of 250-1000, RT ranging from 2 to 27 min, minimal peak duration of 0.2 min, and maximal peak duration of 1.2 min. Chromatogram deconvolution was conducted and then the peak alignment algorithm was performed to adjust for any slight variation in RT (RT tolerance: 0% or 0.15 min) and m/z (m/z tolerance: 0.005 or 5 ppm). To improve data quality, a manual feature evaluation procedure was performed: features present in the blank or subjected to carry over, were excluded. Furthermore a filtering quality procedure was applied to deem as reliable features those present in at least 90% of the QCs with a CV < 20%[220]. Features with more than 20% missing values within the same group (STEMI, NSTEMI, SA or HS) were removed. Missing values imputation was performed using Random Forest algorithm[219]. The datasets were corrected by sample cell number and normalized by sum. The robust lists finally obtained, for positive and negative mode, were defined as compound lists.

4.5.5 Compound identification

Lipids identification was performed for each reliable feature included in the two compounds lists (positive and negative ionization mode). LipidMaps software was used for detected and accurate *m/z* values matching (10 ppm mass error window) The elution rules for different lipids classes were also considered for the identification. To further confirm the lipid putative identification, MS/MS analysis were also performed. Specifically, standards for the main lipid classes were purchased and their MS/MS spectrum was collected for lipid identification validation. The typical fragments for each lipid classes were then matched with the experimental MS/MS fragmentation pattern obtained for the putative identified features. In addition, molecular adducts as $[M+Na]^+$ and $[M+NH_4]^+$ in positive ionization mode and $[M+Cl]^-$, $[M+HCOO]^-$ and $[M+HCOONH_4]^-$ in negative ionization mode were manually annotated based on RT correspondence, m/z and MS/MS fragmentation patterns.

4.5.5.1 LC-QTOF-MS/MS sample analysis

The LC-QTOF-MS/MS experiments were performed for every reliable feature included in the two compounds list, using the same chromatographic separation and the positive or negative ionization conditions previous described. Compounds were targeted using *m/z* value (isolation width 4 Da) and RT (ΔRT 0.6 min), and data were collected applying 30 eV fixed collision energy. Moreover, samples with the highest intensity of each compound were analyzed to optimize MS/MS spectra quality. Different runs were performed so as to avoid fragmentation of significant compounds co-eluting in the same analysis. Subsequently, spectra were processed through MassHunter Qualitative software (Agilent Technologies).

4.6 Lactosylceramide synthase levels

The levels of β-1,4-galactosyltransferase 5, lactosylceramide synthase, was evaluated by ELISA kit (MyBioSource, Labospace, Milan). Monocytes obtained from HS and CAD patients were lysed with 120 µl of β-octyl glucopiranoside lysis buffer and subjected to 3 freeze and thaw cycles. The enzyme expression was evaluated spectrophotometrically at a wavelength of 450 nm and the concentration in the samples is then determined by comparing the absorbance of the samples to the standard curve.

4.7 Statistical analysis

4.7.1 Monocyte characterization

Continuous variables are presented as mean ± standard deviation (SD), variables not normally distributed are presented as median and interquartile ranges (IQR), and categorical variables as absolute numbers and percentages.

Comparisons between the groups were performed using ANOVA test for normally distributed variables, the Kruskal Wallis test for not normally distributed variables. Categorical variables were compared using the chi-square test or Fisher's exact test, as appropriate. Post-hoc testing of main effects was performed using t-tests with Bonferroni adjustments for multiple comparisons (α/[number of comparisons]). Trends of variation from "HS" to "STEMI" were assessed by general linear models. Paired t-test was used for paired-group comparisons.

Further, all analyses were also adjusted for gender and age.

Correlations between variables were determined using the Spearman's rank test.

All tests were two-sided, and a p value < 0.05 was required for statistical significance.

All calculations were computed with the aid of the SAS software package (Version 9.4 SAS Institute Inc., Cary, NC).

4.7.2 Untargeted lipidomic analysis

The compound lists obtained from positive and negative modes were treated independently for statistical analysis. Mass Profiler Professional software (Agilent Technologies) was employed for multivariate analysis as unsupervised PCA and univariate analysis as one-way analysis of variance (ANOVA) test or Moderate t-test. For ANOVA test, performed for the fourth study groups (HV, SA, NSTEMI, STEMI), post hoc Tukey Honest significant difference (HSD) was performed while Benjamini-Hochberg multiple testing correction for controlling the false discovery rate (FDR) was applied for both ANOVA and Moderate t-test. Further volcano plot analysis with fold change (FC) > or < 1.5 and FDR < 0.05 by the Moderate t-test was used to identify significantly differential metabolites between CAD and HV groups.

Heatmaps were obtained using MetaboAnalyst online software (http://www.metaboanalyst.ca). Venn diagrams were drawn by Bioinformatics & Evolutionary Genomics online software (http://bioinformatics.psb.ugent.be/webtools/Venn).

Correlations between variables were performed using the Spearman's rank test. A p value <0.05 was considered to indicate statistical significance.

5. Results

5.1 Study population

The principal demographic, clinical and laboratory characteristics of CAD patient (SA, NSTEMI, STEMI) and of healthy subjects, enrolled in this study, are shown in **Table 2.**

	HS (n=27)	**SA (n=20)**	**NSTEMI (n=21)**	**STEMI (n=21)**	***p* value all subjects**	***p* value CAD groups**
Demographic characteristics						
Age, years	58 ± 11	66 ± 11	62 ± 13	64 ± 10	0.153	0.551
Male gender, n (%)	15 (55)	20 (100)	15 (71)	15 (71)	0.003	0.015
Clinical characteristics						
BMI, Kg/m^2	25.7 ± 3.6	27.6 ± 2.4	27.4 ± 2.9	28.9 ± 2.1°	0.003	0.145
Smoke, n (%)	5 (18)	14 (70)	10 (48)	14 (67)	0.001	0.279
Diabetes, n (%)	1 (4)	6 (30)	5 (24)	8 (38)	0.019	0.602
Dyslipidemia, n (%)	10 (37)	8 (40)	15 (71)	10 (48)	0.092	0.107
Hypertension, n (%)	7 (26)	15 (75)	5 (24)	17 (81)	0.0001	0.0003
Family history of CAD, n (%)	-	10 (50)	11 (52)	12 (57)	0.0001	0.896
Haematological parameters						
WBC, $x10^9/l$	5.8 (5.1;7.1)	7.4 (4.2;9.1)	8.8 (7.5;9.2) [a]	7.5 (7.2;11.2)[a]	0.0001	0.213
RBC, $x10^{12}/l$	4.9 ± 0.4	4.3 ± 0.5[a]	4.6 ± 0.6	4.6 ± 0.7	0.003	0.183
Neutrophils, $x10^9/l$	3.3 (2.6;4)	4.6 (1.6;5.8)	5.1 (4;6.1) [a]	4.9 (4;7.8)[a,b]	0.0002	0.350
Lymphocytes, $x10^9/l$	2 (1.7;2.4)	1.6 (1.1;2.4)	2 (1.7;2.1)	2.1 (1.4;2.7)	0.336	0.299
Eosinophils, $x10^9/l$	0.2 (0.1;0.3)	0.1 (0.1;0.2)	0.3 (0.1;0.7)[a,b]	0.1 (0.1;0.2)	0.013	0.007
Monocytes, $x10^9/l$	0.4 ± 0.1	0.56 ± 0.1[a]	0.58 ± 0.1 [a]	0.62 ± 0.3[a]	0.0001	0.308
Platelets, $x10^9/l$	233.3 ± 46.6	211.6 ± 46.2	227.6 ± 63.2	209.5 ± 27.6	0.248	0.417
Glycaemia, mg/dl	89 (87;95)	125 (91;126)[a]	118(104;139)[a]	118(114;154)[a]	0.0001	0.514
Haemoglobin, g/dl	14.8 ± 1	12.5 ± 1.6 [a]	13.2 ± 1.2 [a]	13.8 ± 1.6[b]	0.0001	0.030
Total cholesterol, mg/dl	211.7 ± 31.1	184.4 ± 31.3 [a]	215.4 ± 50[b]	207.7 ± 42.4[b]	0.054	0.090
LDL, mg/dl	131.3 ± 27.8	98.4 ± 28.7 [a]	146.1 ± 41.2	133.1 ± 35.8	0.0002	0.006
HDL, mg/dl	56 (48;67)	67 (58;78)	43 (40,46)[a,b]	41 (35;45)[a,b]	0.0001	0.0001
Triglycerides, mg/dl	100 (86;125)	70 (59,152)	213(125;224)[ab]	194(108;211)[a,b]	0.0001	0.0001
Pharmacological treatments						
Aspirin, n (%)	-	7 (35)	7 (33)	11 (52)	0.0001	0.380
β-blockers, n(%)	4 (15)	10 (50)	5 (24)	3 (14)	0.033	0.042
ACE-inhibitors, n (%)	3 (11)	13 (65)	2 (9)	7 (33)	0.0001	0.001
Statins, n (%)	-	8 (40)	5 (24)	6 (29)	0.001	0.514

Table 2 **Study population characteristics**
Baseline demographic, clinical and laboratory characteristics of healthy subjects (HS, n=27) and coronary artery disease (CAD, n= 62) patients including patients with stable angina (SA, n=20), non-ST elevation myocardial infarction (NSTEMI, n=21) and ST elevation myocardial infarction (STEMI, n=21) patients. Data are expressed as mean±SD or median and interquartile range. Categorical variables are expressed as number (percentage). p-values for ANOVA t test or Kruskal-Wallis test are shown for comparison of the 4 study groups or only of CAD patients (SA, NSTEMI, STEMI).
[a] $p<0.05$ *vs* HS, [b] $p<0.05$ *vs* SA.
ACE-inhibitors: angiotensin-converting enzyme inhibitors; **BMI**: body-mass index; **HDL**: high-density lipoprotein; **LDL**: low-density lipoprotein; **RBC**: red blood cells; **WBC**: white blood cells.

In the CAD group there is a prevalence of males (about 80%) compared to the HS group in which males are 55%. CAD patients show an older age even if not significant different from HS. Thus, all data are adjusted for sex and age. As expected, classical risk factors such as a high BMI, smoking, diabetes and hypertension are significant higher in CAD group than in the HS group. Patients show higher levels of WBC, sign of their inflammatory condition. Moreover, NSTEMI and STEMI patients are characterized by higher LDL and triglycerides and lower HDL compared to HS. SA patients show an opposite behaviour probably due to a clinical condition monitored by pharmacological treatments such as statins (40%). CAD patients, specifically SA, significantly differ from healthy volunteers for the pharmacological treatments since the former received cardiovascular therapy.

5.2 Monocyte characterization

5.2.1 Monocyte isolation, retrieval and purity

To isolate the monocyte population, peripheral blood mononuclear cells (PBMCs), obtained by Ficoll-Paque density centrifugation were processed through two different protocols which are summarized in **Figure 12**.

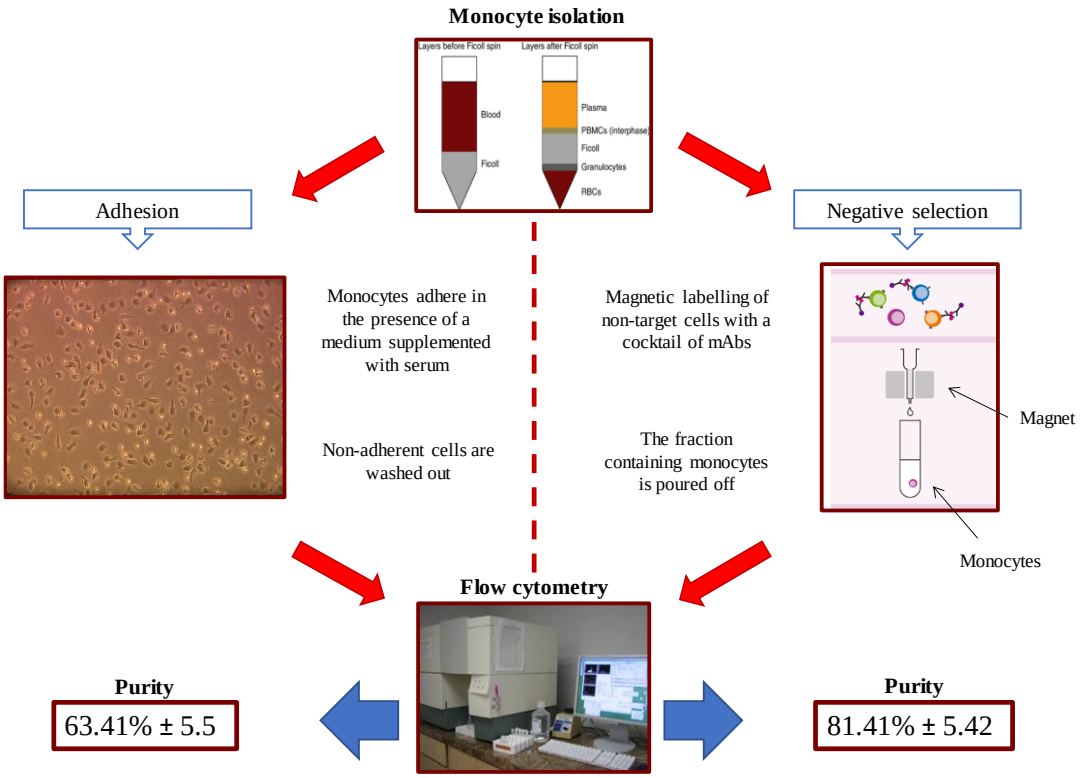

Figure 12 **Monocyte isolation, retrieval and purity**
Schematic representation of the two techniques applied for monocyte isolation. Peripheral blood mononuclear cells (PBMCs) are obtained by Ficoll-Paque density centrifugation and monocytes are isolated by adhesion (on the left) and by negative selection (on the right) obtaining an average purity of the cell population of 63.41% ± 5.5 and 81.41% ± 5.42 respectively, evaluated with flow cytometry.

In the first strategy, the separation of monocytes form lymphocytes could be performed through the adhesion to the plastic, indeed monocytes adhere on plate surface in the presence of a medium supplemented with serum. Then after several wash, non-adherent cells could be removed. Adherent cells were monocytes with a cell population purity of 63.41% ± 5.5 (n=4) defined on the basis of the CD14 expression evaluated by flow cytometry.

Using the second isolation approach, EasySep Negative Selection Human Monocytes Enrichment Kit, the monocyte population purity is higher: 81.41% ± 5.42 (n=4). Indeed, when samples are put into the magnet, the magnetically labelled unwanted cells remain held by the magnetic field on the contrary, the desired fraction (monocytes) could be poured off. A great advantage of this technique is that, through a negative selection, the interaction between monocytes and antibodies or magnetic beams is prevented. The cocktail provided by the isolation kit, also contains an FcR blocker to prevent non-specific binding to monocytes; thus, by this way monocyte activation is avoided.

This second technique allows to obtain monocytes with a higher degree of purity and prevent them from activation. Consequently, in this study we chose to perform the isolation of monocytes by a negative selection.

5.2.2 Monocyte counts

It was first reported in the 1970s that monocytes increase their proliferative activity in bone marrow in response to inflammatory stimuli, leading to monocytosis, a clinical condition reflecting an increase number of circulating monocytes[228]. Given the role of inflammation as a precipitating factor for atherosclerosis development, a relationship between monocyte counts and cardiovascular diseases, is expected.

5.2.2.1 Total monocyte count

As shown in **Figure 13**, CAD patients are characterized by a higher number of monocyte count compared to healthy subjects (0.56±0.1 x10^9/l, 0.58±0.1 x10^9/l and 0.62±0.3 x10^9/l for SA, NSTEMI and STEMI respectively and 0.4±0.1 x10^9/l for HS) (p<0.05, p<0.01 and p<0.001 respectively). Moreover, a progressive increase in the monocyte count going from HS, SA, NSTEMI, STEMI, was observed (p for trend< 0.001).

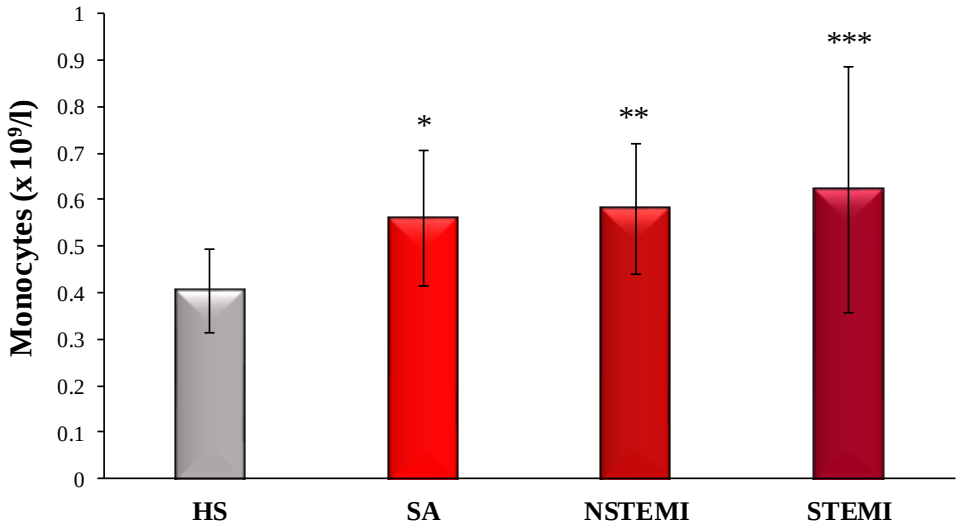

Figure 13 **Total monocytes count**
Total monocyte count in healthy subjects (HS, n=27), and in patients with stable angina (SA, n=20), non-ST elevation myocardial infarction (NSTEMI, n=21) and ST elevation myocardial infarction (STEMI, n=21). Data are represented as mean ± standard deviation. *p<0.05 vs HS, **p<0.01 *vs* HS, ***p<0.001 *vs* HS; p anova<0.01; p for trend< 0.001.

5.2.2.2 Monocyte subset count

The three monocyte subsets were identified on the basis of the CD14 and CD16 expressions.

In **Figure 14**, a representative flow cytometry analysis of monocyte subsets is shown. Overall, despite the inter-individual variability, classical monocytes represent the largest subgroup: 80-90% of the total monocyte count while non-classical and intermediate monocytes represent 2-8% and 2-10% of the total circulating monocytes

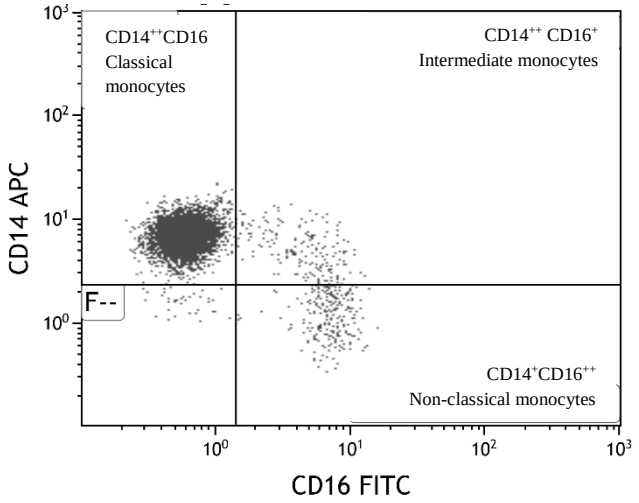

Figure 14 **Flow cytometry analysis of monocyte subsets**
Representative flow cytometry plots of the monocyte subsets. $CD14^{++}CD16^{-}$: classical monocytes, $CD14^{++}CD16^{+}$: intermediate monocytes, $CD14^{+}CD16^{++}$: non-classical monocytes

Specifically, classical monocytes do not show significant differences between the study groups (**Figure 15, panel A**). Interestingly, the number of intermediate monocytes appear to be higher in CAD patients (specifically in NSTEMI patients) compared to HS and this increase goes in parallel with the increase severity of the disease (p for trend< 0.05) (**Figure 15, panel B**). Moreover, a significant positive association between intermediate monocyte count and diagnosis of CAD is observed (R= 0.38, p<0.001).

By contrast, non-classical monocyte count results reduced in CAD patients compared to HS group (**Figure 15, panel C**) and this reduction is marked in SA patients. Moreover, a negative association between non-classical monocyte count and diagnosis of CAD is observed (R= -0.30, p<0.01).

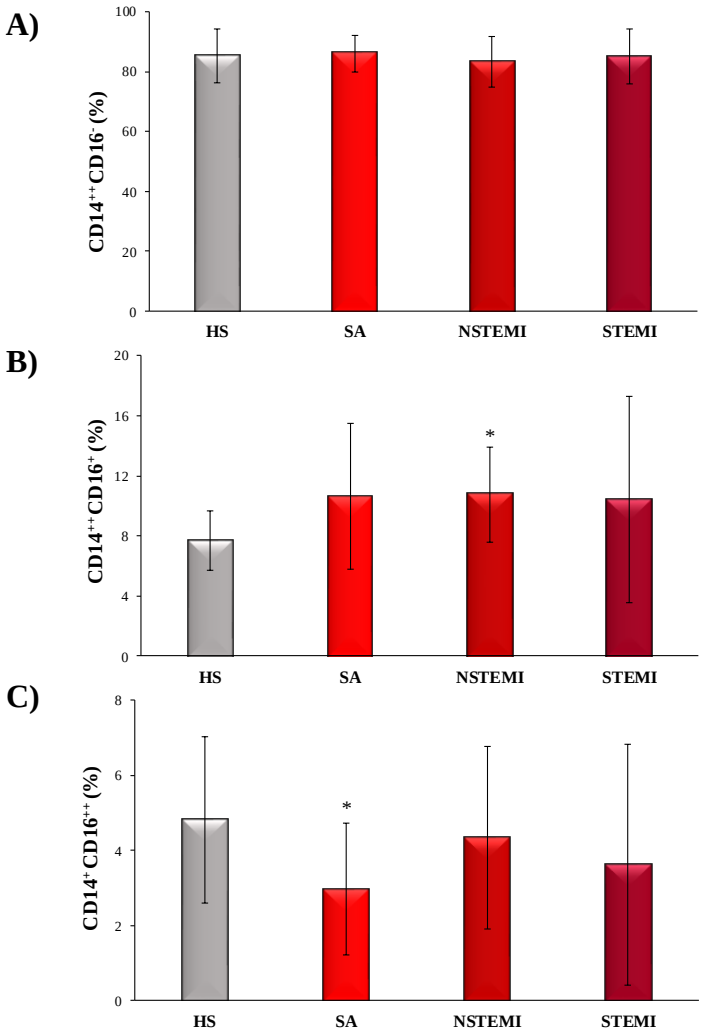

Figure 15 **Monocyte subsets count**
A) Classical monocyte count, B) intermediate monocyte count and C) non-classical monocyte counts in healthy subjects (HS, n=27), and patients with stable angina (SA, n=20), non-ST elevation myocardial infarction (NSTEMI, n=21) and ST elevation myocardial infarction (STEMI, n=21). Data are represented as mean ± standard deviation.
B) *p<0.05 *vs* HS, p anova< 0.001, p for trend< 0.05; C) *p<0.05 *vs* HS, p anova< 0.01.

5.2.3 Monocyte migration

Monocyte trafficking and migration studies could help to better understand the role of monocytes in atherosclerotic disease.

In this study, the CAD patients and HS monocyte migration in the presence of different type of serum which represent a trafficking trigger, was evaluated

5.2.3.1 Monocyte migration towards FBS or autologous serum

Monocytes obtained from all the subjects participating to the study (HS, SA, NSTEMI and STEMI), were seeded in plates with medium supplemented with 10% of FBS or autologous serum. As shown in **Figure 16, panel A,** a progressive increase in monocyte migration is observed as the severity of the disease rises (p for trend<0.001). Moreover, monocytes obtained from STEMI patients have a significantly higher migration ability than HS (Migration Index (%): 6.7 ± 5.1 and 3 ± 1.2 respectively, p<0.01). This result suggests that monocytes obtained from CAD patients (in particular from STEMI patients) are more prone to migrate towards FBS serum.

The same result is also obtained using autologous serum as chemotactic stimulus (**Figure 16, panel B)** and a progressive significantly increase in monocyte migration is observed (p for trend<0.001). Specifically, the migration of STEMI and NSTEMI monocytes is higher compared to the HS group (Migration Index (%): 3.6 ± 2.8, 3.3 ± 3.1 and 1.5 ± 0.9 for STEMI, NSTEMI and HS respectively, p<0.05 *vs* HS). In addition, a significant positive correlation between the migration performed in the presence of FBS (R= 0.24, p<0.05) or autologous serum (R= 0.34, p< 0.01) and CAD diagnosis is observed.

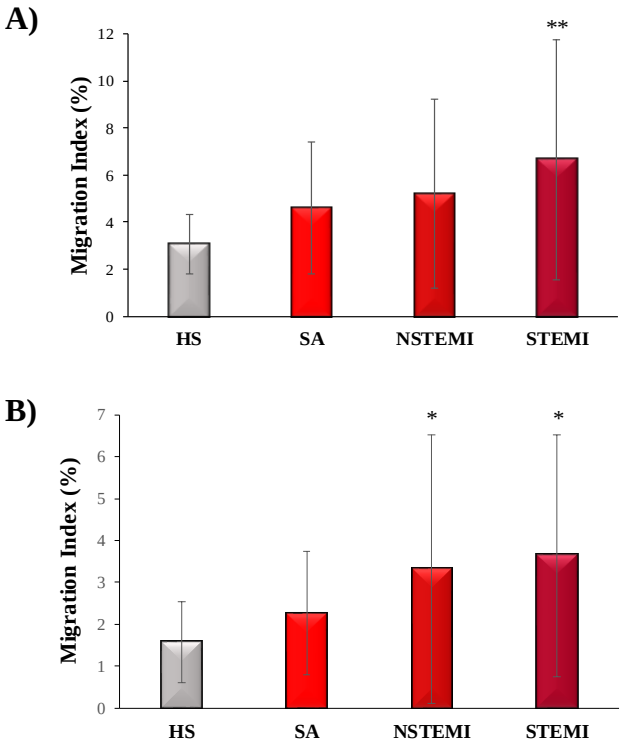

Figure 16 **Monocyte migration towards FBS or autologous serum**
Migration of monocytes obtained from healthy subjects (HS), and patients with stable angina (SA), non-ST elevation myocardial infarction (NSTEMI) and ST elevation myocardial infarction (STEMI). Migration is performed in the presence of A) fetal bovine serum (FBS) (HS, n= 21; SA, n=17; NSTEMI, n=17; STEMI, n=20) or B) autologous serum as chemotactic stimuli (HS, n= 20; SA, n=13; NSTEMI, n=16; STEMI, n=13). Data are represented as mean ± standard deviation. A) $^{**}p<0.01$ *vs* HS, *p* anova<0.01, *p* for trend<0.001; B) $^{*}p<0.05$ *vs* HS, *p* anova<0.05, *p* for trend<0.001.

5.2.3.2 Monocyte migration towards human non-autologous sera

To evaluate the influence of different sera on monocyte migration, the migration assay was performed inducing the migration of monocytes isolated from HS towards a medium supplemented with a pool of sera obtained from CAD patients. As shown in **Figure 17, panel A**, when HS monocytes are exposed to a "non-autologous" serum such as FBS or CAD pool sera, their migration significantly increase compare to the migration obtained in presence of the autologous serum (Migration Index (%): 3.2 ± 1.3, 3.8 ± 3.6 and 1.3 ± 0.8 for FBS, CAD pool and AUTO respectively).

In addition, when CAD patients' monocytes are exposed to a pool of sera obtained from HS, their migration significantly decrease compared to that obtained in presence of the autologous serum (Migration Index (%): 1.7 ± 0.9 and 2.9 ±2.3 for HS pool and AUTO respectively, $p<0.01$).
Similar to that observed for HS monocytes, CAD patients' monocytes show increase migration towards FBS (Migration Index (%): 4.5 ± 2.4) compared to autologous serum ($p<0.001$).

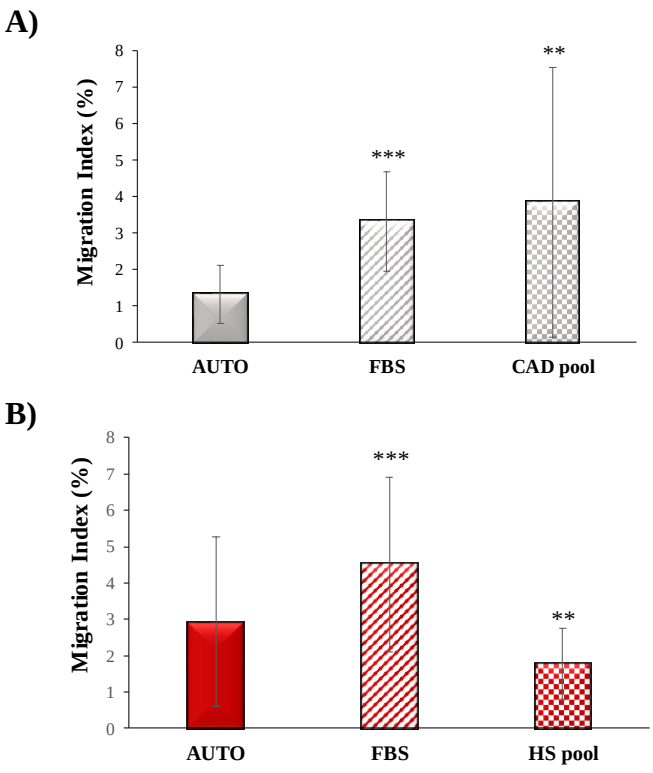

Figure 17 **Monocyte migration towards serum pool obtained from HS or CAD**
Migration of monocytes obtained from A) healthy subjects (HS, n=11), and B) coronary artery disease (CAD, n= 7) patients is performed in the presence of fetal bovine serum (FBS), autologous serum (AUTO) and A) pool of serum obtained from CAD patients (CAD pool) or B) pool of serum obtained from HS (HS pool). Data are represented as mean ± standard deviation. A) ***$p<0.001$ *vs* AUTO, **$p<0.01$ *vs* AUTO; B) ***$p<0.001$ *vs* AUTO, **$p<0.01$ *vs* AUTO

5.2.4 Correlation between monocyte migration and monocyte subsets counts

A positive correlation between the $CD14^{++}CD16^{+}$ monocyte (intermediate monocytes) count and the monocyte migration towards autologous serum is demonstrated. Not significant correlations are observed considering monocyte migration with FBS or human non-autologous sera and classical or non-classical monocyte counts.

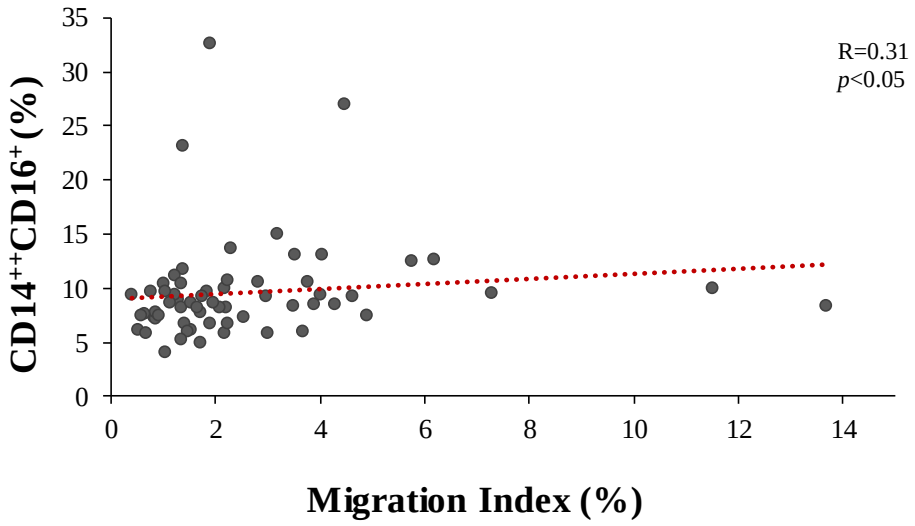

Figure 18 **Monocyte migration and subset count correlation**
Correlation between monocyte migration towards autologous serum and $CD14^{++}CD16^{+}$ intermediate monocyte count. Monocytes are obtained from healthy subjects (HS, n=27), and coronary artery disease (CAD, n= 62) patients.

5.3 Untargeted lipidomics analysis

5.3.1 Method development and validation

The lipidomic profile of monocytes obtained from CAD patients and healthy subject, was defined by an untargeted mass spectrometry method that simultaneously detect a broad range of lipids. Given the complexity and structural variability of lipid molecules, the method development assumes a fundamental role in order to define the widest spectrum of molecules that can be detected simultaneously.

For the development of this method, a standard solution containing standards (2 ng/ml, each) belonging to different lipid classes was prepared (**Table 3**). Thus, different methodological aspects (instrumental parameters, sample preparation, chromatographic separation and instrumental reproducibility) have been evaluated.

Class	**Name**	***m/z +***	***m/z -***
Phosphatidylcholine	PC (16:0/18:1)	760.5851	758.5706
Phosphatidylethanolamine	PE (16:0/18:1)	718.5381	716.5236
Phosphatidylserine	PS (16:0/18:1)	762.528	760.5134
Phosphatidylglycerol	PG (16:0/18:1)	749.5327	747.5182
Phosphatidylinositol	PI (16:0/18:1)	837.5488	835.5342
Phosphatidic acid	PA (16:0/18:1)	675.4959	673.4814
Plasmenyl Phosphatidylcholine	PC (P-36:1) (P-18:0/18:1)	772.6215	770.6070
Plasmenyl Phosphatidylethanolamine	PE (P-36:1) (P-18:0/18:1)	730.5745	728.5600
Sphingomyelin	SM (d34:1) (d18:1/16:0)	703.5748	701.5603
Ceramide	Cer (d34:1) (d18:1/16:0)	538.5194	536.5049
Hexosylceramide	HexCer (d34:1) (d18:1/16:0)	700.5722	698.5577
Lactosylceramide	LacCer (d42:1) (d18:1/24:0)	974.7502	972.7357
Monoacylglycerol	MG (16:0)	331.2843	329.2697
Diacylglycerol	DG (34:1) (18:1/16:0)	595.5296	593.5151
Triacylglycerol	TG (52:1) (18:0/18:1/16:0)	861.7906	859.776
Cholesteryl ester	CE (18:0)	653.6231	651.6086

Table 3 **Lipid standards**
List of lipid standard employed for the development of the untargeted lipidomic method. For each standard, the lipid class, the full name with the fatty acid composition and the m/z values for both positive and negative ionization mode are reported.

5.3.1.1 Instrument parameters

There are two kind of instrument parameters: “compound dependent” and “flow dependent”.
The first ones include voltage of nozzle, capillary, fragmentor and octopole RF peak and are defined on the basis of the type of molecules analyzed. The flow dependent parameters as drying gas temperature and flow, sheath gas temperature and flow, nebulizer pressure, are influenced by the flow rate of the mobile phases. For the evaluation of the instrument parameters, the standard solution was directly infused into the source, without chromatographic separation, and the parameters were evaluated for both negative and positive ionization mode.
Table 4 shows the optimal values defined for this method as those providing the greater intensity of the standards examined.

Instrument parameter	Value for negative ion mode	Value for positive ion mode
Drying gas temperature (°C)	230	230
Drying gas flow (L/min)	12	12
Nebulizer (psig)	35	35
Sheath gas temperature (°C)	350	350
Sheath gas flow (L/min)	12	12
VCap (V)	4000	3500
Nozzle Voltage (V)	1000	1000
Fragmentor (V)	150	150
Skimmer1 (V)	65	65
Octopole RF peak (V)	750	750

Table 4 **Instrument parameters**
Optimized instrument parameter defined for the untargeted lipidomic method.

5.3.1.2 Chromatographic separation

The choice of both stationary and mobile phases can influence the lipid chromatographic separation. The reversed-phase chromatography (C18 column) was chosen since it is the optimal method for lipid separation, and it is mainly based on interaction between hydrophobic stationary phase and acyl carbon chains of the lipids. Thus, lipid can be eluted according to their class and chain length and degree of unsaturation of constituent FA.

Moreover, mobile phase composition could influence ionization efficiency and specifically the mobile phase modifiers can facilitate molecule ionization.

To keep the concentration constant though the entire mobile phase gradient, in our method, the used concentrations of ammonium formate and formic acid, are the same for the mobile phase A and B. These modifiers allow the formation of three adducts of molecules ($[M+H]^+$, $[M+NH_4]^+$, $[M+Na]^+$) in positive ionization mode; while the formate adduct ($[M+HCOO]^-$) is formed in negative ion mode.

Moreover, two different flow rates were evaluated: 300 µl/min and 400 µl/min. Moreover, to obtain the best gradient for lipid separation, the time necessary to reach 100% of mobile phase B was tested as both 20 and 35 minutes. In **Figure 19** an example of two different gradients and their respective chromatograms are reported. For both methods, the time of the isocratic conditions was 5 minutes.

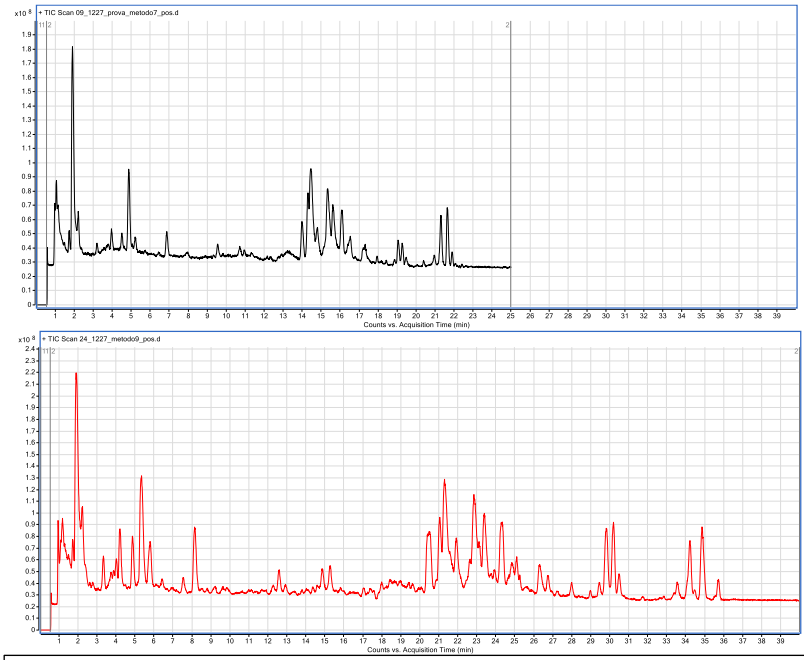

Time (min)	A (%)	B (%)
0	65	35
20	0	100
25	0	100
25.5	65	35
35	65	35

Table 5 **Gradient elution of the mobile phases**

Time (min)	A (%)	B (%)
0	65	35
35	0	100
40	0	100
40.1	65	35
50	65	35

Table 6 **Gradient elution of the mobile phases**

Figure 19 **Chromatographic separation optimization**
Representative chromatograms obtained by standard solution, applying different chromatographic gradient reported in Table 5 and Table 6. In black is represented the chromatogram obtained using a time of 20 min to reach 100% B. In red is represented the chromatogram obtained using a time of 35 min to reach 100% B.

A higher resolution and separation of the chromatographic peaks is observed using a longer time. However, a total running time of 50 min is extremely high and would make the sample analysis excessively long. So, to explore the possibility of shorting the run time, we analyze in detail the lipid elution. As shown in **Figure 20,** the chromatogram obtained running the standard solution in our chromatographic conditions, reveals that in the first 10 min., the most-polar lipids, like LPC and LPE elute, followed by MG. Then a highly crowded range between 10 and 20 min contain PL (PI, PS, PG, PA, PE, PC), and plasmenyl-PL, most of the SP such as SM and CER. In addition, DG are also observed in this range. Finally, in the retention time window from 20 to 27 min, CE and TG elute, the least-polar species. Thus, the method we developed applied a total run time of 27 min and it is a compromise between running time and chromatographic resolution so as to obtain an efficient lipid class separation allowing their identification.

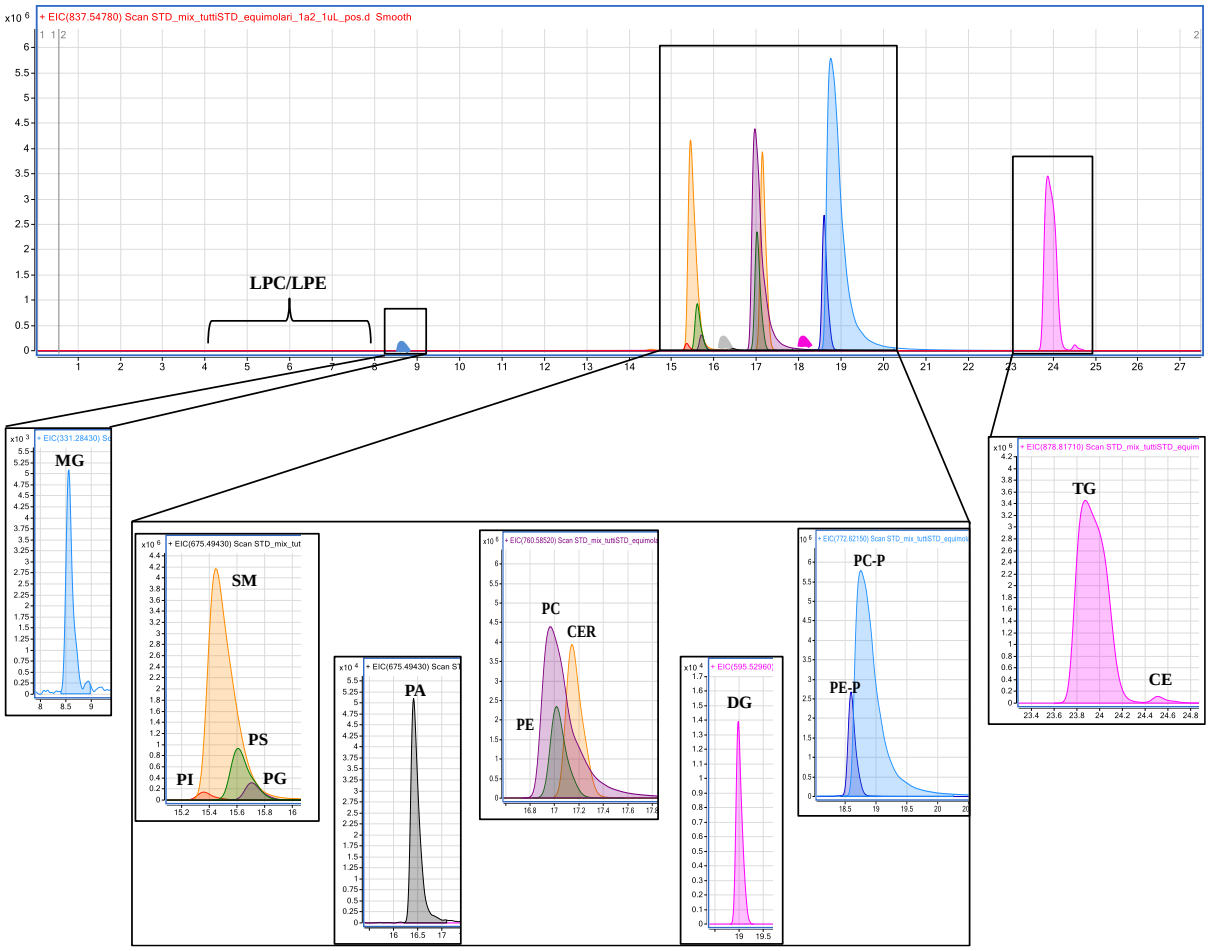

Figure 20 **Lipid classes separation**
Representative chromatogram obtained from the lipid standard solution showing lipid classes separation.
CE: cholesteryl ester; **CER:** ceramide; **DG:** diacylglycerol; **LPC:** lysophosphatidylcholine; **LPE:** lysophosphatidylethanolamine; **PA:** phosphatidic acid; **PC:** phosphatidylcholine; **PC-P:** plasmenyl-phosphatidylcholine; **PE:** phosphatidylethanolamine; **PE-P:** plasmenyl-phosphatidylethanolamine; **PG:** phosphatidylglycerol; **PI:** phosphatidylinositol; **PS:** phosphatidylserine; **MG:** Monoacylglycerol; **SM:** sphingomyelin; **TG:** triacylglycerol.

5.3.1.3 Reproducibility

The reproducibility of our method was tested injecting the same sample for 5 times in 5 consecutive days. As represented below, this method has good reproducibility in terms of both RT and peaks area. **Figure 21** shows chromatograms obtained from different injections of the same sample: their overlap demonstrates the high RT reproducibility. Moreover, a high peaks area reproducibility is revealed in **Figure 22** showing integration of a representative extracted compound for different injections of the same sample. The area of the two peaks related to PC (34:1) show a coefficient of variation (CV) below 10% (**Table 7**).

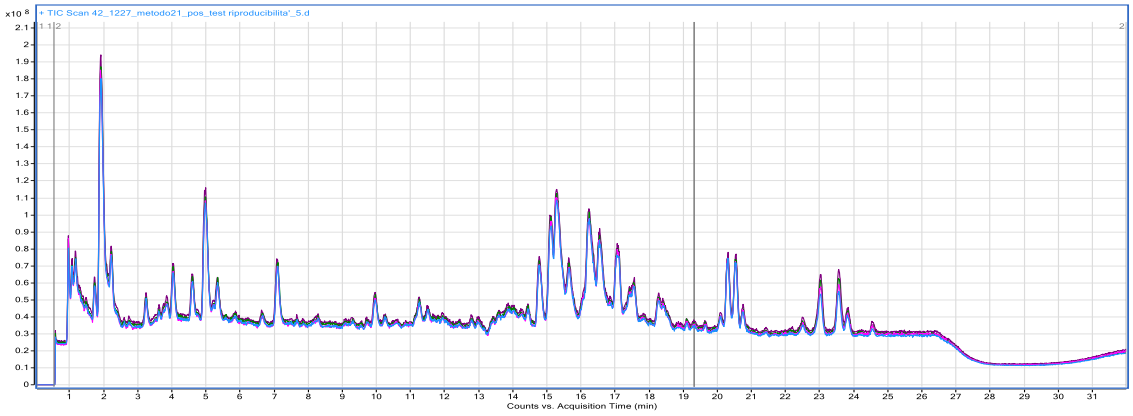

Figure 21 **Retention times reproducibility**
Chromatograms obtained from 5 different injections of the same sample in 5 consecutive days.

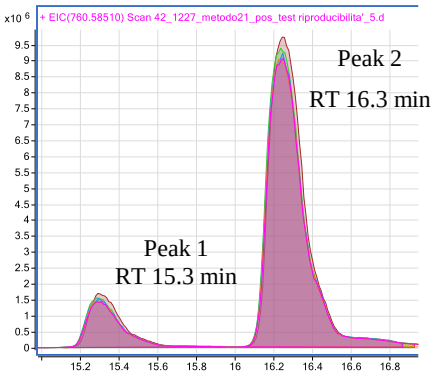

	Peak 1 RT 15.3 min	**Peak 2 RT 16.3 min**
Area mean	18804283	120887420
SD	1014173	3849438
CV%	5.4	3.2

Table 7 **Peak Area**

Figure 22 **Peak area reproducibility**
Integration of the two peaks related to phosphatidylcholine (34:1) for 5 different injections of the same sample in 5 consecutive days.

5.3.1.4 Cell amount

In order to establish the minimum cell number required for adequate lipid coverage, experiments were performed on monocyte samples obtained from 2 different subject. Specifically, samples containing 62500, 125000, 250000 and 500000 monocytes were collected.

An increased number of extracted compounds are observed according to the increased number of cells (**Figure 23**). Analysis of samples containing 500000 monocytes, allows good lipid coverage and enough intensity signal. Thus at least 500000 monocytes aliquots were collected for the untargeted lipidomic analysis.

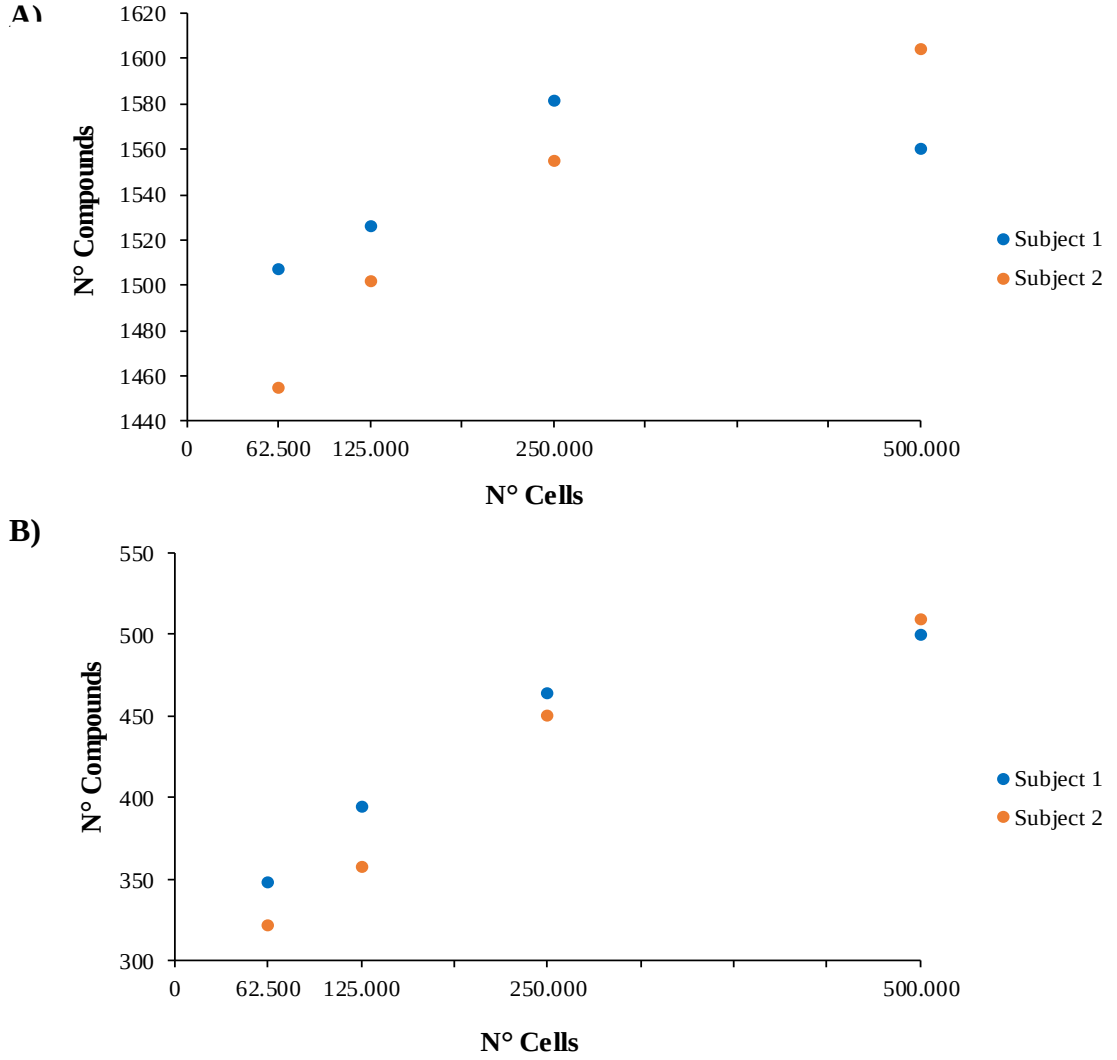

Figure 23 **Sample concentration**
Number of extracted compounds in samples containing 62500, 125000, 250000 and 50000 monocytes obtained from 2 different subject in A) positive and B) negative ionization mode.

5.3.2 Untargeted lipidomic analysis of monocytes

The untargeted method developed was applied to define the lipidomic profile of monocytes obtained from HV and CAD patients and to investigate difference in lipid metabolism.

5.3.2.1 Performance evaluation

The reproducibility of sample preparation and analysis was evaluated by QC samples approach. The total ion current (TIC) of QCs versus the order of injections (**Figure 24**) showed the good reproducibility of the system response during the whole LC-MS analysis both for positive (**panel A**) and negative (**panel B**) ion mode (CV 8.56% and 2.81% respectively). In addition, the TICs of sample replicates showed a very little intra-run variability and no drift was observed.

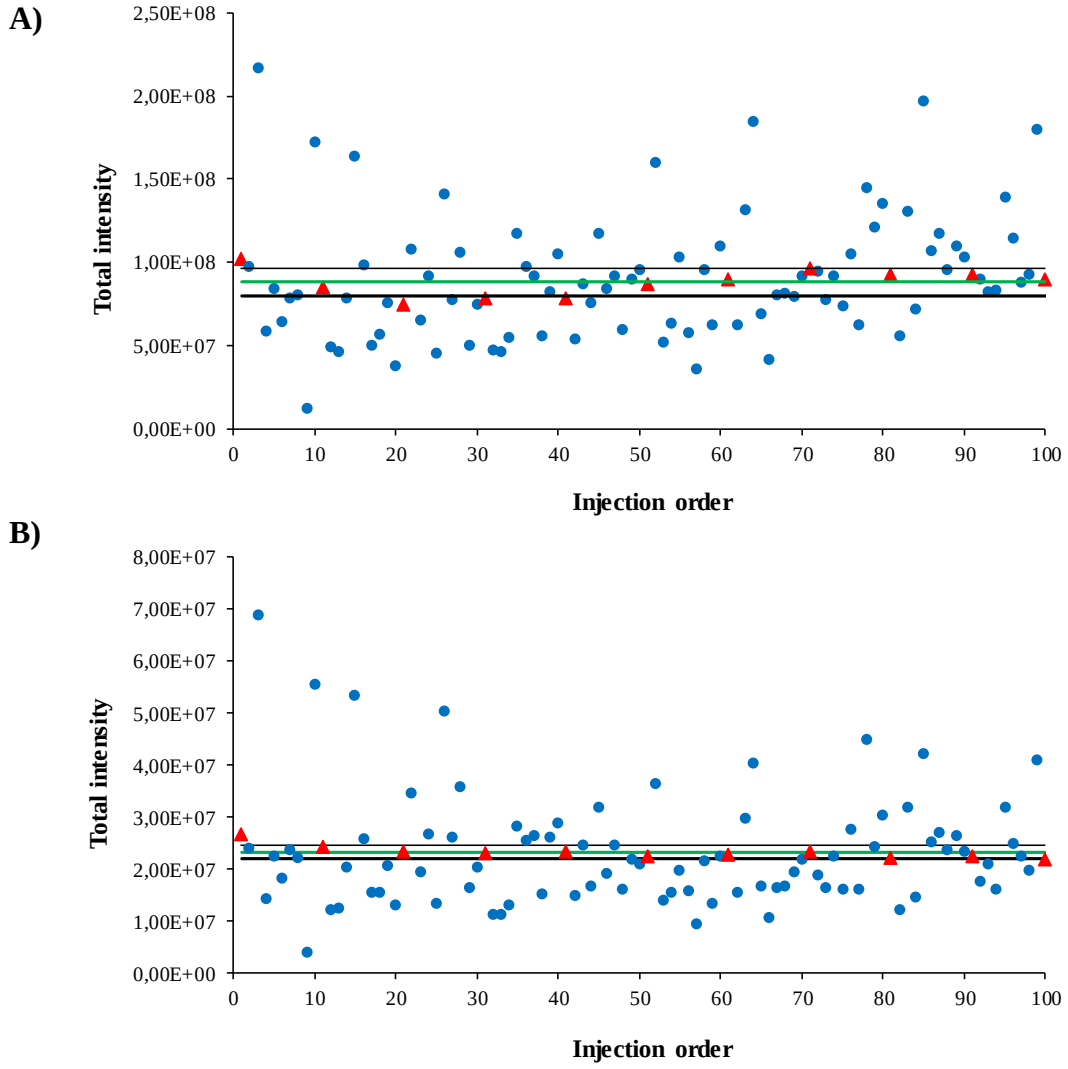

Figure 24 **Performance evaluation**
Total ion current (TIC) values over all observations (100 injections) in A) positive and B) negative ionization mode. Quality controls (QC) are represented by red triangles and samples by blue dots. The green line represents QCs' TIC mean value, the black lines ± standard deviation.

5.3.2.2 Data processing

Raw LC-MS chromatograms obtained from 89 monocyte samples, were processed to extract peak profiles of positive and negative ionization mode independently (**Figure 25**) and converted into two different data matrices.

A)

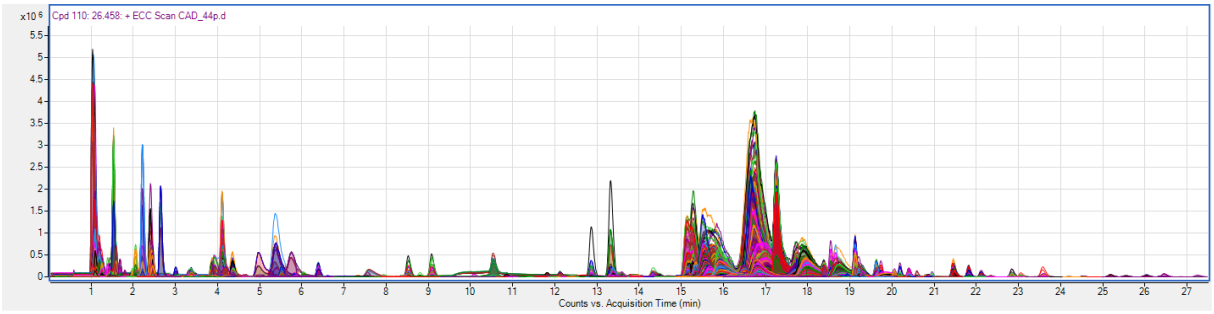

B)

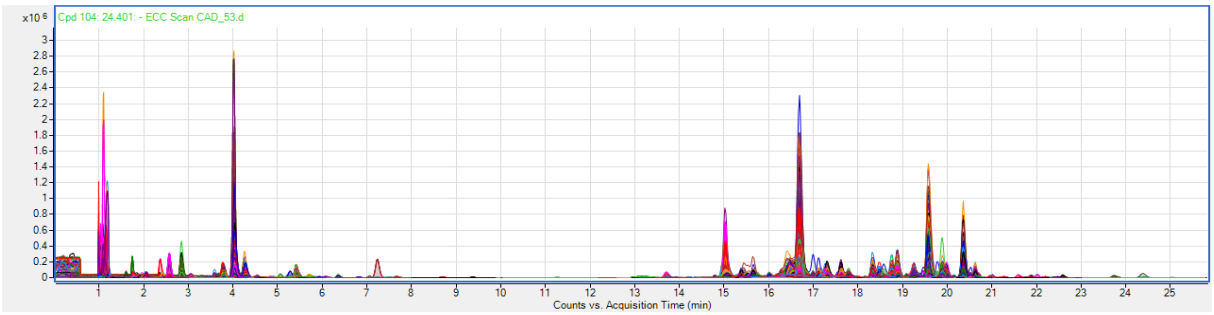

Figure 25 **Extracted compounds chromatograms**
Representative extracted compounds chromatograms obtained from a monocyte sample in A) positive and B) negative ionization mode. Abundance, expressed as counts, is reported on the Y-axis and time, expressed as minutes, on X-axis.

Specifically, the processing of the MS data results in a peak table in which every feature is characterized by m/z, RT, and intensity represented by the area under the peak. A total of 259 and 531 features were detected in positive and negative ionization mode, respectively, and among them, 137 and 323 features were annotated lipids. Identification was attributed by LipidMaps m/z and RT matching and by manual MS/MS spectrum confirmation with specific fragment pattern for different lipid classes as reported in **Appendix A.**

Only reliable lipids were considered for data analysis and statistics. Eleven lipids were removed from the dataset for the negative mode due to the high CV% across samples and to the missing values count >20%. In addition, a sample obtained from a STEMI patient was removed from the analysis in both ionization modes due to reduced lipid detection in this sample. The two define datasets included 137 and 312 lipids for positive and negative ionization mode respectively obtained from HV, n=27, SA, n=20, NSTEMI, n=21 and STEMI, n=20 monocytes samples.

5.3.2.3 Monocyte lipidomic profile

The complete lists of lipids identified are reported in **Appendix B** for positive (**Table B1**) and negative (**Table B2**) ionization mode respectively. Collectively, the following lipid classes were detected: PL as PC (including PC-P and PC-O), PE (including PE-P and PE-O), PG, PS, and PI; LPL (including LPC, LPE, and LPI); SP as SM and CER (including HexCer and LacCer), and TAG. Specifically, PL were detected in both ionization mode due to their amphoteric properties, TAG were only observed in positive ionization mode while CER better ionized in negative mode. In addition, Sph and Cho were also detected (**Figure 26**).

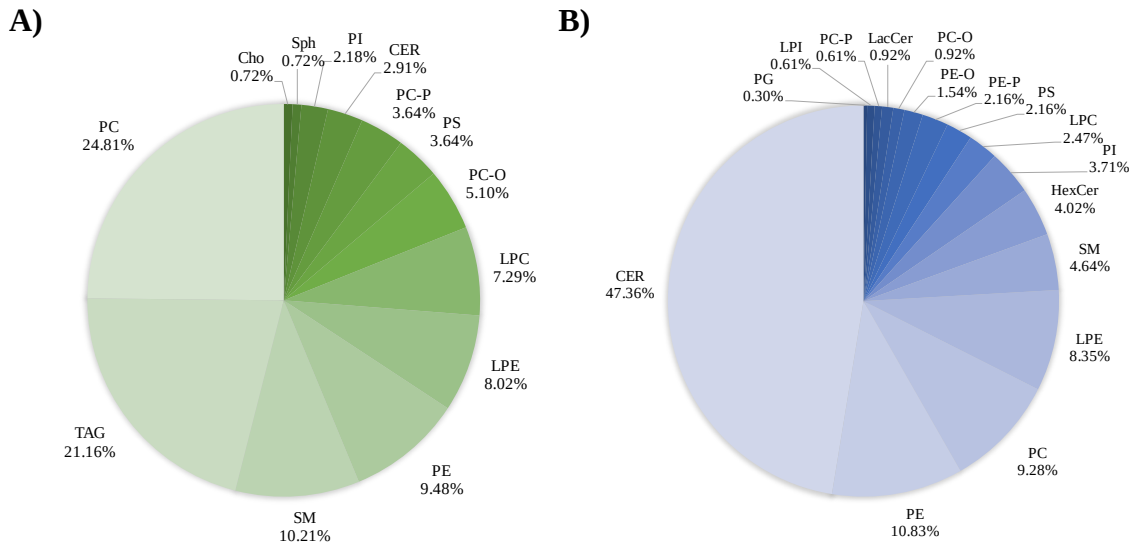

Figure 26 **Lipid classes detected**
Pie chart of the lipid classes detected in A) positive and B) negative ionization mode.
CER: ceramide; **Cho:** cholesterol; **HexCer:** hexosylceramide; **LacCer:** lactosylceramide; **LPC:** lysophosphatidylcholine; **LPE:** lysophosphatidylethanolamine; **LPI:** lysophosphatidylinositol; **PC:** phosphatidylcholine; **PC-O:** plasmanyl-phosphatidylcholine; **PC-P:** plasmenyl-phosphatidylcholine; **PE:** phosphatidylethanolamine; **PE-O:** plasmanyl-phosphatidylethanolamine; **PE-P:** plasmenyl-phosphatidylethanolamine; **PG:** phosphatidylglycerol; **PI:** phosphatidylinositol**; PS:** phosphatidylserine; **SM:** sphingomyelin; **Sph:** sphingosine; **TAG:** triacylglycerol.

The two datasets were first subjected to PCA analysis (**Figure 27**) in order to give a comprehensive view of the clustering trend of the analyzed samples obtained from the four study groups. The first two PCA components explained 22.48% and 12.08% of the total variance for positive ion mode, 17.83% and 13.97% for negative ion mode. The PCA score plots revealed a clustering distribution of samples obtained by HS (grey dots) against CAD samples and it appear to be more prominent in positive detection mode (**panel A**). In contrast, not a clear separation is observed among SA, NSTEMI and STEMI samples for both ionization modes.

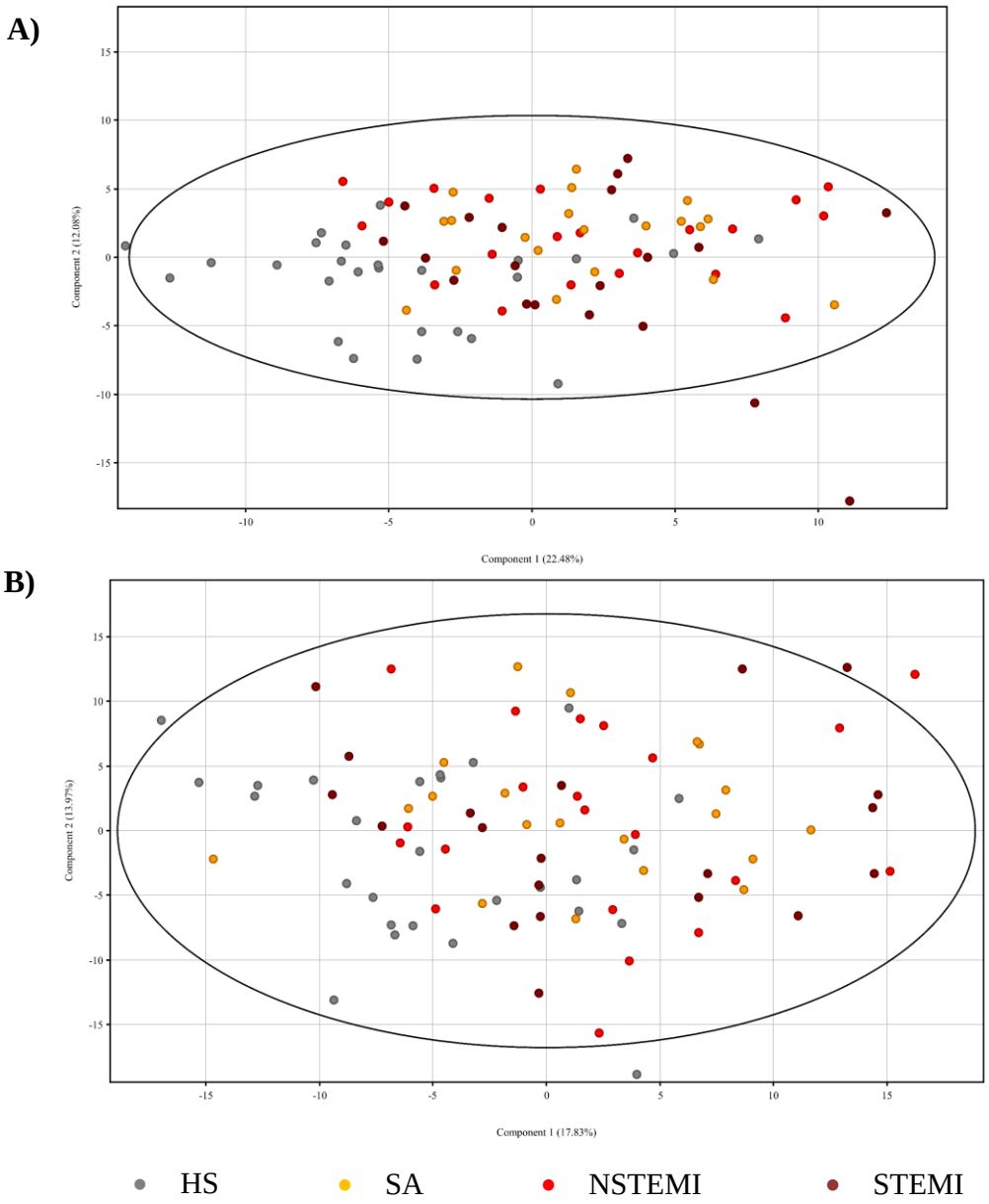

Figure 27 **Principal component analysis score plots**
Score plots of principal component analysis (PCA) models in A) positive and B) negative ionization modes showing the clustering trend of the analysed samples obtained from healthy subjects (HS, n=27), and coronary artery disease (CAD, n= 61) patients including patients with stable angina (SA, n=20), non-ST elevation myocardial infarction (NSTEMI, n=21) and ST elevation myocardial infarction (STEMI, n=20) patients.

Heatmaps as graphical representation of the differential expression of each lipid averaged for the study population were then generated (**Figure 28**). For the positive dataset (**panel A**), the up-regulation of TAG in HS against all the CAD groups is the most prominent result. In addition, LPC and partly LPE, appear strongly up-regulated in STEMI, compared to HS. On the contrary, PC and to a lesser extent PE are down-regulated in STEMI against HS. For these lipid species, SA and NSTEMI seem to show an intermediate expression between the two extreme conditions HS and STEMI. Regarding the negative ionization mode (**panel B**), CER show a clear down-regulation in STEMI compared to HS while SA and NSTEMI appear to be transitional state between the two groups. Moreover, PI and PS are strongly up regulated in STEMI patients.

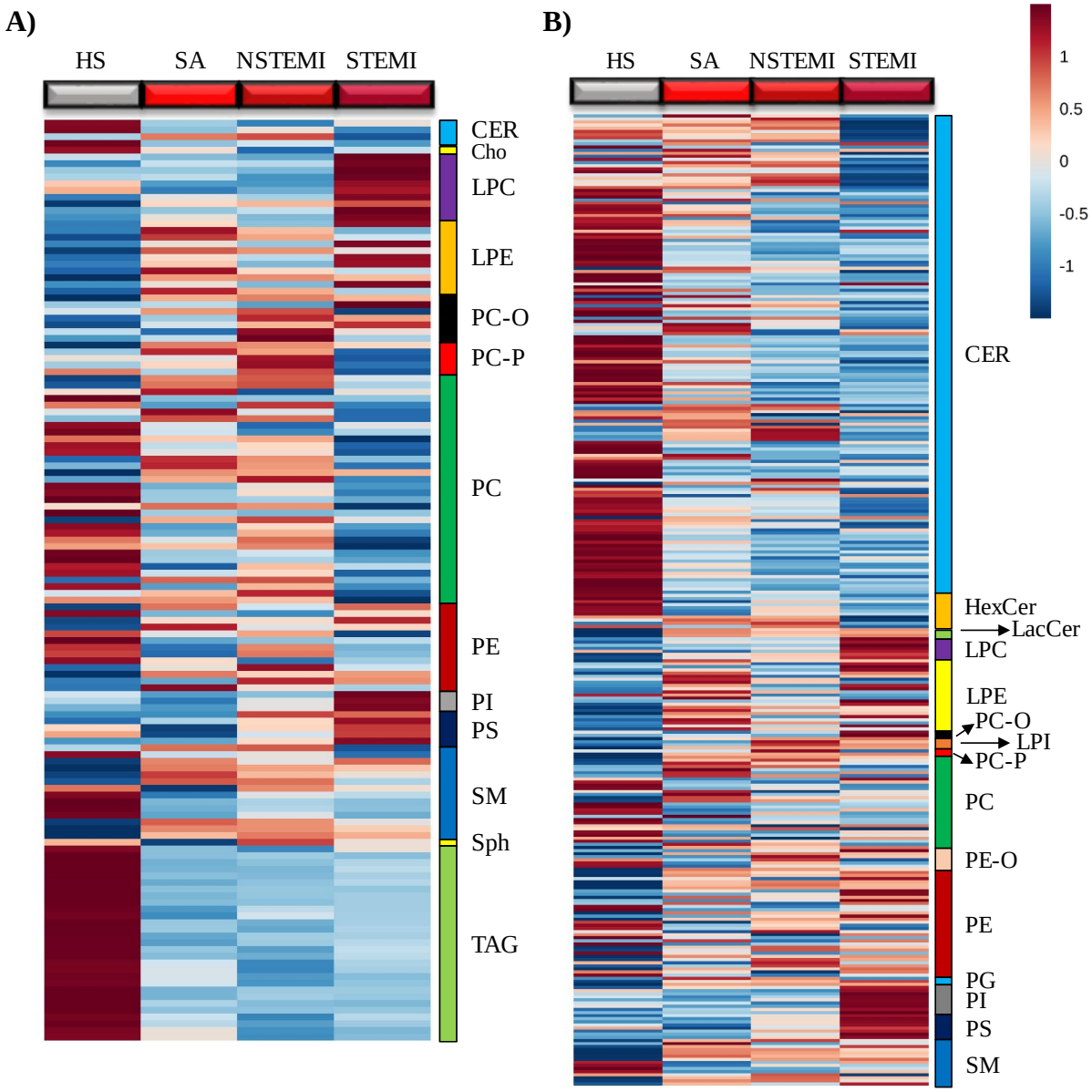

Figure 28 **Heatmap analysis**
Heatmaps showing a graphic representation of the differences in relative lipids expression among healthy subjects (HS), patients with stable angina (SA), non-ST elevation myocardial infarction (NSTEMI) and ST elevation myocardial infarction (STEMI) patients in A) positive and B) negative ionization mode. The colour is correlated with the intensity of the lipid expression, with red indicating up-regulation and blue indicating down-regulation.
CER: ceramide; **Cho:** cholesterol; **HexCer:** hexosylceramide; **LacCer:** lactosylceramide; **LPC:** lysophosphatidylcholine; **LPE:** lysophosphatidylethanolamine; **LPI:** lysophosphatidylinositol; **PC:** phosphatidylcholine; **PC-O:** plasmanyl-phosphatidylcholine; **PC-P:** plasmenyl-phosphatidylcholine; **PE:** phosphatidylethanolamine; **PE-O:** plasmanyl-phosphatidylethanolamine; **PE-P:** plasmenyl-phosphatidylethanolamine; **PG:** phosphatidylglycerol; **PI:** phosphatidylinositol**; PS:** phosphatidylserine; **SM:** sphingomyelin; **Sph:** sphingosine; **TAG:** triacylglycerol.

5.3.2.4 Statistical analysis

For statistical analysis, ANOVA test performed using one-way, followed by the Benjamini-Hochberg multiple testing correction, showed 60 (positive ion mode) and 74 (negative ion mode) lipids significantly dysregulated among the four study groups (**Figure 29**)

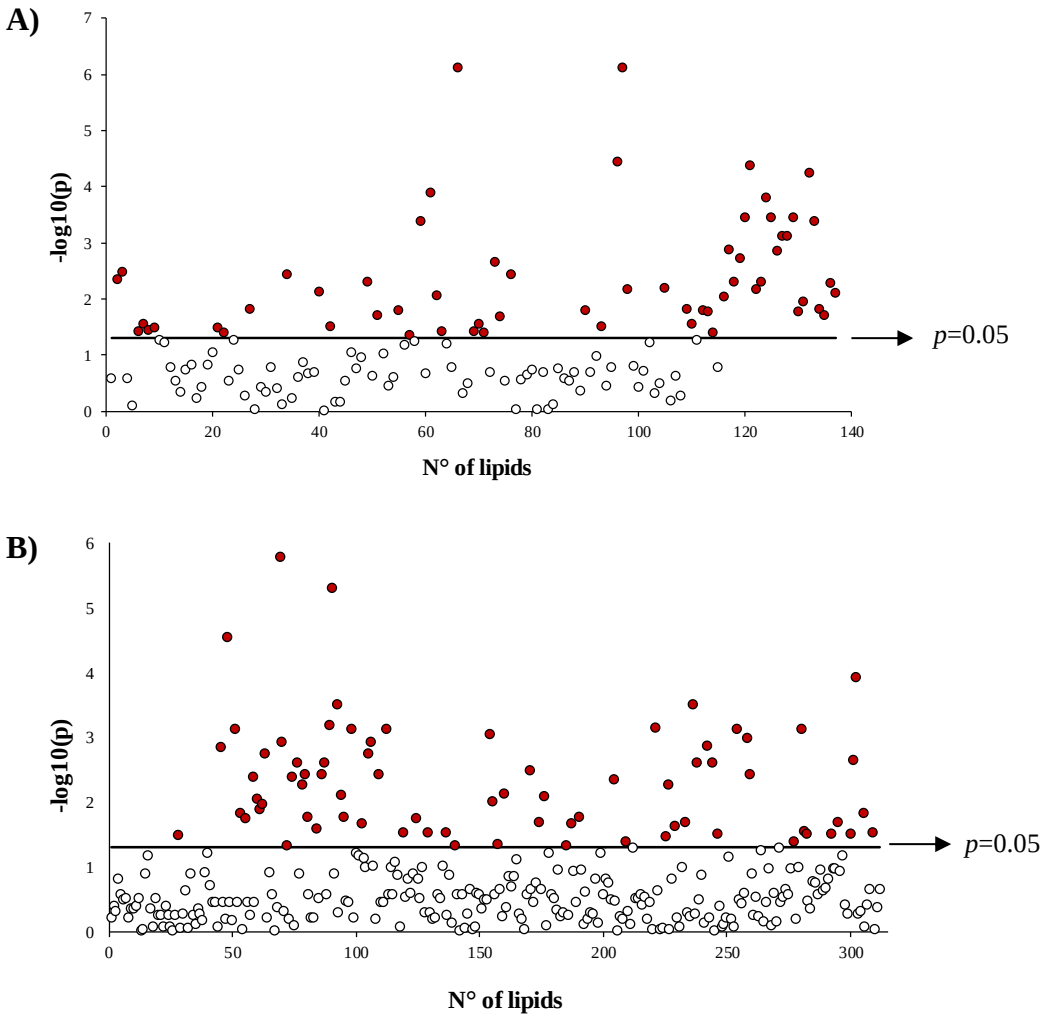

Figure 29 **One-way analysis of variance**
Graphical representation of the results obtained after one-way analysis of variance (ANOVA) test for the dataset in A) positive and B) negative ion mode. On the y-axis -log10(*p*) is reported. The dots represent the lipids and the red colour highlights the lipids significantly regulated ($p < 0.05$; -log10(*p*)>1.3). Black lines represent -log10(p)=1.3 cut off.

For the analysis in positive mode (**Table 5**), mainly TAG, followed by PC, are significantly dysregulated among HS and CAD patients. Others PL that significantly differ are PE and PS. In addition, among LPL, LPE and LPC are observed. SM is another lipid class that is modified.

Lipid	adj *p* *	Pairwise test #	Lipid	adj *p* *	Pairwise test #
CER	0.0044	αβγ	SM (d34:1) [M+H]+	<0.0001	αβγ
CER (d42:1) $[M+H]^+$	0.0032	αγ	SM (d34:1) $[M+Na]^+$	0.0066	βγ
LPC 16:0 $[M+H]^+$	0.0382	-	SM (d42:2) $[M+H]^+$	0.0063	βγ
LPC 16:0 $[M+H]^+$	0.0282	α	TAG 44:0 $[M+Na]^+$	0.0150	βγ
LPC 18:1 $[M+H]^+$	0.0349	-	TAG 44:0 $[M+NH_4]^+$	0.0271	αγ
LPC 18:1 $[M+H]^+$	0.0326	α	TAG 46:0 $[M+Na]^+$	0.0161	βγ
LPE 22:4 $[M+H]^+$	0.0326	α	TAG 46:0 $[M+NH_4]^+$	0.0170	αβγ
LPE 22:5 $[M+H]^+$	0.0405	α	TAG 47:0 $[M+Na]^+$	0.0386	γ
PC (O-32:O) (O-16:0/16:0) $[M+H]^+$	0.0153	αβγ	TAG 48:0 $[M+Na]^+$	0.0088	αβγ
PC (P-34:0) (P-18:0/16:0) $[M+H]^+$	0.0036	αβγ	TAG 48:0 $[M+NH_4]^+$	0.0012	αβγ
PC 32:0 (16:0/16:0) $[M+Na]^+$	0.0073	βγ	TAG 50:0 (16:0/16:0/18:0) $[M+Na]^+$	0.0048	αβγ
PC 33:1 $[M+H]^+$	0.0314	γ	TAG 50:0 (16:0/16:0/18:0) $[M+NH_4]^+$	0.0018	αβγ
PC 36:1 (18:0/18:1) $[M+H]^+$	0.0048	α	TAG 50:1 (16:0/16:0/18:1) $[M+Na]^+$	0.0003	αβγ
PC 36:2 (18:1/18:1) $[M+H]^+$	0.0195	γ	TAG 50:1 (16:0/16:0/18:1) $[M+NH_4]^+$	<0.0001	αβγ
PC 36:4 (16:0/20:4) $[M+H]^+$	0.0161	αγ	TAG 52:0 (16:0/18:0/18:0) (16:0/16:0/20:0) $[M+NH4]^+$	0.0067	αβγ
PC 36:4 (18:2/18:2) $[M+H]^+$	0.0447	α	TAG 52:0 (16:0/18:0/18:0) (16:0/18:0/20:0) $[M+Na]^+$	0.0048	αβγ
PC 38:3 (18:0/20:3) $[M+H]^+$	0.0004	αβγ	TAG 52:1 (16:0/18:0/18:1) $[M+Na]^+$	0.0001	αβγ
PC 38:4 (18:0/20:4) $[M+H]^+$	0.0001	α	TAG 52:1 (16:0/18:0/18:1) $[M+NH_4]^+$	0.0003	αβγ
PC 38:4 (18:0/20:4) $[M+Na]^+$	0.0087	αγ	TAG 52:2 (16:0/18:1/18:1) $[M+Na]^+$	0.0013	αβγ
PC 38:5 (16:0/22:5)(18:1/20:4) $[M+Na]^+$	0.0368	αγ	TAG 52:2 (16:0/18:1/18:1) $[M+NH_4]^+$	0.0007	αβγ
PC 38:6 (18:2/20:4) $[M+H]^+$	<0.0001	αβγ	TAG 52:3 (16:0/18:1/18:2) $[M+Na]^+$	0.0007	αβγ
PC 40:5 (18:1/22:4) $[M+H]^+$	0.0372	β	TAG 52:3 (16:0/18:1/18:2) $[M+NH_4]^+$	0.0003	αβγ
PC 40:6 (18:0/22:6) $[M+H]^+$	0.0271	αγ	TAG 54:0 (18:0/18:0/18:0) $[M+Na]^+$	0.0170	αβγ
PC 40:6 (18:1/22:5)) $[M+H]^+$	0.0405	-	TAG 54:0 (18:0/18:0/18:0) $[M+NH_4]^+$	0.0109	αβγ
PE 34:1 (16:0/18:1) $[M+H]^+$	0.0022	αγ	TAG 54:1 (18:0/18:0/18:1) (16:0/18:1/20:0) $[M+NH_4]^+$	<0.0001	αβγ
PE 36:1 (18:0/18:1) $[M+H]^+$	0.0207	βγ	TAG 54:1 (18:0/18:0/18:1) $[M+Na]^+$	0.0004	αβγ
PE 36:2 (18:1/18:1) $[M+H]^+$	0.0036	γ	TAG 54:2 (18:0/18:1/18:1) (16:0/18:1/20:1) $[M+NH4]^+$	0.0153	β
PS 36:2 (18:0/18:2) (18:1/18:1) $[M+H]^+$	0.0161	α	TAG 54:2 (18:0/18:1/18:1) $[M+Na]^+$	0.0195	αβ
PS 40:5 (18:0/22:5) $[M+H]^+$	0.0299	α	TAG 54:3 (18:1/18:1/18:1) $[M+Na]^+$	0.0051	αβ
SM (d34:0) $[M+H]^+$	<0.0001	αβγ	TAG 54:3 (18:1/18:1/18:1) $[M+NH_4]^+$	0.0077	αβ

Table 5 **One-way analysis of variance for positive dataset**
List of lipids significantly regulated among healthy subjects (HS), patients with stable angina (SA), non-ST elevation myocardial infarction (NSTEMI) and ST elevation myocardial infarction (STEMI) patients.
*: adjusted *p*-value obtained from one-way analysis (ANOVA) and Benjamini-Hochberg multiple testing correction
#: pairwise comparison after post hoc Tukey Honest significant difference
α: STEMI *vs* HS
β: NSTEMI *vs* HS
γ: SA *vs* HS

CER: ceramide; **LPC:** lysophosphatidylcholine; **LPE:** lysophosphatidylethanolamine; **PC:** phosphatidylcholine; **PC-O:** plasmanyl-phosphatidylcholine; **PC-P:** plasmenyl-phosphatidylcholine; **PE:** phosphatidylethanolamine; **PS:** phosphatidylserine; **SM:** sphingomyelin; **TAG:** triacylglycerol.

Concerning the negative dataset (**Table 6**), CER is the class that appears mainly dysregulated and specifically LacCer but not HexCer has a significantly different expression in the study groups. Moreover, PC and PE and the corresponding lyso forms LPC and LPE show a significant variation. Other lipid classes that result after the ANOVA test are PI, PS and SM.

Lipid	adj *p* *	Pairwise test #	Lipid	adj *p**	Pairwise test #
CER (d39:1) $[M+HCOO]^-$	0.0013	αβγ	CER (t42:0) $[M+Cl]^-$	0.0172	α
CER (d39:1) $[M+HCOONH_4]^-$	0.0127	αβγ	CER (t42:0) $[M+HCOO]^-$	0.0017	αβγ
CER (d40:0) $[M+Cl]^-$	0.0146	α	LacCer (d34:1) (d18:1/16:0) $[M+Cl]^-$	0.0008	αβγ
CER (d40:0) $[M+HCOO]^-$	0.0088	αβγ	LacCer (d34:1) (d18:1/16:0) $[M+HCOO]^-$	0.0098	αβγ
CER (d40:0) $[M+HCOO]^-$	0.0073	αβγ	LacCer (d34:1) (d18:1/16:0) $[M+HCOONH_4]^-$	0.0452	αβγ
CER (d40:0) $[M+HCOONH_4]^-$	0.0172	αβ	LPC 16:0 $[M+HCOO]^-$	0.0031	α
CER (d40:1) $[ADDUCT]^-$	0.0287	αγ	LPC 18:1 $[M+HCOO]^-$	0.0201	α
CER (d40:1) $[M+Cl]^-$	0.0007	αβγ	LPC 20:4 $[M+HCOO]^-$	0.0079	αγ
CER (d40:1) $[M+HCOO]^-$	0.0040	αβγ	LPE 22:4 $[M-H]^-$	0.0172	α
CER (d40:1) $[M+HCOONH_4]^-$	0.0024	αβγ	LPE 22:5 $[M-H]^-$	0.0211	βγ
CER (d40:2) $[M+Cl]^-$	<0.0001	αβγ	LPE 22:6 $[M-H]^-$	0.0473	α
CER (d40:2) $[M+HCOO]^-$	0.0179	αβγ	PC (P-34:O) (P-18:0/16:0) $[M+HCOO]^-$	0.0044	αβγ
CER (d40:2) $[M+HCOONH_4]^-$	0.0011	αβγ	PC 36:3 (16:0/20:3) $[ADDUCT]^-$	0.0230	γ
CER (d41:0) $[M+Cl]^-$	0.0017	αβγ	PC 36:4 (16:0/20:4)(18:2/18:2) $[M+HCOO]^-$	0.0402	γ
CER (d41:0) $[M+HCOO]^-$	0.0041	αβγ	PC 38:4 (18:0/20:4) $[ADDUCT]^-$	0.0201	αγ
CER (d41:0) $[M+HCOONH_4]^-$	0.0003	αβγ	PC 38:4 (18:0/20:4) $[M+HCOO]^-$	0.0006	αβγ
CER (d41:1) $[ADDUCT]^-$	0.0287	αβ	PC 40:6 (18:1/22:5) / (18:0/22:6) $[M+HCOO]^-$	0.0052	αγ
CER (d41:1) $[M+Cl]^-$	0.0105	αβ	PC 40:7 (18:1/22:6) $[M+HCOO]^-$	0.0333	γ
CER (d41:1) $[M+HCOO]^-$	<0.0001	αβγ	PE (O-38:5) (O-16:0/22:5) $[M-H]^-$	0.0302	βγ
CER (d41:1) $[M+HCOONH_4]^-$	<0.0001	αβγ	PE 32:0 (16:0/16:0) $[M-H]^-$	0.0003	αβγ
CER (d41:2) $[M+HCOONH_4]^-$	0.0024	αβγ	PE 34:1 (16:0/18:1) $[ADDUCT]^-$	0.0010	αβγ
CER (d42:0) $[ADDUCT]^-$	0.0460	α	PE 34:1 (16:0/18:1) $[M-H]^-$	0.0024	αβγ
CER (d42:0) $[M+HCOO]^-$	0.0006	αβγ	PE 36:1 (18:0/18:1) $[M-H]^-$	0.0024	αβγ
CER (d42:0) $[M+HCOONH_4]^-$	0.0011	αβγ	PE 36:2 (18:1/18:1) $[M-H]^-$	0.0013	αβγ
CER (d42:1) $[M+Cl]^-$	0.0054	αβγ	PE 36:2 $[ADDUCT]^-$	0.0402	α
CER (d42:1) $[M+HCOO]^-$	0.0037	αβγ	PE 38:2 (18:1/20:1) $[M-H]^-$	0.0007	αβγ
CER (d42:2) $[ADDUCT]^-$	0.0287	-	PE 40:7 (18:1/22:6) $[M-H]^-$	0.0037	αβγ
CER (d42:2) $[M+Cl]^-$	0.0460	γ	PI 36:1 (18:0/18:1) $[M-H]^-$	0.0303	α
CER (d42:2) $[M+HCOO]^-$	0.0260	βγ	PI 36:2 (18:1/18:1) $[M-H]^-$	0.0007	αβγ
CER (d43:0) $[M+HCOO]^-$	0.0211	β	PI 36:2 (18:1/18:1) $[M-H]^-$	0.0280	α
CER (d43:1) $[M+HCOO]^-$	0.0007	αβγ	PS 36:1 (18:0/18:1) $[M-H]^-$	0.0302	α
CER (d43:1) $[M+HCOONH_4]^-$	0.0007	αβγ	PS 40:6 (18:0/22:6) $[M-H]^-$	0.0201	α
CER (d44:1) $[M+HCOO]^-$	0.0036	αβγ	SM (d34:0) $[M+HCOO]^-$	0.0001	αβγ
CER (d44:1) $[M+HCOONH_4]^-$	0.0179	βγ	SM (d34:1) $[ADDUCT]^-$	0.0146	βγ
CER (t34:1) $[M+HCOONH_4]^-$	0.0326	γ	SM (d34:1) $[M+HCOO]^-$	0.0022	αβγ
CER (t40:0) $[M+HCOO]^-$	0.0037	αβ	SM (d34:2) $[M+HCOO]^-$	0.0302	γ
CER (t40:0) $[M+HCOONH_4]^-$	0.0077	α	SM (d42:2) $[M+HCOO]^-$	0.0287	βγ

Table 6 **One-way analysis of variance for negative dataset**

List of lipids significantly regulated among healthy subjects (HS), patients with stable angina (SA), non-ST elevation myocardial infarction (NSTEMI) and ST elevation myocardial infarction (STEMI) patients.

*: adjusted *p*-value obtained from one-way analysis (ANOVA) and Benjamini-Hochberg multiple testing correction

#: pairwise comparison after post hoc Tukey Honest significant difference

α: STEMI *vs* HS

β: NSTEMI *vs* HS

γ: SA *vs* HS

CER: ceramide; **LacCer:** lactosylceramide; **LPC:** lysophosphatidylcholine; **LPE:** lysophosphatidylethanolamine; **PC:** phosphatidylcholine; **PC-P:** plasmenyl-phosphatidylcholine; **PE:** phosphatidylethanolamine; **PE-O:** plasmanyl-phosphatidylethanolamine; **PI:** phosphatidylinositol**; PS:** phosphatidylserine; **SM:** sphingomyelin.

Specifically, the performed post hoc Tukey HSD highlights the STEMI *vs* HS, NSTEMI *vs* HS and SA *vs* HS as significant pairwise comparisons in both ionization modes. On the contrary, no lipids appear to be a potential discriminating factor among the patient groups.

In **Figure 30**, the Venn diagrams highlighting the number of lipids that characterize significant pairwise comparisons are depicted. Most of the lipids are common to the three pairwise comparisons: 26 lipids belonging to the CER (and among them LacCer) and PE classes for positive and 39, mainly TAGs for negative ion mode. Considering the single comparison, STEMI *vs* HS is characterized by the highest number of lipids (9 and 13 for the positive and negative modes, respectively). These lipids belong mainly to the LPL (LPC and LPE) and PS lipid classes. Moreover, this result is observed in both datasets. In addition, some PC (for the positive mode) and some CER (for the negative mode) are evidenced. A lower number of lipids characterizes the NSTEMI *vs* HS and SA *vs* HS comparisons.

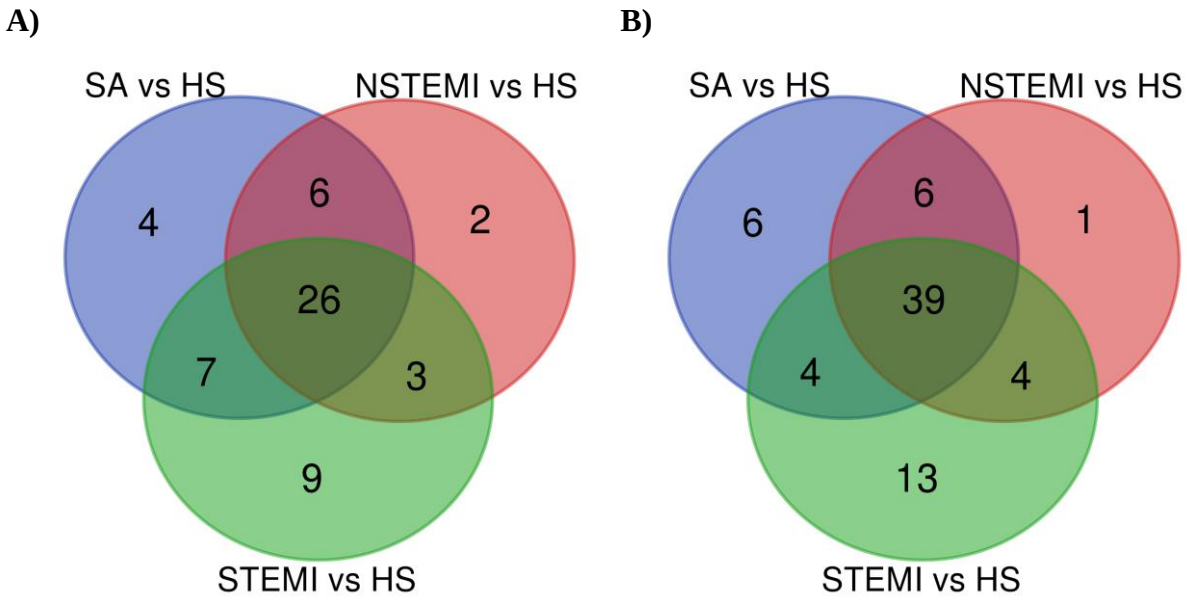

Figure 30 **Venn diagrams**
Venn diagrams of the differentially expressed lipids resulting from the pairwise comparison of STEMI *vs* HS, NSTEMI *vs* HS and SA *vs* HS in A) positive and B) negative ion mode.
HS: healthy subjects; **NSTEMI**: non-ST elevation myocardial infarction patients; **SA**: stable angina patients; **STEMI**: ST elevation myocardial infarction patients.

Overall, the results obtained by the ANOVA test suggest that the lipid composition of monocytes is substantially different between patients and healthy subjects, but it is not possible to highlight particular differences among the three pathological conditions. Moreover, these statistical results are consistent with the results obtained by the PCA analysis.

In order to highlight the major differences in terms of lipid composition of monocytes obtained from healthy subjects and pathological subjects, SA, NSTEMI and STEMI patients were combined into a single group (CAD) and volcano plot analysis was performed (**Figure 31**).

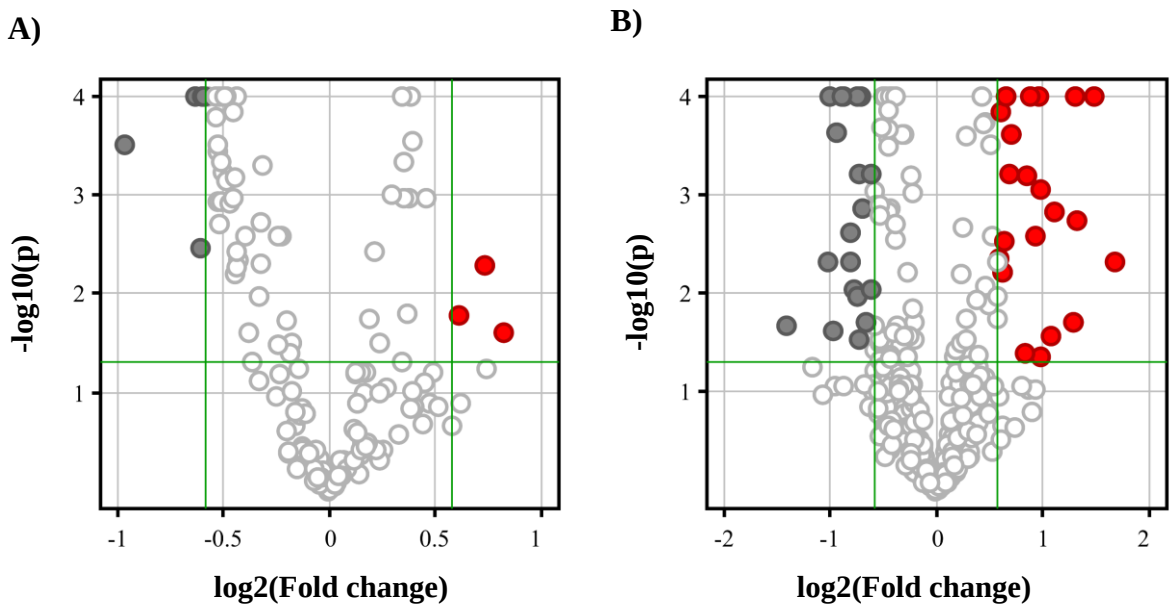

Figure 31 **Volcano plot analysis**
Graphical representation of the results obtained after volcano plot analysis for the dataset in A) positive and B) negative ion mode. On the y-axis, -log10(p) is reported. On the x-axis, log2(Fold change) is reported. The dots represent the lipids. The red colour highlights the lipids significantly up-regulated in patients ($p < 0.05$; -log10(p)>1.3 and fold change > 1.5; log2(Fold change) > 0.58). The grey colour highlights the lipids significantly up-regulated in healthy subjects ($p < 0.05$; -log10(p)>1.3 and fold change < 1.5; log2(Fold change) < 0.58). Green lines represent -log10(p)=1.3 and log2(Fold change) = 0.58 cut offs.

After Moderate t-test followed by Benjamini-Hochberg multiple testing correction and by applying a FC cut off of 1.5, 8 and 40 lipids for positive and negative ionization mode respectively, are significantly dysregulated between CAD and HS groups. Specifically, among the 8 lipids for the positive mode, 3 LPE are up-regulated in patients (FC >1.5) while the others including 2 TAG, PE, PC and CER show increased expression in HS (**Table 7**).

Lipid	adj *p* *	FC#	Lipid	adj *p* *	FC#
CER	0.0003	-1.95	PC 38:6 (18:2/20:4) $[M+H]^+$	<0.0001	-1.54
LPE 22:4 $[M+H]^+$	0.0164	1.52	PE 36:1 (18:0/18:1) $[M+H]^+$	0.0035	-1.52
LPE 22:4 $[M+H]^+$	0.0246	1.76	TAG 50:1 (16:0/16:0/18:1) $[M+Na]^+$	<0.0001	-1.51
LPE 22:5 $[M+H]^+$	0.0052	1.66	TAG 52:3 (16:0/18:1/18:2) $[M+NH_4]^+$	<0.0001	-1.50

Table 7 **Volcano plot analysis for positive dataset**
List of lipids significantly regulated between healthy subjects (HS) and coronary artery disease (CAD) patients.
*: adjusted *p*-value obtained from moderate t-test and Benjamini-Hochberg multiple testing correction
#: fold change (FC) calculated comparing CAD *vs* HS

CER: ceramide; **LPE:** lysophosphatidylethanolamine; **PC:** phosphatidylcholine; P**E:** phosphatidylethanolamine; **TAG**: triacylglycerol

On the other hand, 21 lipids are up-regulated in CAD while 19 are up-regulated in HS for the negative ionization mode. All CER, except for CER (d40:0) $[M+HCOO]^-$ and CER (t42:0) $[M+HCOONH_4]^-$ appear to be increased in HS. On the contrary all the 3 adducts of LacCer (d34:1) are significantly higher in CAD. In addition, PC, PE and their lyso form LPC and LPE characterize CAD patients. In addition, PI 36:2 (18:1/18:1) $[M-H]^-$, PS 40:4 (18:0/20:4) $[M-H]^-$, and SM (d34:2) $[M+HCOO]^-$ show a FC >1.5 (**Table 8**).

Lipid	adj *p* *	FC#	Lipid	adj *p* *	FC#
CER (d39:1) $[M+Cl]^-$	0.0092	-1.69	LacCer (d34:1) (d18:1/16:0) $[M+Cl]^-$	<0.0001	1.96
CER (d39:1) $[M+HCOO]^-$	<0.0001	-1.63	LacCer (d34:1) (d18:1/16:0) $[M+HCOO]^-$	0.0006	1.61
CER (d40:0) $[M+Cl]^-$	0.0024	-1.75	LacCer (d34:1) (d18:1/16:0) $[M+HCOONH_4]^-$	0.0045	1.50
CER (d40:0) $[M+HCOO]^-$	0.0006	-1.66	LPC 16:0 $[M+HCOO]^-$	0.0018	2.51
CER (d40:0) $[M+HCOO]^-$	0.0006	1.80	LPC 18:1 $[M+HCOO]^-$	0.0270	2.12
CER (d40:0) $[M+HCOONH_4]^-$	0.0014	-1.61	LPC 20:4 $[M+HCOO]^-$	0.0008	1.98
CER (d41:0) $[M+Cl]^-$	<0.0001	-1.82	LPE 22:4 $[M-H]^-$	0.0048	3.19
CER (d41:0) $[M+HCOO]^-$	0.0002	-1.91	LPE 22:5 $[M-H]^-$	0.0014	2.16
CER (d41:0) $[M+HCOONH_4]^-$	<0.0001	-1.66	LPE 22:6 $[M-H]^-$	0.0436	1.96
CER (d41:1) $[ADDUCT]^-$	0.0195	-1.57	PC (P-34:0) (P-18:0/16:0) $[M+HCOO]^-$	0.0002	1.62
CER (d42:0) $[ADDUCT]^-$	0.0048	-2.01	PC 36:3 (16:0/20:3) $[ADDUCT]^-$	0.0026	1.91
CER (d42:0) $[M+HCOO]^-$	<0.0001	-1.99	PE 32:0 (16:0/16:0) $[M-H]^-$	<0.0001	2.79
CER (d42:0) $[M+HCOONH_4]^-$	<0.0001	-1.84	PE 34:1 (16:0/18:1) $[ADDUCT]^-$	<0.0001	1.58
CER (d43:0) $[M+HCOO]^-$	0.0048	-1.74	PE 36:2 (18:1/18:1) $[M-H]^-$	0.0001	1.52
CER (d44:1) $[M+HCOO]^-$	0.0237	-1.94	PE 38:2 (18:1/20:1) $[M-H]^-$	<0.0001	2.47
CER (d44:1) $[M+HCOONH_4]^-$	0.0092	-1.51	PE 40:4 (18:0/22:4) $[ADDUCT]^-$	0.0061	1.54
CER (t40:0) $[M+HCOO]^-$	0.0006	-1.52	PE-NMe2 (16:0/20:4) $[ADDUCT]^-$	0.0213	-2.64
CER (t42:0) $[M+Cl]^-$	0.0106	-1.67	PI 36:2 (18:1/18:1) $[M-H]^-$	<0.0001	1.84
CER (t42:0) $[M+HCOONH_4]^-$	0.0195	2.44	PS 40:4 (18:0/20:4) $[M-H]^-$	0.0405	1.79
CER (t44:1) $[M+Cl]^-$	0.0299	-1.65	SM (d34:2) $[M+HCOO]^-$	0.0029	1.56

Table 8 **Volcano plot analysis for negative dataset**
List of lipids significantly regulated between healthy subjects (HS) and coronary artery disease (CAD) patients.
*: adjusted *p*-value obtained from moderate t-test and Benjamini-Hochberg multiple testing correction
#: fold change (FC) calculated comparing CAD *vs* HS

CER: ceramide; **LacCer:** lactosylceramide; **LPC:** lysophosphatidylcholine; **LPE:** lysophosphatidylethanolamine; **PC:** phosphatidylcholine; **PC-P:** plasmenyl-phosphatidylcholine; **PE:** phosphatidylethanolamine; **PI:** phosphatidylinositol**; PS:** phosphatidylserine; **SM:** sphingomyelin

5.3.2.5 Lactosylceramide (d34:1) (d18:1/16:0)

LacCer (d34:1) (d18:1/16:0) has been identified among the lipids capable of discriminating between CAD and HS because all the 3 adducts of this molecule show a high degree of significance associated with high FC.

The identification of LacCer was confirmed through the analysis of the fragmentation spectrum obtained by LC-MS/MS. **Figure 32** shows the structure and fragmentation spectrum of LacCer (d34:1) (d18:1/16:0) $[M+HCOO]^-$. In particular, the $[M-H]^-$ ion m/z 860 is observed which is generated by the loss of a molecule of formate (46 Da). The neutral loss of sugar residues, typical of LacCer, forms the fragments m/z 698 and 536 while the fragment 179 is the residual sugar itself. Finally, fragment 263 identifies a rearrangement of the Sph (d18:1) that constitutes the backbone of LacCer.

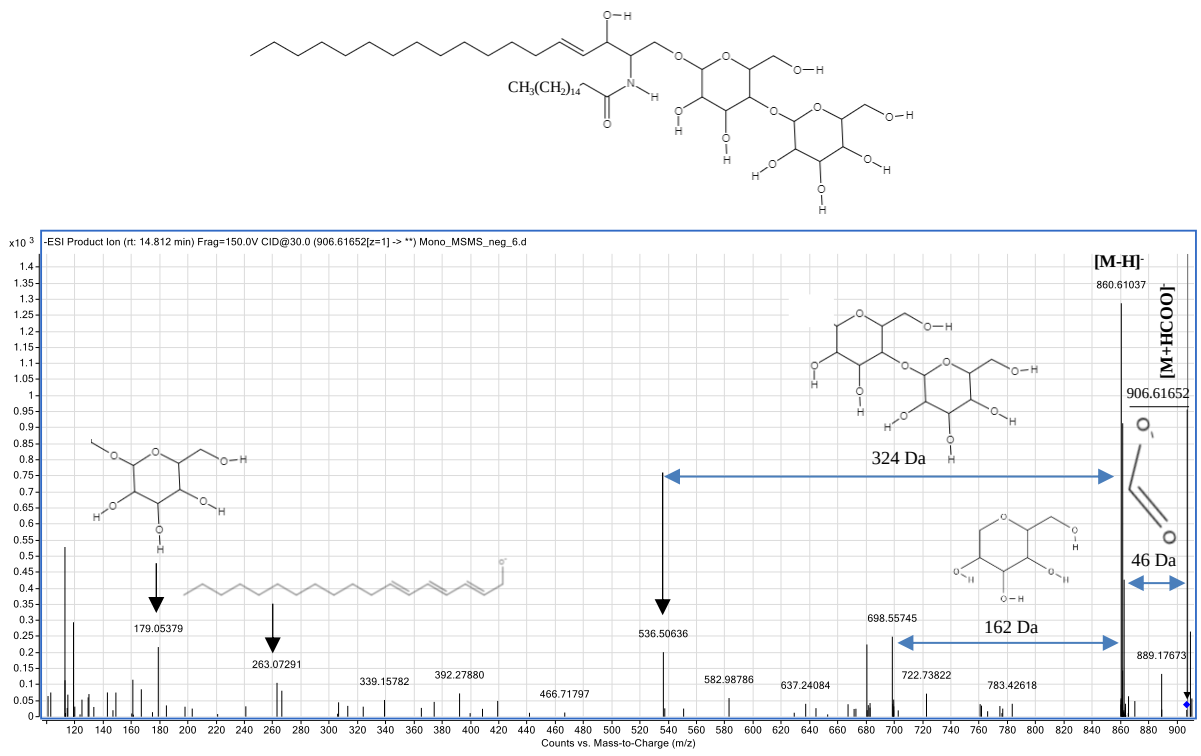

Figure 32 **Lactosylceramide (d34:1) (d18:1/16:0) fragmentation pattern**
Fragmentation pattern of Lactosylceramide (d34:1) (d18:1/16:0) $[M+HCOO]^-$. Blue arrows reported neutral losses. The main fragments and their structures are also reported.

The relative intensity of the 3 molecule adducts ($[M+Cl]^-$, $[M+HCOO]^-$ and $[M+HCOONH_4]^-$) and of their sum are reported in boxplots (**Figure 33**).

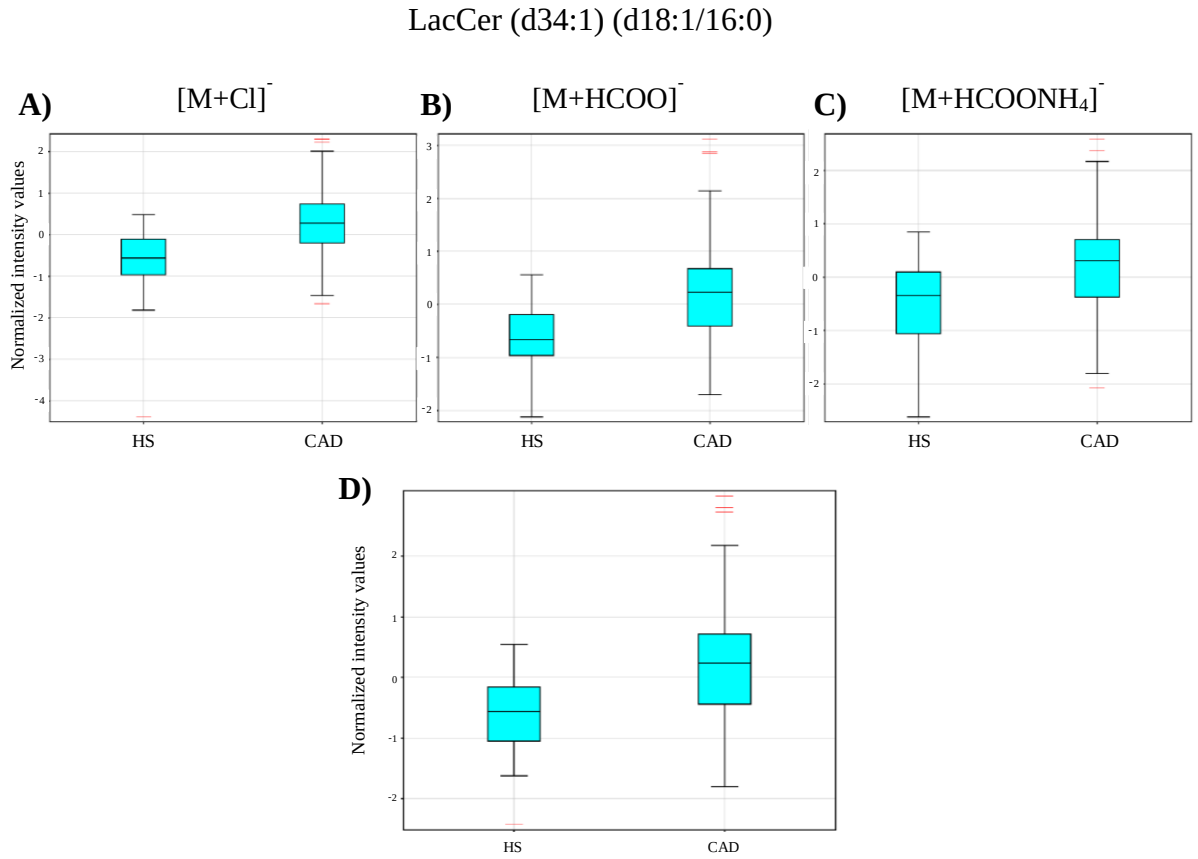

Figure 33 **Lactosylceramide (d34:1) (d18:1/16:0) boxplots**
Normalized intensity values reported by boxplots of Lactosylceramide (d34:1) (d18:1/16:0) A) $[M+Cl]^-$ adduct, B) [M+HCOO]- adduct, C) [M+HCOONH4]- adduct and D) sum of the three adducts in coronary artery disease (CAD) patients and healthy subjects (HS).

5.4 Role of lactosylceramide in monocyte migration

5.4.1 Lactosylceramide synthase levels in monocytes

The level of β-1,4 GalT-V, the lactosylceramide synthase, was evaluated by ELISA analysis.
A significant increase of this enzyme was evidenced in monocytes obtained from CAD patients compared to HS.

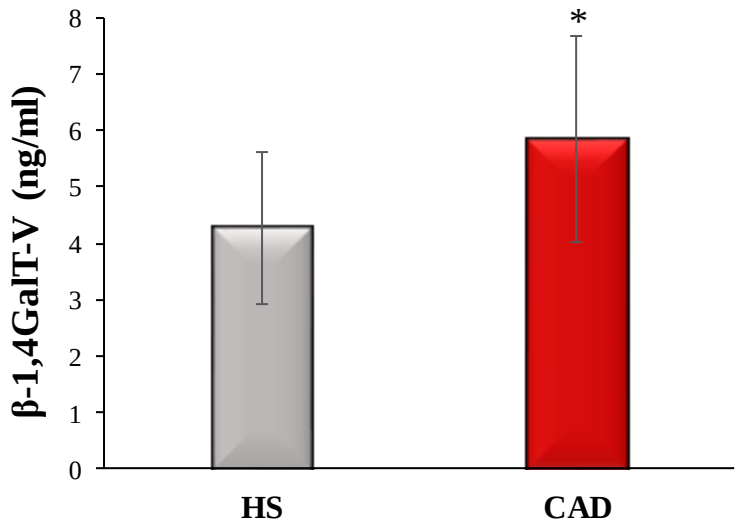

Figure 34 **Lactosylceramide synthase level**
Level of β-1,4 GalT-V, the lactosylceramide synthase enzyme in monocytes obtained from healthy subjects (HS, n=10) and coronary artery disease patients (CAD, n=25); *p<0.05.

5.4.2 Effect of lactosylceramide synthase inhibitor on monocyte migration

To evaluate the involvement of LacCer in monocyte migration, monocytes were treated with D-PDMP, an inhibitor of glucosylceramide synthase and lactosylceramide synthase. TNF-α was used as positive control since TNF-α is known to promote the lactosylceramide synthase activity, leading to a marked production of LacCer[186]

The treatment of monocytes with D-PDMP, markedly reduced the monocyte migration induced by TNF-α (**Figure 35, panel A**). Moreover, D-PDMP significantly reduced the migration of monocyte obtained from CAD patients induced by FBS used as chemotactic stimulus, suggesting that the increased migration showed by patient's monocytes may be partially dependent by the increased levels of LacCer detected (**Figure 35, panel B**).

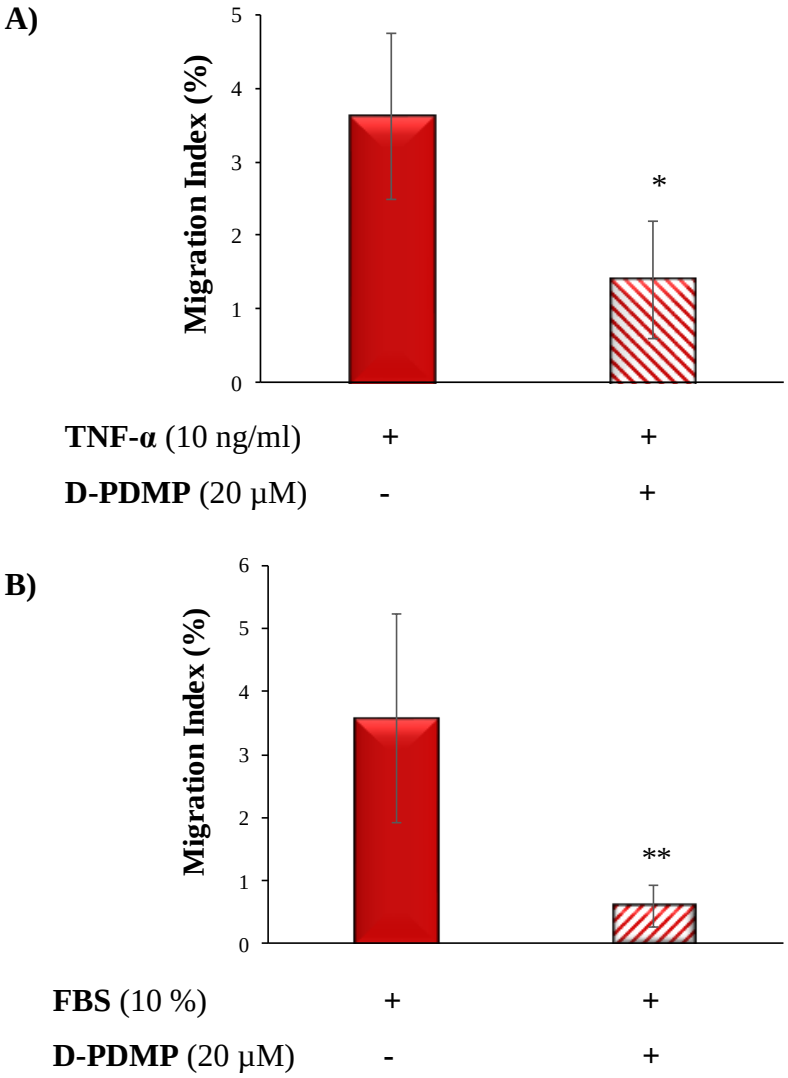

Figure 35 **Effect of lactosylceramide synthase inhibitor on monocyte migration**
Migration of monocytes obtained from coronary disease patients is performed in the presence of A) tumor necrosis factor α (TNF-α, 10 ng/ml) or B) fetal bovine serum (FBS, 10%) as chemotactic stimulus. Monocytes were treated with D-PDMP, the lactosylceramide synthase inhibitor, (20 µM, for 1 hour) were indicated. A) n=3, *p<0.05; B) n=7, **p<0.01

5.4.3 Effect of exogenous lactosylceramide on monocyte migration

Monocytes obtained from HS were treated for 30 min with standard LacCer (d34:1) (d18:1/16:0) at different concentrations: 0.1, 0.5 and 2 µM. The treatment of monocytes with LacCer 2 µM allows to obtain 2-fold increase in the LacCer content (**Figure 36, panel A)** similar to the increased observed in CAD patients monocytes. Moreover, a significantly increase in HS monocytes migration was highlighted after the monocyte treatment with standard LacCer (2 µM) (**Figure 36, panel B)**.

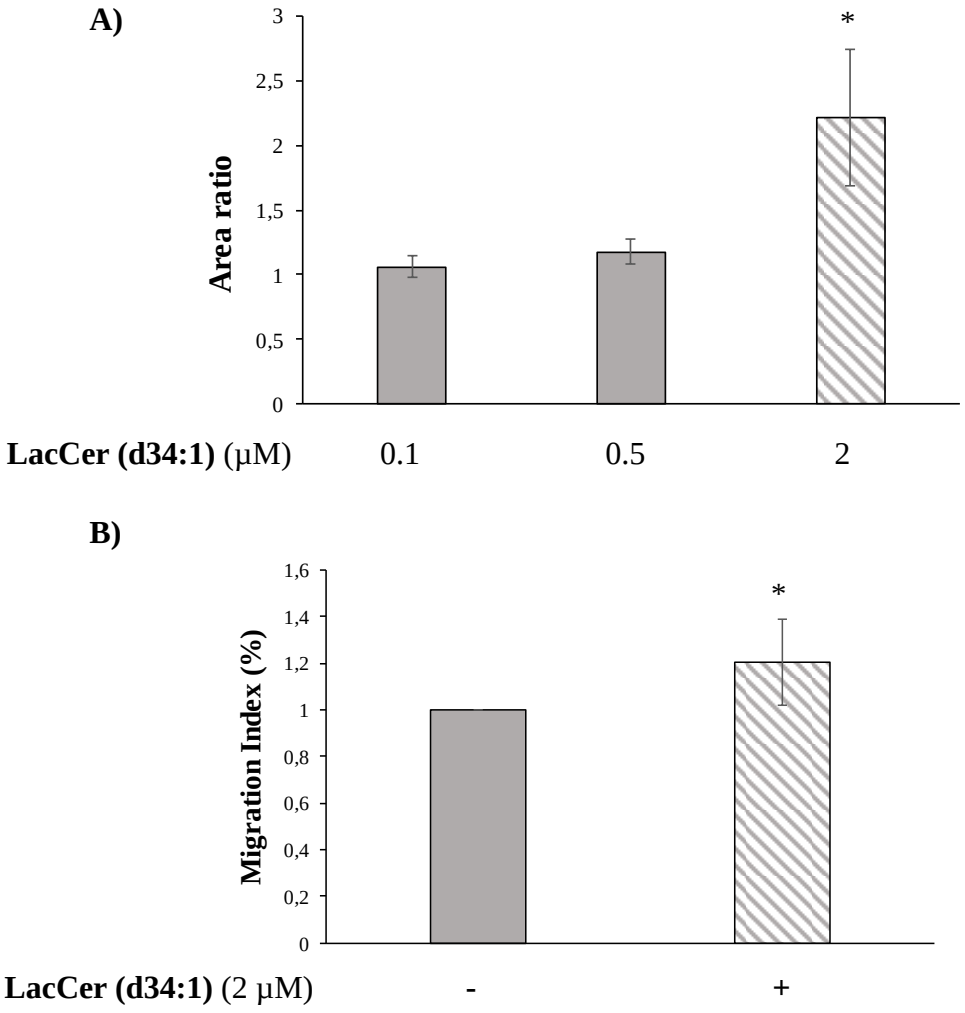

Figure 36 **Effect of exogenous lactosylceramide on monocyte migration**
Monocytes obtained from healthy subjects were treated for 30 min with Lactosylceramide (d34:1) (d18:1/16:0) (LacCer).
A) Monocyte incorporation of LacCer evaluated by mass spectrometry. Data are expressed as the ratio between the LacCer pick area detected before and after the monocyte treatment with LacCer. (n=3); *p<0.05.
B) Monocyte migration performed after the exogenous addition of LacCer (d34:1) (2 µM); (n=7), *p<0.05.

5.4.4 Correlation between endogenous lactosylceramide levels and monocyte subsets

The LacCer endogenous levels showed a positive correlation with the $CD14^{++}CD16^{+}$ monocyte (intermediate monocytes) count. In contrast, a negative correlation between $CD14^{+}CD16^{++}$ non-classical monocyte count and the lipid levels was shown.

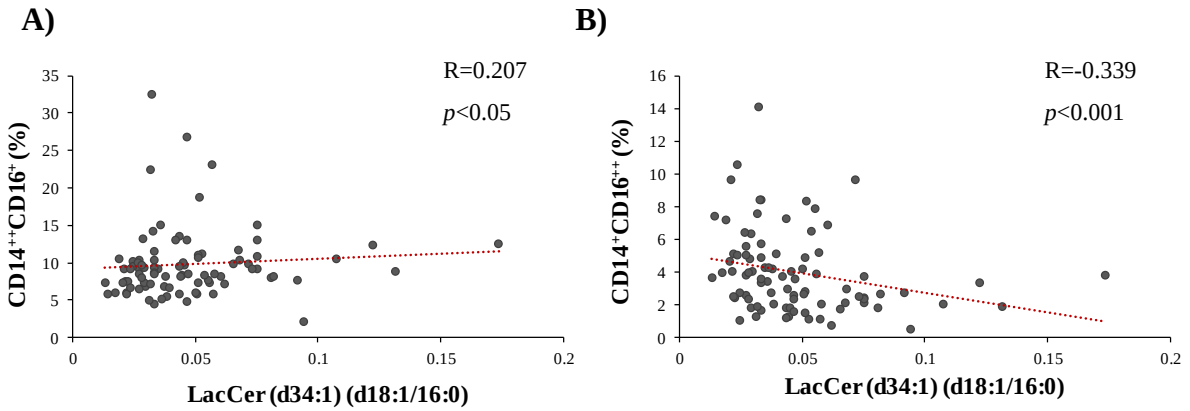

Figure 37 **Correlation between lactosylceramide level and monocyte subsets**
Correlation analysis between lactosylceramide (d34:1)(d18:1/16:0) levels and A) CD14++CD16+ intermediate monocytes, B) CD14+CD16++ non-classical monocytes. Monocytes are obtained from healthy subjects (HS, n=27) and coronary artery disease patients (CAD, n=62).

5.4.5 Correlation between endogenous lactosylceramide levels and monocyte migration

A significant positive correlation between endogenous LacCer levels and the monocyte migration towards autologous serum is demonstrated. In contrast, not a significant correlation is observed considering monocyte migration towards FBS.

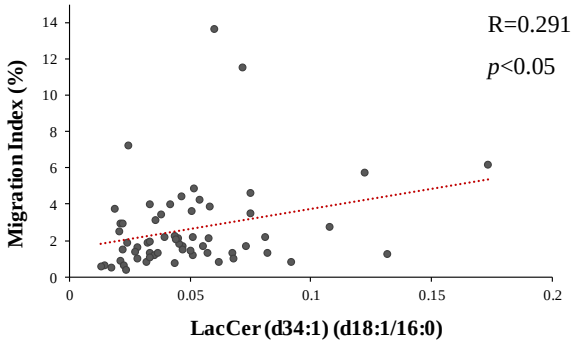

Figure 38 **Correlation between lactosylceramide level and monocyte migration**
Correlation analysis between lactosylceramide (d34:1)(d18:1/16:0) levels and monocyte migration towards autologous serum as chemotactic agent. Monocytes are obtained from healthy subjects (HS, n=27) and coronary artery disease patients (CAD, n=62).

6. Discussion

Atherosclerosis is a chronic inflammatory disease in which the immune response and several metabolic risk factors contribute to the formation and progression of arterial vessel lesions[229]. It is the foremost cause of CAD and specifically the heterogeneity of atherosclerotic plaques leads to different clinical manifestation including SA, NSTEMI and STEMI with an associated increasing degree of severity. SA patients are characterized by an obstructive stable plaque while NSTEMI and STEMI are acute conditions in which the plaque rupture leads to a thrombus formation that will result in heart attack[50].

Immune cells, and among them monocytes, play a key role in plaque progression from the early lesion to the final plaque rupture[229]. In this study we delinate the lipidomic profile and the functional characterization of circulating monocytes in CAD patients compared to HS.

Circulating monocytes represent about 10% of total peripheral leukocytes. Several studies have described an increase in the count of circulating monocytes in subjects with atherosclerotic disease[230, 231] and a reduction in the number of monocytes was reported to suppress the progression of atherosclerosis in animal models[232, 233]. Thus, total blood monocyte count appear to be an independent predictor of cardiovascular events[234, 235] and a risk factor for CAD disease in humans[234]. In this study population, the total monocyte count is higher in CAD group compared to HS and, in particular, a progressive increase that goes in parallel with the severity degree of the disease is observed. STEMI and NSTEMI patients show an elevated monocyte count compared to SA and HS, as symptom of their acute condition. This result is in agreement with a larger cohort study involving ACS patients including UA, NSTEMI and STEMI patients[236]. Moreover, the distribution of the three monocyte subsets, classical $CD14^{++}CD16^{-}$, intermediate $CD14^{++}CD16^{+}$ and non-classical $CD14^{+}CD16^{++}$, was also evaluated. In healthy condition, the three population represents about 85%, 10% and 5% of the whole monocyte population respectively. Several studies have evaluated the changes in the different subsets of circulating monocytes in relation to cardiovascular diseases, and an increase of the intermediate subgroup is considered a predictor of poor cardiovascular outcome[116]. In addition, it was observed that intermediate monocytes increase in subjects with coronary plaque compared to those without, markedly in patients with severe stenosis[237] and in SA patients with a proatherogenic plasma lipoprotein profile[238]. Accordingly, in our study, the intermediate monocyte count is higher in CAD patients, and this increase goes in parallel with the severity of the disease supporting the role of this subgroup in the atherosclerosis onset and progression.

On the contrary, the role of classical and non-classical monocytes is still not completely understood. Recently, Leers et al showed an increase of all three subsets in ACS patients compared to control subjects, at the time of the hospital admission[236]. However, when the time elapsed between the acute event and blood collection is extended, there is no difference in non-classical monocyte count

suggesting that the increase occurs only in the acute phases of ACS[239]. Moreover, a diminish count levels of this subset was observed in CAD patients with cumulative high-risk scores or with established risk factors such as smoking or CAD familiarity compared to low-risk subjects[240]. Overall, patients enrolled in our study show lower non-classical monocytes than HS. Since this subset exhibit patrolling and regenerative potential in ischemic tissue, this result suggests that in CAD patients, a reduced extravasion of non-classical monocytes might be occurred.

Considering classical monocytes, these represent the largest portion of the cell population. However, no differences in the count of classical monocytes was evidenced among CAD patients and HS.

Overall, these results suggest that among the three subsets, the imbalance of the intermediates is associated to CAD disease since the proportion of these cells is increased both in clinical condition with acute or chronic inflammation[114, 241].

Monocyte migration is a crucial step in atherogenesis and plaque progression. The continuous recruitment of monocytes into the subendothelium, contributes to vascular inflammation and promotes plaque progression and the onset of adverse cardiovascular events[242, 243]; while the suppression of monocyte recruitment towards plaques leads to a regression of the disease[244]. Moreover, the trafficking of monocytes towards the aortic wall is proportional to the severity of the disease[245] and an increased migration promotes plaque instability and triggers plaque rupture[246].

In our study, monocyte migration was evaluated using FBS as chemotactic stimulus and monocytes isolated from CAD patients show a greater propensity to migrate than those obtained from HS. In particular, an increase of the migration index from SA to NSTEMI and STEMI patients was observed. This result suggest that the trafficking attitude can be due to intrinsic characteristics of monocytes that are different for CAD and HS. Moreover, similar results are also obtained when migration is evaluated in the presence of autologous serum as a trafficking trigger. These results are in accordance with Zalai et al. who observed increase circulating monocyte activation in patients with unstable coronary syndromes[246]. Nevertheless, the exposure of CAD monocytes to a pool of sera collected from HS reduced the cells trafficking attitude. In parallel, the migration of HS monocytes is increased when a pool of sera obtained from CAD patients is used as a chemotactic agent thus highlighting an additional role of serum and its composition in the modulation of monocyte migration. Overall, these results suggest that CAD monocytes are functionally altered, and that serum is one of the factors that can contribute to their activation.

The up-regulation of cytokines and chemokines that may be present in serum is indeed critical for the recruitment of monocytes to the endothelium and their subsequent migration[247] and it represents a key mechanism for vascular inflammation and atherogenesis[248]. Indeed, high circulating levels of

CCL19 and CCL21 have been observed to be increased in SA patients and even more in UA patients[249]. Moreover, the high expression of these chemokines and their CCR7 receptor in atherosclerotic coronary tissue has been associated with a progression of the atherosclerotic lesion due to a promotion of monocyte adhesion and migration[248]. In contrast, the blocking CCR5, CCR2 or CX3CR1 reduced the migration of murine monocytes [250] with a decrease of the size of the atherosclerotic lesion[251]. Recently Weber et al. have shown the expression of CCR2 to be peculiar of classical and intermediate monocytes in spite of non-classical monocytes[252] while the presence of CX3CR1 on monocyte surface seems to be upregulated in the intermediate and non-classical subsets[236]. Consistent with the increased adhesion and migration of intermediate monocytes, we have observed a positive correlation between the count of intermediate monocytes and the migration of monocytes supporting the pro-inflammatory role of this subsets and their involvement in the atherosclerotic plaque development.

During circulation in the blood stream, monocytes are exposed not only to cytokines and chemokines but also to other agents and among them lipid mediators, systemic signals that can induce functional reprogramming and alter their functions[253, 254]. In particular, altered blood lipid levels may induce an inflammatory phenotype in monocytes[255]. In *in vitro* experiments have shown that even a short exposure of human monocytes to a low concentration of oxLDL, is able to induce a cellular modification resulting in a differentiation of monocyte into a proatherogenic macrophage phenotype[256]. In addition, atherogenic levels of LDL induce changes in monocyte phenotype associated to an increase of the expression of adhesion molecules and to a reduction of apoptosis detected in early phases of monocyte differentiation into macrophages[257]. Alterations in the lipid metabolism of monocytes may lead to the formation of foamy monocytes characterized by the presence of intracellular lipid droplets. For example, it has been observed that a single meal with a high fat content is enough to induce an accumulation of lipids in circulating monocytes[258]. Moreover, monocytes obtained from hypercholesterolemic patients have an enhanced capacity to infiltrate into arterial wall compared to those from healthy subjects[259]. In addition, hypertriglyceridemia promotes the adhesion of monocytes, especially the intermediate subsets, to endothelial cells through VCAM-1 in patients with myocardial infarction[260, 261]. An opposite effect is exerted by reconstituted HDL which administration reduces the expression of CCR2 and CX3CR1 on the surface of monocytes[262]. Overall, lipids play an important role in modulating monocyte phenotype and functions likely because off the plasma membrane lipid bilayer composition is fundamental for cell proliferation, differentiation, migration, cell-cell contacts and signal transduction processes[263]. As regard to lipid effect on monocyte migration, it has been observed that several isoforms of oxidized linoleic acid and LPC were found to be able to stimulate the migration of monocytes through the upregulation of the expression of CCR9 and CX3CR1[264].

In addition, omega-3 FA appear to reduce monocytosis, favorably alter monocyte subsets and reduce monocyte recruitment into atherosclerotic lesions in atherosclerotic mice models[265]. Furthermore, the supplementation of PUFA in physiological concentrations induces profound alterations in the lipid profile of raft and non-raft plasma membranes microdomains by modifying the amount of PUFA substrates available for the synthesis of lipid mediators[263].

On the basis of these observations, in this study, the lipidomic profile of monocytes isolated from CAD patients and subjects without a clinical and family history of cardiovascular disease was defined and it was related to the migratory capacity of these cells. To this end, an untargeted mass spectrometry method was developed that simultaneously detect a broad range of lipid by the use of UHPLC system coupled to a QTOF mass spectrometry detector. This equipment compared to traditional instruments allows a more efficient ionization of molecules, greater sensitivity and linear detector response necessary for this kind of analysis. Moreover, the QTOF instrument consents high-resolution performances, which allow to obtain the accurate mass of the detected unknown compounds. By this analytical platform, it is possible to perform an untargeted lipidomic analysis consisting in the simultaneous detection of different lipid classes so as to obtain a wide lipid profile in biological samples. Given the complexity and structural variability of lipid molecules, the development process of the method assumes a fundamental role in order to define the broadest spectrum of molecules that can be detected simultaneously. For the development of this method, different methodological aspects (instrumental parameters. sample preparation. chromatographic separation and instrumental reproducibility) have been evaluated in order to optimize the conditions for data acquisition so as to obtain reliable results.

Through this method we were able to detect several lipid classes including LPL such as LPC and LPE, PL (PI, PS, PG, PA, PE, PC), and SP such as SM and CER. In addition, among the neutral lipids, DG and TG and CE can be detected.

Overall, in monocytes, 137 and 323 lipids were identified in positive and negative ionization mode respectively. Among these, PL (specifically PE and PC and their lyso-forms), SP (particularly CER and SM) and TG were found to be the most represented lipid classes.

However, in our monocyte samples, DG and CE were not identified probably due to low concentrations that do not exceed the limit of detection of our method. DG, indeed, is a short-life second messenger as it is rapidly metabolized by DG kinase and DG lipase[266] to give products involved in a variety of cell responses such as cell proliferation, survival and migration[267]. Furthermore, DG is an intermediate of the synthesis of PL and precursors of TG[266], which, on the contrary, are detected with high amount in our samples. As regard to CE, a recent study highlights the ability of monocytes and macrophages, obtained from hypercholesterolemic mice, to

accumulate CE when exposed to high concentrations of cholesterol. In addition, a lower activity of cholesterol acyltransferase and CE hydrolase in monocytes was observed compared to macrophages[268]. Thus, in monocytes, free cholesterol is likely incorporate in cell membranes while it is converted to a reduced extent in CE. These observations may explain the low CE concentration in our monocyte samples that do not exceed the limit of detection of our method since

Considering all other detected lipid classes, we compared the lipid profile of monocytes obtained from HS with that obtained from CAD patients. Through the PCA analysis and heatmaps, we observed that the lipid profile is similar for monocytes obtained from patients with different CAD severity degree: SA, NSTEMI and STEMI, while the differences between HS and CAD are considerable. Specifically, we observed elevated levels of LPC against low levels of PC in STEMI monocytes while in HS monocytes an opposite behavior is observed. PC are source of arachidonic acid that acts as precursor for the synthesis of lipid mediators such as eicosanoids[269, 270]. The upregulation of LPC against PC may therefore mean that in monocytes obtained by patients, PC are converted to LPC probably releasing arachidonic acid, mediator needed for the inflammatory response[271]. This result is confirmed by a recent study by Lee et al who defined the lipid profile of macrophages raw264.7 and observed down-regulated PC and up-regulated LPC after stimulation with a pro-inflammatory stimulus[272]. LPC in fact are known to be related to atherosclerotic disease because patients with atherosclerosis show high plasma levels[273, 274] and LPC are also the major components of OxLDL[275]. Moreover, there is a great number of evidence showing the pro-inflammatory and atherogenic effects of LPCs, which are chemotactic factors for monocytes[274], and are able to induce the expression of VCAM-1 and ICAM-1[276] or MCP-1[276, 277].

In addition, the most striking result showed by the heatmaps graphical representation is the low level of CER and TG observed in CAD patients' monocytes.

The high TG levels in HS might suggest an increased ability of HS monocytes to remove TG from the bloodstream. Indeed, high plasma levels of TG-rich lipoproteins are related to CAD and an inefficient clearance induces atherogenesis[278] promoting the adhesion of monocytes to endothelium[279] and the recruitment of monocytes to atherosclerotic plaques[280]. In accordance with these observations, ACS patients enrolled in our study show higher plasma levels of TG than HS, lower TG intracellular levels that are associated with increased monocyte migration.

In addition, the augmented TG intracellular levels observed in HS could be linked to the role of TG that act as storage molecules of metabolic energy and FA. A reduced activity of the enzyme that catalyzes the final step of TG synthesis in the whole body seems to ameliorate atherosclerotic lesion development[281], however an increased synthesis of TG, specifically in macrophages, is sufficient to protect against inflammation which result from diet-induced obesity and counteract the activation of M1 macrophages induced by *in vitro* treatment with cytokines or FA[282]. Indeed, increased

esterification of FA, as palmitate, in TG pool reduces the FA availability for the synthesis of inflammation-related signaling metabolites such as CER, DAG, LPA and eicosanoids[283]. However, we have also observed high levels of CER in HS monocytes, meaning that although the *de-novo* synthesis, starting from palmitate, may be reduced; CER may also derive from SM through sphingomyelinase activity or from Sph by ceramidases[284].

Several papers support CER and their high plasma levels to be related to the development of atherosclerosis[285, 286]. Specifically, CER signaling was also observed to be involved in inflammatory responses during the development of atheromasic plaques[287] and to mediate plaque instability by its pro-apoptotic effect on macrophages and SMCs[288]. However, considering the role of CER as membrane components, high levels of CER cause a change in viscosity[170, 289, 290], and an increase in membrane rigidity resulting in an impaired cell migration as observed in circulating angiogenic cells whose release from bone marrow and extravasation towards retinal vascular injury are reduced following intracellular CER increase[291]. The increase in CER production indeed, induces the formation of CER-enriched microdomains that strongly influence the organization and dynamic properties of the membrane[292]. In addition, CER can be further metabolized into S1P, a mediator that shows proliferation, migration and pro-survival effects[293].

All in all, the high levels of CER observed in HS monocytes may confer membrane rigidity resulting in lower monocyte migration. In contrast, in CAD monocytes, CER could be converted into second messengers such as S1P that stimulate their migration via autocrine mechanism.

The conversion of CER into more complex SP such as GlcCer or LacCer is another potential mechanism for CER levels reduction. Indeed, what we observe is that among the lipids that discriminate CAD patients from HS, LacCer (d34:1) (d18:1/16:0), specifically all three adducts that form $[M+HCOO]^-$, $[M+Cl]^-$ and $[M+HCOONH_4]^-$, appears to be significantly increased in CAD patients compared to HS.

LacCer is a bioactive SP expressed in vascular cells, macrophages, neutrophils, platelets and monocytes[189]. In our study, monocytes obtained from CAD patients show increased levels of LacCer which are also associated with a higher expression of the enzyme β-1,4GalT-V, the lactosylceramide synthase, compared to HS monocytes. This enzyme is the target for activation by TNF-α[187, 188] and OxLDL[199], which leads to increased production of LacCer which in turn stimulates endothelial cells expression of ICAM-1 thus highlighting the role of this enzyme in proliferative disease including atherosclerosis[189]. The activity of lactosylceramide synthase has been reported to be elevated in human atherosclerotic plaques and calcified plaques[189, 202] . Several studies have demonstrated the role of LacCer in atherosclerosis by showing its high levels in human atherosclerotic plaques compared to healthy vascular tissue[202] that positively correlate with plaque content of pro-inflammatory cytokines as IL-6 and MCP-1 and with lipid and macrophage

content[294]. In addition, LacCer modulates different functions in cells involved in the development of atheromasic plaque. In SMCs, LacCer directly stimulates cell proliferation[190] and this lipid is also involved in the OxLDL-mediated increase in SMCs proliferation since OxLDL induce the activation of lactosylceramide synthase and the consequent production of LacCer[200]. In neutrophils, LacCer stimulates their adhesion to endothelial cells through the activation of PLA_2, which catabolizes PC to arachidonate that in turn causes the increase of expression on the cell surface of Mac-1[203]. Moreover, in monocytes, LacCer activates PKC and PLA_2 and stimulates the expression of PECAM-1 and the subsequent adhesion to endothelial cells[193]. The FA moiety of LacCer seems also important for the modulation of the effect induced by this lipid since LacCer, isolated from patients with polycystic kidney disease[295] or from human atherosclerotic plaques[202], rich in C16:0, C22:1 and C24:0, induce higher cell proliferation than synthetic stearoyl LacCer[296]. However, studies on neutrophils revealed that C24:0 and C24:1 but not C16:0 LacCer are preferentially involved in LacCer-mediated neutrophil superoxide generation and migration[297].

Based on these observations, in this study we evidenced that increased levels of C16:0 LacCer, in monocytes may contribute to increase cell migration since a positive correlation between the LacCer levels and the monocyte migration towards autologous serum was observed. Moreover, by treating monocytes with TNF-α we observed a stimulation of migration. TNF-α indeed is known to promote the activity of lactosylceramide synthase leading to an overproduction of LacCer that in turn active nuclear transcription factor NF-κB increasing the expression of ICAM-1 and the adhesion of monocytes to endothelial cells[187]. This signal transduction pathway induced by TNF- α, is abrogated by D-PDMP[187], a non-selective inhibitor of lactosylceramide synthase[191]. In our experimental conditions, D-PDMP is able to inhibit not only the migration of monocytes induced by TNF-α but also the migration obtained toward FBS as chemotactic agent, suggesting the involvement of endogenous LacCer in this process. However, D-PDMP, as a non-selective inhibitor is also able to inhibit GlcCer synthesis[191]. Thus, the reduction in migration observed after treatment of monocytes with D-PDMP, could be the result of the inhibited synthesis of GlcCer, precursor of LacCer[191] , rather than to a direct inhibition of lactosylceramide synthase. However, several papers that have studied the mechanism of action by which LacCer induces cellular proliferation and migration, have shown that LacCer signaling pathway is mitigated by the addition of D-PDMP and bypassed by exogenous LacCer but not by a variety of GSL including GlcCer [187, 188, 298] further endorsing the role of LacCer as a mediator of cellular migration. To further confirm the role of LacCer in monocyte migration, we treated monocytes obtained from HS with exogenous LacCer. The addition of LacCer 2 μM resulted in a 2-fold increase in LacCer levels comparable to that observed for CAD monocytes. Under these conditions, LacCer-loading monocytes showed a significant increase in migration, still supporting the role of LacCer in monocyte migration.

7. Conclusions

In this study, through an untargeted lipidomic approach, a different lipid profile in CAD patient monocytes compared to HS was found. Specifically, a marked increase in lactosylceramide in CAD patient's monocytes was observed which positively correlated with the monocyte migration. In addition, monocytes obtained from CAD patients showed, a significant increase in cell migration, induced by both FBS and autologous serum, compared to HS.

The results obtained in this study suggest that the monocyte lipidomic profile can evidence a specific lipid composition that may lead to changes in cellular function.

In particular, by highlighting the key role of lactosylceramide in monocyte migration and thus in the inflammatory process underlying the progression of atherosclerotic plaque, this study may help to define a potential target for new pharmacological strategies.

8. References

1. Ross, R., Atherosclerosis is an inflammatory disease. *American heart journal* **1999,** *138* (5 Pt 2), S419-20.
2. Bentzon, J. F., et al., Mechanisms of plaque formation and rupture. *Circulation research* **2014,** *114* (12), 1852-66.
3. McLaren, J. E., et al., Cytokines, macrophage lipid metabolism and foam cells: implications for cardiovascular disease therapy. *Progress in lipid research* **2011,** *50* (4), 331-47.
4. Konstantinov, I. E., et al., Nikolai N. Anichkov and his theory of atherosclerosis. *Tex Heart I J* **2006,** *33* (4), 417-423.
5. Keys, A., Human atherosclerosis and the diet. *Circulation* **1952,** *5* (1), 115-8.
6. Goldstein, J. L., et al., The LDL receptor and the regulation of cellular cholesterol metabolism. *Journal of cell science. Supplement* **1985,** *3*, 131-7.
7. Goldstein, J. L., et al., Familial hypercholesterolemia: identification of a defect in the regulation of 3-hydroxy-3-methylglutaryl coenzyme A reductase activity associated with overproduction of cholesterol. *Proceedings of the National Academy of Sciences of the United States of America* **1973,** *70* (10), 2804-8.
8. Jonasson, L., et al., Regional accumulations of T cells, macrophages, and smooth muscle cells in the human atherosclerotic plaque. *Arteriosclerosis* **1986,** *6* (2), 131-8.
9. Epstein, S. E., et al., Insights into the role of infection in atherogenesis and in plaque rupture. *Circulation* **2009,** *119* (24), 3133-41.
10. Fabricant, C. G., et al., Virus-induced atherosclerosis. *The Journal of experimental medicine* **1978,** *148* (1), 335-40.
11. Libby, P., et al., Roles of infectious agents in atherosclerosis and restenosis: an assessment of the evidence and need for future research. *Circulation* **1997,** *96* (11), 4095-103.
12. Libby, P., et al., Inflammation and atherosclerosis. *Circulation* **2002,** *105* (9), 1135-43.
13. Glass, C. K., et al., Atherosclerosis. the road ahead. *Cell* **2001,** *104* (4), 503-16.
14. Rafieian-Kopaei, M., et al., Atherosclerosis: process, indicators, risk factors and new hopes. *International journal of preventive medicine* **2014,** *5* (8), 927-46.
15. Sumino, H., et al., [Investigation of atherosclerosis in postmenopausal women: alteration of atherosclerosis-associated factors and vascular atherosclerosis by oral and transdermal estrogen replacement]. *Rinsho byori. The Japanese journal of clinical pathology* **2013,** *61* (3), 256-62.
16. Humphries, S. E., et al., Genetic risk factors for stroke and carotid atherosclerosis: insights into pathophysiology from candidate gene approaches. *The Lancet. Neurology* **2004,** *3* (4), 227-35.
17. Executive Summary of The Third Report of The National Cholesterol Education Program (NCEP) Expert Panel on Detection, Evaluation, And Treatment of High Blood Cholesterol In Adults (Adult Treatment Panel III). *Jama* **2001,** *285* (19), 2486-97.
18. Ebbesson, S. O., et al., Cardiovascular disease and risk factors in three Alaskan Eskimo populations: the Alaska-Siberia project. *International journal of circumpolar health* **2005,** *64* (4), 365-86.
19. Standards of medical care in diabetes--2007. *Diabetes care* **2007,** *30 Suppl 1*, S4-S41.
20. Son, S. M., Role of vascular reactive oxygen species in development of vascular abnormalities in diabetes. *Diabetes research and clinical practice* **2007,** *77 Suppl 1*, S65-70.
21. Ahmed, N., et al., Advanced glycation endproducts: what is their relevance to diabetic complications? *Diabetes, obesity & metabolism* **2007,** *9* (3), 233-45.
22. Piconi, L., et al., Constant and intermittent high glucose enhances endothelial cell apoptosis through mitochondrial superoxide overproduction. *Diabetes/metabolism research and reviews* **2006,** *22* (3), 198-203.
23. Keller, P. F., et al., Diabetes and acute coronary syndrome. *Minerva medica* **2010,** *101* (2), 81-104.
24. Chobanian, A. V., et al., The Seventh Report of the Joint National Committee on Prevention, Detection, Evaluation, and Treatment of High Blood Pressure: the JNC 7 report. *Jama* **2003,** *289* (19), 2560-72.
25. Asgary, S., et al., Clinical investigation of the acute effects of pomegranate juice on blood pressure and endothelial function in hypertensive individuals. *ARYA atherosclerosis* **2013,** *9* (6), 326-31.
26. Asgary, S., et al., Investigation of the lipid-modifying and antiinflammatory effects of Cornus mas L. supplementation on dyslipidemic children and adolescents. *Pediatric cardiology* **2013,** *34* (7), 1729-35.
27. Winkelmann, B. R., et al., Smoking and atherosclerotic cardiovascular disease: part IV: genetic markers associated with smoking. *Biomarkers in medicine* **2010,** *4* (2), 321-33.
28. Fodor, G., Primary Prevention of CVD: Treating Dyslipidemia. *Am Fam Physician* **2011,** *83* (10), 1207-1208.
29. Mihaylova, B., et al., The effects of lowering LDL cholesterol with statin therapy in people at low risk of vascular disease: meta-analysis of individual data from 27 randomised trials. *Lancet* **2012,** *380* (9841), 581-590.
30. Cannon, C. P., Cardiovascular disease and modifiable cardiometabolic risk factors. *Clinical cornerstone* **2007,** *8* (3), 11-28.
31. Pi-Sunyer, X., et al., Reduction in weight and cardiovascular disease risk factors in individuals with type 2 diabetes: one-year results of the look AHEAD trial. *Diabetes care* **2007,** *30* (6), 1374-83.

32. Wentzel, J. J., et al., Endothelial shear stress in the evolution of coronary atherosclerotic plaque and vascular remodelling: current understanding and remaining questions. *Cardiovascular research* **2012,** *96* (2), 234-43.
33. Steinberg, D., et al., Oxidized low-density lipoprotein and atherosclerosis. *Arteriosclerosis, thrombosis, and vascular biology* **2010,** *30* (12), 2311-6.
34. Libby, P., et al., Progress and challenges in translating the biology of atherosclerosis. *Nature* **2011,** *473* (7347), 317-25.
35. Leitinger, N., et al., Phenotypic polarization of macrophages in atherosclerosis. *Arteriosclerosis, thrombosis, and vascular biology* **2013,** *33* (6), 1120-6.
36. Tabas, I., Macrophage death and defective inflammation resolution in atherosclerosis. *Nature reviews. Immunology* **2010,** *10* (1), 36-46.
37. Kunjathoor, V. V., et al., Scavenger receptors class A-I/II and CD36 are the principal receptors responsible for the uptake of modified low density lipoprotein leading to lipid loading in macrophages. *The Journal of biological chemistry* **2002,** *277* (51), 49982-8.
38. Stary, H. C., Lipid and macrophage accumulations in arteries of children and the development of atherosclerosis. *The American journal of clinical nutrition* **2000,** *72* (5 Suppl), 1297S-1306S.
39. Stary, H. C., et al., A definition of initial, fatty streak, and intermediate lesions of atherosclerosis. A report from the Committee on Vascular Lesions of the Council on Arteriosclerosis, American Heart Association. *Circulation* **1994,** *89* (5), 2462-78.
40. Virmani, R., et al., Lessons from sudden coronary death: a comprehensive morphological classification scheme for atherosclerotic lesions. *Arteriosclerosis, thrombosis, and vascular biology* **2000,** *20* (5), 1262-75.
41. Kolodgie, F. D., et al., Is pathologic intimal thickening the key to understanding early plaque progression in human atherosclerotic disease? *Arteriosclerosis, thrombosis, and vascular biology* **2007,** *27* (5), 986-9.
42. Moore, K. J., et al., Macrophages in the pathogenesis of atherosclerosis. *Cell* **2011,** *145* (3), 341-55.
43. Crisby, M., et al., Cell death in human atherosclerotic plaques involves both oncosis and apoptosis. *Atherosclerosis* **1997,** *130* (1-2), 17-27.
44. Schrijvers, D. M., et al., Phagocytosis of apoptotic cells by macrophages is impaired in atherosclerosis. *Arteriosclerosis, thrombosis, and vascular biology* **2005,** *25* (6), 1256-61.
45. Kolodgie, F. D., et al., Intraplaque hemorrhage and progression of coronary atheroma. *The New England journal of medicine* **2003,** *349* (24), 2316-25.
46. Kumamoto, M., et al., Intimal neovascularization in human coronary atherosclerosis: its origin and pathophysiological significance. *Human pathology* **1995,** *26* (4), 450-6.
47. Sluimer, J. C., et al., Thin-walled microvessels in human coronary atherosclerotic plaques show incomplete endothelial junctions relevance of compromised structural integrity for intraplaque microvascular leakage. *Journal of the American College of Cardiology* **2009,** *53* (17), 1517-27.
48. Finn, A. V., et al., Hemoglobin directs macrophage differentiation and prevents foam cell formation in human atherosclerotic plaques. *Journal of the American College of Cardiology* **2012,** *59* (2), 166-77.
49. Kragel, A. H., et al., Morphometric analysis of the composition of atherosclerotic plaques in the four major epicardial coronary arteries in acute myocardial infarction and in sudden coronary death. *Circulation* **1989,** *80* (6), 1747-56.
50. Stary, H. C., et al., A definition of advanced types of atherosclerotic lesions and a histological classification of atherosclerosis. A report from the Committee on Vascular Lesions of the Council on Arteriosclerosis, American Heart Association. *Circulation* **1995,** *92* (5), 1355-74.
51. Otsuka, F., et al., Has our understanding of calcification in human coronary atherosclerosis progressed? *Arteriosclerosis, thrombosis, and vascular biology* **2014,** *34* (4), 724-36.
52. Stary, H. C., The development of calcium deposits in atherosclerotic lesions and their persistence after lipid regression. *The American journal of cardiology* **2001,** *88* (2A), 16E-19E.
53. Stary, H. C., Natural history and histological classification of atherosclerotic lesions: an update. *Arteriosclerosis, thrombosis, and vascular biology* **2000,** *20* (5), 1177-8.
54. Stary, H. C., Evolution and progression of atherosclerotic lesions in coronary arteries of children and young adults. *Arteriosclerosis* **1989,** *9* (1 Suppl), I19-32.
55. Katz, S. S., et al., Physical chemistry of the lipids of human atherosclerotic lesions. Demonstration of a lesion intermediate between fatty streaks and advanced plaques. *The Journal of clinical investigation* **1976,** *58* (1), 200-11.
56. Nakashima, Y., et al., Early human atherosclerosis: accumulation of lipid and proteoglycans in intimal thickenings followed by macrophage infiltration. *Arteriosclerosis, thrombosis, and vascular biology* **2007,** *27* (5), 1159-65.
57. Geer, J. C., et al., Cholesterol ester fatty acid composition of human aorta fatty streaks and normal intima. *Experimental and molecular pathology* **1965,** *4* (5), 500-7.

58. Sakakura, K., et al., Pathophysiology of atherosclerosis plaque progression. *Heart, lung & circulation* **2013,** *22* (6), 399-411.
59. Stary, H. C., Composition and classification of human atherosclerotic lesions. *Virchows Archiv. A, Pathological anatomy and histopathology* **1992,** *421* (4), 277-90.
60. Timmis, A., et al., European Society of Cardiology: Cardiovascular Disease Statistics 2017. *European heart journal* **2018,** *39* (7), 508-579.
61. Davies, M. J., The pathophysiology of acute coronary syndromes. *Heart* **2000,** *83* (3), 361-6.
62. Falk, E., et al., Coronary plaque disruption. *Circulation* **1995,** *92* (3), 657-71.
63. Kolodgie, F. D., et al., The thin-cap fibroatheroma: a type of vulnerable plaque: the major precursor lesion to acute coronary syndromes. *Current opinion in cardiology* **2001,** *16* (5), 285-92.
64. van der Wal, A. C., et al., Site of intimal rupture or erosion of thrombosed coronary atherosclerotic plaques is characterized by an inflammatory process irrespective of the dominant plaque morphology. *Circulation* **1994,** *89* (1), 36-44.
65. Mittleman, M. A., et al., Physical, psychological and chemical triggers of acute cardiovascular events: preventive strategies. *Circulation* **2011,** *124* (3), 346-54.
66. Hao, H., et al., Phenotypic modulation of intima and media smooth muscle cells in fatal cases of coronary artery lesion. *Arteriosclerosis, thrombosis, and vascular biology* **2006,** *26* (2), 326-32.
67. Otsuka, F., et al., Pathology of coronary atherosclerosis and thrombosis. *Cardiovascular diagnosis and therapy* **2016,** *6* (4), 396-408.
68. Sillesen, H., et al., Carotid plaque burden as a measure of subclinical atherosclerosis: comparison with other tests for subclinical arterial disease in the High Risk Plaque BioImage study. *JACC. Cardiovascular imaging* **2012,** *5* (7), 681-9.
69. Falk, E., Pathogenesis of atherosclerosis. *Journal of the American College of Cardiology* **2006,** *47* (8 Suppl), C7-12.
70. Schaar, J. A., et al., Terminology for high-risk and vulnerable coronary artery plaques. Report of a meeting on the vulnerable plaque, June 17 and 18, 2003, Santorini, Greece. *European heart journal* **2004,** *25* (12), 1077-82.
71. Naghavi, M., et al., From vulnerable plaque to vulnerable patient: a call for new definitions and risk assessment strategies: Part II. *Circulation* **2003,** *108* (15), 1772-8.
72. Sillesen, H., et al., Why not screen for subclinical atherosclerosis? *Lancet* **2011,** *378* (9792), 645-6.
73. Ehrlich, P., Methodologische Beiträge zur Physiologie und Pathologie der verschiedenen formen der Leukocyten. *Z.Klin.Med.* **1880,** *1*, 553-560.
74. Pappenheim, A., Uber die verschiedenen lymphoiden Zellformen des normalen und pathologischen Blutes. *Folia Haematol* **1910,** *10*, 72-208.
75. Ebert, R. H., The extravascular development of the monocyte observed in vivo. *Br.J.Exp. Pathol.* **1939,** *20* (342-356).
76. Ziegler-Heitbrock, L., et al., Nomenclature of monocytes and dendritic cells in blood. *Blood* **2010,** *116* (16), E74-E80.
77. Wong, K. L., et al., Gene expression profiling reveals the defining features of the classical, intermediate, and nonclassical human monocyte subsets. *Blood* **2011,** *118* (5), e16-31.
78. Zawada, A. M., et al., SuperSAGE evidence for CD14++CD16+ monocytes as a third monocyte subset. *Blood* **2011,** *118* (12), e50-61.
79. Patel, A. A., et al., The fate and lifespan of human monocyte subsets in steady state and systemic inflammation. *The Journal of experimental medicine* **2017,** *214* (7), 1913-1923.
80. Guilliams, M., et al., Developmental and Functional Heterogeneity of Monocytes. *Immunity* **2018,** *49* (4), 595-613.
81. Chong, S. Z., et al., CXCR4 identifies transitional bone marrow premonocytes that replenish the mature monocyte pool for peripheral responses. *The Journal of experimental medicine* **2016,** *213* (11), 2293-2314.
82. Serbina, N. V., et al., Monocyte emigration from bone marrow during bacterial infection requires signals mediated by chemokine receptor CCR2. *Nature immunology* **2006,** *7* (3), 311-7.
83. Hettinger, J., et al., Origin of monocytes and macrophages in a committed progenitor. *Nature immunology* **2013,** *14* (8), 821-30.
84. Leuschner, F., et al., Rapid monocyte kinetics in acute myocardial infarction are sustained by extramedullary monocytopoiesis. *The Journal of experimental medicine* **2012,** *209* (1), 123-37.
85. Robbins, C. S., et al., Extramedullary hematopoiesis generates Ly-6C(high) monocytes that infiltrate atherosclerotic lesions. *Circulation* **2012,** *125* (2), 364-74.
86. Sawai, C. M., et al., Hematopoietic Stem Cells Are the Major Source of Multilineage Hematopoiesis in Adult Animals. *Immunity* **2016,** *45* (3), 597-609.
87. Swirski, F. K., et al., Identification of splenic reservoir monocytes and their deployment to inflammatory sites. *Science* **2009,** *325* (5940), 612-6.

88. Ghattas, A., et al., Monocytes in Coronary Artery Disease and Atherosclerosis Where Are We Now? *Journal of the American College of Cardiology* **2013,** *62* (17), 1541-1551.
89. Moore, K. J., et al., Macrophage Trafficking, Inflammatory Resolution, and Genomics in Atherosclerosis: JACC Macrophage in CVD Series (Part 2). *Journal of the American College of Cardiology* **2018,** *72* (18), 2181-2197.
90. Galkina, E., et al., Leukocyte influx in atherosclerosis. *Current drug targets* **2007,** *8* (12), 1239-48.
91. Cybulsky, M. I., et al., A major role for VCAM-1, but not ICAM-1, in early atherosclerosis. *The Journal of clinical investigation* **2001,** *107* (10), 1255-62.
92. Huo, Y., et al., Role of vascular cell adhesion molecule-1 and fibronectin connecting segment-1 in monocyte rolling and adhesion on early atherosclerotic lesions. *Circulation research* **2000,** *87* (2), 153-9.
93. Gerszten, R. E., et al., MCP-1 and IL-8 trigger firm adhesion of monocytes to vascular endothelium under flow conditions. *Nature* **1999,** *398* (6729), 718-23.
94. Fenyo, I. M., et al., The involvement of the monocytes/macrophages in chronic inflammation associated with atherosclerosis. *Immunobiology* **2013,** *218* (11), 1376-84.
95. Drechsler, M., et al., The complexity of arterial classical monocyte recruitment. *Journal of innate immunity* **2013,** *5* (4), 358-66.
96. Johnson, P., et al., CD44 and its role in inflammation and inflammatory diseases. *Inflammation & allergy drug targets* **2009,** *8* (3), 208-20.
97. Hashimoto, K., et al., Live-cell visualization of the trans-cellular mode of monocyte transmigration across the vascular endothelium, and its relationship with endothelial PECAM-1. *The journal of physiological sciences : JPS* **2012,** *62* (1), 63-9.
98. Osterud, B., et al., Role of monocytes in atherogenesis. *Physiological reviews* **2003,** *83* (4), 1069-112.
99. Wolfs, I. M., et al., Differentiation factors and cytokines in the atherosclerotic plaque micro-environment as a trigger for macrophage polarisation. *Thrombosis and haemostasis* **2011,** *106* (5), 763-71.
100. Stanley, E. R., et al., Induction of macrophage production and proliferation by a purified colony stimulating factor. *Nature* **1978,** *274* (5667), 168-70.
101. Martinez, F. O., et al., Transcriptional profiling of the human monocyte-to-macrophage differentiation and polarization: new molecules and patterns of gene expression. *J Immunol* **2006,** *177* (10), 7303-11.
102. Gleissner, C. A., Macrophage Phenotype Modulation by CXCL4 in Atherosclerosis. *Frontiers in physiology* **2012,** *3*, 1.
103. Fleetwood, A. J., et al., Granulocyte-macrophage colony-stimulating factor (CSF) and macrophage CSF-dependent macrophage phenotypes display differences in cytokine profiles and transcription factor activities: implications for CSF blockade in inflammation. *J Immunol* **2007,** *178* (8), 5245-52.
104. Simionescu, M., Cellular dysfunction in inflammatory-related vascular disorders' review series. The inflammatory process: a new dimension of a 19 century old story. *Journal of cellular and molecular medicine* **2009,** *13* (11-12), 4291-2.
105. Mosser, D. M., et al., Exploring the full spectrum of macrophage activation. *Nature reviews. Immunology* **2008,** *8* (12), 958-69.
106. Butcher, M. J., et al., Phenotypic and functional heterogeneity of macrophages and dendritic cell subsets in the healthy and atherosclerosis-prone aorta. *Frontiers in physiology* **2012,** *3*, 44.
107. Stoger, J. L., et al., Distribution of macrophage polarization markers in human atherosclerosis. *Atherosclerosis* **2012,** *225* (2), 461-8.
108. Rothe, G., et al., Peripheral blood mononuclear phagocyte subpopulations as cellular markers in hypercholesterolemia. *Arteriosclerosis, thrombosis, and vascular biology* **1996,** *16* (12), 1437-47.
109. Rothe, G., et al., A more mature phenotype of blood mononuclear phagocytes is induced by fluvastatin treatment in hypercholesterolemic patients with coronary heart disease. *Atherosclerosis* **1999,** *144* (1), 251-61.
110. Rogacev, K. S., et al., Lower Apo A-I and lower HDL-C levels are associated with higher intermediate CD14++CD16+ monocyte counts that predict cardiovascular events in chronic kidney disease. *Arteriosclerosis, thrombosis, and vascular biology* **2014,** *34* (9), 2120-7.
111. Poitou, C., et al., CD14dimCD16+ and CD14+CD16+ monocytes in obesity and during weight loss: relationships with fat mass and subclinical atherosclerosis. *Arteriosclerosis, thrombosis, and vascular biology* **2011,** *31* (10), 2322-30.
112. Timmerman, K. L., et al., Exercise training-induced lowering of inflammatory (CD14+CD16+) monocytes: a role in the anti-inflammatory influence of exercise? *Journal of leukocyte biology* **2008,** *84* (5), 1271-8.
113. Rogacev, K. S., et al., Monocyte heterogeneity in obesity and subclinical atherosclerosis. *European heart journal* **2010,** *31* (3), 369-76.
114. Schlitt, A., et al., CD14+CD16+ monocytes in coronary artery disease and their relationship to serum TNF-alpha levels. *Thrombosis and haemostasis* **2004,** *92* (2), 419-24.

115. Kashiwagi, M., et al., Association of monocyte subsets with vulnerability characteristics of coronary plaques as assessed by 64-slice multidetector computed tomography in patients with stable angina pectoris. *Atherosclerosis* **2010,** *212* (1), 171-6.
116. Rogacev, K. S., et al., CD14++CD16+ monocytes independently predict cardiovascular events: a cohort study of 951 patients referred for elective coronary angiography. *Journal of the American College of Cardiology* **2012,** *60* (16), 1512-20.
117. Nozawa, N., et al., Association between circulating monocytes and coronary plaque progression in patients with acute myocardial infarction. *Circulation journal : official journal of the Japanese Circulation Society* **2010,** *74* (7), 1384-91.
118. Tsujioka, H., et al., Impact of heterogeneity of human peripheral blood monocyte subsets on myocardial salvage in patients with primary acute myocardial infarction. *Journal of the American College of Cardiology* **2009,** *54* (2), 130-8.
119. van der Laan, A. M., et al., A proinflammatory monocyte response is associated with myocardial injury and impaired functional outcome in patients with ST-segment elevation myocardial infarction: Monocytes and myocardial infarction. *American heart journal* **2012,** *163* (1), 57-65.
120. van der Laan, A. M., et al., Monocyte subset accumulation in the human heart following acute myocardial infarction and the role of the spleen as monocyte reservoir. *European heart journal* **2014,** *35* (6), 376-385.
121. Tapp, L. D., et al., The CD14++CD16+ monocyte subset and monocyte-platelet interactions in patients with ST-elevation myocardial infarction. *Journal of thrombosis and haemostasis : JTH* **2012,** *10* (7), 1231-41.
122. Smith, A., Oxford Dictionary of Biochemistry and Molecular Biology. *Oxford University Press* **2000**.
123. Meer, G. v., Cellular lipidomics. *The EMBO journal* **2005,** *24*, 3159-3165.
124. Christie, W., Gas Chromatography and Lipids: A Practical Guide. *Oily, Ayr* **1989**.
125. Lipid Library website, http://lipidlibrary.aocs.org.
126. Cyberlipid Center website, http://www.cyberlipid.org.
127. Fahy, E., et al., Lipid classification, structures and tools. *Biochimica et biophysica acta* **2011,** *1811* (11), 637-47.
128. Fahy, E., et al., A comprehensive classification system for lipids. *Journal of lipid research* **2005,** *46* (5), 839-61.
129. The nomenclature of lipids. Recommendations (1976) IUPAC-IUB Commission on Biochemical Nomenclature. *Lipids* **1977,** *12* (6), 455-68.
130. Burdge, G. C., et al., Introduction to fatty acids and lipids. *World review of nutrition and dietetics* **2015,** *112*, 1-16.
131. Gibellini, F., et al., The Kennedy pathway--De novo synthesis of phosphatidylethanolamine and phosphatidylcholine. *IUBMB life* **2010,** *62* (6), 414-28.
132. Shindou, H., et al., Recent progress on acyl CoA: lysophospholipid acyltransferase research. *Journal of lipid research* **2009,** *50 Suppl*, S46-51.
133. Stith, J. L., et al., Advances in determining signaling mechanisms of ceramide and role in disease. *Journal of lipid research* **2019**.
134. Gurr, M., Lipid Biochemistry. *Blackwell Science* **2002**.
135. van Meer, G., et al., Membrane lipids: where they are and how they behave. *Nat Rev Mol Cell Bio* **2008,** *9* (2), 112-124.
136. Epand, R. M., Membrane lipid polymorphism: relationship to bilayer properties and protein function. *Methods Mol Biol* **2007,** *400*, 15-26.
137. Furt, F., et al., Importance of lipid metabolism for intracellular and mitochondrial membrane fusion/fission processes. *The international journal of biochemistry & cell biology* **2009,** *41* (10), 1828-36.
138. Wu, Y., et al., Phosphatidylserine recognition by phagocytes: a view to a kill. *Trends in cell biology* **2006,** *16* (4), 189-97.
139. Koivuniemi, A., The biophysical properties of plasmalogens originating from their unique molecular architecture. *FEBS letters* **2017,** *591* (18), 2700-2713.
140. Rubio, J. M., et al., Regulation of Phagocytosis in Macrophages by Membrane Ethanolamine Plasmalogens. *Frontiers in immunology* **2018,** *9*, 1723.
141. Thewke, D., et al., Transcriptional homeostatic control of membrane lipid composition. *Biochemical and biophysical research communications* **2000,** *273* (1), 1-4.
142. Bell, M. V., et al., Effects of the fatty acid composition of phosphatidylserine and diacylglycerol on the in vitro activity of protein kinase C from rat spleen: influences of (n-3) and (n-6) polyunsaturated fatty acids. *Comparative biochemistry and physiology. B, Comparative biochemistry* **1987,** *86* (2), 227-32.
143. Schoonjans, K., et al., PPARalpha and PPARgamma activators direct a distinct tissue-specific transcriptional response via a PPRE in the lipoprotein lipase gene. *The EMBO journal* **1996,** *15* (19), 5336-48.
144. Shevchenko, A., et al., Lipidomics: coming to grips with lipid diversity. *Nature reviews. Molecular cell biology* **2010,** *11* (8), 593-8.

145. Weir, J. M., et al., Plasma lipid profiling in a large population-based cohort. *Journal of lipid research* **2013,** *54* (10), 2898-908.
146. Stubiger, G., et al., Targeted profiling of atherogenic phospholipids in human plasma and lipoproteins of hyperlipidemic patients using MALDI-QIT-TOF-MS/MS. *Atherosclerosis* **2012,** *224* (1), 177-86.
147. Bou Khalil, M., et al., Lipidomics era: accomplishments and challenges. *Mass spectrometry reviews* **2010,** *29* (6), 877-929.
148. Davies, M. J., Stability and instability: two faces of coronary atherosclerosis. The Paul Dudley White Lecture 1995. *Circulation* **1996,** *94* (8), 2013-20.
149. Meikle, P. J., et al., Plasma lipidomic analysis of stable and unstable coronary artery disease. *Arteriosclerosis, thrombosis, and vascular biology* **2011,** *31* (11), 2723-32.
150. Kolovou, G., et al., Lipidomics in vascular health: current perspectives. *Vascular health and risk management* **2015,** *11*, 333-42.
151. van der Veen, J. N., et al., The critical role of phosphatidylcholine and phosphatidylethanolamine metabolism in health and disease. *Bba-Biomembranes* **2017,** *1859* (9), 1558-1572.
152. Martinez-Una, M., et al., S-Adenosylmethionine increases circulating very-low density lipoprotein clearance in non-alcoholic fatty liver disease. *Journal of hepatology* **2015,** *62* (3), 673-81.
153. Verkade, H. J., et al., Impaired biosynthesis of phosphatidylcholine causes a decrease in the number of very low density lipoprotein particles in the Golgi but not in the endoplasmic reticulum of rat liver. *The Journal of biological chemistry* **1993,** *268* (33), 24990-6.
154. Rahman, M. S., et al., Effects of dyslipidaemia on monocyte production and function in cardiovascular disease. *Nature reviews. Cardiology* **2017,** *14* (7), 387-400.
155. Saja, M. F., et al., Triglyceride-Rich Lipoproteins Modulate the Distribution and Extravasation of Ly6C/Gr1(low) Monocytes. *Cell reports* **2015,** *12* (11), 1802-15.
156. Peng, J., et al., Hypertriglyceridemia and atherosclerosis. *Lipids in health and disease* **2017,** *16* (1), 233.
157. Bernelot Moens, S. J., et al., PCSK9 monoclonal antibodies reverse the pro-inflammatory profile of monocytes in familial hypercholesterolaemia. *European heart journal* **2017,** *38* (20), 1584-1593.
158. Bernelot Moens, S. J., et al., Remnant Cholesterol Elicits Arterial Wall Inflammation and a Multilevel Cellular Immune Response in Humans. *Arteriosclerosis, thrombosis, and vascular biology* **2017,** *37* (5), 969-975.
159. Jackson, W. D., et al., Very-low and low-density lipoproteins induce neutral lipid accumulation and impair migration in monocyte subsets. *Scientific reports* **2016,** *6*, 20038.
160. Tafesse, F. G., et al., The multigenic sphingomyelin synthase family. *The Journal of biological chemistry* **2006,** *281* (40), 29421-5.
161. Zilversmit, D. B., et al., The synthesis of phospholipids in human atheromatous lesions. *Circulation* **1961,** *23*, 370-5.
162. Pan, W., et al., Elevation of ceramide and activation of secretory acid sphingomyelinase in patients with acute coronary syndromes. *Coronary artery disease* **2014,** *25* (3), 230-5.
163. Nilsson, A., et al., Absorption and lipoprotein transport of sphingomyelin. *Journal of lipid research* **2006,** *47* (1), 154-71.
164. Chatterjee, M., et al., Regulation of oxidized platelet lipidome: implications for coronary artery disease. *European heart journal* **2017,** *38* (25), 1993-2005.
165. Schlitt, A., et al., Further evaluation of plasma sphingomyelin levels as a risk factor for coronary artery disease. *Nutrition & metabolism* **2006,** *3*, 5.
166. Kimura, T., et al., Role of scavenger receptor class B type I and sphingosine 1-phosphate receptors in high density lipoprotein-induced inhibition of adhesion molecule expression in endothelial cells. *The Journal of biological chemistry* **2006,** *281* (49), 37457-67.
167. Shimamura, K., et al., Expression of adhesion molecules by sphingosine 1-phosphate and histamine in endothelial cells. *European journal of pharmacology* **2004,** *486* (2), 141-50.
168. Blaho, V. A., et al., An update on the biology of sphingosine 1-phosphate receptors. *Journal of lipid research* **2014,** *55* (8), 1596-608.
169. Hannun, Y. A., et al., Sphingolipids and their metabolism in physiology and disease. *Nature reviews. Molecular cell biology* **2018,** *19* (3), 175-191.
170. Stancevic, B., et al., Ceramide-rich platforms in transmembrane signaling. *FEBS letters* **2010,** *584* (9), 1728-40.
171. Scheffel, M. J., et al., Adoptive Transfer of Ceramide Synthase 6 Deficient Splenocytes Reduces the Development of Colitis. *Scientific reports* **2017,** *7* (1), 15552.
172. Helke, K., et al., Ceramide Synthase 6 Deficiency Enhances Inflammation in the DSS model of Colitis. *Scientific reports* **2018,** *8* (1), 1627.
173. Samanta, S., et al., Visualization of ceramide channels by transmission electron microscopy. *Biochimica et biophysica acta* **2011,** *1808* (4), 1196-201.

174. Park, J. W., et al., Ceramide synthases as potential targets for therapeutic intervention in human diseases. *Biochimica et biophysica acta* **2014,** *1841* (5), 671-81.
175. Raichur, S., et al., CerS2 Haploinsufficiency Inhibits beta-Oxidation and Confers Susceptibility to Diet-Induced Steatohepatitis and Insulin Resistance. *Cell Metab* **2014,** *20* (5), 919.
176. Turner, N., et al., A selective inhibitor of ceramide synthase 1 reveals a novel role in fat metabolism. *Nat Commun* **2018,** *9* (1), 3165.
177. Lallemand, T., et al., nSMase2 (Type 2-Neutral Sphingomyelinase) Deficiency or Inhibition by GW4869 Reduces Inflammation and Atherosclerosis in Apoe(-/-) Mice. *Arteriosclerosis, thrombosis, and vascular biology* **2018,** *38* (7), 1479-1492.
178. Peterson, L. R., et al., Ceramide Remodeling and Risk of Cardiovascular Events and Mortality. *Journal of the American Heart Association* **2018,** *7* (10).
179. Patterson, G. H., et al., Transport through the Golgi apparatus by rapid partitioning within a two-phase membrane system. *Cell* **2008,** *133* (6), 1055-67.
180. Kasahara, K., et al., Functional roles of glycosphingolipids in signal transduction via lipid rafts. *Glycoconjugate journal* **2000,** *17* (3 -4), 153-62.
181. Hakomori, S., Glycosphingolipids in cellular interaction, differentiation, and oncogenesis. *Annual review of biochemistry* **1981,** *50*, 733-64.
182. Hakomori, S., et al., New insights in glycosphingolipid function: "glycosignaling domain," a cell surface assembly of glycosphingolipids with signal transducer molecules,involved in cell adhesion coupled with signaling. *Glycobiology* **1998,** *8* (10), xi-xix.
183. Degroote, S., et al., The cell biology of glycosphingolipids. *Seminars in cell & developmental biology* **2004,** *15* (4), 375-87.
184. Basu, M., et al., Glycolipids. *Methods in enzymology* **1987,** *138*, 575-607.
185. Chatterjee, S., et al., Regulation of lactosylceramide synthase (glucosylceramide beta1-->4 galactosyltransferase); implication as a drug target. *Current drug targets* **2008,** *9* (4), 272-81.
186. Chatterjee, S., et al., The Yin and Yang of lactosylceramide metabolism: implications in cell function. *Biochimica et biophysica acta* **2008,** *1780* (3), 370-82.
187. Bhunia, A. K., et al., Lactosylceramide mediates tumor necrosis factor-alpha-induced intercellular adhesion molecule-1 (ICAM-1) expression and the adhesion of neutrophil in human umbilical vein endothelial cells. *The Journal of biological chemistry* **1998,** *273* (51), 34349-57.
188. Pannu, R., et al., A novel role of lactosylceramide in the regulation of tumor necrosis factor alpha-mediated proliferation of rat primary astrocytes. Implications for astrogliosis following neurotrauma. *The Journal of biological chemistry* **2005,** *280* (14), 13742-51.
189. Chatterjee, S., Sphingolipids in atherosclerosis and vascular biology. *Arteriosclerosis, thrombosis, and vascular biology* **1998,** *18* (10), 1523-33.
190. Chatterjee, S., Lactosylceramide stimulates aortic smooth muscle cell proliferation. *Biochemical and biophysical research communications* **1991,** *181* (2), 554-61.
191. Chatterjee, S., et al., Studies of the action of ceramide-like substances (D- and L-PDMP) on sphingolipid glycosyltransferases and purified lactosylceramide synthase. *Glycoconjugate journal* **1996,** *13* (3), 481-6.
192. Rajesh, M., et al., Novel role of lactosylceramide in vascular endothelial growth factor-mediated angiogenesis in human endothelial cells. *Circulation research* **2005,** *97* (8), 796-804.
193. Gong, N., et al., Lactosylceramide recruits PKCalpha/epsilon and phospholipase A2 to stimulate PECAM-1 expression in human monocytes and adhesion to endothelial cells. *Proceedings of the National Academy of Sciences of the United States of America* **2004,** *101* (17), 6490-5.
194. Zimmerman, J. W., et al., A novel carbohydrate-glycosphingolipid interaction between a beta-(1-3)-glucan immunomodulator, PGG-glucan, and lactosylceramide of human leukocytes. *The Journal of biological chemistry* **1998,** *273* (34), 22014-20.
195. Grandl, M., et al., E-LDL and Ox-LDL differentially regulate ceramide and cholesterol raft microdomains in human Macrophages. *Cytometry. Part A : the journal of the International Society for Analytical Cytology* **2006,** *69* (3), 189-91.
196. Chatterjee, S., Regulation of synthesis of lactosylceramide in normal and tumor proximal tubular cells. *Biochimica et biophysica acta* **1993,** *1167* (3), 339-44.
197. Chatterjee, S., et al., Regulation of glycosphingolipid glycosyltransferase by low density lipoprotein receptors in cultured human proximal tubular cells. *The Journal of biological chemistry* **1988,** *263* (26), 13017-22.
198. Chatterjee, S., et al., Localization of urinary lactosylceramide in cytoplasmic vesicles of renal tubular cells in homozygous familial hypercholesterolemia. *Proceedings of the National Academy of Sciences of the United States of America* **1983,** *80* (5), 1313-7.
199. Chatterjee, S., Role of oxidized human plasma low density lipoproteins in atherosclerosis: effects on smooth muscle cell proliferation. *Molecular and cellular biochemistry* **1992,** *111* (1-2), 143-7.

200. Chatterjee, S., et al., Oxidized low density lipoproteins stimulate galactosyltransferase activity, ras activation, p44 mitogen activated protein kinase and c-fos expression in aortic smooth muscle cells. *Glycobiology* **1997,** *7* (5), 703-10.
201. Bhunia, A. K., et al., Lactosylceramide stimulates Ras-GTP loading, kinases (MEK, Raf), p44 mitogen-activated protein kinase, and c-fos expression in human aortic smooth muscle cells. *The Journal of biological chemistry* **1996,** *271* (18), 10660-6.
202. Chatterjee, S. B., et al., Accumulation of glycosphingolipids in human atherosclerotic plaque and unaffected aorta tissues. *Glycobiology* **1997,** *7* (1), 57-65.
203. Arai, T., et al., Lactosylceramide stimulates human neutrophils to upregulate Mac-1, adhere to endothelium, and generate reactive oxygen metabolites in vitro. *Circulation research* **1998,** *82* (5), 540-7.
204. Folkman, J., Angiogenesis in cancer, vascular, rheumatoid and other disease. *Nature medicine* **1995,** *1* (1), 27-31.
205. Kishimoto, K., et al., Nondestructive quantification of neutral lipids by thin-layer chromatography and laser-fluorescent scanning: Suitable methods for "lipidome" analysis. *Biochemical and biophysical research communications* **2001,** *281* (3), 657-662.
206. Han, X., et al., Global analyses of cellular lipidomes directly from crude extracts of biological samples by ESI mass spectrometry: a bridge to lipidomics. *Journal of lipid research* **2003,** *44* (6), 1071-9.
207. Han, X., et al., Shotgun lipidomics: electrospray ionization mass spectrometric analysis and quantitation of cellular lipidomes directly from crude extracts of biological samples. *Mass spectrometry reviews* **2005,** *24* (3), 367-412.
208. Dayalan, S., Metabolome Analysis. *Encyclopedia of Bioinformatics and Computational Biology* **2018**.
209. Folch, J., et al., A simple method for the isolation and purification of total lipides from animal tissues. *The Journal of biological chemistry* **1957,** *226* (1), 497-509.
210. Bligh, E. G., et al., A rapid method of total lipid extraction and purification. *Canadian journal of biochemistry and physiology* **1959,** *37* (8), 911-7.
211. Pati, S., et al., Extraction, chromatographic and mass spectrometric methods for lipid analysis. *Biomedical chromatography : BMC* **2016,** *30* (5), 695-709.
212. Axelsen, P. H., et al., Quantitative analysis of phospholipids containing arachidonate and docosahexaenoate chains in microdissected regions of mouse brain. *Journal of lipid research* **2010,** *51* (3), 660-71.
213. Medina-Gomez, G., et al., PPAR gamma 2 prevents lipotoxicity by controlling adipose tissue expandability and peripheral lipid metabolism. *PLoS genetics* **2007,** *3* (4), e64.
214. Perona, J. S., et al., Simultaneous determination of molecular species of monoacylglycerols, diacylglycerols and triacylglycerols in human very-low-density lipoproteins by reversed-phase liquid chromatography. *Journal of chromatography. B, Analytical technologies in the biomedical and life sciences* **2003,** *785* (1), 89-99.
215. Griffiths, W. J., et al., Mass spectrometry: from proteomics to metabolomics and lipidomics. *Chemical Society reviews* **2009,** *38* (7), 1882-96.
216. Blanksby, S. J., et al., Advances in mass spectrometry for lipidomics. *Annu Rev Anal Chem (Palo Alto Calif)* **2010,** *3*, 433-65.
217. Schwudke, D., et al., Shotgun lipidomics on high resolution mass spectrometers. *Cold Spring Harbor perspectives in biology* **2011,** *3* (9), a004614.
218. Bourgon, R., et al., Independent filtering increases detection power for high-throughput experiments. *Proceedings of the National Academy of Sciences of the United States of America* **2010,** *107* (21), 9546-51.
219. Gromski, P. S., et al., Influence of missing values substitutes on multivariate analysis of metabolomics data. *Metabolites* **2014,** *4* (2), 433-52.
220. Godzien, J., et al., Controlling the quality of metabolomics data: new strategies to get the best out of the QC sample. *Metabolomics* **2015,** *11* (3), 518-528.
221. Wishart, D. S., et al., HMDB 3.0--The Human Metabolome Database in 2013. *Nucleic acids research* **2013,** *41* (Database issue), D801-7.
222. Fahy, E., et al., LIPID MAPS online tools for lipid research. *Nucleic acids research* **2007,** *35* (Web Server issue), W606-12.
223. Smith, C. A., et al., METLIN: a metabolite mass spectral database. *Therapeutic drug monitoring* **2005,** *27* (6), 747-51.
224. Kind, T., et al., Identification of small molecules using accurate mass MS/MS search. *Mass spectrometry reviews* **2018,** *37* (4), 513-532.
225. Sumner, L. W., et al., Proposed minimum reporting standards for chemical analysis Chemical Analysis Working Group (CAWG) Metabolomics Standards Initiative (MSI). *Metabolomics* **2007,** *3* (3), 211-221.
226. Gika, H. G., et al., Within-day reproducibility of an HPLC-MS-based method for metabonomic analysis: application to human urine. *Journal of proteome research* **2007,** *6* (8), 3291-303.

227. Mzmine website, www.mzmine.github.io.
228. Meuret, G., et al., Kinetics of human monocytopoiesis. *Blood* **1974,** *44* (6), 801-16.
229. Hansson, G. K., Inflammation, atherosclerosis, and coronary artery disease. *The New England journal of medicine* **2005,** *352* (16), 1685-95.
230. Huang, Z. S., et al., In hypercholesterolemia, lower peripheral monocyte count is unique among the major predictors of atherosclerosis. *Arteriosclerosis, thrombosis, and vascular biology* **1996,** *16* (2), 256-61.
231. Nasir, K., et al., Relationship of monocyte count and peripheral arterial disease: results from the National Health and Nutrition Examination Survey 1999-2002. *Arteriosclerosis, thrombosis, and vascular biology* **2005,** *25* (9), 1966-71.
232. Smith, J. D., et al., Decreased atherosclerosis in mice deficient in both macrophage colony-stimulating factor (op) and apolipoprotein E. *Proceedings of the National Academy of Sciences of the United States of America* **1995,** *92* (18), 8264-8.
233. Stoneman, V., et al., Monocyte/macrophage suppression in CD11b diphtheria toxin receptor transgenic mice differentially affects atherogenesis and established plaques. *Circulation research* **2007,** *100* (6), 884-93.
234. Horne, B. D., et al., Which white blood cell subtypes predict increased cardiovascular risk? *Journal of the American College of Cardiology* **2005,** *45* (10), 1638-43.
235. Olivares, R., et al., Monocyte count: a risk factor for coronary heart disease? *American journal of epidemiology* **1993,** *137* (1), 49-53.
236. Leers, M. P. G., et al., Intermediate and nonclassical monocytes show heterogeneity in patients with different types of acute coronary syndrome. *Cytometry. Part A : the journal of the International Society for Analytical Cytology* **2017,** *91* (11), 1059-1067.
237. Lo, S. C., et al., Intermediate CD14(++)CD16(+) monocyte predicts severe coronary stenosis and extensive plaque involvement in asymptomatic individuals. *The international journal of cardiovascular imaging* **2017,** *33* (8), 1223-1236.
238. Krychtiuk, K. A., et al., Monocyte subset distribution in patients with stable atherosclerosis and elevated levels of lipoprotein(a). *Journal of clinical lipidology* **2015,** *9* (4), 533-41.
239. Leers, M. P., et al., The pro- and anticoagulant role of blood-borne phagocytes in patients with acute coronary syndrome. *Thrombosis and haemostasis* **2013,** *110* (1), 101-9.
240. Hristov, M., et al., Circulating monocyte subsets and cardiovascular risk factors in coronary artery disease. *Thrombosis and haemostasis* **2010,** *104* (2), 412-4.
241. Ziegler-Heitbrock, L., The CD14+ CD16+ blood monocytes: their role in infection and inflammation. *Journal of leukocyte biology* **2007,** *81* (3), 584-92.
242. Gautier, E. L., et al., Regulation of the migration and survival of monocyte subsets by chemokine receptors and its relevance to atherosclerosis. *Arteriosclerosis, thrombosis, and vascular biology* **2009,** *29* (10), 1412-8.
243. Farb, A., et al., Coronary plaque erosion without rupture into a lipid core. A frequent cause of coronary thrombosis in sudden coronary death. *Circulation* **1996,** *93* (7), 1354-63.
244. Potteaux, S., et al., Suppressed monocyte recruitment drives macrophage removal from atherosclerotic plaques of Apoe-/- mice during disease regression. *The Journal of clinical investigation* **2011,** *121* (5), 2025-36.
245. Swirski, F. K., et al., Monocyte accumulation in mouse atherogenesis is progressive and proportional to extent of disease. *Proceedings of the National Academy of Sciences of the United States of America* **2006,** *103* (27), 10340-10345.
246. Zalai, C. V., et al., Increased circulating monocyte activation in patients with unstable coronary syndromes. *Journal of the American College of Cardiology* **2001,** *38* (5), 1340-7.
247. Charo, I. F., et al., The many roles of chemokines and chemokine receptors in inflammation. *The New England journal of medicine* **2006,** *354* (6), 610-21.
248. Cai, W., et al., Contribution of homeostatic chemokines CCL19 and CCL21 and their receptor CCR7 to coronary artery disease. *Arteriosclerosis, thrombosis, and vascular biology* **2014,** *34* (9), 1933-41.
249. Damas, J. K., et al., Enhanced expression of the homeostatic chemokines CCL19 and CCL21 in clinical and experimental atherosclerosis: possible pathogenic role in plaque destabilization. *Arteriosclerosis, thrombosis, and vascular biology* **2007,** *27* (3), 614-20.
250. Tacke, F., et al., Monocyte subsets differentially employ CCR2, CCR5, and CX3CR1 to accumulate within atherosclerotic plaques. *The Journal of clinical investigation* **2007,** *117* (1), 185-94.
251. Combadiere, C., et al., Combined inhibition of CCL2, CX3CR1, and CCR5 abrogates Ly6C(hi) and Ly6C(lo) monocytosis and almost abolishes atherosclerosis in hypercholesterolemic mice. *Circulation* **2008,** *117* (13), 1649-57.
252. Weber, C., et al., Role and analysis of monocyte subsets in cardiovascular disease. Joint consensus document of the European Society of Cardiology (ESC) Working Groups "Atherosclerosis & Vascular Biology" and "Thrombosis". *Thrombosis and haemostasis* **2016,** *116* (4), 626-37.

253. Askenase, M. H., et al., Bone-Marrow-Resident NK Cells Prime Monocytes for Regulatory Function during Infection. *Immunity* **2015,** *42* (6), 1130-42.
254. Quintin, J., et al., Candida albicans infection affords protection against reinfection via functional reprogramming of monocytes. *Cell host & microbe* **2012,** *12* (2), 223-32.
255. Patel, V. K., et al., Monocyte inflammatory profile is specific for individuals and associated with altered blood lipid levels. *Atherosclerosis* **2017,** *263*, 15-23.
256. Bekkering, S., et al., Oxidized low-density lipoprotein induces long-term proinflammatory cytokine production and foam cell formation via epigenetic reprogramming of monocytes. *Arteriosclerosis, thrombosis, and vascular biology* **2014,** *34* (8), 1731-8.
257. Escate, R., et al., LDL accelerates monocyte to macrophage differentiation: Effects on adhesion and anoikis. *Atherosclerosis* **2016,** *246*, 177-86.
258. Khan, I. M., et al., Postprandial Monocyte Activation in Individuals With Metabolic Syndrome. *The Journal of clinical endocrinology and metabolism* **2016,** *101* (11), 4195-4204.
259. Bath, P. M., et al., Human monocyte characteristics are altered in hypercholesterolaemia. *Atherosclerosis* **1991,** *90* (2-3), 175-81.
260. Xue, D., et al., Correlation between CD14+CD16++ monocytes in peripheral blood and hypertriglyceridemia after allograft renal transplantation. *Transplantation proceedings* **2013,** *45* (9), 3279-83.
261. Foster, G. A., et al., On-chip phenotypic analysis of inflammatory monocytes in atherogenesis and myocardial infarction. *Proceedings of the National Academy of Sciences of the United States of America* **2013,** *110* (34), 13944-9.
262. Bursill, C. A., et al., High-density lipoproteins suppress chemokines and chemokine receptors in vitro and in vivo. *Arteriosclerosis, thrombosis, and vascular biology* **2010,** *30* (9), 1773-8.
263. Hellwing, C., et al., Lipid composition of membrane microdomains isolated detergent-free from PUFA supplemented RAW264.7 macrophages. *Journal of cellular physiology* **2018,** *233* (3), 2602-2612.
264. Rolin, J., et al., Oxidized lipids and lysophosphatidylcholine induce the chemotaxis, up-regulate the expression of CCR9 and CXCR4 and abrogate the release of IL-6 in human monocytes. *Toxins* **2014,** *6* (9), 2840-56.
265. Brown, I., et al., Omega-3 N-acylethanolamines are endogenously synthesised from omega-3 fatty acids in different human prostate and breast cancer cell lines. *Prostaglandins, leukotrienes, and essential fatty acids* **2011,** *85* (6), 305-10.
266. Preiss, J., et al., Quantitative measurement of sn-1,2-diacylglycerols present in platelets, hepatocytes, and ras- and sis-transformed normal rat kidney cells. *The Journal of biological chemistry* **1986,** *261* (19), 8597-600.
267. Wattenberg, B. W., et al., The sphingosine and diacylglycerol kinase superfamily of signaling kinases: localization as a key to signaling function. *Journal of lipid research* **2006,** *47* (6), 1128-39.
268. Fernandez-Ruiz, I., et al., Differential lipid metabolism in monocytes and macrophages: influence of cholesterol loading. *Journal of lipid research* **2016,** *57* (4), 574-86.
269. Rouzer, C. A., et al., Lipid profiling reveals glycerophospholipid remodeling in zymosan-stimulated macrophages. *Biochemistry* **2007,** *46* (20), 6026-42.
270. Rouzer, C. A., et al., Lipid profiling reveals arachidonate deficiency in RAW264.7 cells: Structural and functional implications. *Biochemistry* **2006,** *45* (49), 14795-808.
271. Levick, S. P., et al., Arachidonic acid metabolism as a potential mediator of cardiac fibrosis associated with inflammation. *J Immunol* **2007,** *178* (2), 641-6.
272. Lee, J. W., et al., UPLC-QqQ/MS-Based Lipidomics Approach To Characterize Lipid Alterations in Inflammatory Macrophages. *Journal of proteome research* **2017,** *16* (4), 1460-1469.
273. Wells, I. C., et al., Lecithin: cholesterol acyltransferase and lysolecithin in coronary atherosclerosis. *Experimental and molecular pathology* **1986,** *45* (3), 303-10.
274. Quinn, M. T., et al., Lysophosphatidylcholine: a chemotactic factor for human monocytes and its potential role in atherogenesis. *Proceedings of the National Academy of Sciences of the United States of America* **1988,** *85* (8), 2805-9.
275. Schmitz, G., et al., Metabolism and atherogenic disease association of lysophosphatidylcholine. *Atherosclerosis* **2010,** *208* (1), 10-8.
276. Kume, N., et al., Lysophosphatidylcholine, a component of atherogenic lipoproteins, induces mononuclear leukocyte adhesion molecules in cultured human and rabbit arterial endothelial cells. *The Journal of clinical investigation* **1992,** *90* (3), 1138-44.
277. Pan, J. P., et al., Vitamin C protects against lysophosphatidylcholine-induced expression of monocyte chemoattractant protein-1 in cultured human umbilical vein endothelial cells. *Journal of the Formosan Medical Association = Taiwan yi zhi* **2003,** *102* (3), 151-7.
278. Carmena, R., et al., Atherogenic lipoprotein particles in atherosclerosis. *Circulation* **2004,** *109* (23 Suppl 1), III2-7.

279. Wilhelm, M. G., et al., Induction of atherosclerosis by human chylomicron remnants: a hypothesis. *Journal of atherosclerosis and thrombosis* **2003,** *10* (3), 132-9.
280. Jagla, A., et al., Postprandial triglycerides and endothelial function. *Experimental and clinical endocrinology & diabetes : official journal, German Society of Endocrinology [and] German Diabetes Association* **2001,** *109* (4), S533-47.
281. Chandak, P. G., et al., Lack of acyl-CoA:diacylglycerol acyltransferase 1 reduces intestinal cholesterol absorption and attenuates atherosclerosis in apolipoprotein E knockout mice. *Biochimica et biophysica acta* **2011,** *1811* (12), 1011-20.
282. Koliwad, S. K., et al., DGAT1-dependent triacylglycerol storage by macrophages protects mice from diet-induced insulin resistance and inflammation. *The Journal of clinical investigation* **2010,** *120* (3), 756-67.
283. De Lima, T. M., et al., Mechanisms by which fatty acids regulate leucocyte function. *Clin Sci* **2007,** *113* (1-2), 65-77.
284. Samad, F., et al., Altered adipose and plasma sphingolipid metabolism in obesity: a potential mechanism for cardiovascular and metabolic risk. *Diabetes* **2006,** *55* (9), 2579-87.
285. Li, Z., et al., The effect of dietary sphingolipids on plasma sphingomyelin metabolism and atherosclerosis. *Biochimica et biophysica acta* **2005,** *1735* (2), 130-4.
286. Jiang, X. C., et al., Plasma sphingomyelin level as a risk factor for coronary artery disease. *Arteriosclerosis, thrombosis, and vascular biology* **2000,** *20* (12), 2614-8.
287. Auge, N., et al., Role for matrix metalloproteinase-2 in oxidized low-density lipoprotein-induced activation of the sphingomyelin/ceramide pathway and smooth muscle cell proliferation. *Circulation* **2004,** *110* (5), 571-8.
288. Mitchinson, M. J., et al., Cell death in atherosclerotic plaques. *Current opinion in lipidology* **1996,** *7* (5), 324-9.
289. Goni, F. M., et al., Biophysics of sphingolipids I. Membrane properties of sphingosine, ceramides and other simple sphingolipids. *Biochimica et biophysica acta* **2006,** *1758* (12), 1902-21.
290. Song, J., et al., Bending rigidity of SOPC membranes containing cholesterol. *Biophysical journal* **1993,** *64* (6), 1967-70.
291. Chakravarthy, H., et al., Role of Acid Sphingomyelinase in Shifting the Balance Between Proinflammatory and Reparative Bone Marrow Cells in Diabetic Retinopathy. *Stem Cells* **2016,** *34* (4), 972-83.
292. Bollinger, C. R., et al., Ceramide-enriched membrane domains. *Biochimica et biophysica acta* **2005,** *1746* (3), 284-94.
293. Catapano, E. R., et al., Solid character of membrane ceramides: a surface rheology study of their mixtures with sphingomyelin. *Biophysical journal* **2011,** *101* (11), 2721-30.
294. Edsfeldt, A., et al., Sphingolipids Contribute to Human Atherosclerotic Plaque Inflammation. *Arteriosclerosis, thrombosis, and vascular biology* **2016,** *36* (6), 1132-40.
295. Chatterjee, S., et al., Role of lactosylceramide and MAP kinase in the proliferation of proximal tubular cells in human polycystic kidney disease. *Journal of lipid research* **1996,** *37* (6), 1334-44.
296. Bhunia, A. K., et al., Redox-regulated signaling by lactosylceramide in the proliferation of human aortic smooth muscle cells. *The Journal of biological chemistry* **1997,** *272* (25), 15642-9.
297. Iwabuchi, K., et al., Involvement of very long fatty acid-containing lactosylceramide in lactosylceramide-mediated superoxide generation and migration in neutrophils. *Glycoconjugate journal* **2008,** *25* (4), 357-74.
298. Kolmakova, A., et al., Platelet derived growth factor recruits lactosylceramide to induce cell proliferation in UDP Gal:GlcCer: beta1 --> 4Galactosyltransferase (GalT-V) mutant Chinese hamster ovary cells. *Glycoconjugate journal* **2005,** *22* (7-9), 401-7.

9. Appendixes

9.1 Appendix A

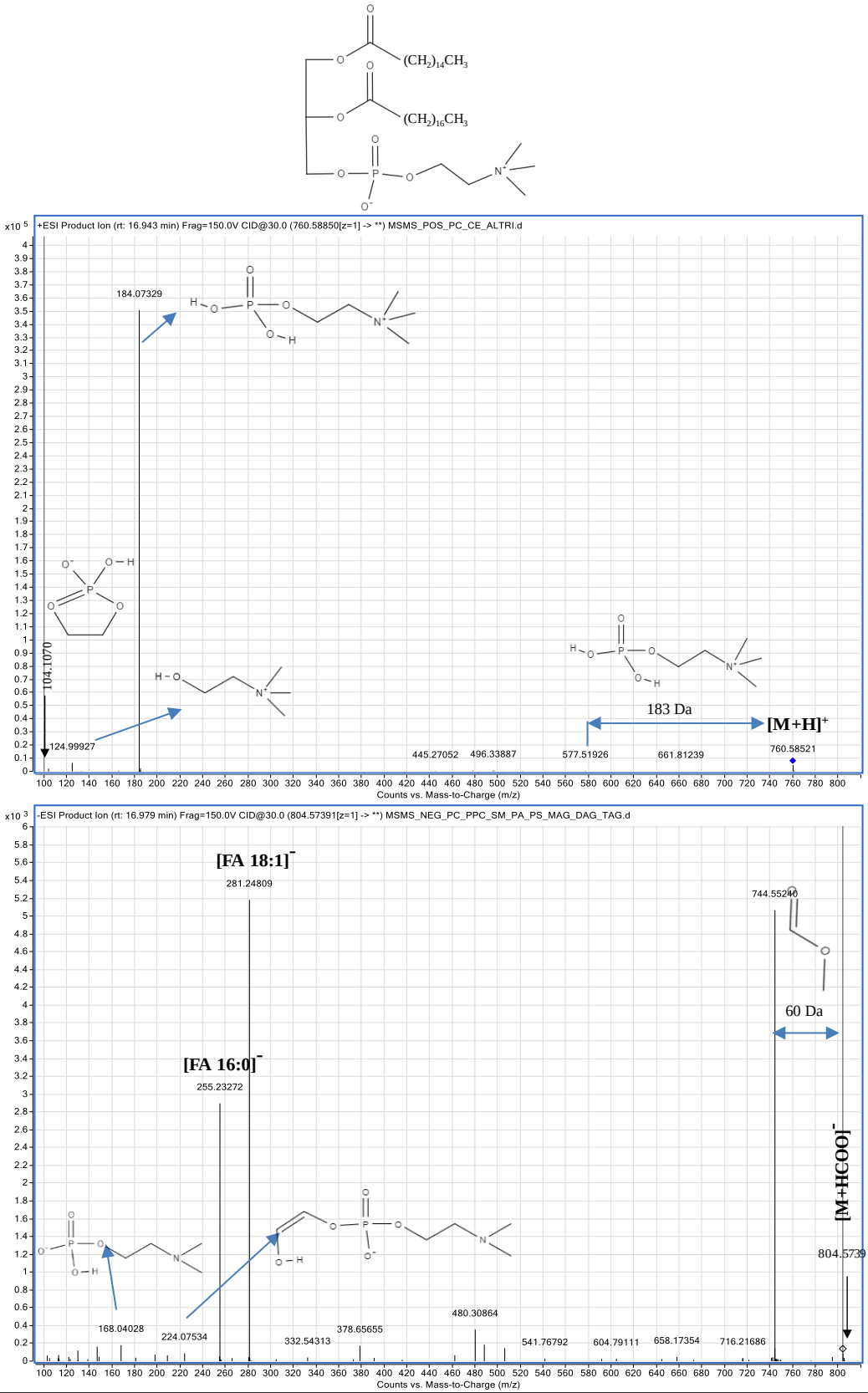

Figure A1 **Phosphatidylcholine fragmentation**
Representative MS/MS spectra for phosphatidylcholine PC (34:1) (16:0/18:1) in A) positive $[M+H]^+$ and B) negative $[M+HCOO]^-$ ionization mode.

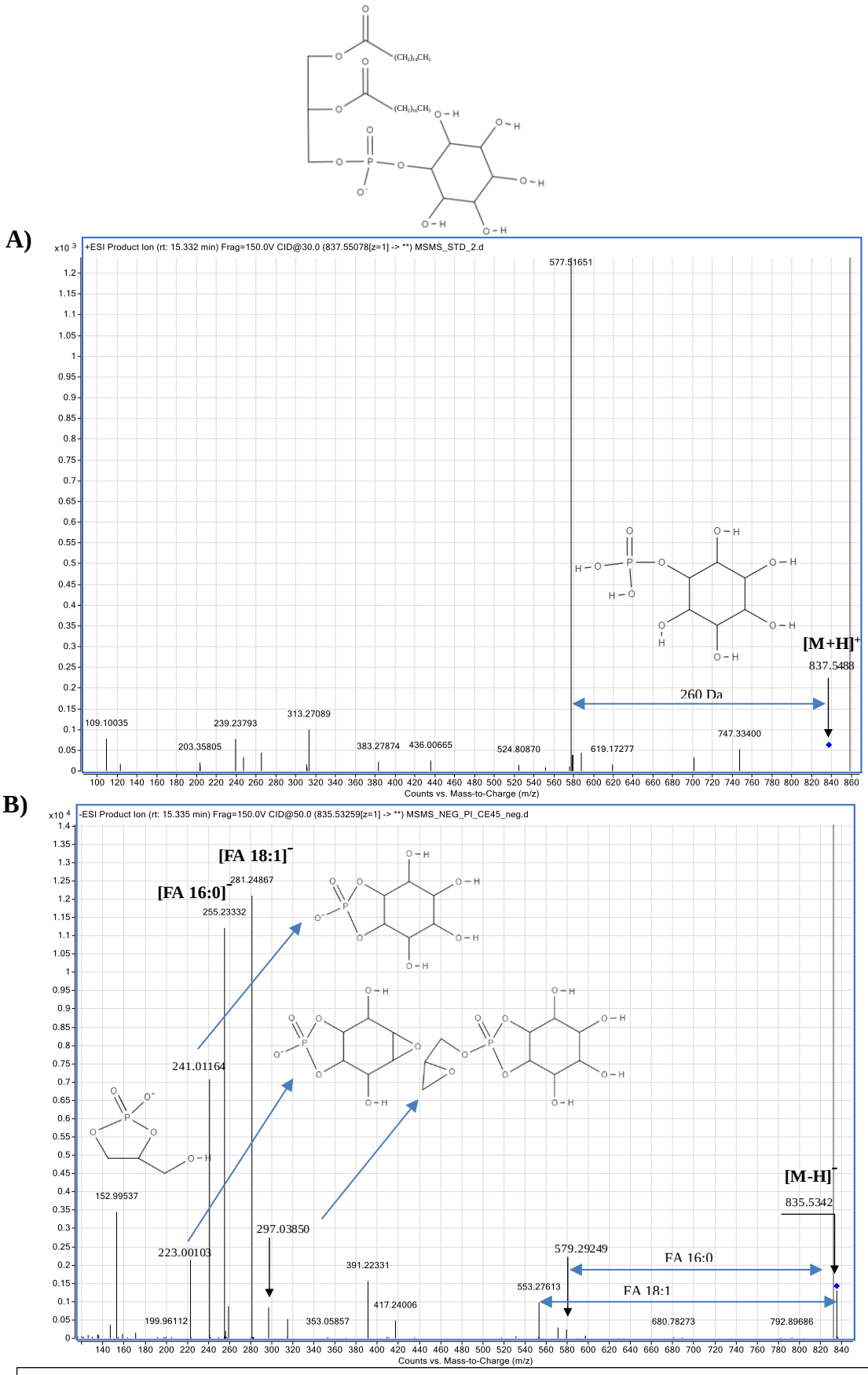

Figure A2 **Phosphatidylinositol fragmentation**
Representative MS/MS spectra for phosphatidylinositol PI (34:1) (16:0/18:1) in A) positive $[M+H]^+$ and B) negative $[M+H]^-$ ionization mode.

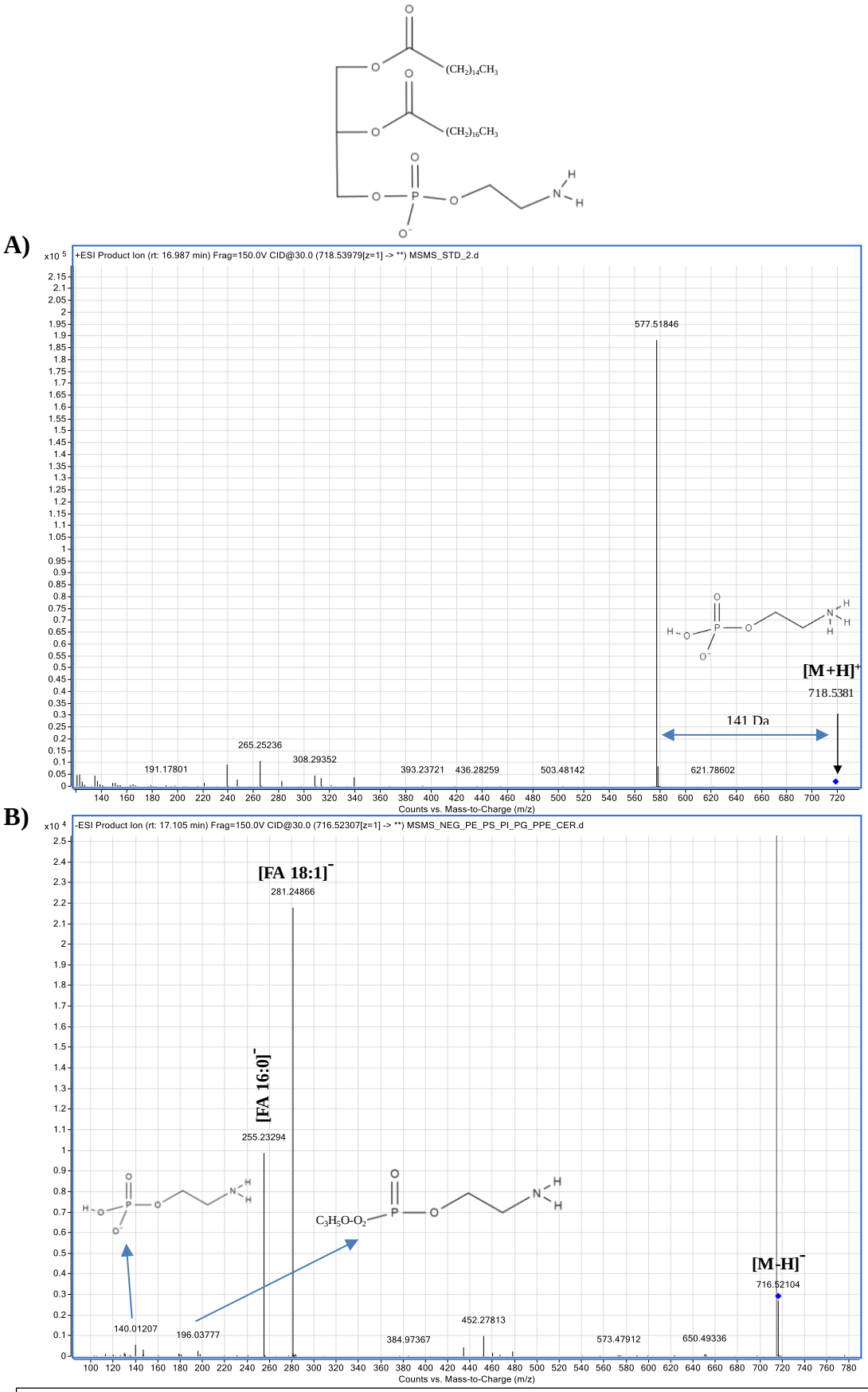

Figure A3 **Phosphatidylethanolamine fragmentation**
Representative MS/MS spectra for phosphatidylethanolamine PE (34:1) (16:0/18:1) in A) positive $[M+H]^+$ and B) negative $[M+H]^-$ ionization mode.

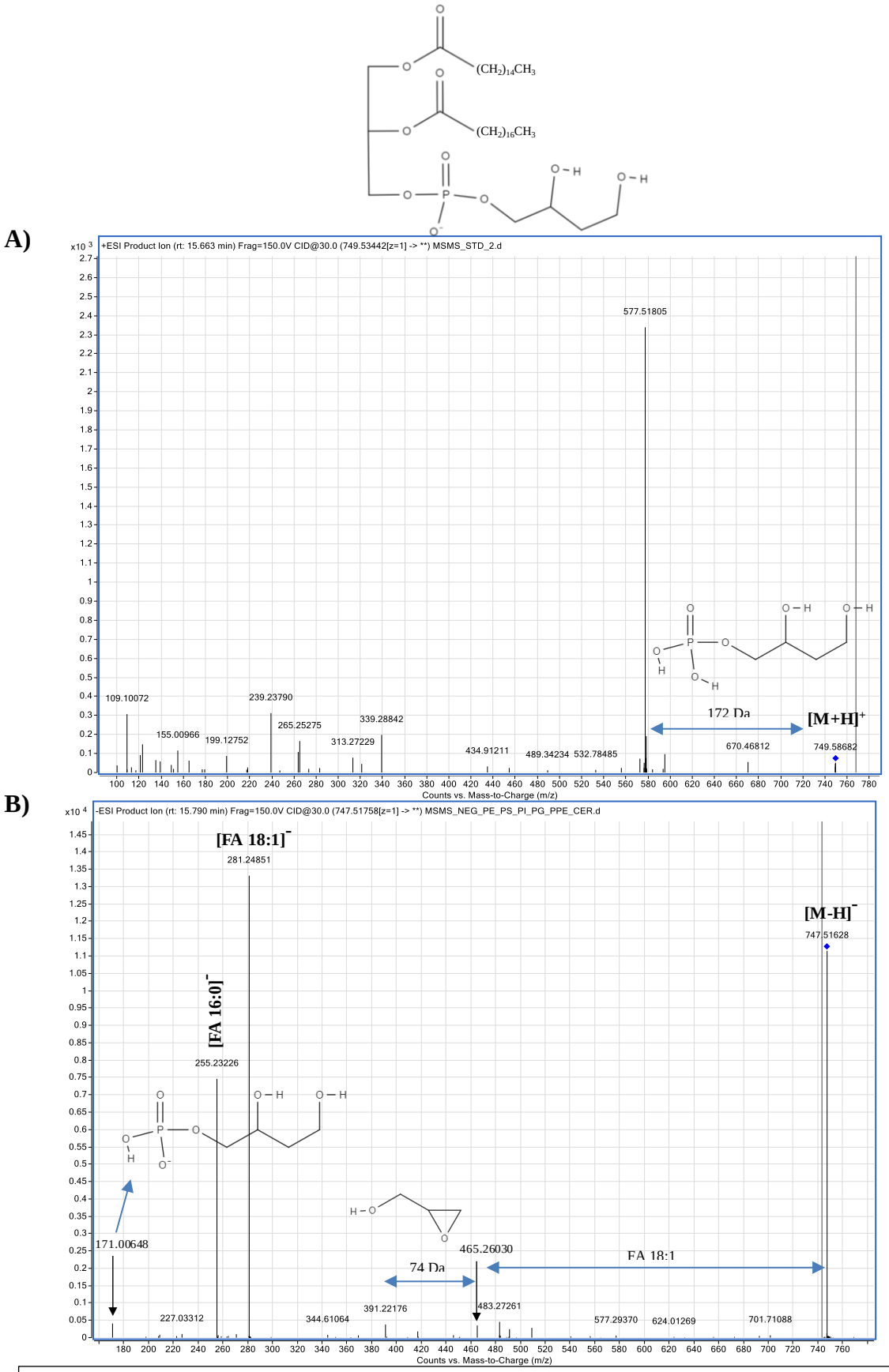

Figure A4 **Phosphatidylglycerol fragmentation**
Representative MS/MS spectra for phosphatidylglycerol PG (34:1) (16:0/18:1) in A) positive $[M+H]^+$ and B) negative $[M+H]^-$ ionization mode.

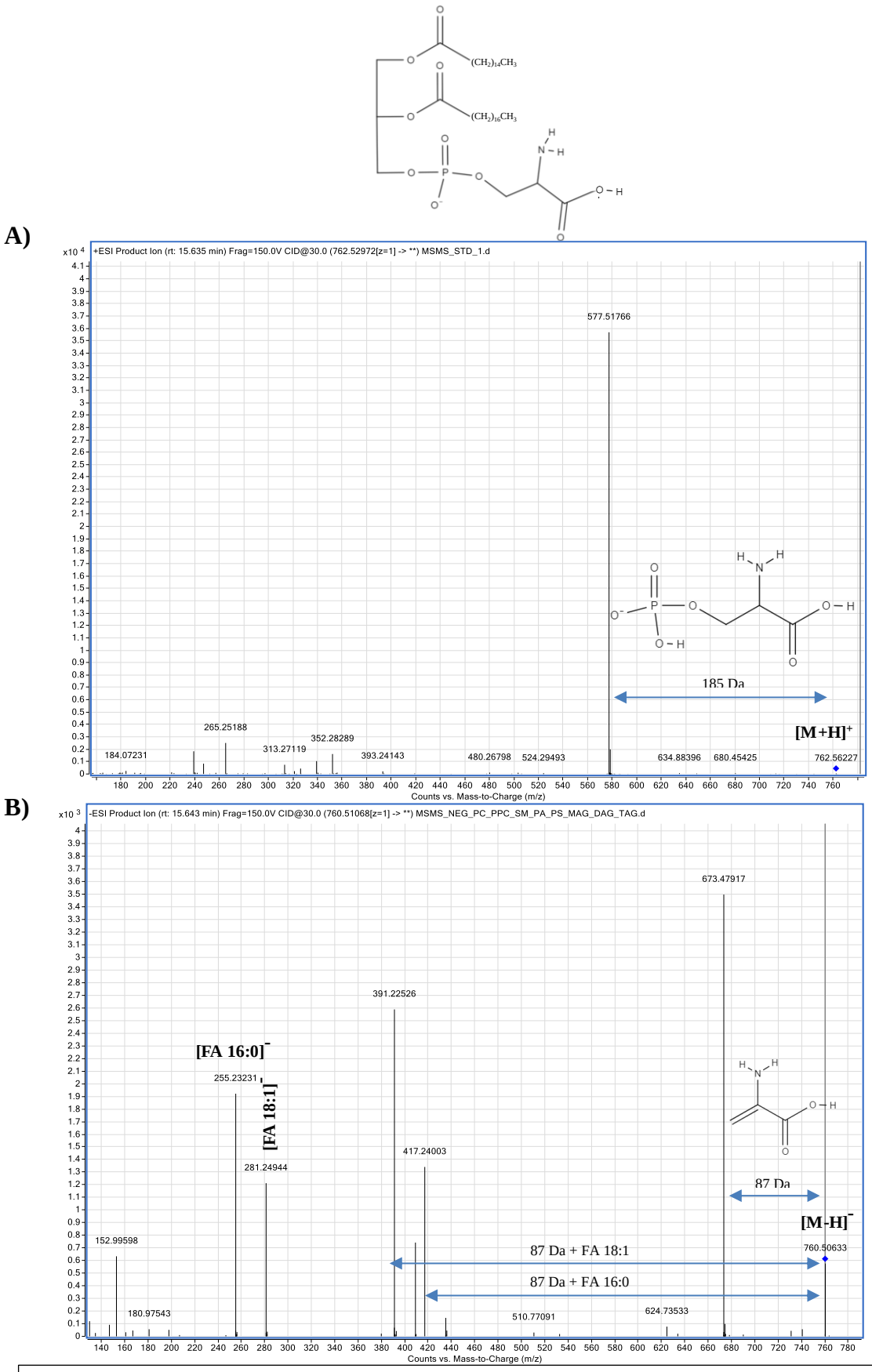

Figure A5 **Phosphatidylserine fragmentation**
Representative MS/MS spectra for phosphatidylserine PS (34:1) (16:0/18:1) in A) positive $[M+H]^+$ and B) negative $[M+H]^-$ ionization mode.

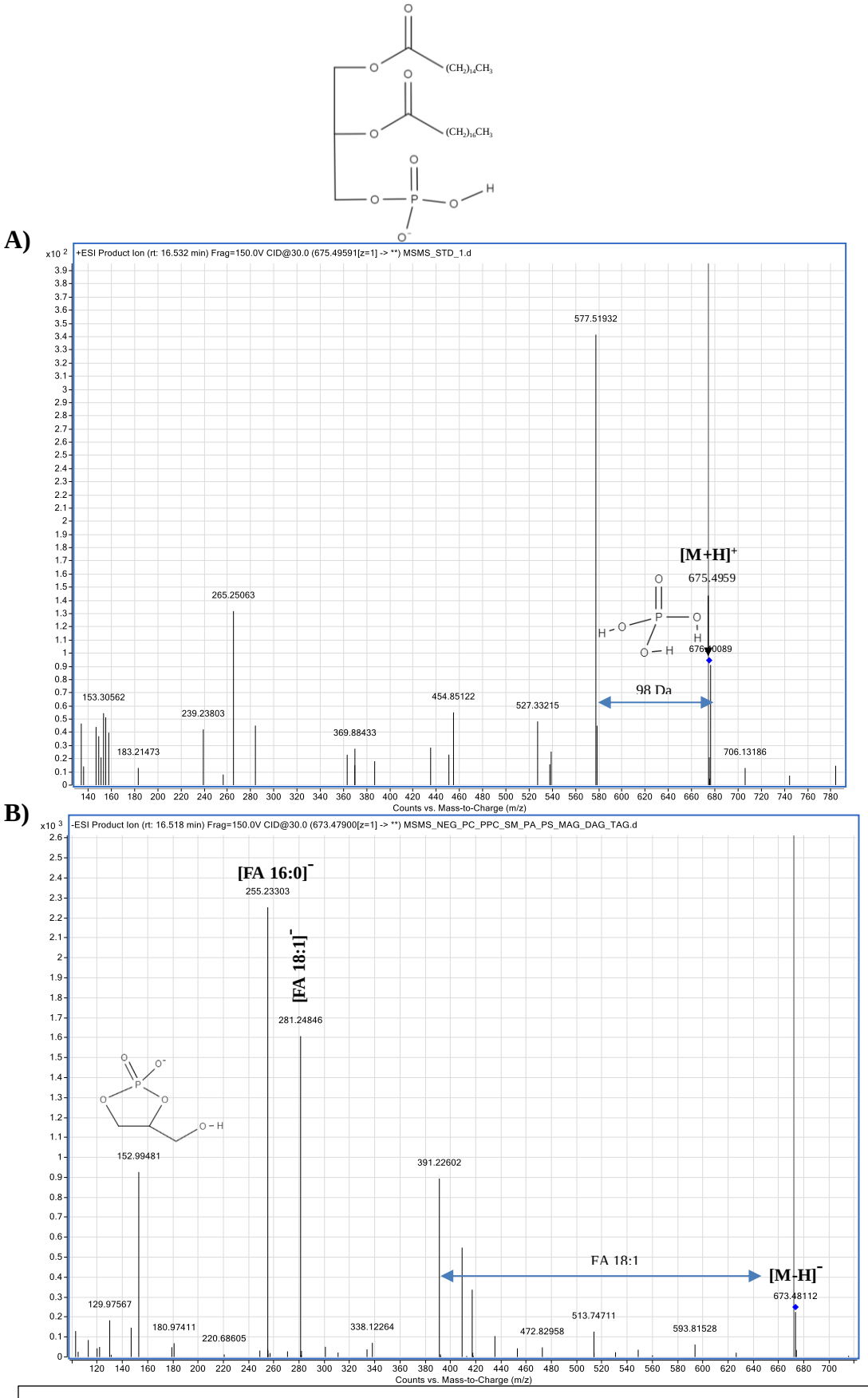

Figure A6 **Phosphatidic acid fragmentation**
Representative MS/MS spectra for phosphatidic acid PA (34:1) (16:0/18:1) in A) positive $[M+H]^+$ and B) negative $[M+H]^-$ ionization mode.

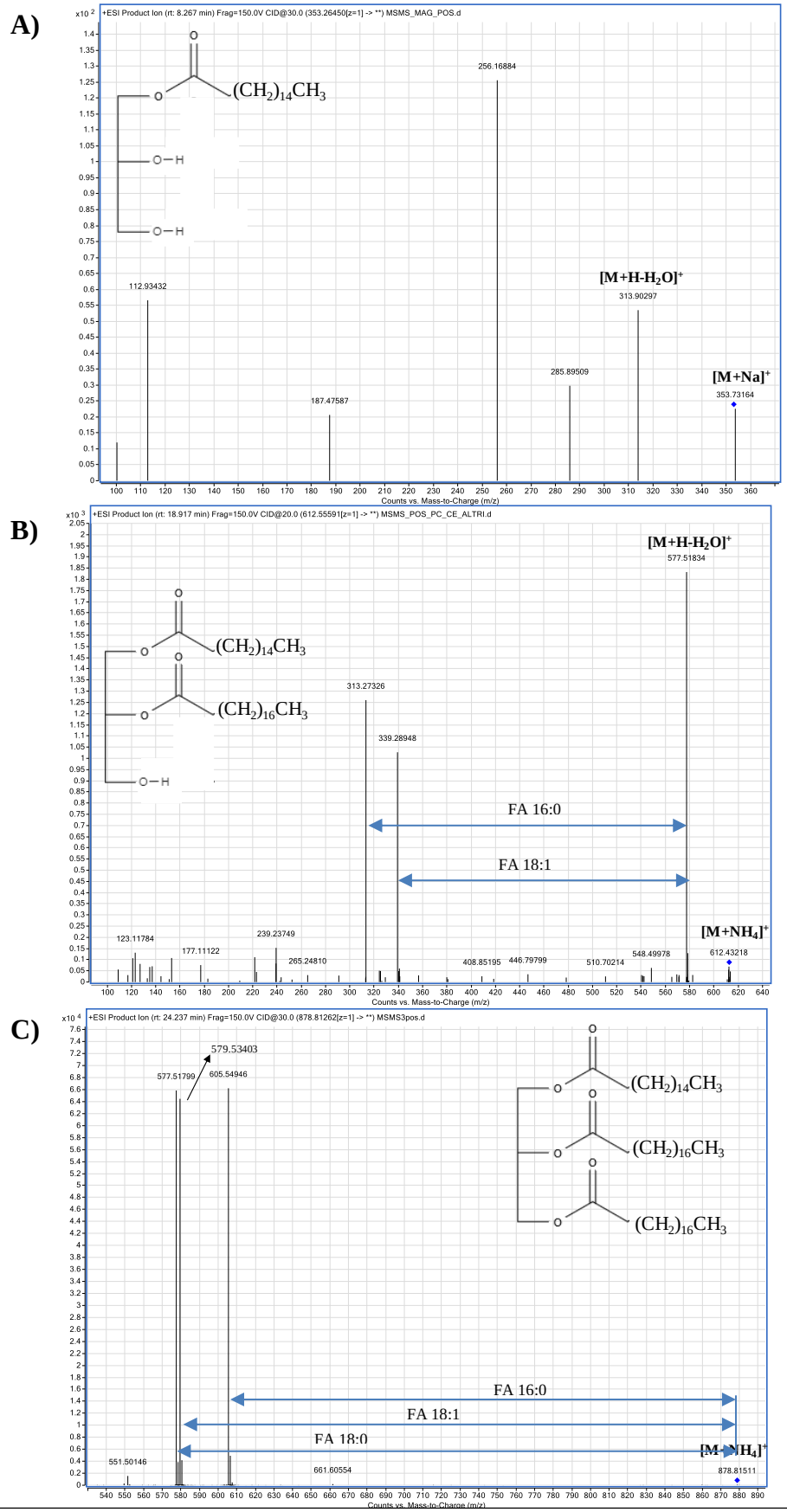

Figure A7 **Glycerolipids fragmentation**
Representative MS/MS spectra for A) monoacylglycerol MG (16:0) $[M+Na]^+$, B) diacylglycerol DG (34:1) (18:1/16:0) $[M+NH_4]^+$, and C) triacylglycerol TG (52:1) (18:0/18:1/16:0) $[M+NH_4]^+$ in positive ionization mode.

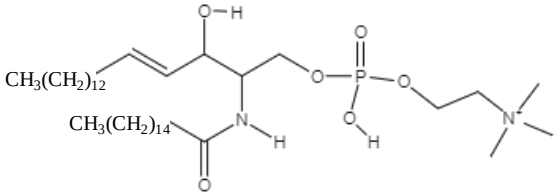

A)

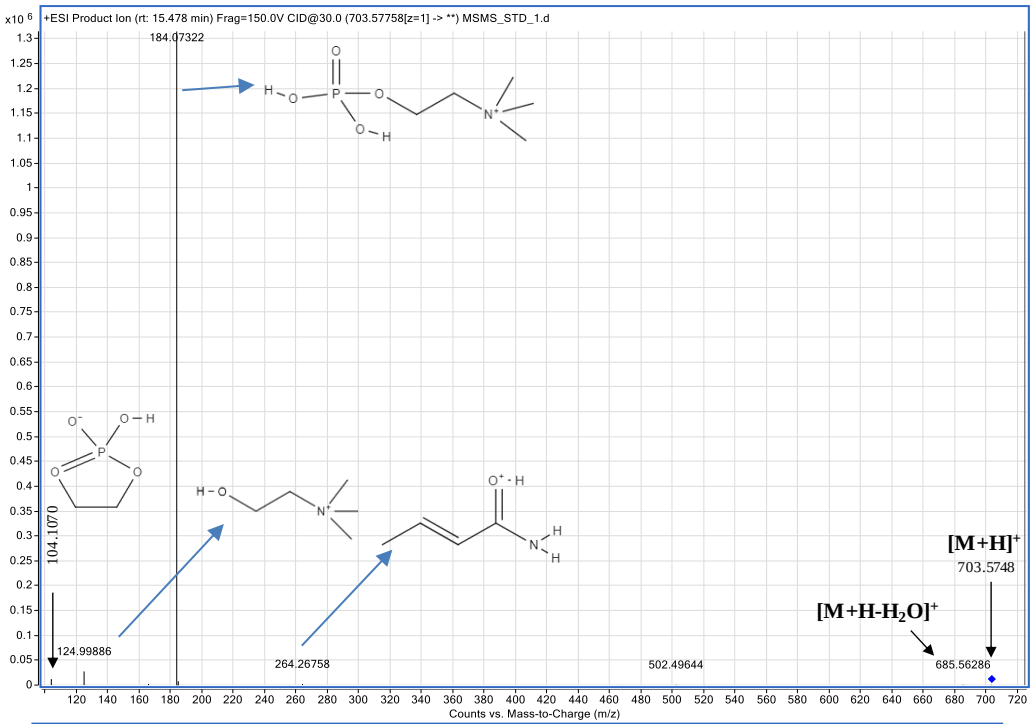

B)

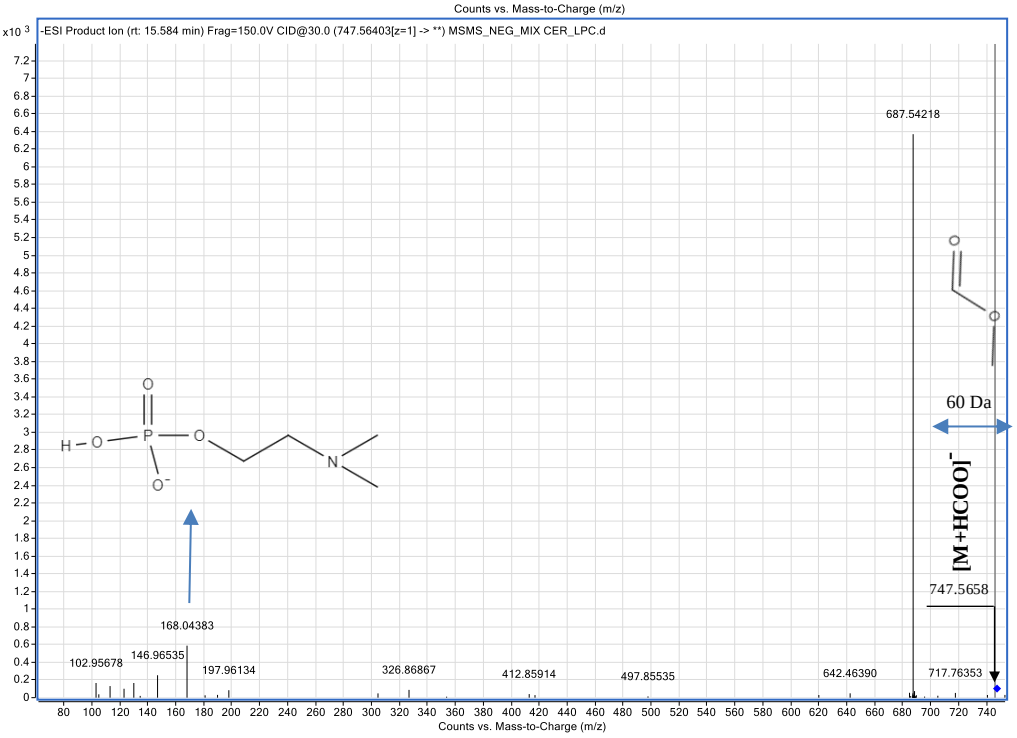

Figure A8 **Sphingomyelin fragmentation**
Representative MS/MS spectra for sphingomyelin SM (d34:1) (d18:1/16:0) in A) positive $[M+H]^+$ and B) negative $[M+HCOO]^-$ ionization mode.

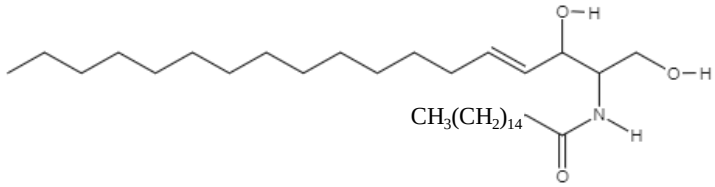

A)

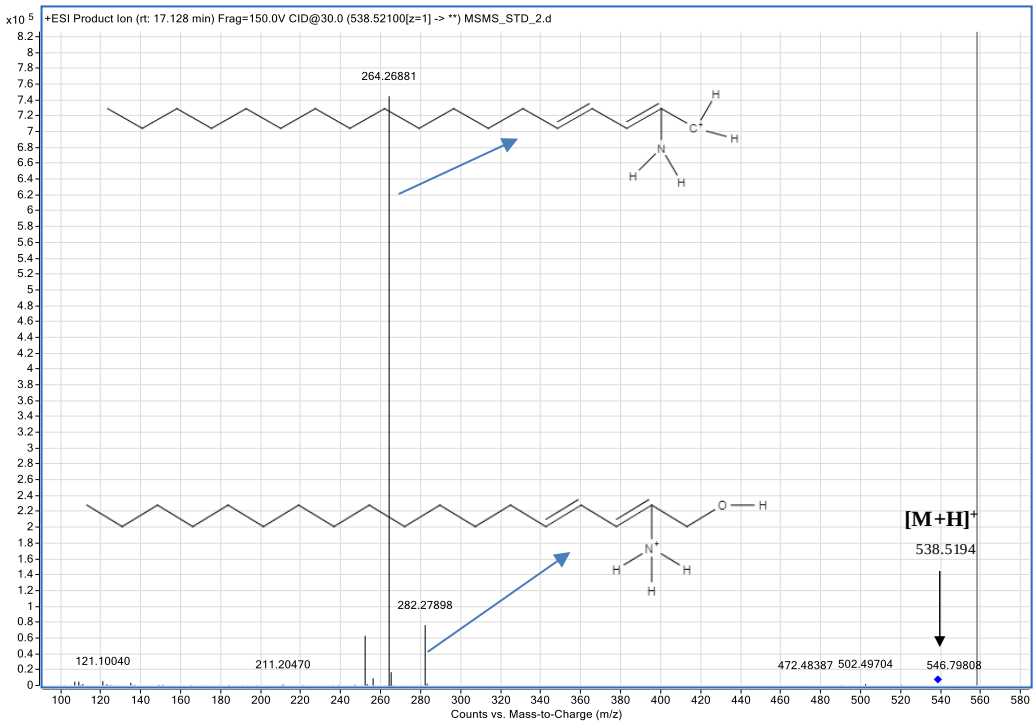

B)

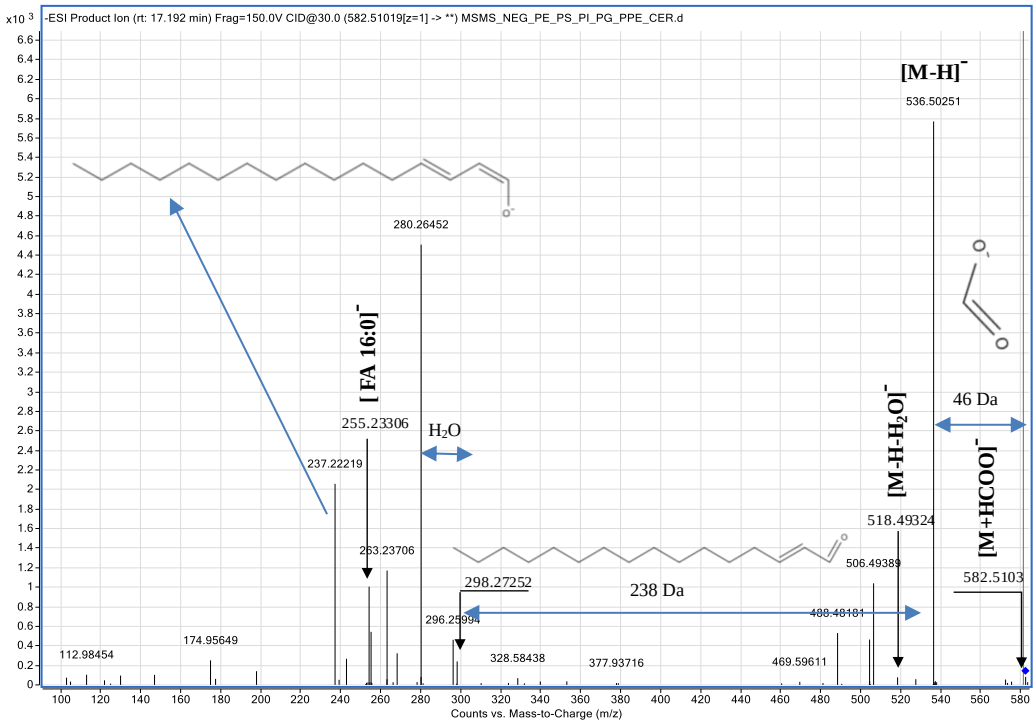

Figure A9 **Ceramide fragmentation**
Representative MS/MS spectra for ceramide CER (d34:1) (d18:1/16:0) in A) positive $[M+H]^+$ and B) negative $[M+HCOO]^-$ ionization mode.

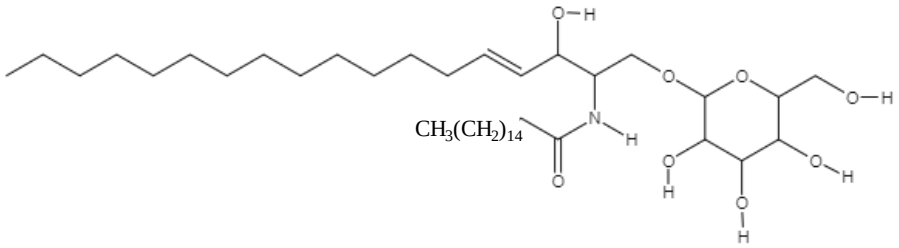

A)

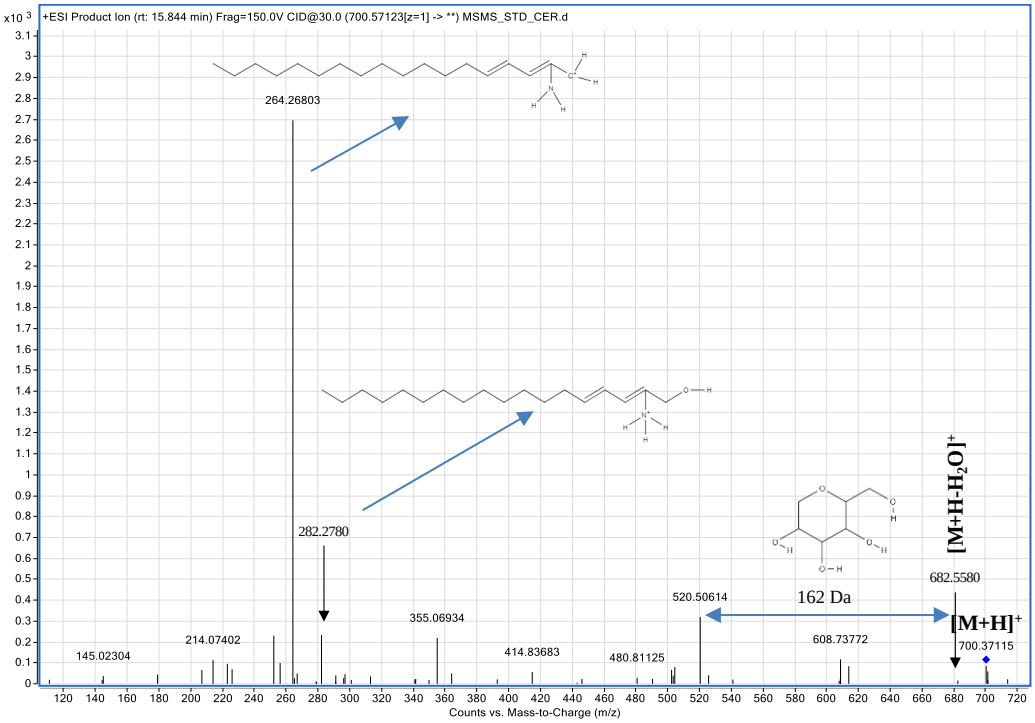

B)

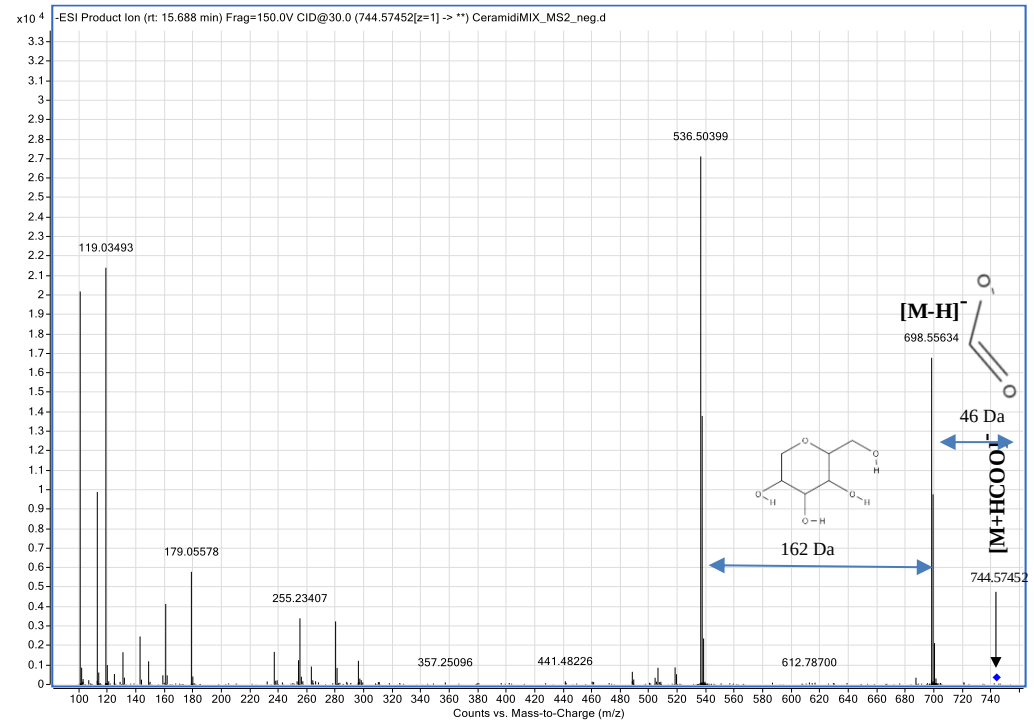

Figure A10 **Hexosylceramide fragmentation**
Representative MS/MS spectra for hexosylceramide HexCer (d34:1) (d18:1/16:0) in A) positive $[M+H]^+$ and B) negative $[M+HCOO]^-$ ionization mode.

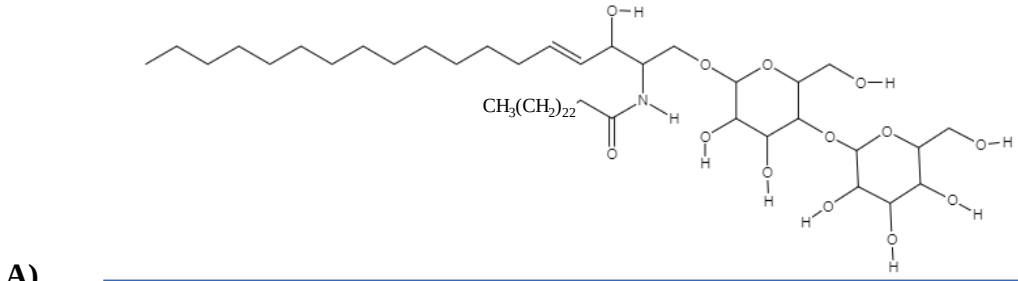

A)

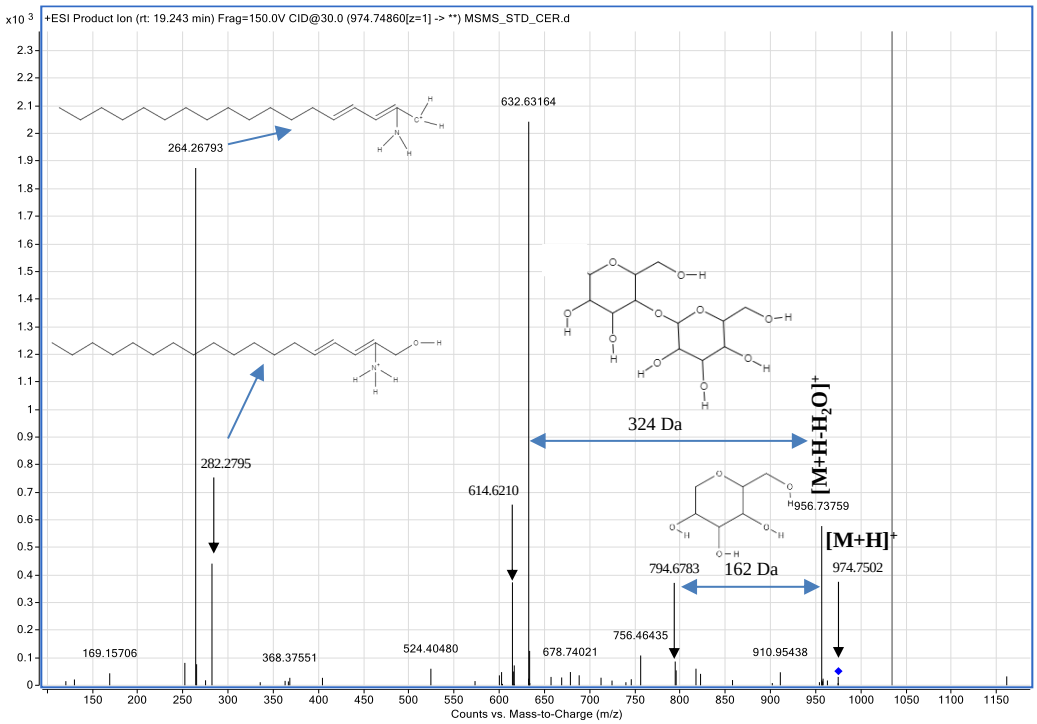

B)

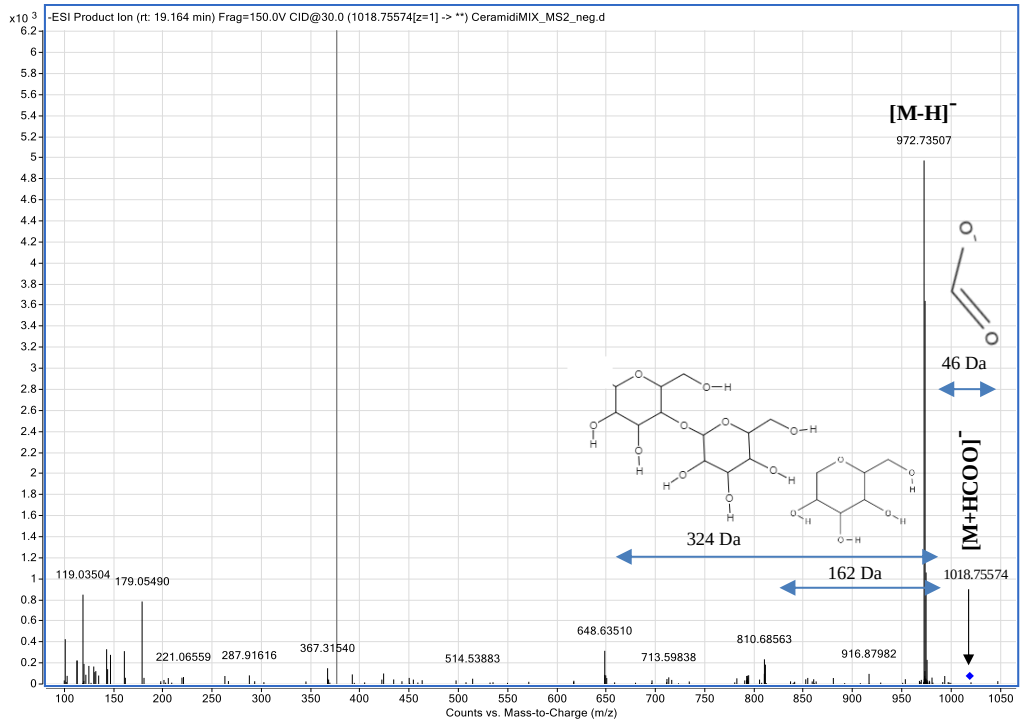

Figure A11 **Lactosylceramide fragmentation**
Representative MS/MS spectra for lactosylceramide LacCer (d42:1) (d18:1/24:0) in A) positive $[M+H]^+$ and B) negative $[M+HCOO]^-$ ionization mode.

9.2 Appendix B

Table B1**: List of lipids detected in positive ionization mode**

Calculated m/z[α]	Measured m/z[β]	Mass error (Da)[γ]	RT (min)[δ]	Lipid Class[ε]	ID[ζ]
538.39683	538.39843	0.0016	17.17	CER	CER
576.56955	576.57196	0.0024	20.80	CER	CER
650.64269	650.64460	0.0019	20.40	CER	CER (d42:1) $[M+H]^+$
648.62729	648.62890	0.0016	19.62	CER	CER (d42:2) $[M+H]^+$
369.35110	369.35213	0.0010	15.31	Cho	CHOLESTEROL
496.33866	496.33980	0.0011	5.40	LPC	LPC 16:0 $[M+H]^+$
496.33869	496.33980	0.0011	4.98	LPC	LPC 16:0 $[M+H]^+$
522.35396	522.35540	0.0015	5.38	LPC	LPC 18:1 $[M+H]^+$
522.35424	522.35540	0.0012	5.76	LPC	LPC 18:1 $[M+H]^+$
520.33396	520.33980	0.0058	4.38	LPC	LPC 18:2 $[M+H]^+$
520.33518	520.33980	0.0046	4.08	LPC	LPC 18:2 $[M+H]^+$
544.33832	544.33980	0.0014	4.11	LPC	LPC 20:4 $[M+H]^+$
544.33842	544.33980	0.0013	3.93	LPC	LPC 20:4 $[M+H]^+$
568.33743	568.33980	0.0023	3.71	LPC	LPC 22:6 $[M+H]^+$
568.33793	568.33980	0.0018	3.86	LPC	LPC 22:6 $[M+H]^+$
502.29169	502.29280	0.0011	4.34	LPE	LPE 20:4 $[M+H]^+$
502.29189	502.29280	0.0009	4.11	LPE	LPE 20:4 $[M+H]^+$
524.27420	524.27480	0.0006	4.12	LPE	LPE 20:4 $[M+Na]^+$
524.27676	524.27480	0.0020	4.35	LPE	LPE 20:4 $[M+Na]^+$
530.32289	530.32410	0.0012	5.52	LPE	LPE 22:4 $[M+H]^+$
530.32304	530.32410	0.0011	5.80	LPE	LPE 22:4 $[M+H]^+$
528.30691	528.30850	0.0015	4.60	LPE	LPE 22:5 $[M+H]^+$
528.30695	528.30850	0.0015	4.37	LPE	LPE 22:5 $[M+H]^+$
528.30698	528.30850	0.0015	4.94	LPE	LPE 22:5 $[M+H]^+$
526.29098	526.29280	0.0018	4.05	LPE	LPE 22:6 $[M+H]^+$
526.29141	526.29280	0.0014	3.87	LPE	LPE 22:6 $[M+H]^+$
720.58840	720.59020	0.0018	17.70	PC	PC (O-32:O) (O-16:0/16:0) $[M+H]^+$
744.58748	744.59020	0.0027	16.76	PC	PC (O-34:2) (O-16:0/18:2)/(P-34:1) (P-16:0/18:1) $[M+H]^+$
772.61932	772.62150	0.0021	17.89	PC	PC (O-36:2) (O:18:0/18:2)/(P-36:1) (P-18:1/18:O) $[M+H]^+$
768.58897	768.59020	0.0012	16.52	PC	PC (O-36:4) (O-18:0/20:4) $[M+H]^+$
796.61704	796.62150	0.0044	17.50	PC	PC (O-38:4) (O-16:0/22:4) $[M+H]^+$
796.61939	796.62150	0.0021	17.78	PC	PC (O-38:4) (O-18:0/20:4) $[M+H]^+$
792.58834	792.59020	0.0018	16.23	PC	PC (O-38:6) (O-16:0/22:6) $[M+H]^+$
746.60402	746.60580	0.0018	17.73	PC	PC (P-34:0) (P-18:0/16:0) $[M+H]^+$
768.58679	768.58780	0.0010	17.71	PC	PC (P-34:0) (P-18:0/16:0) $[M+Na]^+$
794.60417	794.60580	0.0016	16.57	PC	PC (P-38:4) (P-18:0/20:4) $[M+H]^+$
816.58572	816.58780	0.0020	16.58	PC	PC (P-38:4) (P-20:0/20:4) [M+Na]+
818.60367	818.60580	0.0021	16.27	PC	PC (P-40:6) $[M+H]^+$
734.56817	734.56940	0.0013	16.61	PC	PC 32:0 (16:0/16:0) $[M+H]^+$
756.55003	756.55140	0.0013	16.62	PC	PC 32:0 (16:0/16:0) $[M+Na]^+$
732.55058	732.55380	0.0032	15.59	PC	PC 32:1 (16:0/16:1) $[M+H]^+$
746.56474	746.56940	0.0047	16.17	PC	PC 33:1 $[M+H]^+$
762.59843	762.60070	0.0023	17.89	PC	PC 34:0 (16:0/18:0) $[M+H]^+$
760.58385	760.58510	0.0012	16.71	PC	PC 34:1 (16:0/18:1) $[M+H]^+$
782.56637	782.56700	0.0007	16.74	PC	PC 34:1 (16:0/18:1) $[M+Na]^+$
758.56804	758.56940	0.0014	15.79	PC	PC 34:2 (16:0/18:2) $[M+H]^+$
780.54958	780.55140	0.0018	15.79	PC	PC 34:2 (16:0/18:2) $[M+Na]^+$
774.59949	774.60070	0.0012	17.39	PC	PC 35:1 (17:0/18:1) $[M+H]^+$
788.61497	788.61640	0.0014	17.98	PC	PC 36:1 (18:0/18:1) $[M+H]^+$
810.59667	810.59830	0.0017	17.97	PC	PC 36:1 (18:0/18:1) $[M+Na]^+$
786.59939	786.60070	0.0013	16.98	PC	PC 36:2 (18:1/18:1) $[M+H]^+$
808.58161	808.58270	0.0011	16.87	PC	PC 36:2 (18:1/18:1) $[M+Na]^+$
784.58315	784.58510	0.0019	15.95	PC	PC 36:3 (16:0/20:3) $[M+H]^+$

Calculated m/z[α]	Measured m/z[β]	Mass error (Da)[γ]	RT (min)[δ]	Lipid Class[ε]	ID[ζ]
806.56563	806.56700	0.0014	15.94	PC	PC 36:3 (16:0/20:3) $[M+Na]^+$
782.56803	782.56940	0.0014	15.56	PC	PC 36:4 (16:0/20:4) $[M+H]^+$
804.54982	804.55140	0.0015	15.57	PC	PC 36:4 (16:0/20:4) $[M+Na]^+$
782.56714	782.56940	0.0023	14.99	PC	PC 36:4 (18:2/18:2)$[M+H]^+$
814.63028	814.63200	0.0017	18.06	PC	PC 38:2 (18:1/20:1) $[M+H]^+$
812.61338	812.61640	0.0030	17.37	PC	PC 38:3 (18:0/20:3) $[M+H]^+$
810.59769	810.60070	0.0030	16.44	PC	PC 38:4 (16:0/22:4) $[M+H]^+$
810.59895	810.60070	0.0018	16.81	PC	PC 38:4 (18:0/20:4) $[M+H]^+$
832.58129	832.58270	0.0014	16.80	PC	PC 38:4 (18:0/20:4) $[M+Na]^+$
830.56550	830.56700	0.0015	15.68	PC	PC 38:5 (16:0/22:5) (18:1/20:4) $[M+Na]^+$
808.58347	808.58510	0.0016	15.68	PC	PC 38:5 (18:1/20:4) (16:0/22:5) $[M+H]^+$
806.56759	806.56940	0.0018	15.28	PC	PC 38:6 (16:0/22:6) $[M+H]^+$
806.56791	806.56940	0.0015	14.72	PC	PC 38:6 (18:2/20:4) $[M+H]^+$
838.63013	838.63200	0.0019	17.71	PC	PC 40:4 (18:0/22:4) $[M+H]^+$
836.61460	836.61640	0.0018	16.87	PC	PC 40:5 (18:0/22:5) $[M+H]^+$
836.61315	836.61640	0.0032	16.55	PC	PC 40:5 (18:1/22:4) $[M+H]^+$
834.59964	834.60070	0.0011	16.50	PC	PC 40:6 (18:0/22:6) $[M+H]^+$
834.60089	834.60070	0.0002	15.86	PC	PC 40:6 (18:1/22:5) $[M+H]^+$
832.58328	832.58510	0.0018	15.34	PC	PC 40:7 (18:1/22:6) $[M+H]^+$
718.53760	718.53810	0.0005	16.65	PE	PE 34:1 (16:0/18:1) $[M+H]^+$
746.57841	746.56940	0.0090	17.70	PE	PE 36:1 (18:0/18:1) $[M+H]^+$
744.55311	744.55380	0.0007	16.92	PE	PE 36:2 (18:0/18:2) $[M+H]^+$
744.55294	744.55380	0.0008	16.77	PE	PE 36:2 (18:1/18:1) $[M+H]^+$
742.53650	742.53810	0.0016	15.92	PE	PE 36:3 (18:1/18:2) $[M+H]^+$
740.52105	740.52250	0.0014	15.62	PE	PE 36:4 (16:0/20:4) $[M+H]^+$
768.55289	768.55380	0.0009	16.77	PE	PE 38:4 (18:0/20:4) $[M+H]^+$
790.53690	790.53570	0.0012	16.77	PE	PE 38:4 $[M+Na]^+$
764.52128	764.52250	0.0012	15.31	PE	PE 38:6 (16:0/22:6) $[M+H]^+$
796.58688	796.58510	0.0018	17.51	PE	PE 40:4 (18:0/22:4) $[M+H]^+$
794.56848	794.56940	0.0010	16.81	PE	PE 40:5 (18:0/22:5) $[M-H]^+$
792.55470	792.55380	0.0009	16.49	PE	PE 40:6 $[M+H]^+$
790.53875	790.53810	0.0006	15.41	PE	PE 40:7 (18:1/22:6) $[M+H]^+$
887.56316	887.56440	0.0012	15.07	PI	PI 38:4 (18:0/20:4) $[M+H]^+$
909.54448	909.54630	0.0019	15.07	PI	PI 38:4 (18:0/20:4) $[M+Na]^+$
904.58949	904.59100	0.0015	15.07	PI	PI 38:4 (18:0/20:4) $[M+NH_4]^+$
790.56736	790.55930	0.0081	16.45	PS	PS 36:1 (18:0/18:1) $[M+H]^+$
788.54059	788.54360	0.0030	15.33	PS	PS 36:2 (18:0/18:2) (18:1/18:1) $[M+H]^+$
812.54327	812.54360	0.0003	15.34	PS	PS 38:4 (18:0/20:4) $[M+H]^+$
834.52388	834.52560	0.0017	15.35	PS	PS 38:4 (18:0/20:4) $[M+Na]^+$
838.55775	838.55930	0.0015	15.38	PS	PS 40:5 (18:0/22:5) $[M+H]^+$
675.54181	675.54350	0.0017	13.74	SM	SM (d32:1) $(M+H)^+$
689.54849	689.55920	0.0107	14.49	SM	SM (d33:1) $(M+H)^+$
705.58803	705.59050	0.0025	15.70	SM	SM (d34:0) $[M+H]^+$
703.57327	703.57480	0.0016	15.22	SM	SM (d34:1) $[M+H]^+$
725.55518	725.55680	0.0016	15.20	SM	SM (d34:1) $[M+Na]^+$
701.55758	701.55920	0.0016	13.99	SM	SM (d34:2) $[M+H]^+$
731.60446	731.60610	0.0017	16.50	SM	SM (d36:1) $[M+H]^+$
759.63580	759.63740	0.0016	17.74	SM	SM (d38:1) $[M+H]^+$
787.66714	787.66870	0.0016	18.82	SM	SM (d40:1) $[M+H]^+$
785.65147	785.65310	0.0016	17.84	SM	SM (d40:2) $[M+H]^+$
815.69844	815.70000	0.0016	19.91	SM	SM (d42:1) $[M+H]^+$
813.68309	813.68440	0.0013	18.74	SM	SM (d42:2) $[M+H]^+$
835.66477	835.66630	0.0016	18.76	SM	SM (d42:2) $[M+Na]^+$
811.66716	811.66870	0.0016	17.87	SM	SM (d42:3) $[M+H]^+$
300.28898	300.28970	0.0007	4.02	Sph	Sph d18:1
773.66133	773.66300	0.0016	22.27	TAG	TAG 44:0 $[M+Na]^+$

Calculated m/z[α]	Measured m/z[β]	Mass error (Da)[γ]	RT (min)[δ]	Lipid Class[ε]	ID[ζ]
768.70598	768.70760	0.0016	22.27	TAG	TAG 44:0 $[M+NH_4]^+$
782.72165	782.72320	0.0016	22.56	TAG	TAG 45:0 $[M+NH_4]^+$
801.69252	801.69430	0.0017	22.88	TAG	TAG 46:0 $[M+Na]^+$
796.73727	796.73890	0.0016	22.88	TAG	TAG 46:0 $[M+NH_4]^+$
815.70745	815.70990	0.0025	23.18	TAG	TAG 47:0 $[M+Na]^+$
810.75308	810.75450	0.0014	23.18	TAG	TAG 47:0 $[M+NH_4]^+$
829.72395	829.72560	0.0016	23.51	TAG	TAG 48:0 $[M+Na]^+$
824.76881	824.77020	0.0013	23.51	TAG	TAG 48:0 $[M+NH_4]^+$
857.75537	857.75690	0.0015	24.16	TAG	TAG 50:0 (16:0/16:0/18:0) $[M+Na]^+$
852.79983	852.80150	0.0016	24.16	TAG	TAG 50:0 (16:0/16:0/18:0) $[M+NH_4]^+$
855.73987	855.74120	0.0013	23.53	TAG	TAG 50:1 (16:0/16:0/18:1) $[M+Na]^+$
850.78427	850.78580	0.0015	23.53	TAG	TAG 50:1 (16:0/16:0/18:1) $[M+NH_4]^+$
880.83082	880.83280	0.0019	24.82	TAG	TAG 52:0 (16:0/18:0/18:0) (16:0/16:0/20:0) $[M+NH_4]^+$
885.78627	885.78820	0.0019	24.82	TAG	TAG 52:0 (16:0/18:0/18:0) (16:0/18:0/20:0) $[M+Na]^+$
883.77080	883.77250	0.0017	24.18	TAG	TAG 52:1 (16:0/18:0/18:1) $[M+Na]^+$
878.81462	878.81710	0.0025	24.17	TAG	TAG 52:1 (16:0/18:0/18:1) $[M+NH_4]^+$
881.75530	881.75690	0.0016	23.56	TAG	TAG 52:2 (16:0/18:1/18:1) $[M+Na]^+$
876.79982	876.80150	0.0016	23.56	TAG	TAG 52:2 (16:0/18:1/18:1) $[M+NH_4]^+$
879.73995	879.74120	0.0013	23.02	TAG	TAG 52:3 (16:0/18:1/18:2) $[M+Na]^+$
874.78445	874.78580	0.0014	23.03	TAG	TAG 52:3 (16:0/18:1/18:2) $[M+NH_4]^+$
913.81735	913.81950	0.0021	25.49	TAG	TAG 54:0 (18:0/18:0/18:0) $[M+Na]^+$
908.86224	908.86410	0.0018	25.49	TAG	TAG 54:0 (18:0/18:0/18:0) $[M+NH_4]^+$
906.83977	906.84840	0.0086	24.84	TAG	TAG 54:1 (18:0/18:0/18:1) (16:0/18:1/20:0) $[M+NH_4]^+$
911.79810	911.80380	0.0057	24.84	TAG	TAG 54:1 (18:0/18:0/18:1) $[M+Na]^+$
904.83021	904.83280	0.0025	24.19	TAG	TAG 54:2 (18:0/18:1/18:1) (16:0/18:1/20:1) $[M+NH_4]^+$
909.78631	909.78820	0.0018	24.20	TAG	TAG 54:2 (18:0/18:1/18:1) $[M+Na]^+$
907.77072	907.77250	0.0018	23.59	TAG	TAG 54:3 (18:1/18:1/18:1) $[M+Na]^+$
902.81532	902.81710	0.0018	23.59	TAG	TAG 54:3 (18:1/18:1/18:1) $[M+NH_4]^+$

Table 9 **List of lipids detected in positive ionization mode**

α: theoretical m/z values matched in Lipid Maps database;
β: experimental m/z values as calculated by MZmine 2.3 software;
γ: mass error calculated as difference between theoretical m/z and observed m/z
δ: retention time values as calculated by MZmine 2.3 software;
ε: lipid class assign according to Lipid Maps Lipid Classification
ζ: putative ID assign through m/z matched to databases, retention time and MS/MS spectra interpretation.

CER: ceramide; **Cho:** cholesterol; **LPC:** lysophosphatidylcholine; **LPE:** lysophosphatidylethanolamine; **PC:** phosphatidylcholine; **PC-O:** plasmanyl-phosphatidylcholine; **PC-P:** plasmenyl-phosphatidylcholine; **PE:** phosphatidylethanolamine; **PI:** phosphatidylinositol**; PS:** phosphatidylserine; **SM:** sphingomyelin; **Sph:** sphingosine; **TAG:** triacylglycerol.

Table B2**: List of lipids detected in negative ionization mode**

Calculated m/z[α]	Measured m/z[β]	Mass error (Da)[γ]	RT (min)[δ]	Lipid Class[ε]	ID[ζ]
622.46586	622.46590	0.0001	15.45	CER	CER (d32:1) [ADDUCT]$^-$
544.44968	544.45020	0.0005	15.45	CER	CER (d32:1) [M+Cl]$^-$
554.47828	554.47900	0.0007	15.45	CER	CER (d32:1) [M+HCOO]$^-$
571.46881	571.50500	0.0362	15.45	CER	CER (d32:1) [M+HCOONH$_4$]$^-$
558.46532	558.46590	0.0005	16.09	CER	CER (d33:1) [M+Cl]$^-$
568.49206	568.49470	0.0026	16.09	CER	CER (d33:1) [M+HCOO]$^-$
585.48455	585.52060	0.0361	16.09	CER	CER (d33:1) [M+HCOONH$_4$]$^-$
652.51309	652.51282	0.0003	17.12	CER	CER (d34:0) [ADDUCT]$^-$
574.49670	574.49720	0.0005	17.14	CER	CER (d34:0) [M+Cl]$^-$
574.49698	574.49720	0.0002	17.37	CER	CER (d34:0) [M+Cl]$^-$
584.52525	584.52600	0.0007	17.12	CER	CER (d34:0) [M+HCOO]$^-$
584.52553	584.52600	0.0004	17.38	CER	CER (d34:0) [M+HCOO]$^-$
601.51595	601.55195	0.0360	17.12	CER	CER (d34:0) [M+HCOONH$_4$]$^-$
601.51603	601.55195	0.0359	17.38	CER	CER (d34:0) [M+HCOONH$_4$]$^-$
582.51026	582.51030	0.0000	16.69	CER	CER (d34:1) (d18:1/16:0) [M+HCOO]$^-$
650.49759	650.49717	0.0004	16.69	CER	CER (d34:1) [ADDUCT]$^-$
572.48142	572.48150	0.0001	16.69	CER	CER (d34:1) [M+Cl]$^-$
599.50056	599.53630	0.0357	16.69	CER	CER (d34:1) [M+HCOONH$_4$]$^-$
536.50406	536.50480	0.0008	16.69	CER	CER (d34:1) [M-H]$^-$
648.48156	648.48152	0.0000	15.66	CER	CER (d34:2) [ADDUCT]$^-$
570.46597	570.46590	0.0001	15.66	CER	CER (d34:2) [M+Cl]$^-$
580.49418	580.49470	0.0005	15.66	CER	CER (d34:2) [M+HCOO]$^-$
597.48445	597.52065	0.0362	15.66	CER	CER (d34:2) [M+HCOONH$_4$]$^-$
596.52493	596.52600	0.0010	17.26	CER	CER (d35:1) [M+HCOO]$^-$
602.52808	602.52850	0.0004	18.19	CER	CER (d36:0) [M+Cl]$^-$
612.55486	612.55730	0.0024	18.17	CER	CER (d36:0) [M+HCOO]$^-$
629.54804	629.58325	0.0352	18.17	CER	CER (d36:0) [M+HCOONH$_4$]$^-$
678.52860	678.52847	0.0001	17.79	CER	CER (d36:1) [ADDUCT]$^-$
600.51403	600.51280	0.0012	17.79	CER	CER (d36:1) [M+Cl]$^-$
610.54136	610.54160	0.0002	17.79	CER	CER (d36:1) [M+HCOO]$^-$
627.53180	627.56760	0.0358	17.79	CER	CER (d36:1) [M+HCOONH$_4$]$^-$
598.50004	598.49720	0.0029	16.88	CER	CER (d36:2) [M+Cl]$^-$
608.52549	608.52600	0.0005	16.88	CER	CER (d36:2) [M+HCOO]$^-$
625.51588	625.55195	0.0361	16.88	CER	CER (d36:2) [M+HCOONH$_4$]$^-$
624.55472	624.55730	0.0025	18.31	CER	CER (d37:1) [M+HCOO]$^-$
641.54711	641.58325	0.0361	18.30	CER	CER (d37:1) [M+HCOONH$_4$]$^-$
630.55924	630.55980	0.0005	19.10	CER	CER (d38:0) [M+Cl]$^-$
640.58302	640.58860	0.0055	19.05	CER	CER (d38:0) [M+HCOO]$^-$
657.57904	657.61455	0.0355	19.09	CER	CER (d38:0) [M+HCOONH$_4$]$^-$
706.55982	706.55977	0.0000	18.76	CER	CER (d38:1) [ADDUCT]$^-$
628.54675	628.54410	0.0027	18.76	CER	CER (d38:1) [M+Cl]$^-$
638.57266	638.57290	0.0002	18.76	CER	CER (d38:1) [M+HCOO]$^-$
655.56313	655.59890	0.0358	18.76	CER	CER (d38:1) [M+HCOONH$_4$]$^-$
636.55672	636.55730	0.0005	17.97	CER	CER (d38:2) [M+HCOO]$^-$
653.54733	653.58325	0.0359	17.97	CER	CER (d38:2) [M+HCOONH$_4$]$^-$
642.55962	642.55980	0.0001	19.22	CER	CER (d39:1) [M+Cl]$^-$
652.58770	652.58860	0.0009	19.22	CER	CER (d39:1) [M+HCOO]$^-$
669.57851	669.61455	0.0360	19.21	CER	CER (d39:1) [M+HCOONH$_4$]$^-$
736.60839	736.60672	0.0017	19.90	CER	CER (d40:0) [ADDUCT]$^-$
658.59059	658.59110	0.0005	19.90	CER	CER (d40:0) [M+Cl]$^-$
668.61188	668.61990	0.0080	20.30	CER	CER (d40:0) [M+HCOO]$^-$
668.61948	668.61990	0.0004	19.90	CER	CER (d40:0) [M+HCOO]$^-$
685.60974	685.64585	0.0361	19.90	CER	CER (d40:0) [M+HCOONH$_4$]$^-$

Calculated m/z[α]	Measured m/z[β]	Mass error (Da)[γ]	RT (min)[δ]	Lipid Class[ε]	ID[ζ]
734.59136	734.59107	0.0003	19.61	CER	CER (d40:1) [ADDUCT]$^-$
656.57640	656.57540	0.0010	19.61	CER	CER (d40:1) [M+Cl]$^-$
656.57639	656.57540	0.0010	19.13	CER	CER (d40:1) [M+Cl]$^-$
666.60396	666.60420	0.0002	19.61	CER	CER (d40:1) [M+HCOO]$^-$
666.60275	666.60420	0.0015	19.09	CER	CER (d40:1) [M+HCOO]$^-$
683.59460	683.63020	0.0356	19.60	CER	CER (d40:1) [M+HCOONH$_4$]$^-$
683.59340	683.63020	0.0368	19.10	CER	CER (d40:1) [M+HCOONH$_4$]$^-$
732.57642	732.57540	0.0010	18.77	CER	CER (d40:2) [ADDUCT]$^-$
732.57596	732.57540	0.0006	18.88	CER	CER (d40:2) [ADDUCT]$^-$
654.56116	654.55980	0.0014	18.78	CER	CER (d40:2) [M+Cl]$^-$
654.56183	654.55980	0.0021	18.90	CER	CER (d40:2) [M+Cl]$^-$
664.58827	664.58860	0.0003	18.77	CER	CER (d40:2) [M+HCOO]$^-$
664.58822	664.58860	0.0003	18.91	CER	CER (d40:2) [M+HCOO]$^-$
681.57888	681.61455	0.0357	18.77	CER	CER (d40:2) [M+HCOONH$_4$]$^-$
681.57870	681.61455	0.0358	18.90	CER	CER (d40:2) [M+HCOONH$_4$]$^-$
652.54499	652.54410	0.0009	18.01	CER	CER (d40:3) [M+Cl]$^-$
662.57221	662.57290	0.0007	18.00	CER	CER (d40:3) [M+HCOO]$^-$
679.56265	679.59890	0.0363	18.00	CER	CER (d40:3) [M+HCOONH$_4$]$^-$
672.60575	672.60670	0.0009	20.26	CER	CER (d41:0) [M+Cl]$^-$
682.63296	682.63550	0.0025	20.28	CER	CER (d41:0) [M+HCOO]$^-$
699.62543	699.66150	0.0361	20.28	CER	CER (d41:0) [M+HCOONH$_4$]$^-$
748.60926	748.60672	0.0025	20.00	CER	CER (d41:1) [ADDUCT]$^-$
670.59093	670.59110	0.0001	20.01	CER	CER (d41:1) [M+Cl]$^-$
680.61963	680.61990	0.0002	20.00	CER	CER (d41:1) [M+HCOO]$^-$
697.61012	697.64585	0.0357	20.00	CER	CER (d41:1) [M+HCOONH$_4$]$^-$
668.57547	668.57540	0.0001	19.19	CER	CER (d41:2) [M+Cl]$^-$
678.60369	678.60420	0.0005	19.19	CER	CER (d41:2) [M+HCOO]$^-$
678.60357	678.60420	0.0006	19.34	CER	CER (d41:2) [M+HCOO]$^-$
695.59427	695.63020	0.0359	19.19	CER	CER (d41:2) [M+HCOONH$_4$]$^-$
695.59418	695.63020	0.0360	19.33	CER	CER (d41:2) [M+HCOONH$_4$]$^-$
764.63849	764.63802	0.0005	20.62	CER	CER (d42:0) [ADDUCT]$^-$
696.65100	696.65120	0.0002	20.62	CER	CER (d42:0) [M+HCOO]$^-$
713.64096	713.67715	0.0362	20.63	CER	CER (d42:0) [M+HCOONH$_4$]$^-$
762.62298	762.62237	0.0006	20.36	CER	CER (d42:1) [ADDUCT]$^-$
762.62355	762.62237	0.0012	19.88	CER	CER (d42:1) [ADDUCT]$^-$
684.60686	684.60670	0.0002	20.36	CER	CER (d42:1) [M+Cl]$^-$
684.60482	684.60670	0.0019	19.87	CER	CER (d42:1) [M+Cl]$^-$
694.63560	694.63550	0.0001	20.36	CER	CER (d42:1) [M+HCOO]$^-$
694.63465	694.63550	0.0009	19.88	CER	CER (d42:1) [M+HCOO]$^-$
711.62606	711.66150	0.0354	20.36	CER	CER (d42:1) [M+HCOONH$_4$]$^-$
711.62532	711.66150	0.0362	19.87	CER	CER (d42:1) [M+HCOONH$_4$]$^-$
760.60765	760.60672	0.0009	19.57	CER	CER (d42:2) [ADDUCT]$^-$
682.59117	682.59110	0.0001	19.57	CER	CER (d42:2) [M+Cl]$^-$
682.59301	682.59110	0.0020	19.22	CER	CER (d42:2) [M+Cl]$^-$
692.61989	692.61990	0.0000	19.57	CER	CER (d42:2) [M+HCOO]$^-$
692.61945	692.61990	0.0004	19.74	CER	CER (d42:2) [M+HCOO]$^-$
692.61874	692.61990	0.0011	19.21	CER	CER (d42:2) [M+HCOO]$^-$
709.60904	709.64585	0.0368	19.21	CER	CER (d42:2) [M+HCOONH$_4$]$^-$
709.61025	709.64585	0.0356	19.57	CER	CER (d42:2) [M+HCOONH$_4$]$^-$
758.59206	758.59110	0.0010	18.88	CER	CER (d42:3) [ADDUCT]$^-$
680.57535	680.57540	0.0000	18.88	CER	CER (d42:3) [M+Cl]$^-$
690.60390	690.60420	0.0003	18.88	CER	CER (d42:3) [M+HCOO]$^-$
707.59432	707.63020	0.0359	18.88	CER	CER (d42:3) [M+HCOONH$_4$]$^-$
710.66520	710.66680	0.0016	20.95	CER	CER (d43:0) [M+HCOO]$^-$
727.65664	727.69280	0.0362	20.95	CER	CER (d43:0) [M+HCOONH$_4$]$^-$
708.65095	708.65120	0.0002	20.71	CER	CER (d43:1) [M+HCOO]$^-$

Calculated m/z[α]	Measured m/z[β]	Mass error (Da)[γ]	RT (min)[δ]	Lipid Class[ε]	ID[ζ]
725.64126	725.67715	0.0359	20.71	CER	CER (d43:1) $[M+HCOONH_4]^-$
706.63476	706.63550	0.0007	19.95	CER	CER (d43:2) $[M+HCOO]^-$
723.62546	723.66150	0.0360	19.95	CER	CER (d43:2) $[M+HCOONH_4]^-$
724.68193	724.68250	0.0005	21.25	CER	CER (d44:0) $[M+HCOO]^-$
741.67265	741.70845	0.0358	21.26	CER	CER (d44:0) $[M+HCOONH_4]^-$
722.66655	722.66680	0.0003	21.03	CER	CER (d44:1) $[M+HCOO]^-$
722.66536	722.66680	0.0014	20.55	CER	CER (d44:1) $[M+HCOO]^-$
739.65713	739.69280	0.0357	21.03	CER	CER (d44:1) $[M+HCOONH_4]^-$
739.66151	739.69280	0.0313	20.63	CER	CER (d44:1) $[M+HCOONH_4]^-$
720.65044	720.65120	0.0007	20.31	CER	CER (d44:2) $[M+HCOO]^-$
737.64125	737.67715	0.0359	20.31	CER	CER (d44:2) $[M+HCOONH_4]^-$
752.71442	752.71380	0.0007	21.79	CER	CER (d46:0) $[M+HCOO]^-$
769.70487	769.73975	0.0349	21.82	CER	CER (d46:0) $[M+HCOONH_4]^-$
588.47602	588.47640	0.0004	16.11	CER	CER (t34:1) $[M+Cl]^-$
598.50558	598.50520	0.0004	16.11	CER	CER (t34:1) $[M+HCOO]^-$
615.48716	615.53121	0.0441	16.27	CER	CER (t34:1) $[M+HCOONH_4]^-$
684.61025	684.61480	0.0045	19.18	CER	CER (t40:0) $[M+HCOO]^-$
701.60452	701.64076	0.0362	19.17	CER	CER (t40:0) $[M+HCOONH_4]^-$
698.62697	698.63040	0.0034	19.62	CER	CER (t41:0) $[M+HCOO]^-$
715.62009	715.65651	0.0364	19.61	CER	CER (t41:0) $[M+HCOONH_4]^-$
702.61345	702.61730	0.0038	19.98	CER	CER (t42:0) $[M+Cl]^-$
712.64038	712.64610	0.0057	19.92	CER	CER (t42:0) $[M+HCOO]^-$
729.57734	729.67206	0.0947	19.98	CER	CER (t42:0) $[M+HCOONH_4]^-$
700.60079	700.60160	0.0008	19.16	CER	CER (t42:1) $[M+Cl]^-$
710.62804	710.63040	0.0024	19.16	CER	CER (t42:1) $[M+HCOO]^-$
727.62058	727.65641	0.0358	19.16	CER	CER (t42:1) $[M+HCOONH_4]^-$
726.65937	726.66170	0.0023	20.35	CER	CER (t43:0) $[M+HCOO]^-$
743.65162	743.68771	0.0361	20.34	CER	CER (t43:0) $[M+HCOONH_4]^-$
740.67649	740.67740	0.0009	20.67	CER	CER (t44:0) $[M+HCOO]^-$
757.66754	757.70336	0.0358	20.67	CER	CER (t44:0) $[M+HCOONH_4]^-$
728.63055	728.63290	0.0024	19.95	CER	CER (t44:1) $[M+Cl]^-$
738.66120	738.66170	0.0005	19.95	CER	CER (t44:1) $[M+HCOO]^-$
738.66102	738.66170	0.0007	20.64	CER	CER (t44:1) $[M+HCOO]^-$
755.65215	755.68771	0.0356	19.94	CER	CER (t44:1) $[M+HCOONH_4]^-$
755.65196	755.68771	0.0358	20.65	CER	CER (t44:1) $[M+HCOONH_4]^-$
754.69208	754.69300	0.0009	20.97	CER	CER (t45:0) $[M+HCOO]^-$
771.68365	771.71901	0.0354	20.97	CER	CER (t45:0) $[M+HCOONH_4]^-$
758.67717	758.67990	0.0027	21.28	CER	CER (t46:0) $[M+Cl]^-$
768.70883	768.70870	0.0002	21.27	CER	CER (t46:0) $[M+HCOO]^-$
785.69926	785.73466	0.0354	21.27	CER	CER (t46:0) $[M+HCOONH_4]^-$
766.69343	766.69300	0.0004	20.62	CER	CER (t46:1) $[M+HCOO]^-$
783.68413	783.71901	0.0349	20.63	CER	CER (t46:1) $[M+HCOONH_4]^-$
782.72634	782.72430	0.0020	21.54	CER	CER (t47:0) $[M+HCOO]^-$
796.74210	796.74000	0.0021	21.83	CER	CER (t48:0) $[M+HCOO]^-$
761.55339	761.58912	0.0357	15.45	CER	HexCer (d34:1) $[M+HCOONH_4]^-$
734.53419	734.53430	0.0001	15.44	CER	HexCer (d34:1) $[M+Cl]^-$
744.56319	744.56310	0.0001	15.44	CER	HexCer (d34:1) $[M+HCOO]^-$
828.65741	828.65700	0.0004	18.59	CER	HexCer (d40:1) $[M+HCOO]^-$
924.68203	924.67520	0.0068	19.40	CER	HexCer (d42:1) $[ADDUCT]^-$
846.66390	846.65950	0.0044	19.40	CER	HexCer (d42:1) $[M+Cl]^-$
856.68920	856.68830	0.0009	19.39	CER	HexCer (d42:1) $[M+HCOO]^-$
873.67992	873.71430	0.0344	19.40	CER	HexCer (d42:1) $[M+HCOONH_4]^-$
922.66462	922.65955	0.0051	18.55	CER	HexCer (d42:2) $[ADDUCT]^-$
844.64500	844.64390	0.0011	18.55	CER	HexCer (d42:2) $[M+Cl]^-$
854.67328	854.67270	0.0006	18.55	CER	HexCer (d42:2) $[M+HCOO]^-$
871.66388	871.69867	0.0348	18.55	CER	HexCer (d42:2) $[M+HCOONH_4]^-$

Calculated m/z[α]	Measured m/z[β]	Mass error (Da)[γ]	RT (min)[δ]	Lipid Class[ε]	ID[ζ]
760.55677	760.55800	0.0013	15.05	CER	HexCer (t34:1) $[M+HCOO]^-$
896.58722	896.58720	0.0001	14.81	CER	LacCer (d34:1) (d18:1/16:0) $[M+Cl]^-$
906.61654	906.61600	0.0006	14.80	CER	LacCer (d34:1) (d18:1/16:0) $[M+HCOO]^-$
923.60696	923.64195	0.0350	14.80	CER	LacCer (d34:1) (d18:1/16:0) $[M+HCOONH_4]^-$
540.33003	540.33070	0.0007	5.26	LPC	LPC 16:0 $[M+HCOO]^-$
540.33018	540.33070	0.0005	4.87	LPC	LPC 16:0 $[M+HCOO]^-$
566.34522	566.34640	0.0011	5.25	LPC	LPC 18:1 $[M+HCOO]^-$
566.34549	566.34640	0.0009	5.62	LPC	LPC 18:1 $[M+HCOO]^-$
564.33025	564.33070	0.0004	3.97	LPC	LPC 18:2 $[M+HCOO]^-$
564.33004	564.33070	0.0007	4.14	LPC	LPC 18:2 $[M+HCOO]^-$
588.33010	588.33070	0.0006	3.84	LPC	LPC 20:4 $[M+HCOO]^-$
588.33006	588.33070	0.0006	3.96	LPC	LPC 20:4 $[M+HCOO]^-$
452.27527	452.27830	0.0030	5.09	LPE	LPE 16:0 $[M-H]^-$
452.27730	452.27830	0.0010	5.46	LPE	LPE 16:0 $[M-H]^-$
480.30908	480.30960	0.0005	7.66	LPE	LPE 18:0 $[M-H]^-$
478.29328	478.29390	0.0006	5.49	LPE	LPE 18:1 $[M-H]^-$
478.29313	478.29390	0.0008	5.83	LPE	LPE 18:1 $[M-H]^-$
476.27762	476.27830	0.0007	4.16	LPE	LPE 18:2 $[M-H]^-$
476.27786	476.27830	0.0004	4.44	LPE	LPE 18:2 $[M-H]^-$
502.29318	502.29390	0.0007	4.73	LPE	LPE 20:3 $[M-H]^-$
704.23984	704.23999	0.0001	4.04	LPE	LPE 20:4 $[ADDUCT]^-$
568.26526	568.26514	0.0001	4.04	LPE	LPE 20:4 $[ADDUCT]^-$
568.26535	568.26514	0.0002	4.24	LPE	LPE 20:4 $[ADDUCT]^-$
500.27804	500.27830	0.0002	4.03	LPE	LPE 20:4 $[M-H]^-$
500.27782	500.27830	0.0005	4.26	LPE	LPE 20:4 $[M-H]^-$
498.26153	498.26260	0.0011	3.13	LPE	LPE 20:5 $[M-H]^-$
498.26023	498.26260	0.0024	3.30	LPE	LPE 20:5 $[M-H]^-$
596.29664	596.29644	0.0002	5.41	LPE	LPE 22:4 $[ADDUCT]^-$
596.29677	596.29644	0.0003	5.61	LPE	LPE 22:4 $[ADDUCT]^-$
528.30938	528.30960	0.0002	5.42	LPE	LPE 22:4 $[M-H]^-$
528.30937	528.30960	0.0002	5.71	LPE	LPE 22:4 $[M-H]^-$
594.28126	594.28079	0.0005	4.28	LPE	LPE 22:5 $[ADDUCT]^-$
526.29374	526.29390	0.0002	4.28	LPE	LPE 22:5 $[M-H]^-$
526.29322	526.29390	0.0007	4.53	LPE	LPE 22:5 $[M-H]^-$
526.29318	526.29390	0.0007	4.84	LPE	LPE 22:5 $[M-H]^-$
526.28626	526.29390	0.0077	5.09	LPE	LPE 22:5 $[M-H]^-$
592.26547	592.26514	0.0003	3.79	LPE	LPE 22:6 $[ADDUCT]^-$
524.27790	524.27830	0.0004	3.79	LPE	LPE 22:6 $[M-H]^-$
524.27779	524.27830	0.0005	3.95	LPE	LPE 22:6 $[M-H]^-$
619.28853	619.28890	0.0004	2.99	LPI	LPI 20:4 $[M-H]^-$
619.28851	619.28890	0.0004	3.16	LPI	LPI 20:4 $[M-H]^-$
764.58084	764.58110	0.0003	17.52	PC	PC (O-32:0) (O-16:0/16:0) $[M+HCOO]^-$
812.58101	812.58110	0.0001	16.36	PC	PC (O-36:4) (O-18:0/20:4) $[M+HCOO]^-$
840.61228	840.61240	0.0001	17.66	PC	PC (O-38:4) (O-16:0/22:4) (O-18:0/20:4) $[M+HCOO]^-$
790.59669	790.59680	0.0001	17.57	PC	PC (P-34:0) (P-18:0/16:0) $[M+HCOO]^-$
838.59650	838.59680	0.0003	16.41	PC	PC (P-38:4) (P-20:0/20:4) $[M+HCOO]^-$
846.54792	846.54723	0.0007	16.47	PC	PC 32:0 (16:0/16:0) $[ADDUCT]^-$
914.53538	914.53466	0.0007	16.47	PC	PC 32:0 (16:0/16:0) $[ADDUCT]^-$
778.56054	778.56040	0.0002	16.46	PC	PC 32:0 (16:0/16:0) $[M+HCOO]^-$
776.54426	776.54470	0.0005	15.43	PC	PC 32:1 (16:0/16:1) $[M+HCOO]^-$
806.59146	806.59170	0.0002	17.74	PC	PC 34:0 (16:0/18:0) $[M+HCOO]^-$
872.56343	872.56288	0.0006	16.56	PC	PC 34:1 (16:0/18:1) $[ADDUCT]^-$
940.55031	940.55031	0.0000	16.57	PC	PC 34:1 (16:0/18:1) $[ADDUCT]^-$
804.57627	804.57600	0.0003	16.56	PC	PC 34:1 (16:0/18:1) $[M+HCOO]^-$
870.54774	870.54723	0.0005	15.65	PC	PC 34:2 (16:0/18:2) $[ADDUCT]^-$
802.56043	802.56040	0.0001	15.65	PC	PC 34:2 (16:0/18:2) $[M+HCOO]^-$

Calculated m/z[α]	Measured m/z[β]	Mass error (Da)[γ]	RT (min)[δ]	Lipid Class[ε]	ID[ζ]
900.59450	900.59418	0.0003	17.84	PC	PC 36:1 (18:0/18:1) [ADDUCT]$^-$
832.60727	832.60730	0.0000	17.81	PC	PC 36:1 (18:0/18:1) [M+HCOO]$^-$
898.57891	898.57853	0.0004	16.86	PC	PC 36:2 (18:1/18:1) [ADDUCT]$^-$
830.59184	830.59170	0.0002	16.82	PC	PC 36:2 (18:1/18:1) [M+HCOO]$^-$
896.56307	896.56288	0.0002	15.80	PC	PC 36:3 (16:0/20:3) [ADDUCT]$^-$
828.57573	828.57600	0.0003	15.80	PC	PC 36:3 (16:0/20:3) [M+HCOO]$^-$
894.54755	894.54723	0.0003	15.43	PC	PC 36:4 (16:0/20:4) [ADDUCT]$^-$
826.56045	826.56040	0.0001	15.43	PC	PC 36:4 (16:0/20:4) (18:2/18:2) [M+HCOO]$^-$
840.57440	840.57600	0.0016	16.04	PC	PC 37:4 (17:0/20:4) [M+HCOO]$^-$
856.60676	856.60730	0.0006	17.23	PC	PC 38:3 (18:0/20:3) [M+HCOO]$^-$
854.59135	854.59170	0.0003	16.33	PC	PC 38:4 (16:0/22:4) [M+HCOO]$^-$
922.57897	922.57853	0.0004	16.67	PC	PC 38:4 (18:0/20:4) [ADDUCT]$^-$
854.59178	854.59170	0.0001	16.66	PC	PC 38:4 (18:0/20:4) [M+HCOO]$^-$
852.57603	852.57600	0.0000	16.28	PC	PC 38:5 (16:0/22:5) [M+HCOO]$^-$
852.57610	852.57600	0.0001	15.54	PC	PC 38:5 (18:1/20:4) [M+HCOO]$^-$
850.56039	850.56040	0.0000	15.56	PC	PC 38:6 (16:0/22:6) [M+HCOO]$^-$
850.56009	850.56040	0.0003	15.09	PC	PC 38:6 (18:2/20:4) [M+HCOO]$^-$
880.60647	880.60730	0.0009	16.72	PC	PC 40:5 (18:0/22:5) / (18:1/22:4) [M+HCOO]$^-$
878.59156	878.59170	0.0001	16.36	PC	PC 40:6 (18:1/22:5) / (18:0/22:6) [M+HCOO]$^-$
876.57587	876.57600	0.0001	15.20	PC	PC 40:7 (18:1/22:6) [M+HCOO]$^-$
724.52829	724.52870	0.0004	16.38	PE	PE (O-36:4) (O-16:0/20:4) [M-H]$^-$
752.55956	752.56000	0.0004	17.46	PE	PE (O-38:4) (O-18:0/20:4) [M-H]$^-$
750.54439	750.54430	0.0001	16.44	PE	PE (O-38:5) (O-16:0/22:5) [M-H]$^-$
748.52938	748.52870	0.0007	16.26	PE	PE (O-38:6) (O-16:0:/22:6) / (P-38:5) (P-18:1/20:4) [M-H]$^-$
778.57100	778.57560	0.0046	18.26	PE	PE (O-40:5) / (P-40:4) [M-H]$^-$
778.56999	778.57560	0.0056	17.97	PE	PE (O-40:5) / (P-40:4) [M-H]$^-$
776.56032	776.56000	0.0003	17.25	PE	PE (O-40:6) (O-18:0/22:6) [M-H]$^-$
722.51315	722.51300	0.0001	16.19	PE	PE (P-36:4) (P-16:0/20:4) [M-H]$^-$
750.54556	750.54430	0.0012	16.93	PE	PE (P-38:4) (P-16:0/22:4) [M-H]$^-$
750.54407	750.54430	0.0002	17.30	PE	PE (P-38:4) (P-18:0/20:4) [M-H]$^-$
746.51374	746.51300	0.0007	15.83	PE	PE (P-38:6) (P-16:0/22:6) [M-H]$^-$
774.54717	774.54430	0.0029	17.04	PE	PE (P-40:6) (P-18:0/22:6) [M-H]$^-$
690.50765	690.50790	0.0003	16.45	PE	PE 32:0 (16:0/16:0) [M-H]$^-$
784.51084	784.51045	0.0004	16.58	PE	PE 34:1 (16:0/18:1) [ADDUCT]$^-$
716.52360	716.52360	0.0000	16.58	PE	PE 34:1 (16:0/18:1) [M-H]$^-$
714.50764	714.50790	0.0003	15.71	PE	PE 34:2 (16:0/18:2) [M-H]$^-$
744.55503	744.55490	0.0001	17.62	PE	PE 36:1 (18:0/18:1) [M-H]$^-$
812.54249	812.54175	0.0007	17.62	PE	PE 36:1 [ADDUCT]$^-$
880.52978	880.52918	0.0006	17.63	PE	PE 36:1 [ADDUCT]$^-$
810.52676	810.52610	0.0007	16.84	PE	PE 36:2 (18:0/18:2) [ADDUCT]$^-$
742.53923	742.53920	0.0000	16.85	PE	PE 36:2 (18:0/18:2) [M-H]$^-$
742.53921	742.53920	0.0000	16.70	PE	PE 36:2 (18:1/18:1) [M-H]$^-$
810.52694	810.52610	0.0008	16.29	PE	PE 36:2 [ADDUCT]$^-$
740.52334	740.52360	0.0002	15.84	PE	PE 36:3 (18:1/18:2) [M-H]$^-$
806.49543	806.49480	0.0006	15.55	PE	PE 36:4 (16:0/20:4) [ADDUCT]$^-$
738.50805	738.50790	0.0001	15.54	PE	PE 36:4 (16:0/20:4) [M-H]$^-$
770.56991	770.57050	0.0006	17.68	PE	PE 38:2 (18:1/20:1) [M-H]$^-$
768.55486	768.55490	0.0000	17.13	PE	PE 38:3 (18:0/20:3) [M-H]$^-$
766.53912	766.53920	0.0001	16.38	PE	PE 38:4 [M-H]$^-$
834.52679	834.52610	0.0007	16.70	PE	PE 38:4 (18:0/20:4) [ADDUCT]$^-$
902.51393	902.51353	0.0004	16.70	PE	PE 38:4 (18:0/20:4) [ADDUCT]$^-$
896.49706	896.55031	0.0532	16.70	PE	PE 38:4 (18:0/20:4) [ADDUCT]$^-$
766.53966	766.53920	0.0004	16.70	PE	PE 38:4 (18:0/20:4) [M-H]$^-$
764.52682	764.52360	0.0032	15.78	PE	PE 38:5 (16:0/22:5) [M-H]$^-$
764.52402	764.52360	0.0004	15.67	PE	PE 38:5 (18:1/20:4) / (18:0/20:5) [M-H]$^-$
832.51136	832.51045	0.0009	15.67	PE	PE 38:5 (18:1/20:4) [ADDUCT]$^-$

Calculated m/z[α]	Measured m/z[β]	Mass error (Da)[γ]	RT (min)[δ]	Lipid Class[ε]	ID[ζ]
762.50797	762.50790	0.0000	15.23	PE	PE 38:6 (16:0/22:6) [M-H]$^-$
862.55797	862.55740	0.0006	17.42	PE	PE 40:4 (18:0/22:4) [ADDUCT]$^-$
794.57066	794.57050	0.0001	17.42	PE	PE 40:4 (18:0/22:4) [M-H]$^-$
794.57059	794.57050	0.0001	17.72	PE	PE 40:4 [M-H]$^-$
792.55535	792.55490	0.0005	16.73	PE	PE 40:5 (18:0/22:5) [M-H]$^-$
792.55964	792.55490	0.0048	17.12	PE	PE 40:5 [M-H]$^-$
858.52692	858.52610	0.0008	16.41	PE	PE 40:6 (18:0/22:6) [ADDUCT]$^-$
790.54187	790.53920	0.0026	16.41	PE	PE 40:6 (18:0/22:6) [M-H]$^-$
788.52562	788.52360	0.0020	15.37	PE	PE 40:7 (18:1/22:6) [M-H]$^-$
802.56044	802.52102	0.0394	16.51	PE	PE-NMe2 (16:0/18:1) [ADDUCT]$^-$
824.54473	824.50537	0.0394	15.56	PE	PE-NMe2 (16:0/20:4) [ADDUCT]$^-$
773.53315	773.53380	0.0007	14.60	PG	PG 36:2 (18:1/18:1) [M-H]$^-$
863.56628	863.56550	0.0008	15.99	PI	PI 36:1 (18:0/18:1) [M-H]$^-$
861.54945	861.54990	0.0004	15.00	PI	PI 36:2 (18:1/18:1) [M-H]$^-$
861.54964	861.54990	0.0002	15.16	PI	PI 36:2 (18:1/18:1) [M-H]$^-$
857.51868	857.51860	0.0001	13.78	PI	PI 36:4 (16:0/20:4) [M-H]$^-$
887.56543	887.56550	0.0001	15.47	PI	PI 38:3 (18:0/20:3) [M-H]$^-$
953.53710	953.53673	0.0004	15.03	PI	PI 38:4 (18:0/20:4) [ADDUCT]$^-$
885.55038	885.54990	0.0005	15.03	PI	PI 38:4 (18:0/20:4) [M-H]$^-$
883.53461	883.53420	0.0004	13.93	PI	PI 38:5 (18:1/20:4) [M-H]$^-$
883.53485	883.53420	0.0006	14.09	PI	PI 38:5 [M-H]$^-$
913.58105	913.58120	0.0001	15.81	PI	PI 40:4 (18:0/22:4) [M-H]$^-$
911.56550	911.56550	0.0000	15.08	PI	PI 40:5 (18:0/22:5) [M-H]$^-$
909.54974	909.54990	0.0001	14.74	PI	PI 40:6 (18:0/22:6) [M-H]$^-$
788.54512	788.54470	0.0004	16.29	PS	PS 36:1 (18:0/18:1) [M-H]$^-$
786.52902	786.52910	0.0000	15.44	PS	PS 36:2 (18:0/18:2) (18:1/18:1) [M-H]$^-$
812.54474	812.54470	0.0000	15.76	PS	PS 38:3 (18:0/20:3) [M-H]$^-$
810.52928	810.52910	0.0002	15.32	PS	PS 38:4 (18:0/20:4) [M-H]$^-$
838.56140	838.56040	0.0010	16.10	PS	PS 40:4 (18:0/20:4) [M-H]$^-$
836.54484	836.54470	0.0001	15.36	PS	PS 40:5 (18:0/22:5) [M-H]$^-$
834.52918	834.52910	0.0001	15.00	PS	PS 40:6 (18:0/22:6) [M-H]$^-$
719.53434	719.53450	0.0001	13.63	SM	SM (d32:1) (M+HCOO]$^-$
733.54990	733.55010	0.0002	14.37	SM	SM (d33:1) [M+HCOO]$^-$
749.58075	749.58140	0.0007	15.59	SM	SM (d34:0) [M+HCOO]$^-$
815.55329	815.55265	0.0006	15.05	SM	SM (d34:1) [ADDUCT]$^-$
747.56597	747.56580	0.0002	15.05	SM	SM (d34:1) [M+HCOO]$^-$
745.54989	745.55010	0.0002	13.88	SM	SM (d34:2) [M+HCOO]$^-$
775.59636	775.59710	0.0007	16.39	SM	SM (d36:1) [M+HCOO]$^-$
803.62831	803.62840	0.0001	17.63	SM	SM (d38:1) [M+HCOO]$^-$
899.64925	899.64655	0.0027	18.70	SM	SM (d40:1) [ADDUCT]$^-$
831.66013	831.65970	0.0004	18.68	SM	SM (d40:1) [M+HCOO]$^-$
829.64434	829.64400	0.0003	17.76	SM	SM (d40:2) [M+HCOO]$^-$
859.69285	859.69100	0.0019	19.77	SM	SM (d42:1) [M+HCOO]$^-$
925.66573	925.66220	0.0035	18.62	SM	SM (d42:2) [ADDUCT]$^-$
857.67609	857.67530	0.0008	18.62	SM	SM (d42:2) [M+HCOO]$^-$
855.66032	855.65970	0.0006	17.75	SM	SM (d42:3) [M+HCOO]$^-$

Table 10 **List of lipids detected in positive ionization mode**

α: theoretical m/z values matched in Lipid Maps database;
β: experimental m/z values as calculated by MZmine 2.3 software;
γ: mass error calculated as difference between theoretical m/z and observed m/z
δ: retention time values as calculated by MZmine 2.3 software;
ε: lipid class assign according to Lipid Maps Lipid Classification
ζ: putative ID assign through m/z matched to databases, retention time and MS/MS spectra interpretation.

CER: ceramide; **HexCer:** hexosylceramide; **LacCer:** lactosylceramide; **LPC:** lysophosphatidylcholine; **LPE:** lysophosphatidylethanolamine; **LPI:** lysophosphatidylinositol; **PC:** phosphatidylcholine; **PC-O:** plasmanyl-phosphatidylcholine; **PC-P:** plasmenyl-phosphatidylcholine; **PE:** phosphatidylethanolamine; **PE-O:** plasmanyl-phosphatidylethanolamine; **PE-P:** plasmenyl-phosphatidylethanolamine; **PG:** phosphatidylglycerol; **PI:** phosphatidylinositol**; PS:** phosphatidylserine; **SM:** sphingomyelin.

Acknowledgement